

**Impact of the lack of cross-presenting
dendritic cells on the generation of
inflammatory immune responses in
experimental *Plasmodium berghei*
ANKA infection and therapeutic
possibilities to limit excessive brain
inflammation with doxycycline**

Dissertation

zur

Erlangung des Doktorgrades (Dr. rer. nat.)

der

Mathematisch-Naturwissenschaftlichen Fakultät

der

Rheinischen Friedrich-Wilhelms-Universität Bonn

Fach Molekulare Biomedizin

vorgelegt von

Janina Melanie Küpper

aus Radolfzell am Bodensee

Bonn, November 2016

Angefertigt mit Genehmigung der Mathematisch-Naturwissenschaftlichen Fakultät der
Rheinischen Friedrich-Wilhelms-Universität Bonn

1. Gutachter Prof. Dr. med. Achim Hörauf
2. Gutachter Prof. Dr. rer. nat. Waldemar Kolanus

Tag der Promotion: 21.04.2017

Erscheinungsjahr: 2017

Diese Arbeit wurde von Januar 2012 bis November 2016 am Institut für medizinische Mikrobiologie, Immunologie und Parasitologie unter der Leitung von Prof. Dr. Achim Hörauf angefertigt.

Ich versichere an Eides statt, dass die vorgelegte Arbeit persönlich, selbständig und ohne Benutzung anderer als der ausdrücklich angegebenen Hilfsmittel angefertigt wurde. Die aus anderen Quellen direkt oder indirekt übernommenen Daten und Konzepte wurden unter Angabe der Quelle kenntlich gemacht. Ich habe die vorgelegte Arbeit oder ähnliche Arbeiten an keiner anderen Universität als Dissertation eingereicht und habe für die Erstellung der vorgelegten Arbeit keine fremde Hilfe, insbesondere keine entgeltliche Hilfe von Vermittlungs- bzw. Beratungsdiensten (Promotionsberatern / -vermittlern oder anderen Personen) in Anspruch genommen.

Bonn, den 10.11.2016

Bonn, den 13.06.2017

(Redaktionell korrigierte Version)

Summary

Malaria is a vector-transmitted disease caused by unicellular parasites of the *Plasmodium* species and resulted in over 400,000 deaths in 2015, most of them in African children below the age of five. *Plasmodium* parasites are transmitted to a vertebrate intermediate host during blood-meals of female *Anopheles* mosquitoes, the definitive host of the parasite.

Infections with *P. falciparum* are responsible for the severest form of malaria in humans, cerebral malaria (CM). CM is thought to be a multi-factorial process, where sequestration of infected erythrocytes and immune cells in the cerebral microvasculature and overwhelming pro-inflammatory immune responses result in severe cerebral damage. Previous research using experimental models revealed that T cells that have been primed in the spleens of infected individuals and migrated to the brain, play an important role in the development of experimental CM. However, the exact mechanisms that lead to CM in some cases of *P. falciparum* infection remain elusive.

Cross-presenting dendritic cells (DCs) have been shown to be the major cell subset in priming cytotoxic CD8⁺ T cells during *Plasmodium* infection. *Batf3*^{-/-} mice, which genetically lack cross-presenting DCs, are completely protected from experimental CM. We demonstrated here, that the protection was accompanied by reduced immune cell migration to the brain and impaired cytotoxic T lymphocyte (CTL) responses in the spleens of *Batf3*^{-/-} mice after *P. berghei* ANKA-infection. Additionally, we found elevated expression of immune regulating factors in these mice, which could further contribute to the ECM-resistance in *Batf3*^{-/-} mice.

In summary, these results underlined the importance of cross-presenting DCs in the pathogenesis of ECM. Furthermore, they improved our understanding of the disease de-

velopment by adding important details about the alterations in the immune responses that result from the lack of cross-presenting DCs.

Another important question in understanding ECM pathology is how these immune responses can be modified later in *Plasmodium* infection, before cerebral symptoms occur, in order to prevent brain inflammation.

The lack of specific treatment of cerebral malaria and increasing drug resistance of *Plasmodium* species requires new approaches to fight this disease. Here, we demonstrated that the antibiotic doxycycline did not only reduce the parasitemia in *P. berghei* ANKA infected mice but also generally dampened the pro-inflammatory milieu and antigen-specific cytotoxicity of immune cells in the spleens and brains of infected animals. Different approaches in our experimental setup suggest that the reduced inflammation in doxycycline-treated mice was not exclusively dependent on doxycycline's anti-plasmodial effect. Thus, a combined treatment of doxycycline, which is relatively well-tolerated with few side effects, and another fast-acting anti-parasitic drug might offer a reasonable therapeutic option to target parasite load and cerebral inflammation at the same time.

Zusammenfassung

Malaria ist eine durch Vektoren übertragene Krankheit, die allein im Jahr 2015 über 400.000 Leben gefordert hat; die meisten davon in Afrika bei Kindern unter fünf Jahren. Die Krankheit wird durch eine Infektion mit einzelligen Parasiten der Gattung *Plasmodium* ausgelöst, die während der Blutmahlzeit ihres Endwirtes, der *Anopheles* Mücke, auf ein Wirbeltier als Zwischenwirt übertragen werden.

Die schwerwiegendste Form der Malaria in Menschen ist die sogenannte zerebrale Malaria (ZM), deren Ursache eine Infektion mit *P. falciparum* ist. ZM wird als eine Krankheit mit multi-faktoriellen Ursachen angesehen, bei der sowohl die Sequestration infizierter Erythrozyten und Immunzellen in den zerebralen Blutgefäßen als auch eine überschießende Entzündungsreaktion zum Schaden im Gehirn beitragen.

Frühere Studien in Tierversuchen haben gezeigt, dass T Zellen, die nach einer Infektion in der Milz aktiviert werden und dann ins Gehirn einwandern, eine wichtige Rolle in der Entwicklung der experimentellen ZM einnehmen. Der genaue Mechanismus der in manchen Fällen der *P. falciparum* Infektion zur Entstehung von ZM führt, konnte bisher allerdings nicht vollständig aufgeklärt werden.

Da Erythrozyten keine MHC Klasse I Moleküle exprimieren, übernehmen sogenannte kreuz-präsentierende dendritische Zellen (DZs) das Priming von zytotoxischen CD8⁺ T Zellen in einer *Plasmodium* Infektion. *Batf3*^{-/-} Mäuse, denen kreuz-präsentierende DZs genetisch bedingt fehlen, sind vor der Entstehung von experimenteller zerebraler Malaria (EZM) im Mausmodell vollständig geschützt. Dieser Schutz vor EZM ging einher mit einer deutlich eingeschränkten Migration der Immunzellen ins Gehirn sowie einer beeinträchtigten zytotoxischen T Zell (CTL) Immunantwort in der Milz der *Plasmodium berghei* ANKA infizierten *Batf3*^{-/-} Mäuse. Zudem fanden wir in diesen Mäusen eine

erhöhte Expression von immun-regulierenden Faktoren, die zusätzlich zum Schutz vor EZM beitragen könnten.

Zusammengefasst unterstreichen diese Ergebnisse die zentrale Bedeutung kreuz-präsentierender DZs in der Entwicklung von EZM in Mäusen und verbessern damit unser Verständnis des Krankheitsablaufes auf immunologischer Ebene und die veränderten Immunantworten, die durch das Fehlen dieser Zellen hervorgerufen werden.

Untersuchungen humaner Erkrankungen, wie ZM, in knock-out Mäusen lassen uns Änderungen der Immunantwort charakterisieren, die durch das Fehlen einzelner Faktoren hervorgerufen werden. Eine weitere wichtige Frage ist, ob die Immunantworten auch im späteren Krankheitsverlauf, kurz vor dem Auftreten neurologischer Symptome, noch beeinflusst werden können.

Der Mangel an spezifischen Behandlungsmöglichkeiten der zerebralen Malaria und das vermehrte Auftreten von Resistenzen der *Plasmodien* gegenüber herkömmlichen Medikamenten erfordert neue Lösungen im Kampf gegen die Krankheit. Wir konnten zeigen, dass eine Behandlung mit dem Antibiotikum Doxycyclin nicht nur die Parasitämie in PbA-infizierten Mäusen verringerte, sondern auch insgesamt die Entzündungsreaktion sowie vor allem die antigen-spezifische Zytotoxizität der Immunzellen in Milz und Gehirn verringerte. Mithilfe unterschiedlicher experimenteller Behandlungsansätze konnten wir zeigen, dass der Schutz vor EZM in Doxycyclin-behandelten Mäusen nicht nur auf den antiparasitären Effekt des Medikaments zurückzuführen war, sondern höchstwahrscheinlich auch zum großen Teil auf dessen entzündungshemmende Eigenschaften.

Da Doxycyclin sehr gut vertragen wird und nur geringe Nebenwirkungen auftreten, bietet die Behandlung mit Doxycyclin in Kombination mit einem weiteren, schneller wirkenden Medikament gegen die *Plasmodien*, eine Möglichkeit bei Malaria-Patienten mit neurologischen Symptomen gleichzeitig den Parasiten und die Entzündungsreaktion im Gehirn zu bekämpfen.

Contents

Summary	i
Zusammenfassung	iii
Contents	v
List of Figures	xi
List of Tables	xiv
List of Abbreviations	xv
1 Introduction	1
1.1 General introduction to Malaria	1
1.1.1 <i>Plasmodium</i> life cycle	2
1.2 Pathogenesis of cerebral malaria	3
1.2.1 Mouse models for malaria	4
1.2.2 Sequestration theory in cerebral malaria	6
1.2.3 Cytokine theory and immune responses in cerebral malaria	7
1.2.3.1 Cytotoxic effector immune responses in cerebral malaria	8
1.2.3.2 Immune regulation in malaria	11
1.3 Treatment of <i>Plasmodium</i> infection	13
1.3.1 Doxycycline treatment in malaria	13
1.4 Aims and objectives	14

2	Material and Methods	17
2.1	Buffers and Materials	17
2.1.1	Anesthesia - short term	17
2.1.2	Anesthesia - long term	17
2.1.3	Cell culture medium	17
2.1.4	CFSE stock	18
2.1.5	FACS buffer	18
2.1.6	FarRed stock	18
2.1.7	MACS buffer	18
2.1.8	Machines	18
2.1.9	Analysis software	18
2.2	Methods	19
2.2.1	Mouse handling	19
2.2.1.1	Infection of mice with <i>Plasmodium berghei</i> ANKA	19
2.2.1.2	Experimental cerebral malaria score and rapid murine coma and behavior scale for ECM surveillance	20
2.2.1.3	Determination of parasitemia	21
2.2.1.4	Administration of doxycycline	21
2.2.1.5	Administration of BrdU and proliferation analysis	22
2.2.1.6	Preparation of organs and plasma for analysis	22
2.2.2	Cell culture preparation for cytokine analysis	23
2.2.3	Cell culture preparation for generation of bone-marrow derived den- dritic cells	24
2.2.4	Cross-presentation assay for brain microvessels	24
2.2.5	Enzyme-linked immunosorbent assay (ELISA)	24
2.2.6	Evans blue assay	26
2.2.7	Flow cytometric analysis	27
2.2.8	<i>In vivo</i> cytotoxicity assay	27
2.2.9	Magnetic-activated cell sorting (MACS)	28
2.2.10	Natural killer (T) cell assay	29
2.2.11	Phagocytosis assay	29
2.2.12	Quantitative real-time polymerase chain reaction (PCR)	30
2.2.13	Transmigration assay	31
2.2.14	Statistical analysis	32

3 Results	33
3.1 <i>Batf3</i> ^{-/-} mice were protected from experimental cerebral malaria after PbA-infection	33
3.1.1 <i>Batf3</i> ^{-/-} mice did not develop ECM upon PbA-infection with extracted sporozoites	34
3.1.2 Brains of PbA-infected <i>Batf3</i> ^{-/-} mice did not show signs of cellular infiltration and inflammation	35
3.1.2.1 Immune cell infiltration to the brain was reduced in PbA-infected <i>Batf3</i> ^{-/-} mice	35
3.1.2.2 Brains of PbA-infected <i>Batf3</i> ^{-/-} mice showed reduced inflammation	41
3.1.2.3 Phagocytic capacity of microglia was impaired in <i>Batf3</i> ^{-/-} mice	44
3.1.3 Immune responses in early PbA-infection were less pronounced in spleens of PbA-infected <i>Batf3</i> ^{-/-} mice and led to reduced T cell activation in the late phase of ECM development	45
3.1.3.1 Spleens of PbA-infected <i>Batf3</i> ^{-/-} mice contained less CD8 ⁺ T cells compared to infected WT mice at 3 and 6 dpi . . .	47
3.1.3.2 Cytotoxicity and activation of splenic CD8 ⁺ T cells was reduced in PbA-infected <i>Batf3</i> ^{-/-} mice on dpi 6	50
3.1.3.3 NK cells were more activated in the spleens of PbA-infected <i>Batf3</i> ^{-/-} mice on dpi 6	55
3.1.3.4 CD4 ⁺ dendritic cells from <i>Batf3</i> ^{-/-} mice expressed more CD40 on their surface after PbA-infection	59
3.1.3.5 Antigen-presenting cells in <i>Batf3</i> ^{-/-} mice showed a reduced pro-inflammatory milieu on 3 dpi, compared to WT controls	62
3.1.3.6 Phagocytic capacity of CD11b ⁺ cells from PbA-infected <i>Batf3</i> ^{-/-} mice was reduced on 6 dpi compared to WT mice	65
3.1.3.7 Immune regulatory mechanisms in PbA-infected <i>Batf3</i> ^{-/-} mice were elevated on 6 dpi	67

3.2	ECM development after doxycycline administration from 4 dpi	74
3.2.1	Increased splenocyte numbers in doxycycline treated mice was neither caused by altered migration patterns nor by increased proliferation	77
3.2.2	Higher infective dose in doxycycline treated animals allowed the comparison between treated and untreated animals with similar parasite loads	80
3.2.3	Blood-brain barrier remained stable after doxycycline treatment despite high parasitemia	82
3.2.4	Immune cell infiltration and activation was reduced in brains of doxycycline treated mice	83
3.2.4.1	Brain infiltrated T cell were less activated but did not differ in frequencies after doxycycline treatment	85
3.2.4.2	Antigen presenting cell frequencies were not altered in brains of doxycycline treated mice, but they expressed less activation markers	87
3.2.4.3	Microglia showed reduced expression of MHC class II molecules in doxycycline-treated PbA-infected mice	90
3.2.4.4	Cytokine production was reduced in brains of mice treated with doxycycline	91
3.2.4.5	Cross-presentation by brain microvessels was not altered after doxycycline treatment	92
3.2.5	Cytotoxicity in the spleen was reduced after doxycycline treatment .	93
3.2.5.1	T cell numbers did not differ in spleens of doxycycline treated mice, but their cytotoxicity was significantly reduced	94
3.2.5.2	Antigen presenting cells were less activated in doxycycline treated mice	99
3.2.6	Reduction of doxycycline dose to sub-antimicrobial doses still improved survival independent of parasite killing	101
4	Discussion	105
4.1	Cross-presenting dendritic cells were required for development of ECM in a PbA mouse model	106

4.1.1	PbA-infected <i>Batf3</i> ^{-/-} mice maintained a stable blood-brain barrier and lacked infiltration of effector T cells into the brain	107
4.1.2	ECM-protected <i>Batf3</i> ^{-/-} mice showed no signs of cerebral inflammation 6 days after PbA-infection	109
4.1.2.1	Cells in brains of PbA-infected <i>Batf3</i> ^{-/-} mice produced less effector molecules	109
4.1.2.2	Reduced ICAM-1 expression could prevent adhesion of cells in brains of PbA-infected <i>Batf3</i> ^{-/-} mice	110
4.1.2.3	Phagocytosis is reduced in microglia of PbA-infected and naive <i>Batf3</i> ^{-/-} mice	111
4.1.3	Protection from brain pathology in PbA-infected <i>Batf3</i> ^{-/-} mice apparently resulted from altered immune responses in the spleen	112
4.1.3.1	PbA-infected <i>Batf3</i> ^{-/-} mice displayed an impaired, but not fully absent CTL response	112
4.1.3.2	The lack of <i>Batf3</i> resulted in a shift from inflammation to a more regulatory milieu after PbA-infection	117
4.1.4	Relevance of impaired CTL responses for PbA-infection in <i>Batf3</i> ^{-/-} mice	120
4.2	Doxycycline prevented ECM by exerting anti-inflammatory properties in susceptible Bl/6 mice	123
4.2.1	Doxycycline treatment in mice infected with higher parasite loads prevented ECM and protected the blood-brain barrier	124
4.2.1.1	PbA-infected mice showed reduced cerebral inflammation after doxycycline treatment: less cellular infiltrates and impaired activity of effector T cells	126
4.2.1.2	(Antigen-specific) immune cell activation in spleens of PbA-infected mice was reduced by doxycycline but the treatment did not affect the composition of cell subsets	129
4.2.2	Sub-antimicrobial doses of doxycycline prevented ECM without affecting parasitemia	131
4.2.3	Outlook - Prevention of ECM due to altered shedding of microparticle	132
4.2.4	Anti-inflammatory drugs offer promising treatment options in ECM	134

CONTENTS

Supplements	153
Scientific Contributions	165
Curriculum Vitae	167
Acknowledgments	169

List of Figures

1.1	Life cycle of <i>Plasmodium</i> spp. in human and mosquito	2
1.2	No ECM in PbA-infected <i>Batf3</i> ^{-/-} mice	15
2.1	Principle of the <i>in vivo</i> kill.	28
2.2	Principle of the migration assay	32
3.1	<i>Batf3</i> ^{-/-} mice did not develop ECM after infection with PbA sporozoites	34
3.2	FACS gating scheme for brain cells	36
3.3	Less CD45 ^{hi} cells infiltrated the brains of PbA-infected <i>Batf3</i> ^{-/-} mice	37
3.4	Levels of CD8 ⁺ T cell infiltration were not increased in brains of PbA-infected <i>Batf3</i> ^{-/-} mice at 6 dpi	38
3.5	Composition of brain-infiltrated leukocytes did not differ between d+6 PbA-infected <i>Batf3</i> ^{-/-} mice and naive controls	40
3.6	T cells from <i>Batf3</i> ^{-/-} mice produced less granzyme B and general inflammation in the brain was reduced	42
3.7	Microglia from brains of <i>Batf3</i> ^{-/-} mice were in general less capable of phagocytosis than WT microglia.	45
3.8	Total amount of splenocytes did increase in PbA-infected <i>Batf3</i> ^{-/-} mice at 6 dpi	46
3.9	FACS gating scheme for spleen cells	48
3.10	Increased CD4 ⁺ vs. CD8 ⁺ T cell ratios in spleens of <i>Batf3</i> ^{-/-} mice at all tested time points after PbA-infection	49
3.11	Cytotoxicity was reduced in spleens of <i>Batf3</i> ^{-/-} mice	52
3.12	Impaired cytotoxicity in spleens of PbA-infected <i>Batf3</i> ^{-/-} mice on 6 dpi	53

3.13 NK and NKT cells were elevated in spleens of <i>Batf3</i> ^{-/-} mice after PbA-infection, compared to infected WT mice	55
3.14 NK and NKT cells from spleens of <i>Batf3</i> ^{-/-} mice produced significantly more granzyme B after PbA-infection than infected WT mice	56
3.15 NK cells from spleens of d+6 PbA-infected <i>Batf3</i> ^{-/-} mice displayed enhanced activity in both, cytotoxic and regulatory markers	58
3.16 Dendritic cell numbers decreased in spleens of PbA-infected WT and <i>Batf3</i> ^{-/-} mice	59
3.17 CD40 was increased on splenic DCs in d+6 PbA-infected <i>Batf3</i> ^{-/-} mice	61
3.18 Inflammatory monocytes were not increased in spleens of <i>Batf3</i> ^{-/-} but in WT mice on dpi 3	63
3.19 TNF production in the spleen was increased 3 days after PbA-infection, but CCL2 levels remained unchanged	64
3.20 Phagocytosis of APCs in the spleen was impaired in <i>Batf3</i> ^{-/-} mice on 6 dpi but not changed in early PbA-infection (3 dpi)	66
3.21 IL-10 and IL-6 production from splenic CD11b ⁺ cells was increased in PbA-infected <i>Batf3</i> ^{-/-} mice	68
3.22 The total amount of T _{regs} was increased in spleens of PbA-infected <i>Batf3</i> ^{-/-} mice on 6 dpi	71
3.23 Splenic CD11b ⁺ cells from d+6 PbA-infected <i>Batf3</i> ^{-/-} mice contained higher frequencies of alternatively activated macrophages	73
3.24 Intravenous doxycycline prevented ECM when given from 4 dpi	75
3.25 Doxycycline treatment from 4 dpi resulted to a stable BBB and reduced cytotoxicity in PbA-infected mice	76
3.26 Migration of spleen cells towards <i>in vitro</i> cultured brain cells was not altered in samples from doxycycline-treated mice	78
3.27 Splenocytes from doxycycline-treated mice had a similar proliferation rate as untreated mice on 5 dpi	79
3.28 ECM was prevented in mice infected with high parasite load and treated with doxycycline	81
3.29 Stable Blood-brain barrier in 1e6 iRBC infected mice after doxycycline treatment	83
3.30 The total number of brain infiltrated cells was reduced after doxycycline treatment	84

3.31	T cells in the brains of PbA-infected mice showed no alteration in their frequencies after doxycycline treatment	86
3.32	CD8 ⁺ T cells found in the brains of PbA-infected mice were less activated after doxycycline treatment	87
3.33	Dendritic cells in the brain expressed less ICAM-1 after doxycycline treatment in PbA-infection	88
3.34	CD11b ⁺ cells in the brain were less activated in PbA-infected mice after doxycycline treatment	89
3.35	Microglia expressed less I-Ab in PbA-infected mice after doxycycline treatment	90
3.36	TNF and CCL5 release were slightly downregulated in brains of "PbA 1e6 + DOX" mice compared to untreated "PbA 5e4" mice	92
3.37	Brain microvessels of doxycycline treated PbA-infected mice were able to cross-present antigen	93
3.38	Total number of spleen cells did not differ between doxycycline treated and untreated mice	94
3.39	T cell numbers in the spleen did not differ after doxycycline treatment of PbA-infected mice	95
3.40	Activation markers were decreased in splenic CD8 ⁺ T cells from doxycycline treated, PbA-infected mice	96
3.41	Cytotoxicity was reduced in spleens and serum of PbA-infected mice after doxycycline treatment	97
3.42	Activation markers on splenic dendritic cells were reduced in doxycycline treated, PbA-infected mice	99
3.43	Less Ly6C ⁺ monocytes in spleens of doxycycline treated mice but similar activation in CD11b ⁺ cells in general, compared to untreated mice	100
3.44	Mice treated with different doses of doxycycline showed better survival compared to untreated mice.	102
3.45	Doxycycline was able to protect mice from ECM without affecting parasitemia.	103
4.1	<i>Batf3</i> ^{-/-} mice did not develop ECM as a consequence of impaired T cell priming and subsequent reduction of inflammation in the brain	121
4.2	Doxycycline treatment protected PbA-infected WT mice from ECM by dampening their inflammatory immune responses	134

S1	XCR1 ⁺ cross-presenting dendritic cells were missing in <i>Batf3</i> ^{-/-} mice	153
S2	Supplementary figure for Fig. 1.2 and 3.1	153
S3	Supplementary figure for Fig. 3.4 and 3.5	154
S4	Supplementary figure for Fig. 3.8	154
S5	Supplementary figure for Fig. 3.10	155
S6	Supplementary figure for Fig. 3.11	156
S7	Supplementary figure for Fig. 3.11 and 3.12	157
S8	Supplementary figure for Fig. 3.13	157
S9	Supplementary figure for Fig. 3.14	158
S10	Supplementary figure for Fig. 3.15	159
S11	Supplementary figure for Fig. 3.16	160
S12	Supplementary figure for Fig. 3.17	161
S13	Supplementary figure for Fig. 3.18	162
S14	Supplementary figure for Fig. 3.21	163
S15	Supplementary figure for Fig. 3.22	163
S16	Supplementary figure for Chapter 3.1.5.7	164
S17	Supplementary figure for Fig. 3.32	164

List of Tables

2.1	Phagocytosis assay - Combination of serum opsonized beads and cells	29
-----	---	----

List of Abbreviations

ACT	Artemisinin-based combination therapy
B_{reg}	B regulatory cell
T_{reg}	T regulatory cell
μ	micro- (10 ⁻⁶)
AAM	alternatively activated macrophages
APC	antigen presenting cell
app.	approximately
ATF	activating transcription factor
BATF	basic leucine zipper transcriptional factor ATF-like
BBB	blood-brain barrier
BCP	1-bromo-3-chloropropane
BL/6	C57 BL/6 mice
BMDC	bone-marrow derived dendritic cells
BrdU	bromodeoxyuridine
BSA	bovine serum ovalbumin
C	Celsius
Ca	calcium
CCL	CC chemokine ligand
CCR	CC chemokine receptor
CFSE	carboxy fluorescein di-amino succinimidyl ester
CM	cerebral malaria
CTL	cytotoxic T lymphocyte
CXCL	CXC chemokine ligand

LIST OF ABBREVIATIONS

CXCR	CXC chemokine receptor
d	day
DC	dendritic cell
DMSO	dimethyl sulfoxide
DNA	deoxyribonucleic acid
dNTP	deoxyribonucleotide
DOX	doxycycline
dpi	days post infection
e.g.	<i>exempli gratia</i> (for example)
ECM	experimental cerebral malaria
EDTA	ethylenediaminetetraacetate dehydrate
ELISA	enzyme-linked immunosorbent assay
EMP	erythrocyte membrane protein
et al.	<i>et alteres</i> (and others)
FACS	fluorescent activated cell sorter
FCS	fetal calf serum
g	Gram
GFP	Green fluorescent protein
GM-CSF	granulocyte-macrophage colony-stimulating factor
grzmB	granzyme B
gzmB	granzyme B
h	hour(s)
HIV	human immunodeficiency virus
HSTaq	HotStar Taq DNA Polymerase
i.e.	<i>id est</i> (that is)
i.p.	intraperitoneal
i.v.	intravenous
ICAM	intracellular adhesion molecule
IFN γ	interferon gamma
Ig	immunoglobulin
IL	interleukin
IMDM	Iscove's Modified Dulbecco's Medium
iRBC	infected red blood cell

kg	kilogram
KO	knock out
LT- α	lymphotoxin alpha
M	molar
m	meter, milli (10 ⁻³)
MACS	magnetic-activated cell sorting
MCP-1	monocyte chemo-attractant protein 1
MgCl ₂	magnesium chloride
MHC	major histocompatibility complex
min	minute(s)
MMP	matrix metalloproteinase
MSP	merozoite surface protein
n	nano (10 ⁻⁹); number
NaCl	sodium chloride
NF κ B	nuclear factor kappa B
NK	natural killer
NO	nitric oxide
OD	optical density
OVA	ovalbumin
<i>P.</i>	<i>Plasmodium</i>
p.i.	post infection
p.o.	<i>per os</i> (oral administration)
PAMP	pathogen associated molecular pattern
PbA	<i>Plasmodium berghei</i> ANKA
PBS	phosphate buffered saline
PbTG	transgenic strain of <i>P. berghei</i> ANKA expressing ovalbumin
PCR	Polymerase chain reaction
PfEMP-1	<i>Plasmodium falciparum</i> erythrocyte membrane protein 1
PSGL-1	P-selectin glycoprotein ligand 1
RANTES	regulated upon activation, normal T-Cell expressed, and secreted
RBC	red blood cell
RMCBS	rapid murine coma and behavior scale
rpm	rounds per minute

LIST OF ABBREVIATIONS

RPMI	Roswell Park Memorial Institute, cell culture medium developed by G.E. Moore et al.
RT	room temperature
sec	second(s)
SPF	specific pathogen free
<i>spp.</i>	<i>species pluralis</i>
TCR	T cell receptor
tg	transgenic
T _h	T helper
TMB	tetramethylbenzidine
TNF	tumor necrosis factor
vs.	<i>versus</i>
vWF	von Willebrand factor
WHO	World Health Organization
WT	wild type
Zn	zinc

Chapter 1

Introduction

1.1 General introduction to Malaria

Malaria is a vector-transmitted disease that is known for over 4,000 years, but it took several centuries before the actual parasite and the transmitting vector, the *Anopheles* mosquito, were discovered in the late 19th century [Centers for Disease Control and Prevention, 2016b]. Today we know, that human malaria can be caused by five different unicellular *Plasmodium* species: *P. falciparum*, *P. vivax*, *P. ovale*, *P. malariae* and *P. knowlesi*. These species share the general life cycle but lead to different clinical manifestations, that might progress to life-threatening complications such as severe anemia or cerebral malaria. Malaria occurs in tropical and subtropical countries, mostly in Africa and South-East Asia and currently half of the world population lives at risk of *Plasmodium* infection. In 2015, 214 Mio. people were infected with *Plasmodium* parasites and 438,000 died from following complications; most of them being African children under the age of five [WHO, 2016]. Despite enormous progress regarding prevention of fatality in the last decade, with a drop of mortality rates of almost 47%, *Plasmodium* infection still remains a big burden in tropical and sub-tropical countries [WHO, 2014]. Not only does the tropical climate in these countries promote parasite replication within its definitive host, the *Anopheles* mosquito, but also incomplete comprehension and limited availability of convenient treatment options are important factors that make these countries more vulnerable to the disease. Luckily, in most regions of the world, treatment for *Plasmodium* infections is available today and malaria death's have been decreasing constantly.

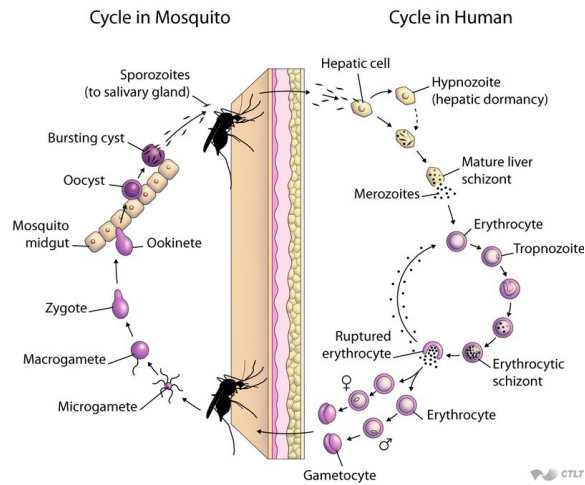


Figure 1.1: **Life cycle of *Plasmodium* spp. in humans and mosquitoes.** Sporozoites of *Plasmodium* spp. are injected into the human host during the blood meal of an infected female *Anopheles* mosquito. Thereafter the parasite enters the liver through the blood stream and develops there before entering the erythrocytic cycle; in case of *P. vivax* or *P. ovale* infection hypnozoites can form and remain in the liver before starting the blood stage cycle at a later time point. The parasite further replicates in the red blood cells and finally forms gametocytes which are taken up by *Anopheles* mosquitoes with their next blood meal. The *Plasmodium* gametocytes undergo sexual reproduction in the mosquito and develop till they reach sporozoite stage in the salivary glands from where a new cycle starts [Picture ©Johns Hopkins Bloomberg School of Public Health].

However, an unsolved problem is the development of cerebral malaria, that accounts for almost all deaths after *P. falciparum* infection. Till today, neither the reason why this disease form develops in only 1% of *P. falciparum* infections nor the mechanisms responsible for disease progression are completely understood. An estimated 5 - 20% of people who present themselves at hospitals with severe neurological symptoms like convulsion or coma will still succumb to the disease despite immediate anti-plasmodial treatment [de Souza et al., 2010]. Therefore, profound research is needed to understand disease development and consequential prevent and treat cerebral malaria.

1.1.1 *Plasmodium* life cycle

The life cycle of all *Plasmodium* species (Fig. 1.1) starts when an infected female *Anopheles* mosquito takes a blood meal and transfers sporozoites from its salivary glands to a vertebrate host. Here, sporozoites enter the blood stream and are transported to the liver where they infect hepatocytes. During exo-erythrocytic schizogony, schizonts containing thousands of merozoites are formed. In this clinically silent phase, the parasite replicates for 6 - 30 days before single merozoites are released to the blood stream and start the erythrocytic cycle. In *P. vivax* and *P. ovale* infections, schizonts can develop into so-called

hypnozoites which remain dormant in the liver for up to several years before they are reactivated and enter the erythrocytic cycle.

In the blood stream, merozoites infect erythrocytes where they develop into trophozoites and start the erythrocytic schizogony. Multiplication of parasites within erythrocytes finally leads to rupture of the cells and another release of merozoites that infect other red blood cells and can either start another asexual replication or mature into gametocytes of both sexes.

Gametocytes are then taken up by a female *Anopheles* during its next blood meal. Sexual reproduction takes place in the mosquito gut when microgametes (male) penetrate macrogametes (female) which leads to the formation of zygotes. In the midgut, the zygote matures into an ookinete and then into an oocyst. In the oocyst, up to thousand sporozoits develop which are released and then migrate into the salivary gland from where they can start another infection cycle with the next blood meal [Centers for Disease Control and Prevention, 2016a].

1.2 Pathogenesis of cerebral malaria

Infection with *Plasmodium* spp. can result in different clinical outcomes depending on the parasite strain and several host factors like genetics or immunization status. In general, clinical manifestations are divided into mild / uncomplicated and severe / complicated malaria. Mild symptoms are the typical fever rhythms accompanied by phases of chill, heat and sweating, headache and nausea. Complicated forms of malaria include severe anemia, acute respiratory distress syndrome, multi organ failure and cerebral malaria. Out of these, cerebral malaria is the most deadly form, which is caused almost solely by infection with *P. falciparum*. Cerebral malaria develops in 1% of *P. falciparum* infection and manifests with severe neurological symptoms like impaired consciousness, convulsion and coma and leads to death within 48h after first symptoms occur, if not treated immediately. However, even if treated at the onset of neuro-specific symptoms, only 80-90% of the patients survive, some of them with life-long neurological limitations [de Souza et al., 2010]. Interestingly, the disease outcome does not only depend on the parasite strain but also host factors, as infection with the same parasite can cause a variety of disease outcomes in humans. Today, many genetic factors are known to influence the disease outcome, but still a huge knowledge gap remains regarding the question why some people develop cerebral malaria or other severe outcomes and others do not. An answer to this

question would help to establish diagnostic predictions on the disease outcome and therefore prevent fatal progression [Centers for Disease Control and Prevention, 2015].

Despite promising research, the mechanisms that lead to cerebral malaria in some *P. falciparum* infections, is still a point of discussion. First observations in deceased patient revealed a massive sequestration of infected erythrocytes in brain microvessels. These findings led to the so-called "sequestration theory" that suggests mechanical blockade of brain microvasculature leading to a critical shortage of oxygen supply in the brain and subsequent neurological deficits, causing death in the end. The "cytokine theory" is another common approach to explain development of cerebral malaria as a result of an overreacting host immune response toward the parasite. Both theories have strong arguments on their side and in the end, a combination of both approaches is very likely [Hunt et al., 2006]. Due to ethical concerns, in-depth research is also relying animal models, which allow more detailed analysis of all organs at different time points after infection. Therefore, we will discuss the need and validity of mouse models before further introduction to the sequestration and cytokine theory, with a focus on immune mechanisms that might be involved in CM development.

1.2.1 Mouse models for malaria

Despite intensive research for several decades, the mechanisms that underlie the development of CM are still unknown. Studies in humans are limited to non- or minimally invasive procedures (e.g. analysis of blood or urine) or postmortem samples due to obvious ethical reasons. Brain tissue from fatal cases of cerebral malaria has provided valuable insights to the development of the disease in past and present studies, but these analyses also have their limitations. Adequate controls from non-fatal cases of *Plasmodium* infection or uninfected patients are difficult to access and analyses of postmortem tissue can reveal misleading information due to physiological changes after death of the patient. These issues limit the parameters that can be investigated in human CM, which emphasizes the need for convenient research models [de Souza et al., 2010].

In the last decades, several animal models have been established for research of *Plasmodium* infections. Next to non-human primate models and rat models, the murine models are by far the most extensively investigated [Craig et al., 2012]. A good number of rodent *Plasmodium* species are available for laboratory research and can be used to mimic differ-

ent aspects of malaria development. Both, parasite and mouse strain influence the disease outcome, which covers experimental forms of self-limiting, non-lethal models, models for severe anemia, severe respiratory distress or cerebral malaria [Langhorne et al., 2002]. Experimental infections are mostly performed by intraperitoneal (i.p.) or intravenous (i.v.) injection of parasitized red blood cells (pRBCs = infected RBCs (iRBC)), but can also be performed by injection of sporozoites, extracted from salivary gland of infected *Anopheles* mosquitoes or naturally by bites of infective mosquitoes.

Experimental cerebral malaria (ECM) is the most common and accepted experimental model for CM. Here, C57Bl/6 or CBA mice are infected (i.p. or i.v.) with RBCs that are parasitized with *P. berghei* ANKA (PbA). This model mimics many features of human CM like rapid and fatal disease development after first neuro-specific symptoms, i.e. convulsion or coma, occur [de Souza et al., 2010]. Both, human and murine CM, are accompanied by sequestration of blood vessels in the brain and cerebral inflammation. Besides numerous similarities, there are also distinct differences. While in human CM the adherence of infected erythrocytes in the cerebral vasculature is a common feature, iRBC accumulation is less prominent in the mouse model. However, when comparing ECM-inducing infection and non-ECM-infections, iRBC accumulation is only seen in mice developing ECM [Baptista et al., 2010]. As a matter of limited samples and appropriate controls, it is unclear whether parasite accumulation in human brains is necessary for CM development [Clark and Cowden, 2003]. Another difference is the characteristic of the cerebral inflammation. The rodent models of CM strongly support the relevance of an intense inflammatory response in ECM, along with leukocyte sequestration in the brain and an opening of the blood-brain barrier. In contrast, leukocyte adherence is less common in human postmortem brain tissues, but hemorrhages and BBB destruction in the brain and signs of endothelial activation are also indicating cerebral inflammation [White et al., 2010]. To overcome differences in human and murine *Plasmodium* infection, current research is conducted to generate humanized mouse models [Vaughan et al., 2013].

In summary, mouse models provide a unique and useful way to investigate mechanisms underlying CM development. We are able to gain valuable insights in the disease development of ECM, that would not be possible in human studies. However, one always has to be careful about how results from murine studies translate to the human disease.

1.2.2 Sequestration theory in cerebral malaria

Finding sequestered iRBCs in cerebral blood vessels of patients that had died from cerebral malaria led to one of the first theories to explain the pathogenesis of the disease [MacPherson et al., 1985]. Survival of the *Plasmodium* parasite in its intermediate host is dependent on its ability to prevent recognition and removal of infected red blood cells (iRBCs). Therefore, the parasite has developed different methods to circumvent detection. Sequestration of *Plasmodium*-infected erythrocytes to blood vessels is one method for the parasite to impede transport to the spleen where abnormal blood cells are usually removed from the blood stream. Other methods are binding of iRBCs to uninfected RBCs (rosetting) or platelets (clumping), which does not only hamper the recognition in the spleen but also hides the infected cells from peripheral immune cells which would not attack the agglutinated healthy cells. While sequestration, rosetting and clumping help the parasite to survive, they harm the host by microvessel occlusion in the brain but also other organs with high blood flow-through like lungs or kidneys.

Sequestration is directly caused by the parasite that induces the formation of knobs on the RBC surface with expression of specific erythrocyte membrane proteins (EMPs). Specifically, *P. falciparum* infection leads to expression of PfEMP-1 (*P. falciparum* EMP) on knobs of infected erythrocytes which mediates their binding to host tissue via receptors and adhesion molecules like CD36 or intracellular adhesion molecule-1 (ICAM-1) [Sherman et al., 2003].

In most CM cases, sequestration of iRBCs in brain microvessels and the severity of the disease correlate positively [MacPherson et al., 1985]. However, later studies have challenged the picture of sequestration being the sole mediator of CM: not all fatal CM cases showed sequestration of iRBCs in their brains [Clark et al., 2003] and the proposed receptors for PfEMP (CD36 and ICAM-1) have been shown to be dispensable on endothelial cells in development of ECM [Sherman et al., 2003, Ramos et al., 2013].

Interestingly, the immunoglobulin (Ig) superfamily member ICAM-1 was shown to be dispensable on endothelial cells, but its expression on leukocytes was needed for ECM development in a mouse model [Ramos et al., 2013]. However, co-localization with iRBCs and upregulated ICAM-1 levels in brains of CM patients suggest that this interaction could at least exaggerate the course of disease [Sherman et al., 2003].

A combination of sequestration of iRBCs and a profound pro-inflammatory immune

response in the brain is most likely the cause of pathology with endothelial activation being a linking factor and both events further augmenting the other [Schofield and Grau, 2005]. For example, *in vitro* stimulation of murine endothelial cells with the pro-inflammatory molecules IFN γ and TNF led to an increased expression of ICAM-1 and the cerebral sequestration of iRBCs and also other immune cells, which initiates a local immune response [Coisne et al., 2006, Schofield and Grau, 2005].

1.2.3 Cytokine theory and immune responses in cerebral malaria

Next to sequestration of parasites and peripheral lymphocytes in brains, inflammatory responses in the periphery and brains of CM patients have come into focus. The pathogenesis of CM is seen as a result caused by an overwhelming immune response that is initiated for parasite elimination but accidentally damages the brain, rather than a direct harm by the parasite [Clark et al., 2004]. The so-called cytokine theory was initiated by Clark et al., due to numerous parallels between malaria and septic conditions i.e. strong similarities of cytokine patterns. They also suggested parasite-induced nitric oxide (NO) in addition to cytokine production as the final cause of cerebral symptoms and death in CM [Clark and Rockett, 1994]. Rising cytokine levels in the blood after infection are often correlated with severity of the disease and clear evidence for inflammation in the brain was found in experimental models of CM [Day et al., 1999, de Kossodo and Grau, 1993]). Finally, a tightly regulated balance of pro-inflammatory and cytotoxic responses and anti-inflammatory immune regulation does likely decides whether or not (E)CM develops.

Among the pro-inflammatory cytokines, **tumor necrosis factor (TNF)** was one of the first mediators associated with fatal outcome during *Plasmodium falciparum* infection [Grau et al., 1987]. TNF levels in serum of human and murine studies, correlated positively with disease severity and were suggested as a diagnostic marker for disease progression [Sahu et al., 2013, de Kossodo and Grau, 1993, Kinra and Dutta, 2013]. *In vivo* depletion of TNF in usually ECM-susceptible mouse strains protected mice from disease development and therefore provided more evidence for the importance of TNF in ECM [Grau et al., 1987].

Interestingly, not only the quantity of TNF is determining the outcome of cerebral malaria, but also the reactivity of endothelial cells to TNF was shown to be a crucial factor. Upon *in vitro* simulation, cultured endothelial cells from brains of ECM-susceptible mice

expressed more ICAM-1 and produced higher amounts of IL-6 compared to cells derived from ECM-resistant mice [Lou et al., 1998]. Similar results were found in cell cultures from patients with or without CM [Wassmer et al., 2010].

Meanwhile, recent results rather favor a role for other members of the TNF family and their receptors such as lymphotoxin- α (LT- α) and LIGHT-lymphotoxin- β receptor than for TNF [Togbe et al., 2008, Randall et al., 2008]. Also, the activity of cytotoxic T cells including their capacity to produce powerful effector molecules such as IFN γ and granzyme B, moved into the focus of ECM with help of the experimental models.

1.2.3.1 Cytotoxic effector immune responses in cerebral malaria

Cytotoxic T lymphocytes (CTLs) are crucial in ECM development, where they accumulate in brains of susceptible mice and contribute to the local tissue damage. Several studies have shown the importance of CD8⁺ T cells by use of RAG deficient mice or by depletion experiments that protected mice from ECM. Protection was still achieved when anti-CD8⁺ antibodies were administered shortly before the onset of neurological symptoms [Rénia et al., 2006, Belnoue et al., 2002].

Upon blood stage PbA infection, cells of the innate immune system engulf parasitized red blood cells and induce an inflammatory response due to the presence of multiple innate triggers (e.g. toll-like receptor ligands). Since infection *Plasmodium* spp. is a systemic incident, the generation of adaptive immune responses takes place in the spleen, involving splenic macrophages that preferably pick erythrocytes in order to recycle the iron as well as dendritic cells, which finally prime the T lymphocytes. The involved processes have been studied extensively during the last years and added valuable knowledge to the understanding of inflammatory immune responses during malaria.

Recognition of specific peptides that are presented on major histocompatibility complex (MHC) class I molecules, which are expressed by all nucleated cells, and additional co-stimulation initiates the activation of CD8⁺ T cells. In *Plasmodium* infection, T cells first encounter parasite antigen in the spleens of infected individuals where they are primed by **cross-presenting dendritic cells (DCs)** [Lundie et al., 2008]. This small subset of DCs, which was formerly characterized by CD8 or Clec9A expression and more recently by expression of XCR1 (CD141 in humans), is able to take up exogenous antigen and pro-

cess it for presentation over MHC class I (= cross-presentation) in order to prime CD8⁺ T cells [Bachem et al., 2012]. As *Plasmodium* parasites infect erythrocytes, which lack a nucleus and consistently do not express any MHC molecules, cross-presentation of antigen by these specialized cross-presenting DCs is the only way to generate a CD8⁺ T cell response against the parasite. Detailed studies showed that indeed, cross-presentation from these DCs is required for CTL priming [Lundie et al., 2008] and consequently, depletion of Clec9A⁺ DCs protected mice from ECM [Piva et al., 2012].

Upon activation, **T cells migrate** toward a chemokine gradient into the brain. Accumulation of CD8⁺ T cells in the brain is commonly seen in mice that develop ECM, but was also found in brains of human CM patients. However research on that matter in human patients is difficult due to limited samples and obvious ethical concerns [Hunt, 2003].

CCL5 (RANTES) binds to chemokine receptors CCR5, but also -1 and -3, on T cells, and is one cytokine that is likely involved in T cell attraction to the brain. It is released by many different cell types including T cells, platelets, endothelial cells and also astrocytes and microglia [Murphy et al., 2008] and might also enhance inflammation by activation of brain resident cells like endothelial cells, microglia and astrocytes [Sarfo et al., 2004].

Studies in post-mortem samples from human CM patients and experimental analysis of mouse models correlated increased expression of CCL5 in the brain with malaria [Sarfo et al., 2004, Sarfo et al., 2005, Miu et al., 2008]. However, while upregulation of CCL5 and its receptors were also found in a non-ECM model, CCR5 deficient mice are not susceptible to ECM, which could further verify the importance of the CCL5 / CCR5 axis in CM [Belnoue et al., 2003a, Sarfo et al., 2005]. Possible triggers of CCL5 release include TNF, which can induce CCL5 secretion and is associated with cerebral malaria [Chen et al., 2011].

The development of ECM in mice is then strongly linked to ability of these activated T cells to produce perforin and granzyme B, as mice deficient for one of these cytotoxic mediators are protected from ECM [Nitcheu et al., 2003, Haque et al., 2011] and ECM-induction by adoptive transfer of CD8⁺ T cells was dependent on granzyme B and perforin from antigen-specific CD8⁺ T cells, but independent from CD8⁺ T cell-derived IFN γ [Haque et al., 2011]. Unfortunately, these findings have not been confirmed in human studies, as limitations in analysis and low numbers of T cells in brains of deceased

patients impede detailed studies. Interestingly, it was shown that the blood-brain barrier (BBB) breakdown is most likely T cell mediated in a perforin-dependent manner by alteration of tight-junction proteins but not through apoptosis [Suidan et al., 2008].

IFN γ is a well-known cytotoxic cytokine, that was associated with (E)CM in murine and human studies [Rudin et al., 1997, Koch et al., 2002]. However, according to more recent findings, IFN γ is more likely an activation marker for CD8⁺ T cells than an effector molecule from these cells [Haque et al., 2011].

More importantly, IFN γ production by **NK cells** and **T_h1 CD4⁺ T cells** was shown to initiate CD8⁺ T cell migration and accumulation in the brains of PbA-infected animals, thereby contributing to ECM [Villegas-Mendez et al., 2012, Hansen et al., 2007, Belnoue et al., 2008]. Both, NK cells and CD4⁺ T cells could also serve a role as cytotoxic effector cells in CM, however, their role in CM, is less studied and an involvement of these cells in ECM is not yet clear [Roetynck et al., 2006, Rénia et al., 2006, Yañez et al., 1996].

After reaching the brain, T cells need a second stimulus to be exert their cytotoxic functions, most likely by cross-presentation from endothelial brain vessel cells [Howland et al., 2013, Howland et al., 2015].

In *Plasmodium* infection, **macrophages** and later also brain residential **microglia**, are associated with initiation of an inflammatory immune response in periphery and then in the brain and therefore with the development of CM [Pais and Chatterjee, 2005]. Macrophages were shown to accumulate in brains of CM patients and, together with microglia, to cause pathophysiological alterations including release of cytokines (e.g. TNF, IL-1 β , IL-6), activation of endothelial tissue, attraction of more immune cells to the brain and local T cell proliferation. These processes promote the blood-brain barrier breakdown and thus the fatal outcome of Plasmodium infection [Deininger et al., 2002, Pais and Chatterjee, 2005].

Inflammatory monocytes and neutrophils are APCs that have been less studied in the context of CM. Neutrophils were long thought to be required for development of cerebral malaria, as depletion with GR-1 antibodies prevented ECM development in mice [Chen et al., 2000]. Based on newer observations, that GR-1 antibodies recognize Ly6C and Ly6G isoforms, these findings were recently challenged by our lab: we found

that only depletion of inflammatory monocytes with CCR2-antibodies, but not specific depletion of neutrophils prevented ECM in C57Bl/6 mice by preventing immune cell accumulation and inflammation in the brain [Schumak et al., 2015]. Furthermore, the ligand of CCR2, **CCL2**, also known as monocyte chemo-attractant protein 1 (MCP-1), is released from various immune cells and also neuronal cells to attract monocytes and macrophages [Murphy et al., 2008, Banisadr et al., 2005]. CCL2 receptor CCR2 was found on CD8a⁺ cell, promoting their migration to the brain of PbA-infected mice, but ECM-susceptibility was similar in WT and CCR2 knock-out mice [Belnoue et al., 2003a], which can be explained by development of compensating mechanisms and chemokine receptor redundancy.

Finally, **interleukin 6 (IL-6)** is considered as a link between innate and adaptive immunity by regulation of T and B cell differentiation [Murphy et al., 2008]. Like CCL5, the release of pro-inflammatory IL-6 can be mediated by TNF, which supports its role in CM development [de Kossodo and Grau, 1993]. Importantly, IL-6 is multi-functional and can also exhibit immune regulatory functions.

1.2.3.2 Immune regulation in malaria

In addition to ECM prevention by inhibition of pro-inflammatory immune responses as discussed above, initiation of a regulatory immune response could also be beneficial for survival after *Plasmodium* infection.

IL-10 is a typical anti-inflammatory cytokine that executes immune regulatory function by shifting T_h1 to T_h2 responses and inhibiting the release of IFN γ and TNF, which are both associated with pro-inflammatory responses and promotion CM after *Plasmodium* infection. The importance of IL-10 in immune regulation after *Plasmodium* infection was elegantly shown in experimental models using ECM-resistant mice depleted from IL-10 that consequently succumbed to ECM. Furthermore, application of recombinant IL-10 protected usually ECM-susceptible mice from disease development [Kossodo et al., 1997]. Interestingly, serum levels of IL-10 are generally higher in patients with severe and cerebral malaria when compared to uncomplicated malaria, but these levels decrease steadily when death approaches [Day et al., 1999].

$CD4^+$ T_{regs} are known to be a major source of IL-10 in the context of immune regulation. They are characterized by secretion of IL-4, -10 and TGF- β as well as expression of CD25 and FoxP3. Murine studies showed that ECM-resistant mouse strains present higher amounts of T_{regs} and IL-10 in their spleens compared to susceptible strains [Wu et al., 2010]. In cases of cerebral malaria, the T_H1 immune response is presumably too strong to be effectively regulated by T_{regs} [Finney et al., 2010]

Data on T_{regs} in human cases of CM are currently not available, but their presence is associated with a higher parasite burden as a result of down-regulated anti-parasitic immune responses after *Plasmodium* infection which correlates with findings in murine studies [Finney et al., 2010].

Next to T_{regs} , also other cells such as **macrophages** and **B cells (B_{regs})** are possible sources of IL-10. Current studies support IL-10 production by regulatory B cells (B_{regs}) as a crucial factor in immune regulation of cerebral malaria [Liu et al., 2013]. Recently, usually susceptible C57Bl/6 mice were protected from ECM by induction of alternatively activated macrophages (AAMs) by administration of pro- T_H2 cytokine IL-33 [Besnard et al., 2015]. These results indicate the existence of several possibilities that might interfere with an inflammatory outcome of PbA-infection.

While immune regulation is beneficial in malaria to prevent CM development, a profound immune response is also needed to clear the parasite from the blood. In a usually non-lethal malaria model, where C57Bl/6 mice were infected with *P. chabaudi* AS, IFN γ knock-out mice showed decreased survival which was linked to increased parasitemia and production of T_H2 cytokine IL-10 [Su and Stevenson, 2000]. However, patients with severe malaria anemia showed lower serum levels of IL-10 than uncomplicated or cerebral malaria patients, which might be explained by increased $CD8^+$ T cell-dependent erythrocyte clearance in the spleen [Kurtzhals et al., 1998, Safeukui et al., 2015]. These findings support a role as a double-edged sword for the role of immune regulation in malaria which needs careful balancing in order to fight the parasite without harming its host.

1.3 Treatment of *Plasmodium* infection

Treatment of *Plasmodium* infection has to start as early as possible to prevent development of a severe course of disease. Especially in suspected cases of cerebral malaria after *P. falciparum* infection, immediate start of treatment is inevitable as this disease form is 100% lethal if not treated. To this day, the gold standard of diagnosis is microscopic examination of blood samples. Additionally, rapid diagnostic tests were developed to provide an easy tool for rural areas where access to microscopes is limited. After diagnosis, the World Health Organization (WHO) recommends oral artemisinin-based combination therapy (ACT) in uncomplicated cases of infections with all *Plasmodium* spp. or chloroquine in non-resistant infections with *P. vivax*, *P. ovale*, *P. malariae* or *P. knowlesi*. In severe cases artesunate (an artemisinin derivative) can be given intravenous or intramuscular till oral treatment is tolerated [WHO, 2015]. Next to these standard treatment regimens, appropriate precautions have to be taken in special risk groups like pregnant women, small infants or HIV-positive people.

All antiplasmodial treatment recommendations are based on the need of rapid parasite clearance. While this is indisputably important, other aspects of disease are not considered. In cases of cerebral malaria lethality is still 5-20% after first neuro-specific symptoms like convulsion are obvious and neurological longterm effects in surviving patients are a huge burden. Targeting and preventing the neuropathology that underlies the disease outcome might therefore be beneficial in all cases of *P. falciparum* infection, especially in cases with manifested neuropathology.

1.3.1 Doxycycline treatment in malaria

Doxycycline (DOX) was originally developed as a broad-spectrum antibiotic from the tetracycline group, which works by binding to the ribosomal 30S unit of bacteria.

Interestingly, doxycycline has also been shown to exhibit antiplasmodial activities *in vitro* and *in vivo* [Budimulja et al., 1997, Batty et al., 2007] by acting on the apicoplast genes in the parasite. However, impaired gene expression only shows effects in the next generation of daughter parasites, which leads to a rather slow action of doxycycline that is noticeable two days after treatment start [Dahl et al., 2006]. In previous WHO recommendations, doxycycline was included as second-line treatment in combination with another fast-acting anti-plasmodium drug and was also given intravenous in severe cases [WHO,

2010]. However, the newest guidelines maintain doxycycline only as follow-up treatment and possible prophylaxis for travelers [WHO, 2015].

Since its discovery in the 1960s, many additional properties of doxycycline and other antibiotics in the tetracycline group have been examined. Drugs in this group have been shown to inhibit matrix metalloproteinases (MMPs) directly via binding Zn^{2+} at the proteases active site [Griffin et al., 2011], to regulate tight junctions [Wang et al., 2011] and also different anti-inflammatory effects have been found: decline of T cell activation (maybe Ca^{2+} -mediated), modulation of mononuclear phagocytes and reduced microglia activation, among others [Kloppenborg et al., 1995, Enose-Akahata et al., 2012, Giuliani and Hader, 2005]. Those additional properties of doxycycline might be beneficial in treatment of cerebral malaria, as the disease outcome is linked to strong neuro-inflammation. While the original tetracycline is discussed to work less anti-inflammatory [Castro et al., 2011], other derivatives like minocycline or tigecycline were shown to have similar properties as doxycycline and are also active against *Plasmodium* parasites [Griffin et al., 2011, Starzengruber et al., 2009, Kast, 2008].

1.4 Aims and objectives

This thesis consists of two different projects, which aim at understanding immunological mechanisms in the development of experimental cerebral malaria and in therapeutic interventions after PbA-infection in mice with Bl/6 background.

First, we analyzed the changes in immune responses of *Batf3*^{-/-} mice, that genetically lack cross-presenting dendritic cells, towards infection with *Plasmodium berghei* ANKA in comparison to wild type mice. *Plasmodium* parasites infect red blood cells, which lack MHC class I molecules and can therefore not directly present antigen to CD8⁺ T cells. This problem is compensated by presentation of antigen by specialized dendritic cells that can digest external antigen and process it for presentation over MHC class I molecules, a well-described mechanism called cross-presentation.

The lack of (cross-presenting) dendritic cells (genetically or by depletion), protects Bl/6 mice from developing ECM [DeWalick et al., 2007, Piva et al., 2012, Zhao et al., 2014]. Initial experiments from our lab confirmed that in contrast to PbA-infected C57Bl/6 WT mice that develop severe cerebral symptoms, *Batf3*^{-/-} mice were completely protected from ECM, despite similar parasitemia in both groups of mice (Fig. 1.2A-C), ruling out that

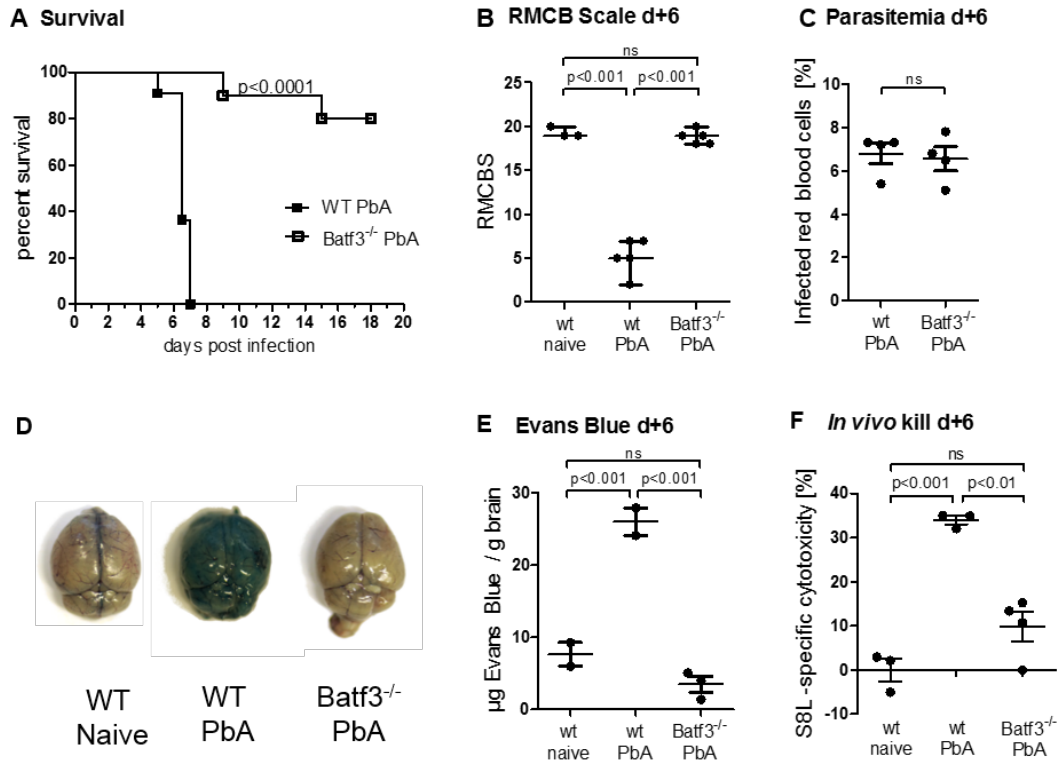


Figure 1.2: **No ECM in PbA-infected *Batf3*^{-/-} mice.** A: Survival of WT Bl/6 mice (filled squares, n = 10) and *Batf3*^{-/-} mice (empty squares, n = 10) after infection with 5e4 iRBC i.v. till 20 dpi. B: Rapid murine coma and behavior scale analysis for WT and *Batf3*^{-/-} mice 6 days after PbA-infection (n = 6). Naive WT mice served as control (n = 5). C: Parasitemia in infected WT and *Batf3*^{-/-} mice 6 dpi (n = 4). D + E: d+6 PbA-infected WT and *Batf3*^{-/-} mice received an i.v. injection of Evans blue. When mice were sacrificed 1h later, brains were photographed (D) and weighed before incubation in formamide for 48h in order to extract the dye that had leaked into the brain. Naive WT mice were used as reference. The amount of dye in mice brains was read in an ELISA reader and quantified with defined standard (E). The amount of Evans blue is calculated per mg of brain weight. E: OVA S8L specific lysis in PbA-infected WT and *Batf3*^{-/-} mice was measured 18h after S8L-labeled target and control cells injection. Cytotoxicity was calculated by comparing the ratio of recovered target cells to control cells in naive mice to experimental mice (n=3-4). Differences in survival were tested for significance with log-rank test. Significance for RMCBS scale and parasitemia was tested with Man-Whitney and t-test and with ANOVA with Tukey correction for Evans Blue analysis and *in vivo* kill. p values below 0.05 were considered significant. (*Unpublished data set from Schumak et al.*)

the protection was due to reduced parasitemia.

Absence of ECM correlated with a stable blood-brain barrier and impaired antigen-specific lytic capacity of splenic T cells in PbA-infected *Batf3*^{-/-} mice on 6 dpi (Fig. 1.2D-F).

Based on these findings from our lab, here we aimed to elucidate alterations of the immune response due to the lack of cross-presenting DCs that might be responsible for the protection of *Batf3*^{-/-} mice.

In this thesis the following questions were addressed:

1. Which differences can be observed in brains of ECM-positive WT mice and ECM-negative *Batf3*^{-/-} mice 6 days after *P. berghei* infection?
2. How does the composition of splenic immune effector cells and their activity differ in *Batf3*^{-/-} and WT mice at the time point of ECM onset in WT mice?
3. Are differences in the immune response between *Batf3*^{-/-} and WT mice already visible at an early time point of infection when infected mice do not yet show any signs of ECM?

In the second part, we studied the effects of doxycycline, an antibiotic that has been described to have anti-plasmodial and also anti-inflammatory properties, regarding the immune response in mice infected with PbA. In previous observations that were part of my diploma thesis, we found that mice treated with doxycycline from 4 dpi did not develop cerebral malaria. However, we also observed a significant drop in parasitemia on 6 dpi which made it difficult to distinguish between direct anti-inflammatory properties and diminished inflammation as a consequence of reduced parasitemia. This thesis aimed to optimize the previous model in regard to this problem and to analyze the immune response in doxycycline treated mice.

1. Can we establish a model where the anti-plasmodial effect of doxycycline is negligible in the analysis of the immune response in treated mice after PbA-infection?
2. How do brains of doxycycline-treated mice differ in regard to infiltrated immune cells and cytokine production?
3. Are anti-inflammatory effects of doxycycline treatment detectable in spleens of doxycycline-treated mice?

Chapter 2

Material and Methods

2.1 Buffers and Materials

2.1.1 Anesthesia - short term

Isofluran (Abbott (Wiesbaden, Germany)) was given for inhalation.

2.1.2 Anesthesia - long term

10µl Rompun 2% (Bayer (Leverkusen, Germany)) + 40µl Ketamin 50mg/ml (Ratiopharm GmbH (Ulm, Germany)) was given intramuscular.

2.1.3 Cell culture medium

RPMI medium (PAA Laboratories (Pasching, Austria)) for cell culture analysis of splenocyte and brain cell suspensions was supplemented with 10% FCS (PAA), 100IU/ml penicillin (PAA), 100µg/ml streptomycin (PAA) and 2mM L-glutamine (PAA).

IMDM medium (PAA) for culturing bone-marrow derived dendritic cells (BMDCs) was supplemented with 10% FCS (fetal calf serum; PAA), 100IU/ml penicillin (PAA), 100µg/ml streptomycin (PAA), 2mM L-glutamine (PAA) and 0.2% (GM-CSF).

Media were stored at 4°C.

2.1.4 CFSE stock

5,6-carboxy-succinimidyl-fluoresceine-ester (CFSE; Invitrogen (Darmstadt, Germany)) was dissolved in DMSO (Merck KGaA (Darmstadt, Germany)) to 5mM and stored at -20°C.

2.1.5 FACS buffer

PBS (PAA) was supplemented with 1% FCS and stored at 4°C.

2.1.6 FarRed stock

CellTrace Far Red DDAO-SE (short FarRed; Invitrogen (Darmstadt, Germany)) was dissolved in DMSO to 1mM and stored in aliquots at -20°C.

2.1.7 MACS buffer

PBS (PAA) was supplemented with 1% FCS and 2mM EDTA (Ethyldiamintetraacetate dehydrate; Roth (Karlsruhe, Germany)) and stored at 4°C.

2.1.8 Machines

autoMACS® Pro Separator	Miltenyi Biotec GmbH (Bergisch Gladbach, Germany)
BD FACS Canto™ I	BD Biosciences (Heidelberg, Germany)
BD FACS Canto™ II	BD Biosciences (Heidelberg, Germany)
BD LSRFortessa™	BD Biosciences (Heidelberg, Germany)
Rotorgene RG-3000, Corbett Research	Qiagen (Hilden, Germany)
Spectra Max 340pc384m, Photometer	Molecular Devices (Sunnyvale, USA)

2.1.9 Analysis software

BD FACS Diva™ flow cytometer	BD Biosciences (Heidelberg, Germany)
FlowJo	TreeStar Software (Ashland, USA)
Prism 5	GraphPad Software (La Jolla, USA)
Rotor-Gene 6.1, Corbett Research	Qiagen (Hilden, Germany)
SoftMax® Pro 3.0 Pro	Molecular Devices (Sunnyvale, USA)

2.2 Methods

2.2.1 Mouse handling

Female C57Bl/6 mice (further referred to as WT mice) were purchased from Janvier (Le Genest Saint Isle, France) or Charles River (Sulzfeld, Germany). *Batf3*^{-/-} mice on C57 Bl/6 background (first described by Hildner et al. (2008)) were kindly provided by I.R. Dunay (Institut für Medizinische Mikrobiologie und Krankenhaushygiene, University Hospital Magdeburg, Germany).

Animals were kept in our in-house animal facility under SPF (specific pathogen free) conditions. Food and water was provided *ad libitum*.

All animal procedures were licensed by local regulatory agencies (Landesamt für Natur, Umwelt und Verbraucherschutz Nordrhein-Westfalen (LANUV NRW) §84–02.04.2012.A264 and §84-02.04.2012.A295). All people working with the mice were holding a FELSA B certificate (Federation of Laboratory Animal Science Associations, category B) or equivalent or were supervised by an appropriate person.

2.2.1.1 Infection of mice with *Plasmodium berghei* ANKA

C57 Bl/6 mice were infected with *Plasmodium berghei* ANKA (PbA) parasites. We used two different PbA strains: the wild type *Plasmodium berghei* ANKA and a transgenic PbA variant which is modified to express the model antigen ovalbumin (OVA) (kindly provided by Ann-Kristin Müller (Heidelberg, Germany)). Both strains were compared and no difference in the disease outcome was observed. For simplification, "PbA" is used throughout the document for both strains.

Infection with infected erythrocytes from stock mice Parasite stocks were prepared from blood of sporozoite infected mice and stored, mixed with glycerin, in liquid nitrogen. In order to obtain a uniformly infectious dose *in vivo*, 200-250µl of the parasite stock was injected intraperitoneally (i.p.) into stock mice. After 4-5 days, parasitemia was determined and the blood of these mice was diluted in PBS to reach the final injection concentration. Experimental mice were infected with either 5e4 or 1e6 (as stated in the text) infected red blood cells (iRBCs) in 200µl PBS intravenously (i.v.)

Infection with sporozoites isolated from infected mosquitoes Stock mice were prepared as described above. On day 5 p.i., blood of these mice was stained with

Giemsa and checked for the presence of gametocytes. Gametocyte-positive mice were anesthetized with Rompun / Ketanest before they were shaved and placed on a net over adult mosquitoes. Taken up gametocytes reproduced sexually in the mosquitoes and developed into sporozoites within 17 days. After this time mosquitoes were dissected and salivary glands were extracted and crushed in PBS. Sporozoites were counted in a Neubauer chamber and adjusted to a concentration of 5000 sporozoites / ml. 1000 sporozoites in 200 μ l PBS were injected i.v. into experimental animals.

Parasitemia was determined in all ex vivo experiments on the day of analysis to confirm successful infection. In survival experiments blood smears were analyzed from 4-8 days post infection (dpi).

2.2.1.2 Experimental cerebral malaria score and rapid murine coma and behavior scale for ECM surveillance

In our experimental conditions, WT mice usually started to display first signs of disease from 6 dpi on. Therefore, mice were monitored from 5 dpi for symptoms of disease.

For this thesis, two different scoring schemes were used due to changing regulations in between, ordered by the local regulatory agencies for animal health. The first scoring system is a disease score (higher scores indicate sick mice) and was adapted from Amante et al. [Amante et al., 2007]:

- 0 no symptoms
- 1 ruffled fur, hunching, wobbly gait or swollen eyes
- 2 two or more symptoms from 1 but agile moving
- 3 at least one symptom from 1 and reduced willingness to move
- 4 limb paralysis, rarely moving without exogenous stimuli
- 5 no controlled reaction to exogenous stimuli (e.g. convulsion after touching), virtually no voluntary movement
- 6 coma (no reaction to exogenous stimuli)

In addition, convulsions, heavy weight loss or other abnormal behavior was noted. In this scoring system a score of 4 or above is considered to be neuro specific.

The other scoring system is a health score (higher scores indicate healthy mice) named "*Rapid Murine Coma and Behavior Scale*" (RMCBS) for quantitative assessment of murine cerebral malaria developed by Carroll et al. [Carroll et al., 2010]. The scoring is

based on 10 different parameters (gait, balance, motor performance, body position, limb strength, touch escape, pinna reflex, toe pinch, aggression, grooming), which are evaluated with 0 to 2 points, with the latter being the optimal score of a healthy mouse. This system gives a score between 0 (dead / coma) to 20 (completely healthy). Naive (uninfected) mice usually reach a score between 18 and 20 points according to this system; mice under 10 are notably ill and mice with a score below 5 are severely ill.

Due to ethical reasons and in agreement with our license for animal testing mice were killed when they reached a point of severe illness which was defined by either reaching a score of 5 or higher in the ECM score or a score of 5 or below in the RMCBS. Mice with a weight loss of more than 20% were also put down.

2.2.1.3 Determination of parasitemia

Parasitemia of *Plasmodium* infected mice was determined by Giemsa staining of thin blood smears. Blood for analysis was collected from the tail vein and fixed with 100% methanol on glass slides. After drying blood smears were stained in Giemsa solution (1:20 solution adjusted to pH 7.2; Giemsa's azur-eosin-methylene blue, Merck KGaA (Darmstadt, Germany)) for approximately 15 minutes. A minimum of 800 red blood cells was counted and infected and uninfected red blood cells were differentiated to calculate the percent parasitemia ($= (\text{iRBC} / \text{all red blood cells}) * 100$).

2.2.1.4 Administration of doxycycline

Doxycycline (DOX, Merck KGaA (Darmstadt, Germany)) was solved in PBS and injected i.v. in a volume of 200 μ l into the tail veins. If not stated otherwise mice received 80mg/kg bodyweight once daily from 4-6 dpi. Mice that were analyzed on 6 dpi did not receive treatment on that day. The standard concentration of 80mg/kg/d was chosen according to Prall et al. [Prall et al., 2002] who compared plasma level of doxycycline in mice and human after oral administration and found that 200mg/d doxycycline in human resembles 50-100mg/kg/d given to mice in drinking water. 200mg/d is also the standard dose in malaria treatment [Lalloo et al., 2007].

2.2.1.5 Administration of BrdU and proliferation analysis

Bromodeoxyuridine (BrdU; BrdU Flow Kit, BD Biosciences (Heidelberg, Germany)) is integrated in newly synthesized DNA instead of thymidine and therefore allows detection of proliferating cells by subsequent intracellular FACS staining of BrdU in mouse organs. To obtain optimal results we chose to administer PBS-solved BrdU to living mice once 2 days before analysis intraperitoneal (2.4 mg/mouse) and 1.5 and 0.5 days before analysis per oral route (1.5 mg/mouse). The given amount was based on the provided protocol from BD Biosciences (Heidelberg, Germany). On the day of analysis, the spleen was removed from BrdU treated mice and single cell suspensions were stained for BrdU detection according to the manufacturers protocol. Shortly, cells were first stained for surface antibodies to distinguish between different cell populations. Cells were fixed and permeabilized with the help of the provided buffers. Cells were then intracellularly stained for BrdU and acquired on a flow cytometer.

2.2.1.6 Preparation of organs and plasma for analysis

Animals were anesthetized with long term anesthesia (Rompun + Ketamin) before procedures. In order to eliminate cells from blood vessels within the organs, mice were perfused with PBS for 5 min prior to organ removal, but after blood was collected. Organs were prepared according to their further usage.

Preparation of organs for mRNA extraction Organs used for mRNA extraction were immediately snap frozen in liquid nitrogen and stored at -80°C until further use.

Preparation of blood for serum and FACS analysis

Serum Blood was directly drawn from the heart of anesthetized mice and collected in uncoated tubes. The blood was left at RT till clots formed and centrifuged at 8,000 rpm for 10 min the next day. Serum was transferred to new tubes and directly used for analysis or stored at -20°C .

FACS analysis Blood was drawn from anesthetized mice from the orbital vein prior to perfusion and collected in EDTA coated collection tubes. In order to analyze the immune cell subsets in the blood stream, blood was enriched for lymphocytes via ficoll

gradient (Pancoll, Pan-Biotech (Aidenbach, Germany)) before staining with FACS antibodies.

Preparation of brain for cell culture and FACS analysis Brains were cut into small pieces and incubated in 0.05% collagenase A (Sigma-Aldrich (Munich, Germany)) for 30 min at 37°C on a shaker. Following this digestion, 10ml MACS buffer was added to the brains in collagenase and the tissue was homogenized by a fine metal sieve. A small section of the homogenate was kept on ice for primary cell culture, the rest was centrifuged (1500rpm, 7min). The resulting pellet was taken up in 30% percoll (Sigma-Aldrich (Munich, Germany)) and carefully underlayered with 70% percoll. Centrifugation with 2000rpm for 20min at room temperature without brake led to an interphase between the two percoll concentrations. This interphase, consisting of mainly lymphocytes and microglia, was removed and washed with MACS buffer before further proceedings.

Preparation of liver for FACS analysis Liver was carefully cropped into small pieces and incubated in 0.05% collagenase A (Sigma-Aldrich (Munich, Germany)) for 30 min at 37°C on a shaker. Following this digestion, 10ml MACS buffer was added and the tissue was homogenized by a fine metal sieve. The homogenate was centrifuged (1500rpm, 7min) and the resulting pellet was taken up in 40% percoll and carefully underlayered with 80% percoll. Centrifugation with 2000rpm for 20min at room temperature without brake led to an interphase between the two percoll concentrations. This interphase of lymphocytes, was removed and washed with MACS buffer before further proceedings.

Preparation of spleen for cell culture and FACS analysis After removal spleens were perfused with 0.05% collagenase A, cut into small pieces and were then incubated in 2-3ml collagenase solution at 37°C for 20 min on a shaker. After incubation approximately 10ml MACS buffer were added and a single cell suspension was generated by pushing the spleen pieces through a fine metal sieve. Cells were washed with MACS buffer and taken up in RPMI medium.

2.2.2 Cell culture preparation for cytokine analysis

Cell homogenates from spleen or brain were taken in a defined volume of RPMI cell culture medium (PAA Laboratories (Pasching, Austria)) and cell concentration was determined by counting cells with CASY® TT Cell Counter (Schärfe Systems (Reutlingen, Germany)).

After counting cells were adjusted to $1e6$ cells/ml (spleen) and $1.25e6$ cells/ml (brain), respectively. $100\mu\text{l}$ of adjusted cells were plated in 96-well-plates (U-bottom, Greiner Bio-One GmbH (Frickenhausen, Germany)) and incubated over night at 37°C / $5\%\text{CO}_2$. To test antigen specific immune responses, some cells were incubated with additional $1\mu\text{M}$ OVA S8L peptide. Supernatans from cell culture were collected the next day and either processed directly or frozen at -20°C .

2.2.3 Cell culture preparation for generation of bone-marrow derived dendritic cells

Bone-marrow derived dendritic cells (BMDCs) were prepared by carefully flushing leg bones of C57Bl/6 donor mice with PBS with the help of a small syringe. Cells were then cultured in IMDM medium supplemented with GM-CSF in a petri dish for at least 6 days before usage at 37°C / $\% \text{CO}_2$. Cells were splitted and medium was renewed once within this time.

Cells were removed from petri dishes by incubation with 3ml 2mM EDTA for 4 minutes. Remaining cells were carefully removed with the help of a cell scraper. All cells were collected together, centrifuged and taken up in IMDM before further usage.

2.2.4 Cross-presentation assay for brain microvessels

The cross-presentation assay was kindly performed by Shanshan Wu Howland in the lab of Laurent Rénia according to their publication [Howland et al., 2013].

In short: microvessel fragments were isolated from experimental mice by mincing, homogenization and followed by fractioning by 15% dextran gradient centrifugation. Pelleted Microvessels were retained on a $40\mu\text{m}$ cell strainer and digested with collagenase and DNaseI for 90 min. Microvessels were plated on to a filter plate and incubated with NFAT-lacZ reporter cells (LR-BSL8.4 cells) that were transduced with a T cell receptor (TCR) recognizing the S QLLNAKYL epitope. After 6h co-culture, interaction was analyzed by β -galactosidase staining and blue spots were imaged and counted in an ImmunoSpot Analyser.

2.2.5 Enzyme-linked immunosorbent assay (ELISA)

Sandwich ELISA were used to determine cytokine level in cell culture supernatants and plasma. ELISA were purchased from eBioscience (Frankfurt am Main, Germany), R&D

Systems (Minneapolis, USA) and BD Biosciences (Heidelberg, Germany) and performed according to the manufacturers' protocols.

Shortly: An unlabeled capture antibody (1st antibody) was incubated over night in a high-binding 96-well-plate. After this incubation the plate was blocked for at least two hours and samples and a defined standard for quantification was applied subsequently for another over night incubation. On the next day the plate a biotinylated detection antibody (2nd antibody) was added for 2 hours, followed by an incubation for 30 min with an enzyme-linked secondary antibody that binds to the detection antibody. In the next step tetramethylbenzidine (TMB) was used as a substrate and is converted to a colorimetric signal by the antibody bound enzyme. The reaction was stopped by adding H₂SO₄ (Merck KGaA (Darmstadt, Germany)) and the optical density (OD) was measured with a photometer at 450nm wavelength. The protein amount was calculated with the help of a standard curve. Appropriate washing was done between the different steps.

Used antibodies and kits

Cytokine	Company	Kit
CCL5	R&D	DuoSet
CCL2	R&D	DuoSet
granzyme B	R&D	DuoSet
IFN γ	eBioscience	Ready-Set-Go!
IL-6	eBioscience	Ready-Set-Go!
IL-10	BD Biosciences (Heidelberg, Germany)	
TNF	R&D	DuoSet
ICAM-1	R&D	DuoSet

Buffers not included in kits

buffer	composition	for ELISA
Coating buffer	PBS 0.1 M Na ₂ HPO ₄ (Merck)	all DuoSets, IL-10
Working solution	PBS + 1% BSA (PAA)	all DuoSets, IL-10
Enzyme solution	Streptavidin-POD conjugate (Roche (Mannheim, Germany))	all DuoSets, IL-10
Substrat	0.1M Na ₂ HPO ₄ *H ₂ O (pH 5.5) + 2% TMB solution (60mg 3,3',5,5'tetramethylbenzidine Roth (Karlsruhe, Germany) in 10ml DMSO) + 0.02% H ₂ O ₂	all DuoSets, IL-10
Stop solution	2M H ₂ SO ₄	all ELISA
Washing buffer	0.05% Tween20 (Sigma-Aldrich) in PBS (pH 7.2)	all ELISA

2.2.6 Evans blue assay

To determine the integrity of the blood-brain barrier (BBB) we performed an Evans blue assay. The Evans blue dye (Sigma-Aldrich (Munich, Germany)) binds to serum albumin and is only able to cross the BBB when it is already damaged. The BBB destruction can be directly observed by the color of the brain and can be further quantified by extraction of the dye with formamide (Sigma-Aldrich).

For the assay 200µl of 2% Evans blue in 0.95% NaCl (natrium chloride; AppliChem GmbH (Darmstadt, Germany)) was injected i.v. into mice. The dye was left circulating with the blood in the animals for one hour before they were sacrificed and their brains removed. Brains were photographed for documentation of visual assessment, weighed and then transferred to 2ml formamide. Brains were incubated for 48h at 37°C on a shaker. In this time the dye that had extravasated to the brain was extracted and the amount of dye in the formamide solution could be quantified with a defined standard by reading in a photometer at 620nm. Results were calculated as mg / g brain.

2.2.7 Flow cytometric analysis

Flow cytometry (also fluorescence-activated cell sorting (FACS)) was used to define the different cell populations in blood, brain, liver and spleen of experimental animal and the activation status of these cells.

For surface staining fluorescent labeled antibodies were diluted in FACS buffer and incubated with single cell suspensions from the different organs for 20 minutes on ice. Cells were washed with MACS buffer twice after staining and filtered before acquisition on a LSRFortessa™ flow cytometer (BD Biosciences (Heidelberg, Germany)).

Intracellular (IC) staining was done using the "Foxp3 / Transcription Factor Staining Buffer Set" from eBioscience (Frankfurt am Main, Germany) according to the described procedure for surface staining. Subsequently, the cells were permeabilized and fixed by incubation in fixation/permeabilization reagent (1 part fixation/permeabilization concentrate + 3 parts fixation/permeabilization diluent) for 30 minutes at 4°C followed by washing with permeabilization buffer and 1 hour incubation of the desired antibody diluted in permeabilization buffer. The cells were washed again and filtered before analysis on a LSRFortessa™ flow cytometer (BD Biosciences (Heidelberg, Germany)).

Anti-mouse antibodies were purchased from Biolegend (Fell, Germany), eBioscience (Frankfurt am Main, Germany) or Invitrogen (Darmstadt, Germany). Importantly, the antibody for granzyme B was originally developed as anti-human granzyme B, but worked likewise in mice (clone GB11, Invitrogen).

2.2.8 *In vivo* cytotoxicity assay

The specificity of CD8⁺ T cells can be determined with an *in vivo* cytotoxicity assay (adapted from [Coles et al., 2002]). After infection of mice with an OVA-expressing *Plasmodium berghei* strain, T cells are primed for endogenous parasite peptides as well as the OVA peptide. Spleen cells from syngenic naive mice are loaded *ex vivo* with fluorescently labeled MHC class I peptides from OVA (= target cells) and subsequently transferred into a mouse 5 days after infection. Labeling the spleen cells with a CFSE allows detection and quantification of remaining cells in the recipient mouse the next day.

For the generation of target cells, splenocytes from donor mice were splitted into two fraction which were either incubated with 1 μM S8L (MHC I OVA peptide) or without peptide (control) for 20 min at 37°C, following an incubation with the fluorescent dyes for 25 min at 37°C. To distinguish between loaded and unloaded cells, the pep-

target loaded cells were incubated with a high dose of CFSE (1 μ M) while the unloaded cells were labeled with a low dose CFSE (0.1 μ M). Both subsets could be recognized as independent populations with flow cytometry. All mice received 5×10^6 cells of each type intravenously on 5 dpi. Spleens of recipient mice were extracted the next day (18h incubation) and the amount of remaining CFSE-positive cells counted with FACS. The presence of OVA specific T cells can be calculated from the elimination of labeled target cells, as depicted in Fig. 2.1. The specific *in vivo* cytotoxicity is determined by comparing the infected (immunized) animals with uninfected (naive) ones with the following formula:

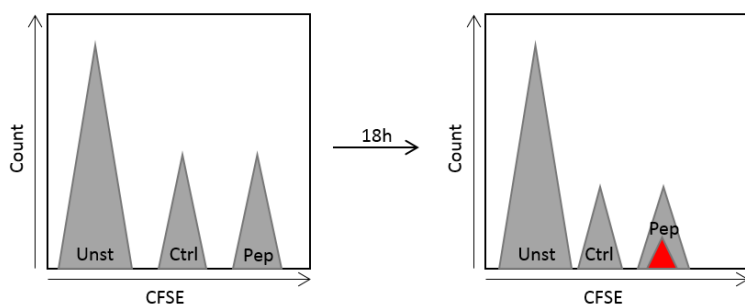
$$\text{specific cytotoxicity [\%]} = 100 \cdot \frac{\text{ratio exp group}}{\text{ratio ctrl group}} * 100$$


Figure 2.1: **Principle of the *in vivo* kill.** The left graphic shows the cell populations before injection, the right one after 18h incubation. Unst = unstained and unlabeled cells from recipient mouse, Ctrl = fluorescently stained cells (0.1 μ M CFSE) not labeled with peptide as reference for unspecific killing, Pep = fluorescently stained cells (1 μ M CFSE) labeled with a MHC I peptid. After injection of the amount of peptide-labeled and unlabeled cells, both populations shrink likewise unspecifically in uninfected mice ("Ctrl" and "Pep" in right graph), while peptide-labeled target cells are specifically killed in PbA-infected mice, which leads to a comparably smaller target cell population (depicted by red triangle).

2.2.9 Magnetic-activated cell sorting (MACS)

To analyze specific cell populations, cells were separated using the autoMACS from Miltenyi Biotec GmbH (Bergisch Gladbach, Germany). Cells were taken in 300 μ l MACS buffer and incubated with cell population specific MACS beads (magnetic beads attached to antibodies; Miltenyi Biotec GmbH (Bergisch Gladbach, Germany)) for 15 minutes at 4°C. Afterwards cells were washed twice and filtered before proceeding with the actual separation step in the autoMACS. Here, cells were separated into beads-bound cells and those that were not bound, allowing either positive or negative selection. After separation, cells were counted and adjusted to the desired concentration.

2.2.10 Natural killer (T) cell assay

Cytokine production by NK and NKT cells was determined in supernatant of NK and NKT cell culture, MACS-sorted by DX5 (present on both subsets). Purified cells were incubated with recombinant IL-2 (final concentration 1e3 units per ml; Biolegend) alone or on previously prepared BMDCs in a final volume of 200 μ l. Additional wells without IL-2 served as negative controls. Supernatant was analyzed for cytokines after 24h incubation at 37°C / 5% CO₂.

2.2.11 Phagocytosis assay

Phagocytic capacity of MACS-purified CD11b⁺ splenocytes and lymphocyte / microglia enriched brain cells (percoll gradient after perfusion) was analyzed *ex vivo* with the help of plasma opsonized beads.

Fluorescently labeled beads (Sigma-Aldrich) were first opsonized with plasma from experimental mice at 37 °C for 30 min to optimize uptake by cells. Thereafter, the bead solution was diluted 1:10 with PBS and 50 μ l of the beads were added to 0.5e5 cells in a volume of 250 μ l. Beads and cells were incubated 1h at 37°C / 5% CO₂ to allow uptake of beads by phagocytosing cells. The reaction was stopped by adding 2 ml ice-cold PBS / 1% BSA and spinning of cells at 1500 rpm for 7 min, 4°C. This step was repeated twice. The cells were then stained for surface markers to differentiate between cell subsets. Flow cytometry analysis revealed which cells had taken up the fluorescently labeled beads.

Table 2.1: Combination of serum opsonized beads and cells

Cells*:	Plasma**:	WT Naive	WT PbA	<i>Batf3</i> ^{-/-} Naive	<i>Batf3</i> ^{-/-} PbA
CD11b ⁺ WT Naive		X	X	X	X
CD11b ⁺ WT PbA		X	X	X	X
CD11b ⁺ <i>Batf3</i> ^{-/-} Naive		X	X	X	X
CD11b ⁺ <i>Batf3</i> ^{-/-} PbA		X	X	X	X
Brain WT Naive		X			
Brain WT PbA			X		
Brain <i>Batf3</i> ^{-/-} Naive				X	
Brain <i>Batf3</i> ^{-/-} PbA					X

*Source of potential phagocytosing cells; single approaches for all animals per group

** Source of plasma for bead opsonation; pooled plasma from all animals in one group

2.2.12 Quantitative real-time polymerase chain reaction (PCR)

Isolation of mRNA

Isolation of mRNA from cryo tissue was performed with a single step method with TRIzol® (Invitrogen) and 1-bromo-3-chloropropane (BCP; Sigma-Aldrich). TRIzol® contains guanidinium thiocyanate to lyse the cells and inactivate enzymes, especially RNase. Adding BCP leads to three phases: a lower phase containing proteins, an intermediate phase with DNA and an upper, aqueous phase which contains the desired RNA. The RNA was then precipitated with isopropyl alcohol (Merck) and ethanol (Merck). The precipitate was centrifuged and the formed pellet dried and subsequently dissolved in RNase free water. DNA digestion (reagents from Ambion® (Invitrogen)) was performed before reverse transcription (Qiagen OmniScript® RT Kit 200, OligoDT and RNase inhibitor from Invitrogen). The samples were 1:10 diluted and stored in aliquots at -20°C.

qRT-PCR procedure

Analysis of mRNA expression in brain tissue of mice was done by quantitative real-time PCR. With the help of a standard curve (1:10 dilution) from samples with known concentration of DNA, the amount of copies per μ l can be determined. To avoid variations of concentration due to extraction and purification of the mRNA, a so called house-keeping gene is measured first. A house-keeping gene is constitutively expressed and can be used for normalization (i.e. copies gene X per copies of housekeeping gene). Our house-keeping gene was β -actin.

Primer

Primers were purchased from Invitrogen (Darmstadt, Germany)

β -actin forward	5' AGA GGG AAA TCG TGC GTG AC 3'
β -actin reverse	5' CAA TAG TGA TGA CCT GGC GGT 3'
granzyme b forward	5' CTG CTC TGA TTA CCC ATC GTC 3'
granzyme b reverse	5' GTG AAT GGA CAT GAA GCC AGT 3'
PbA 18S rRNA forward	5' CTA ACA TGG CTT TGA CGG GTA 3'
PbA 18S rRNA reverse	5' CTG CTG CCT TCC TTA GAT GTG 3'

qRT-PCR master mix

A master mix was prepared containing the following substances in optimized concentrations. The volumes are given for one reaction. To a total volume of 18 μl in each reaction tube, 2 μl of cDNA were added. All samples were measured in triplicates.

	β -actin	grzmB	PbA	
H ₂ O	10.8 μl	14 μl	10.4 μl	
10x buffer	2.0 μl	2.0 μl	2.0 μl	Qiagen
MgCl ₂ (25 mM)	2.4 μl	0.4 μl	1.2 μl	Qiagen
dNTPs (40 mM)	0.1 μl	0.1 μl	0.1 μl	Fermentas, St. Leon-Roth, Germany
primer forward (5 μM)	1.2 μl	0.6 μl	2 μl	Invitrogen
primer reverse (5 μM)	1.2 μl	0.6 μl	2 μl	Invitrogen
SYBR Green (1:100)	0.2 μl	0.2 μl	0.2 μl	Invitrogen
HSTaq (250 U)	0.1 μl	0.1 μl	0.1 μl	Qiagen
total volume	18 μl	18 μl	18 μl	

Cycling

All samples were run in a Rotor-Gene 3000 (Corbett Research, Qiagen (Hilden, Germany)) using the following protocol:

	β -actin	grzmB	PbA
Hold	95°C / 15 min	95°C / 15 min	95°C / 15 min
45x cycle	94°C / 15 sec	94°C / 30 sec	95°C / 15 sec
	58°C / 20 sec	58°C / 30 sec	53°C / 20 sec
	72°C / 20 sec	72°C / 30 sec	72°C / 20 sec
Melt	59-95°C / 0.8°C steps	72-99°C / 1°C steps	52-95°C / 0.8°C steps
	1 st 10 sec	1 st 10 sec	1 st 10 sec
	all other 2 sec	all other 2 sec	all other 2 sec

2.2.13 Transmigration assay

We designed a transmigration assay using transwell plates (polycarbonate membrane, VWR Lab Shop (Batavia, USA)) to assess the *ex vivo* migration of spleen cells towards a

brain cell generated cytokine gradient. Therefore, whole brain homogenate (1,25e6 cells / well) was cultured in the bottom of a transwell plate together with FarRed labeled splenocytes (1e6 cells / well, 1 μ M FarRed, 20 min incubation at 37°C) in the upper well (depicted in Fig. 2.2). The pores of the upper chamber were 5 μ m to allow mainly active migration of lymphocytes to the chemotactic attractants produced by the brain cells in contrast to unidirectional floating of cells through the pores. Cells were incubated together for 6h at 37°C. After this incubation time the plate was placed in 4°C for 20 min to remove leukocytes sticking to the underparts of the upper chamber. The upper chamber was removed carefully and cells in the lower well were collected. The amount of FarRed labeled cells was calculated among the total amount of measured cells (same number for all samples). Additional FACS surface staining after migration allowed to distinguish between different cell subsets.



Figure 2.2: **Principle of the migration assay.** Brain and spleen cells were removed from experimental animals and cultured for 6h in a transwell plate as with brain cells in the lower and fluorescently (FarRed) labeled spleen cells in the upper chamber. After incubation cells were analyzed by flow cytometry.

2.2.14 Statistical analysis

Most statistical analysis was done using GraphPad Prism software. P-values below 0.05 were considered significant. Survival curves were analyzed with the Log-rank test. Data up to 20 dpi were taken into calculation. ECM scores are displayed as median values and significance was tested with Kruskal-Wallis with Bunn's post-test (>2 groups) or Mann Whitney test (2 groups). If not stated otherwise, all other graphs represent mean values (\pm SD or SEM, as indicated). Differences between groups (>2) were evaluated with ANOVA followed by Tukey post-test, groups with 2 animals were tested with t test. Analysis of the PCR array was done with R version 3.1.0. using the Mann-Whitney test (non-parametric without assumptions on the distribution of Ct values). Adjustment for multiple testing was performed by Benjamini-Hochberg.

Chapter 3

Results

3.1 *Batf3*^{-/-} mice were protected from experimental cerebral malaria after PbA-infection

Batf3^{-/-} mice genetically lack the transcription factor *Batf3* which is required in the development of XCR1⁺ dendritic cells (DCs), a DC subpopulation, which is known to be the major cell type for cross-presentation of antigen via MHC class I to CD8⁺ T cells. During their blood stage phase, *Plasmodium* parasites infect vertebrate erythrocytes, which do not express any MHC molecules on their own. Cross-presentation is therefore indispensable to prime CD8⁺ T cells for a fully functional T_h1 immune response to the parasite. The development of cerebral malaria is well associated with a strong T_h1 response of CD8⁺ T cells. In this study we were interested how ECM development is altered in *Batf3*^{-/-} mice, since the crucial cell population responsible for priming of CD8⁺ T cells via cross-presentation is lacking in these mice. We confirmed the *Batf3* knock-out by flow cytometry analysis on spleen cells (Fig. S1). In initial experiments our lab could demonstrate that PbA-infected *Batf3*^{-/-} mice are completely protected from ECM, as shown by survival and a stable blood-brain barrier in these mice (Schumak et al., (unpublished), summarized in Fig. 1.2A-E).

3.1.1 *Batf3*^{-/-} mice did not develop ECM upon PbA-infection with ex- tracted sporozoites

Infection of mice with infected red blood cells (iRBCs) is a common technique for using experimental mouse models for malaria, but only focuses on the blood stage aspects of the disease. We wanted to confirm that the disease outcome was comparable to a more natural infection, that also includes the liver stages of the parasite's life cycle. To address this point, mice were infected intravenously with 1,000 sporozoites, which were extracted from salivary glands of mosquitoes that had ingested PbA gametocytes 17 days earlier. Mice were observed for survival, disease outcome and parasitemia. ECM development was monitored according to the rapid murine coma and behavior scale (RMCBS, [Carroll et al., 2010]), a fitness score composed of 10 parameters with a maximum score of 2 points each.

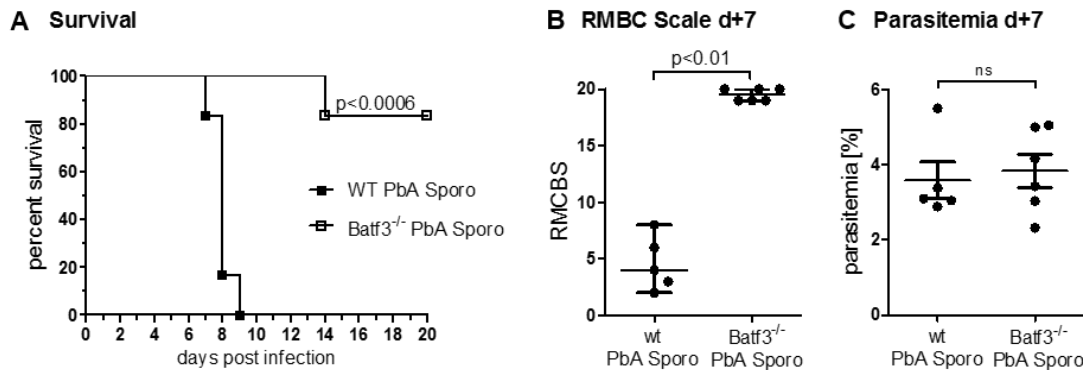


Figure 3.1: *Batf3*^{-/-} mice did not develop ECM after infection with PbA sporozoites. A: Survival of WT (filled squares, n=6) and *Batf3*^{-/-} mice (empty squares, n =6) after inoculation with 1,000 sporozoites from 17 dpi infected mosquitoes is shown. B and C: RMCBS and parasitemia, are shown for 7 dpi. Differences in survival were tested for significance with log-rank test. Significance for RMCBS scale and parasitemia was tested with Man-Whitney and t-test. p values below 0.05 were considered significant.

After sporozoite infection, WT mice developed cerebral symptoms and died after 7 dpi, while *Batf3*^{-/-} mice survived the infection without any signs of disease (Fig. 3.1). In comparison to blood-stage infection (Fig. 1.2A, B), disease development and ECM phase was delayed for 1-2 days in WT mice. This observation could be explained with the different stages of parasites that were injected: sporozoites have to develop in the liver before reentering the blood stream, while parasites in RBCs can directly start blood cycle divisions. ECM onset was observed in WT mice on dpi 7 (B: RMCBS of 4-7 dpi) while PbA-infected *Batf3*^{-/-} mice were still healthy at that time point (RMCBS of 19.5 7 dpi). Similar to

iRBC-infected *Batf3*^{-/-} mice, sporozoite-infected knock-out mice did also not develop specific neurological symptoms later in infection (Fig. S2). Importantly, parasitemia did not differ between WT and *Batf3*^{-/-} mice on 7 dpi, when WT mice developed severe ECM symptoms (3.6% vs. 3.8%; Fig. 3.1C).

Thus, *Batf3*^{-/-} mice did not develop ECM after PbA-infection, neither with iRBCs nor sporozoites. As disease development in WT mice was also comparable, we performed blood-stage infection for all following experiments.

3.1.2 Brains of PbA-infected *Batf3*^{-/-} mice did not show signs of cellular infiltration and inflammation

It is widely accepted that cerebral malaria is a combination of sequestration of blood cells in the microvessels within the brain and local inflammation, caused by an overreaction of the host's immune system [Hunt et al., 2006]. Therefore, it is inevitable to have a closer look at the brains of PbA-infected *Batf3*^{-/-} mice to analyze ongoing immune responses and compare them to infected WT mice and naive mice.

3.1.2.1 Immune cell infiltration to the brain was reduced in PbA-infected *Batf3*^{-/-} mice

Cells of hematopoietic origin can be distinguished from other cells by their high expression of the cell surface marker CD45. Especially in the brain this marker is extremely helpful to differentiate between CD45^{hi} cells, identifying as infiltrated immune cells and CD45^{lo} cells, which are mostly brain resident microglia and still present after percoll gradient purification of a brain homogenate.

To get a first idea of possibly infiltrated cells in the brain of *Batf3*^{-/-} mice vs. WT mice after infection with *Plasmodium berghei* ANKA, we did a FACS analysis of immune cells that were isolated from the brain 6 days after infection and compared them to naive control animals. Therefore we anesthetized the experimental animals and perfused them intracardially with PBS to remove the majority of the cells that were present in the vessels due to blood circulation. Brains were taken out, cut into small pieces and digested in collagenase for 30 min at 37°C before homogenization through a metal sieve. The brain homogenate was then applied to a percoll gradient in order to enrich leukocytes and remove brain parenchyma. The forming layer of mainly leukocytes and microglia was then stained with FACS antibodies for surface markers to distinguish between different cell

subtypes. For analysis of the cells that infiltrated the brain, we first gated purified cells for expression of CD45 and CD11b to discriminate between leukocytes from the periphery ($CD45^{hi}$), brain-resident microglia ($CD45^{lo}CD11b^{+}$) and other brain cells that were not excluded by the gradient ($CD45^{-}CD11b^{-}$). The latter were not included in our analysis.

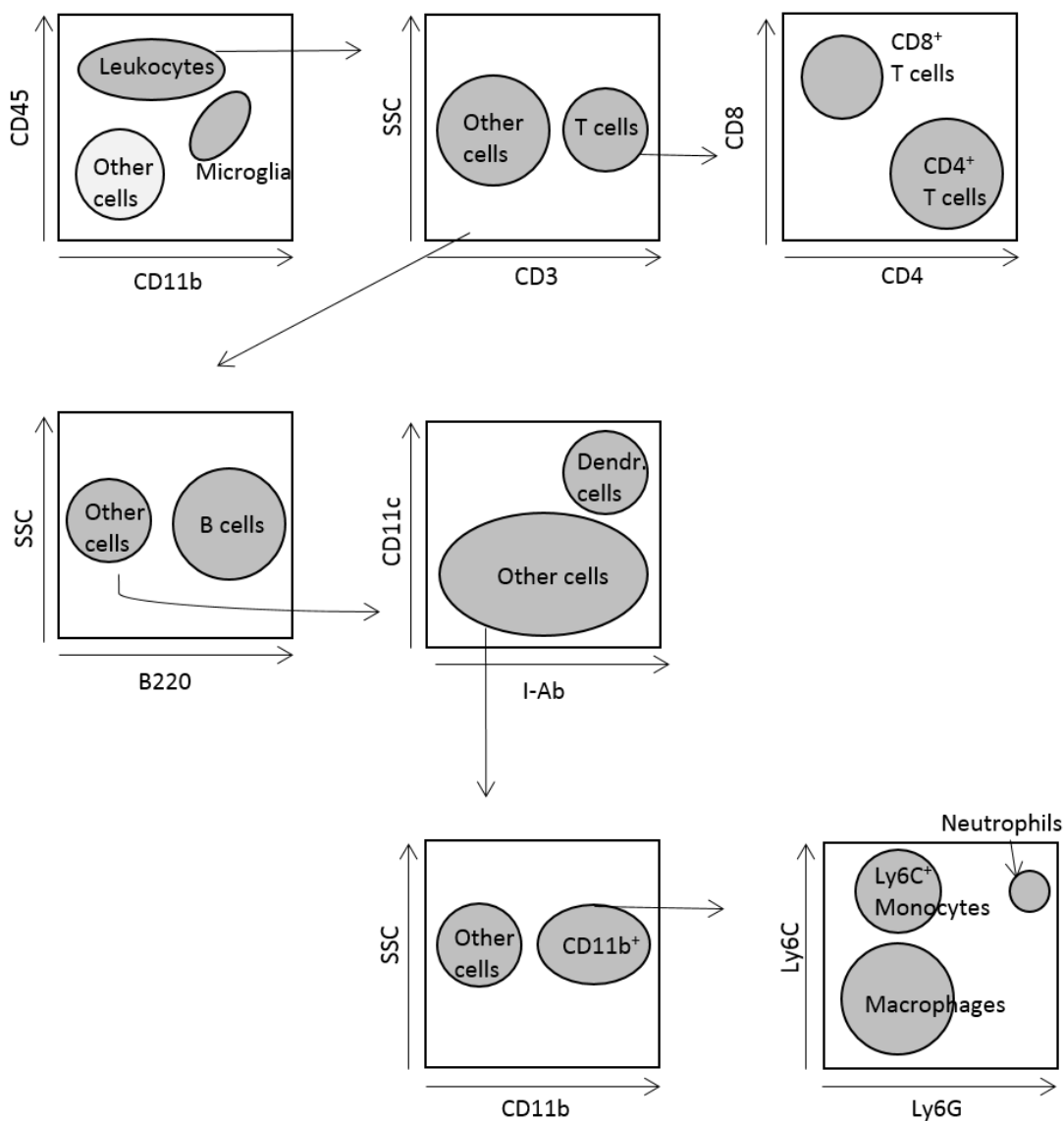


Figure 3.2: **FACS gating scheme for brain cells.** Schematic drawn to show the different population in brains from mice that were isolated after PBS perfusion and enrichment for leukocytes via a percoll gradient. Cells are stained for CD45 and CD11b to distinguish between resident microglia ($CD45^{lo} CD11b^{+}$) and infiltrated immune cells ($CD45^{hi}$). Cells are stained for CD3 to identify T cells ($CD3^{+}$). $CD3^{+}$ cells were separated into $CD8^{+}$ and $CD4^{+}$ T cells. Cells negative for CD3 were analyzed for B cells ($B220^{+}$), $B220^{-}$ cells were gated for dendritic cells ($CD11c^{+}I-Ab^{+}$). Other cells were analyzed for the presence of CD11b and were further separated into macrophages ($Ly6C^{-}Ly6G^{-}$), $Ly6C^{+}$ monocytes ($Ly6C^{+}Ly6G^{-}$) and neutrophils ($Ly6C^{+}Ly6G^{+}$).

3.1. *Batf3*^{-/-} MICE WERE PROTECTED FROM EXPERIMENTAL CEREBRAL MALARIA AFTER PBA-INFECTION

Figure 3.2 illustrates the general gating scheme for brain derived cells after a percoll gradient for leukocyte enrichment in PbA-infected WT mice. The plot shows the CD45^{hi} population which represents cells with hematopoietic origin, present in blood vessels in the brain or cells that had crossed the blood-brain barrier and infiltrated the brain. These cells were further divided into different cell types according to additional surface markers and were analyzed for activation markers. The other population of gated cells contains microglia (CD45^{lo}CD11b⁺) which were also analyzed for activation markers.

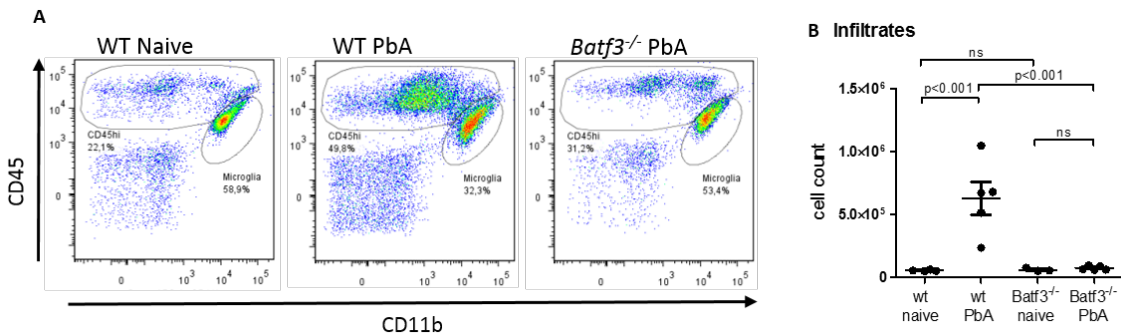


Figure 3.3: **Less CD45^{hi} cells infiltrated the brains of PbA-infected *Batf3*^{-/-} mice.** Brain cells were prepared from d+6 PbA-infected mice (n=4-5) and stained for CD45 and CD11b for flow cytometry analysis. Naive mice from both strains were used as control (n=3-4). CD45^{hi} cells were gated as shown before in fig. 3.2. A: FACS dot plots from representative naive WT, PbA-infected WT and *Batf3*^{-/-} mice. B: The absolute amount of brain infiltrated cells calculated by multiplying the relative amount of CD45^{hi} cells by the total cell number counted after the leukocytes gradient. Significance was tested by ANOVA following Tukey post test. p values below 0.05 were considered significant.

Flow cytometric analysis of naive mice and PbA-infected mice revealed that naive mice contained almost no cellular infiltrates or adherent cells in their brains, while PbA-infected C57Bl/6 mice displayed a prominent CD45^{hi} population (Fig. 3.3A). In comparison, this population was less prominent in PbA-infected *Batf3*^{-/-} mice. The difference seen in figure 3.3A, was also quantified by cell counting. With an average total amount of 6.31e5 cells, infected WT mice showed more than 10-fold increase (p < 0.001) in leukocytes infiltration compared to naive WT mice as well as naive PbA-infected *Batf3*^{-/-} mice ("WT Naive": 5.63e4 cells, "WT PbA: 6.31e5 cells, "*Batf3*^{-/-} Naive": 6.22e4 cells, "*Batf3*^{-/-} PbA": 7.57e4 cells, p < 0.001 between "WT PbA" vs. "*Batf3*^{-/-} PbA"; Fig. 3.3B).

We were first interested in the different cell subsets that migrated from the periphery into the brain. It is assumed that effector cells, such as CD8⁺ T cells, are primed in the spleens of infected animals but migrate to the brain where they cause substantial damage

[Rénia et al., 2006]. Therefore, we analyzed the $CD45^{hi}$ cells from 6 dpi infected WT and $Batf3^{-/-}$ mice for different surface markers to get an impression of the cell subsets that had infiltrated the brain after PbA-infection. It has to be kept in mind, that PbA-infected $Batf3^{-/-}$ mice had 10-fold less cell infiltration to their brains, which led to lower total cell numbers in general (Fig. 3.3).

First of all, we focused on T cells, as especially $CD8^{+}$ T cells are well-known for their major role in the pathogenesis of experimental cerebral malaria [Rénia et al., 2006]. In order to identify T cells, we gated for $CD3^{+}$ cells, which were further differentiated into $CD4^{+}$ and $CD8^{+}$ T cells.

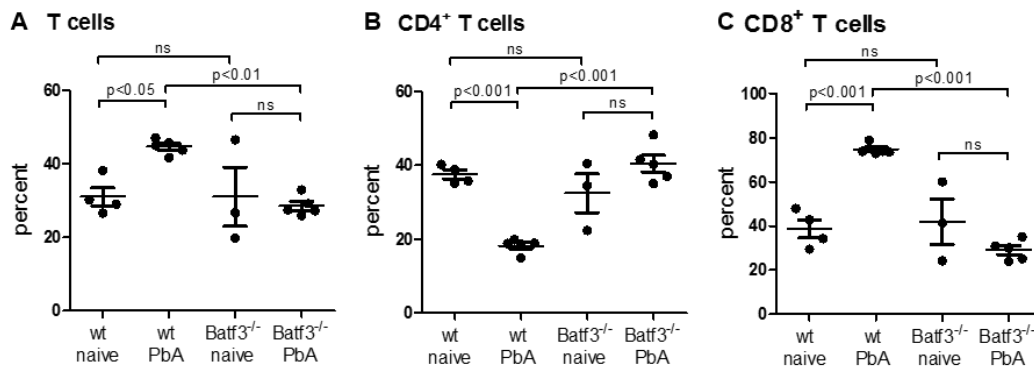


Figure 3.4: **Levels of $CD8^{+}$ T cell infiltration were not increased in brains of PbA-infected $Batf3^{-/-}$ mice at 6 dpi.** Brain infiltrated leukocytes from PbA-infected mice 6 dpi (n=5) or naive mice (n=3) were first gated for $CD45^{high}$ cells as shown before and then analyzed for T cell marker CD3 (A). These $CD3^{+}$ cells were further differentiated in $CD4^{+}$ and $CD8^{+}$ T cells (B and C). Significance was tested by ANOVA following Tukey post test. p values below 0.05 were considered significant.

Of the few cell that were found in the brains of naive WT and $Batf3^{-/-}$ mice, 31% were T cells in both strains (Fig. 3.4A). In brains of PbA-infected WT mice on 6 dpi, the T cell proportion from all brain infiltrated cells was significantly increased (44.6%), in contrast to brains of infected $Batf3^{-/-}$ mice that contained unchanged proportions of T cells in relation to naive mice (28.5%). Among the gated $CD3^{+}$ cells, PbA-infected WT mice contained mostly $CD8^{+}$ T cells (18.2% $CD4^{+}$ vs. 74.6% $CD8^{+}$, ratio 0.25), whereas brains of PbA-infected $Batf3^{-/-}$ mice showed more $CD4^{+}$ T cells among the few cells that had infiltrated to the brain (40.5% $CD4^{+}$ vs. 29.6% $CD8^{+}$, ratio 1.4; Fig. 3.4B and C). In naive mice, the frequencies of $CD4^{+}$ and $CD8^{+}$ cells was were similar ("WT Naive": 35.2% $CD4^{+}$ vs. 38.7% $CD8^{+}$, ratio 1,01, " $Batf3^{-/-}$ Naive": 32.5% $CD4^{+}$ vs.

41.9% CD8⁺, ratio 0.96). Additionally to these significant differences of T cells subset proportions between PbA-infected WT and knock-out mice ($p < 0.001$ in both subsets), the different amount of cells infiltrating the brain has to be considered. *Batf3*^{-/-} mice had significantly less leukocytes migrating to their brains (Fig. 3.3B), which means, that the total cell number for both CD8⁺ but also CD4⁺ T cells was higher in PbA-infected WT mice compared to infected *Batf3*^{-/-} mice and naive controls (Fig. S3).

Next, we examined the other cell populations that were purified with help of a percoll gradient of homogenized brains from PbA-infected WT and *Batf3*^{-/-} mice and their respective naive controls. Flow cytometry staining was performed in order to divide CD45^{hi}CD3⁻ cells into B cells (BCs, B220⁺), dendritic cells (CD11c⁺I-Ab⁺ but no B or T cells) and CD11b⁺ cells that were neither TCs, BCs cells nor DCs. CD11b⁺ mononuclear cells were further differentiated into Ly6C⁺ monocytes (Ly6C⁺Ly6G⁻), neutrophils (Ly6C⁺Ly6G⁺) and macrophages (Ly6C⁻Ly6G⁻).

B cell frequencies in brains of PbA-infected Bl/6 dropped significantly compared to the frequencies in naive WT mice (1.5% vs. 14.5%; $p < 0.001$), but *Batf3*^{-/-} mice (\pm PbA) showed similar results to naive WT mice ("*Batf3*^{-/-} Naive" 13.0%, "*Batf3*^{-/-} PbA": 10.7%; Fig. 3.5A). As brains of PbA-infected WT mice contained significantly more infiltrated cells, the absolute numbers of B cells were similar in all groups (Fig. S3D).

The percentage of dendritic cells found in brains of the experimental animals was very low and did not differ between all analyzed groups ("WT Naive" 1.3%, "WT PbA": 1.9%, "*Batf3*^{-/-} Naive" 1.5%, "*Batf3*^{-/-} PbA": 1.6%; Fig. 3.5B), which led to an increase of total DC numbers in PbA-infected WT mice compared to all other groups (Fig. S3E).

Analysis of CD11b⁺ cells isolated from brains of the described groups revealed a significant increase of Ly6C⁺ monocytes in WT mice that were infected with PbA 6 days before when compared to their naive controls (23.9% vs. 9.4%, $p < 0.001$; Fig. 3.5C). This increase was not observed in PbA-infected *Batf3*^{-/-} mice (8.3%; $p < 0.001$ to "WT PbA"), that did not differ from their uninfected control mice (8.8%). Due to higher total cell numbers in brains of PbA-infected WT mice, these differences in total monocyte numbers were even more prominent (Fig. S3F). Neutrophils numbers were rather low in all investigated groups and showed a high standard deviation. Naive mice from both groups, showed the highest percentages of neutrophils in their brains ("WT Naive": 3.8%, "*Batf3*^{-/-} Naive": 3.2%; Fig. 3.5D). Six days after PbA-infection, the number of neutrophils dropped in WT (0.2%; $p < 0.01$) and *Batf3*^{-/-} mice (1.0%; not significant; Fig. 3.5D), despite higher cell

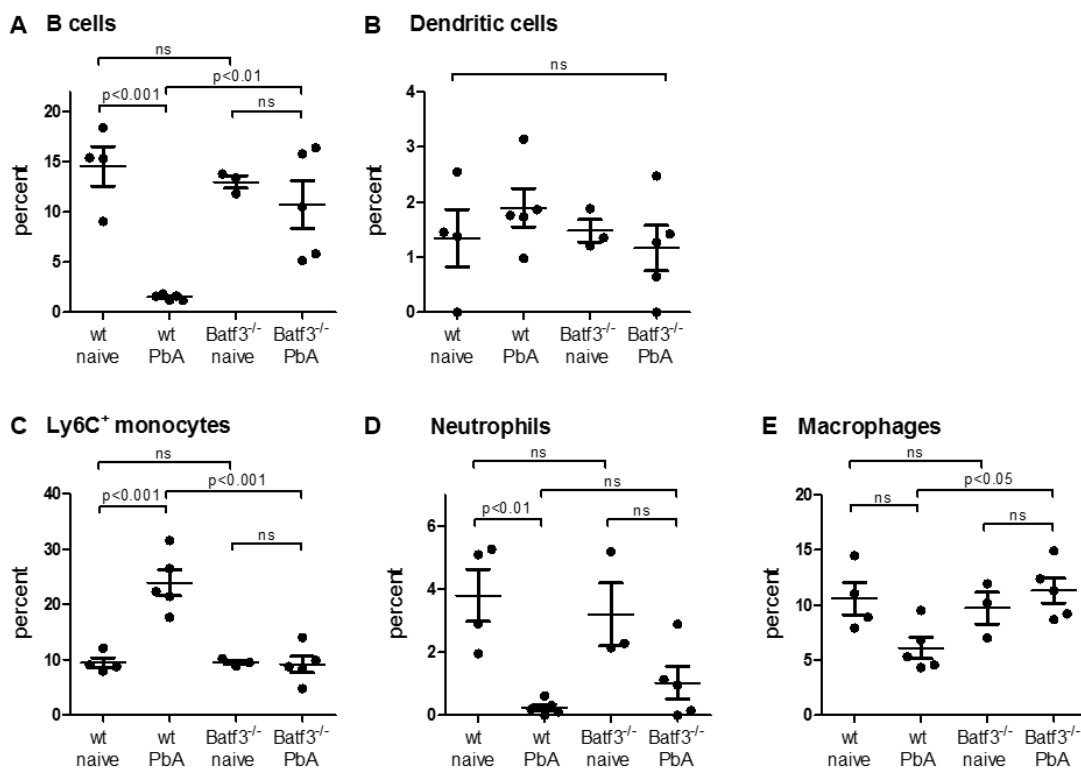


Figure 3.5: **Composition of brain-infiltrated leukocytes did not differ between d+6 PbA-infected *Batf3*^{-/-} mice and naive controls.** Brain-infiltrated leukocytes from PbA-infected (6 dpi) and naive WT and *Batf3*^{-/-} mice were differentiated by flow cytometry (n=3-5). B cells were defined as CD3⁻B220⁺ (A), dendritic cells were gated for CD11c⁺I-Ab⁺ from CD3⁻B220⁻ (B) and CD11b⁺ cells, that were neither of the other cell types, were subdivided into Ly6C⁺ monocytes (Ly6C⁺Ly6G⁻; C), neutrophils (Ly6C⁺Ly6G⁺; D) and macrophages (Ly6C⁻Ly6G⁻; E). Differences were statistically analyzed with ANOVA and Tukey post-test; p < 0.05 was considered significant.

numbers in PbA-infected WT mice, the differences in percentages led to reduction of total neutrophils in both infected groups (Fig. S3G). The small difference between infected mice from both strains was not significant. Macrophage frequencies were around 10% in both naive groups ("WT Naive" 10.6%, "*Batf3*^{-/-} Naive" 9.7%; Fig. 3.5E). In PbA-infected WT mice this number changed only marginally to 6.1% while there was a small increase in *Batf3*^{-/-} mice after infection (11.3%). Differences within both strains were not significant, but the PbA-infected *Batf3*^{-/-} showed an elevated frequency of macrophages among their infiltrates in their brains compared to PbA-infected WT mice (p < 0.05; Fig. 3.5E), however the total number in *Batf3*^{-/-} mice was only half the amount compared to infected WT mice (Fig. S3H).

Taken together, the analysis of the different cell types of brain-infiltrated cells on 6 dpi

revealed a strong increase in T cells (Fig. 3.4) and Ly6C⁺ monocytes (Fig. 3.5C) in PbA-infected WT mice, which were not present in infected *Batf3*^{-/-} mice. Due to the relative increase of these two cell subsets, the frequencies of B cells and neutrophils were lower in the "WT PbA" group. However, as the absolute number of infiltrated cells to the brains of PbA-infected WT was significantly higher compared to that of infected *Batf3*^{-/-} mice (Fig. 3.3), the absolute cell numbers did not differ in these cell populations and differences in T cells and monocytes were even more prominent.

3.1.2.2 Brains of PbA-infected *Batf3*^{-/-} mice showed reduced inflammation

We had observed significantly reduced levels of T cells and Ly6C⁺ monocytes in the brains of PbA-infected *Batf3*^{-/-} mice (relative amount and absolute numbers) compared to high numbers of these cell types that had infiltrated the brains of PbA-infected WT mice. Next, we addressed the question whether there were functional differences between these T cell populations and / or other signs of inflammation, as *Batf3*^{-/-} mice showed no symptoms of ECM and maintained an intact BBB upon PbA-infection.

Granzyme B is an important marker for cytotoxicity of CD8⁺ T cells and was reported to play a major role in experimental cerebral malaria [Haque et al., 2011]. Therefore it was important to test if the cellular production in brain infiltrated CD8⁺ T cells as well as the actual release of granzyme B was altered in infected *Batf3*^{-/-} mice (6 dpi) compared to infected WT mice (6 dpi). Naive mice from both strains served as controls.

We analyzed the production of granzyme B on different levels using quantitative real time PCR, FACS and ELISA (Fig. 3.6A-C).

We extracted mRNA from brains of d+6 infected mice and the transcribed cDNA was then subjected to qPCR. Results were normalized to the house-keeping gene β -actin and are displayed as copies granzyme B per 1e6 copies β -actin. Samples from PbA-infected WT mice showed a strong upregulation of granzyme B (912 copies granzyme B per 1e6 copies β -actin) compared to naive controls (9.17 copies granzyme B per 1e6 copies β -actin) and infected *Batf3*^{-/-} mice (60 copies granzyme B per 1e6 copies β -actin, $p < 0.05$ to WT PbA). Brain samples from naive WT and infected *Batf3*^{-/-} mice did not show significant differences in granzyme B expression (Fig. 3.6A).

After measuring expression levels, we analyzed the amount of granzyme B that was stored specifically in CD8⁺ T cells from brains of d+6 infected mice. The geometric mean

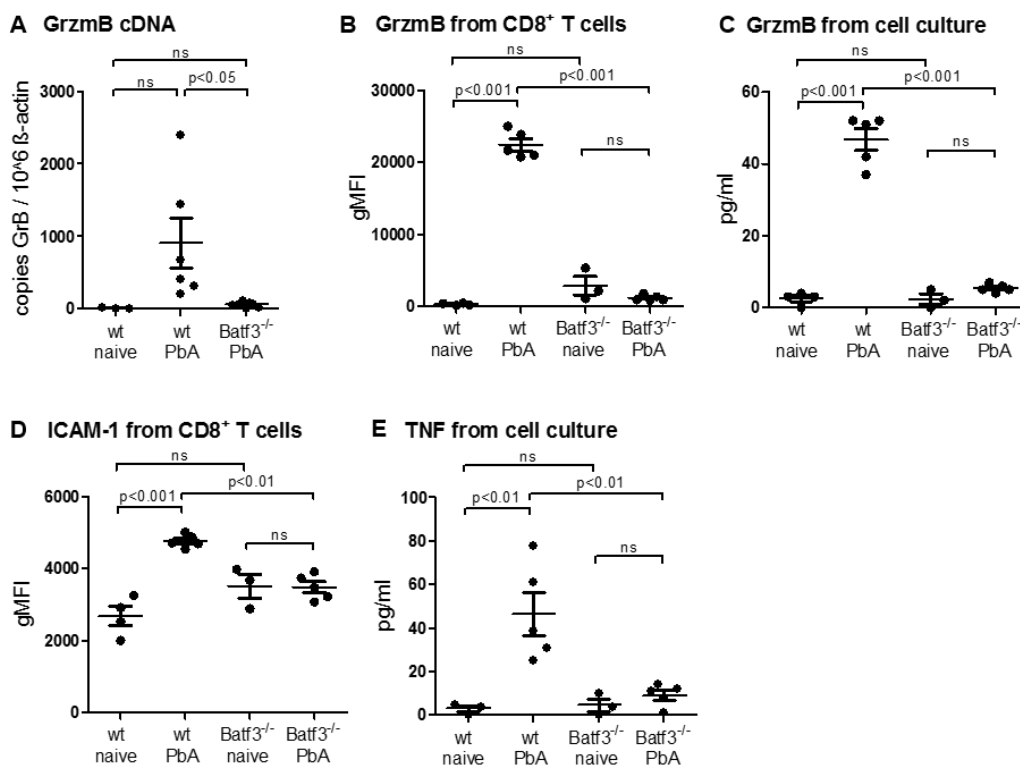


Figure 3.6: T cells from *Batf3*^{-/-} mice produced less granzyme B and general inflammation in the brain was reduced. Granzyme B production was analyzed 6 dpi in brains of PbA-infected *Batf3*^{-/-} and WT mice by qPCR (A), FACS (B) and ELISA (C), naive mice served as controls. (A) mRNA was extracted from snap frozen brains and transcribed to cDNA. cDNA was subjected to quantitative real time PCR for granzyme B and standardized with β -actin as house keeping gene. (B) For FACS analysis, cells were gated for CD8⁺ T cells and the geometric mean fluorescence intensity (gMFI) was calculated with the low cytometry analysis program FlowJo. (C) Granzyme B production *ex vivo* was determined by measuring the cytokines from unpurified brain homogenate supernatant after 24h incubation at 37°C / 5% CO₂ with ELISA. D: ICAM-1 expression was analyzed on brain infiltrating CD8⁺ T cells by flow cytometry. The gMFI was calculated on cells from PbA-infected mice 6 days p.i. and naive mice from WT and *Batf3*^{-/-} strains. E: TNF was measured in brain homogenates that had been cultured over night at 37°C / 5% CO₂ and supernatants were subjected to an ELISA. Values are displayed as mean (n=3-6). Significance was tested by ANOVA following Tukey post test. p values below 0.05 were considered significant.

fluorescence intensity (gMFI) for granzyme B from these cells was significantly upregulated in WT mice after PbA-infection (22,507 units) compared to uninfected mice (301 units, $p < 0.001$; Fig. 3.6B). In contrast to WT animals, granzyme B levels in PbA-infected *Batf3*^{-/-} mice did not increase (1,173 units, $p < 0.001$ to "WT PbA") and was comparable to their naive controls (2869 units; Fig. 3.6B).

As granzyme B can be stored in cells and is secreted when needed, it was also important to check the actual release from cultured brain cells. Therefore, we extracted brains from PbA-infected mice on 6 dpi and prepared brain single cell suspensions which were cultured *ex vivo* in medium for 24h at 37°C / 5% CO₂. The supernatant was collected

the next day and measured for cytokines. ELISA measurements on these supernatants revealed a significant increase (about 20-fold) in granzyme B release in samples from infected WT mice as compared to naive control animals (46.8 pg/ml vs. 2.5 pg/ml, $p < 0.001$) as well as an 10-fold increase in samples from infected WT mice compared to PbA-infected *Batf3*^{-/-} mice (5.4 pg/ml, $p < 0.001$). Cytokine levels from brains of PbA-infected *Batf3*^{-/-} mice did not differ from that in naive *Batf3*^{-/-} controls (2.33 pg/ml; Fig.3.6C).

ICAM-1 is an adhesion molecule which supports cell-cell-interactions and is upregulated on activated T cells. Its importance on T cells in disease development of experimental cerebral malaria was shown before [Ramos et al., 2013]. We analyzed the ICAM-1 expression of brain infiltrated CD8⁺ T cells in PbA-infected WT and *Batf3*^{-/-} mice on 6 dpi as well as their respective naive controls via flow cytometry.

We observed a significant increase in ICAM-1 expression on CD8⁺ T cells in brains of PbA-infected WT mice compared to uninfected control mice (gMFI 4,547 in PbA-infected vs. gMFI 2,679 in naive; $p < 0.001$; Fig. 3.6D). While CD8⁺ T cells in brains cells from naive *Batf3*^{-/-} mice showed a small, but not significant increase in ICAM-1 expression in general ("*Batf3*^{-/-} Naive" gMFI 3,517), PbA-infection did not result in upregulation of this adhesion molecule ("*Batf3*^{-/-} PbA" gMFI 3,481). However, the ICAM-1 expression was significantly lower in PbA-infected *Batf3*^{-/-} than and WT mice ($p < 0.01$).

Brains from ECM-positive mice do not only show T cell activation but a general inflammatory milieu in the brain. In order to analyze the immune responses in the brain of PbA-infected WT versus *Batf3*^{-/-} mice in more detail, we analyzed the brain cell culture for TNF, which can be produced by various immune cells.

We determined very low levels of TNF in supernatants from naive WT (3.0 pg/ml) and *Batf3*^{-/-} derived brain samples (4.7%; Fig. 3.6E). After PbA-infection the measured amount of TNF from cultured brain cells increased significantly in samples from WT mice (46.8 pg/ml; $p < 0.01$) but not from *Batf3*^{-/-} mice (9.2 pg/ml). The comparison between both infected groups showed significant less TNF in samples from *Batf3*^{-/-} than from WT mice ($p < 0.01$; Fig. 3.6E).

In summary, brains of PbA-infected *Batf3*^{-/-} mice showed less cellular infiltration and a strongly reduced activation of the few T cells that migrated to the brains of *Batf3*^{-/-} mice upon PbA-infection, thus mirroring the absent brain inflammation in these mice (brains

of naive and PbA-infected *Batf3*^{-/-} mice showed similar results).

3.1.2.3 Phagocytic capacity of microglia was impaired in *Batf3*^{-/-} mice

Microglia are immune-competent resident brain cells, which can phagocyte and present antigen and also contribute to the development of ECM [Medana et al., 1997].

We wanted to clarify whether microglia, the brain resident macrophages, from WT and *Batf3*^{-/-} mice differed in their ability to take up antigen, as this might influence the ECM pathogenesis. Presentation of antigen to immune cells stimulates functional immune responses *in vivo*; phagocytosis - the uptake of particles and cellular fragments - is the first step in antigen processing. As the presentation of antigen might be important before the onset of disease symptoms, we analyzed mice 3 and 6 days after infection with PbA. Naive mice from both strains served as controls. To test phagocytosis *ex vivo*, we performed a bead-phagocytosis assay. Therefore, we opsonized fluorescent labeled beads with serum from the respective groups to enforce potential bead-uptake. These opsonized beads were then incubated with brain cells that had been isolated with the help of a percoll gradient. After one hour, we stopped the uptake processes by adding ice-cold PBS and identified the percentage of microglia that had taken up the beads by flow cytometry.

Combination of serum opsonized beads and cells (see also Table 2.1)

Cells* \ Plasma**:	WT Naive	WT PbA	<i>Batf3</i> ^{-/-} Naive	<i>Batf3</i> ^{-/-} PbA
Brain WT Naive	X			
Brain WT PbA		X		
Brain <i>Batf3</i> ^{-/-} Naive			X	
Brain <i>Batf3</i> ^{-/-} PbA				X

*Source of potential phagocytosing cells; single approaches for all animals per group

** Source of plasma for bead opzonation; pooled plasma from all animals in one group

Microglia in all groups were able to take up beads. Interestingly, at both time points of the analysis (3 and 6 dpi), we found differences in the phagocytic capacity of microglia from naive mice from WT and *Batf3*^{-/-} strains, as microglia from the latter took up significantly less beads than cells from uninfected WT mice (14.2% to 10.1%; $p < 0.05$ and 10.3% to 4.3%; $p < 0.01$, respectively; Fig. 3.7). We did not observe any differences in phagocytosis in cells from infected mice of both groups on 3 dpi (Fig. 3.7A). However,

3.1. *Batf3*^{-/-} MICE WERE PROTECTED FROM EXPERIMENTAL CEREBRAL MALARIA AFTER PBA-INFECTION

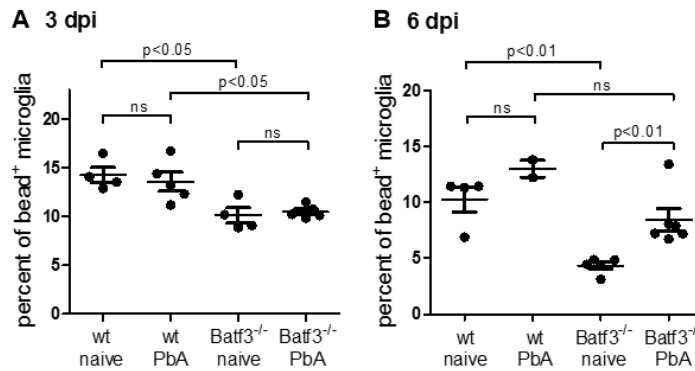


Figure 3.7: Microglia from brains of *Batf3*^{-/-} mice were in general less capable of phagocytosis than WT microglia. The capability of microglia to take up beads was tested 3 (A) and 6 (B) days p.i. in *Batf3*^{-/-} and WT mice (n=2-6). Naive mice from both groups served as control (n=4-5). In this phagocytosis assay brain cells were purified for leukocytes and microglia before 1h incubation with fluorescent labeled beads. Following this incubation time, cell were stained with FACS antibodies to distinguish between different cell subset. Microglia were defined as CD45^{low}CD11b⁺. Values are displayed as mean. Significance was tested by ANOVA following Tukey post test. p values below 0.05 were considered significant.

6 days post infection, the capacity for phagocytosis was increased in both strains with PbA-infection (10.3% to 13% in WT (not significant but strong trend), 4.3% to 8.4% (p < 0.01) in *Batf3*^{-/-}; Fig. 3.7B).

These results indicate, that PbA-infection enhances phagocytosis in microglia. Interestingly, microglia from *Batf3*^{-/-} mice are less efficient in bead-uptake in general, but phagocytic ability was improved upon infection.

3.1.3 Immune responses in early PbA-infection were less pronounced in spleens of PbA-infected *Batf3*^{-/-} mice and led to reduced T cell activation in the late phase of ECM development

As the term cerebral malaria implies, the brain is a critical organ in this disease. It was shown that brain infiltrating immune cells, that cause fatal damage during ECM, are primed in the spleen of infected individuals [Engwerda et al., 2005]. Therefore, it is also important to analyze immune responses towards PbA blood stage infections in the spleen as a secondary lymphoid organ, which plays a crucial role in blood-borne infections.

Different outcomes in the late phase of PbA-infection were associated with differences in infiltrating cell subsets, which are active at the time point when cerebral symptoms are visible. Analyzing these cells subsets not only in the brain but also in the spleen could provide important insights of potential mechanisms that are involved in pathology or

immune regulations. However, the priming of immune effector cells takes probably place at an earlier time point. On day 3 after PbA-infection, the immune system should already have initiated a response against the *Plasmodium* parasites, but neither ECM symptoms nor parasitemia is yet detectable at this early stage. Therefore, we decided to analyze the immune status in the spleen on day 3 and 6 after PbA-infection in WT and *Batf3*^{-/-} mice. In order to illustrate differences between WT and *Batf3*^{-/-} mice at both time points during ECM development, we normalized all values to naive WT mice and displayed them in joined graphs. Graphs with absolute numbers of individual experiments can be found in the appendix.

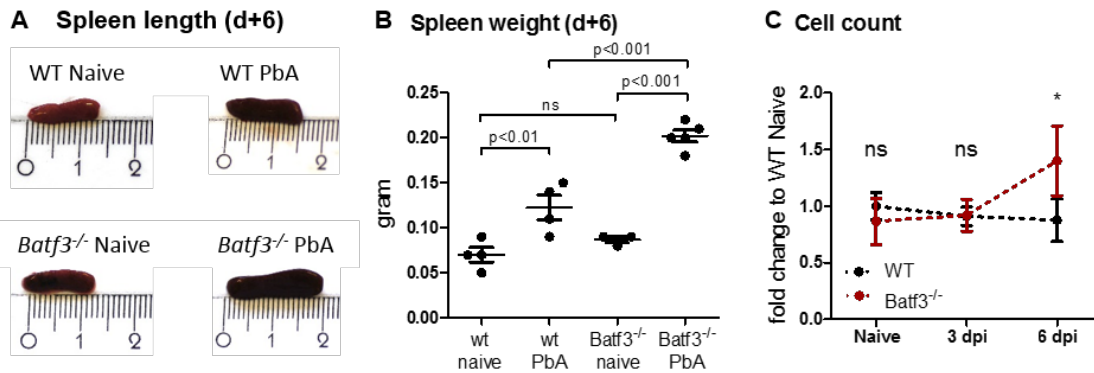


Figure 3.8: **Total amount of splenocytes did increase in PbA-infected *Batf3*^{-/-} mice at 6 dpi.** A: Spleen length was measured and one representative picture from each group is shown. B: Spleens from experimental mice were weighed directly after perfusion on 6 dpi (n = 3-5). C: Spleens from dpi 3 and 6 infected WT and *Batf3*^{-/-} mice (n=5-6) as well as naive control mice (n=3-4) were digested with collagenase and homogenized. The cell concentration of in this suspension was counted and the total amount of splenocytes was calculated. Values from different time points of analysis are presented as mean fold change (\pm SD (standard deviation)) to naive WT mice. Dashed lines are shown for better visualization but time points were analyzed in different mice. Values from 6 dpi are presented as mean \pm SEM. Significance was tested with ANOVA followed by Tukey post-test, $p < 0.05$ was considered significant (* = $p < 0.05$, ** = $p < 0.01$, *** = $p < 0.001$).

Removal of spleens from WT and *Batf3*^{-/-} mice 6 dpi showed obvious splenomegaly in both infected groups when compared to their naive controls as shown by representative pictures from one spleen per group and spleen weights as measured directly after perfusion (Fig. 3.8A, B). Interestingly, spleens from PbA-infected *Batf3*^{-/-} mice were significantly enlarged regarding length and weight compared to all other groups (Fig. 3.8A, "WT Naive": 0.07g, "WT PbA": 0.12g, "*Batf3*^{-/-} Naive": 0.09g, "*Batf3*^{-/-} PbA": 0.20g, $p < 0.001$; Fig. 3.8B).

Interestingly, the physical appearance of the spleens was only partially mirrored by the counted splenocyte number: Before differentiation of individual cell subsets, the total amounts of splenocytes were calculated from spleens of WT and *Batf3*^{-/-} mice 3 and 6 days after PbA-infection versus naive controls. Cell counts from naive mice or on d+3 infected mice did not differ significantly between both strains. However, on 6 dpi, splenocyte counts from PbA-infected *Batf3*^{-/-} mice were significantly increased in comparison to WT controls (fold change to "WT Naive" on 6 dpi: WT 0.88 vs. *Batf3*^{-/-} 1.40, $p < 0.05$; Fig. 3.8A). In contrast to visual observations, we did not find increased cell counts in spleens of d+6 PbA-infected WT mice, which might be due to dead cells which were not counted.

First of all we analyzed the cellular composition in the spleens from PbA-infected WT and *Batf3*^{-/-} mice by flow cytometry analysis. Naive mice of both strains were used as controls. Spleens were first digested with collagenase to recover also antigen-presenting cells, then homogenized to obtain a single cell solution and subsequently prepared for FACS staining as described before.

Identification of immune effector cells in the spleen was performed accordingly to the gating scheme for analysis of the infiltrated brain cells. As the number of splenocytes was sufficient, in contrast to the limited number of cells obtained from the brain after percoll gradient, we could perform a more detailed analysis of spleen cells. The gating strategy after gating for live cells is shown in figure 3.9.

3.1.3.1 Spleens of PbA-infected *Batf3*^{-/-} mice contained less CD8⁺ T cells compared to infected WT mice at 3 and 6 dpi

After determination of the total cell number, we stained the splenocytes for FACS analysis to identify different subsets of immune cells, as described in the gating scheme before (Fig. 3.9). For all analyses of splenic immune cell subsets and activities in our PbA-mouse model, we infected WT and *Batf3*^{-/-} mice with PbA-infected RBCs and isolated their spleens 3 or 6 days later. Naive mice of both strains were included in all experiments as controls.

As the onset of ECM after PbA-infection could be correlated with infiltration of T cells into the brain, these effector cells were of major interest in the spleen. After gating on live cells using forward and sideward scatter on the flow cytometer, these cells were

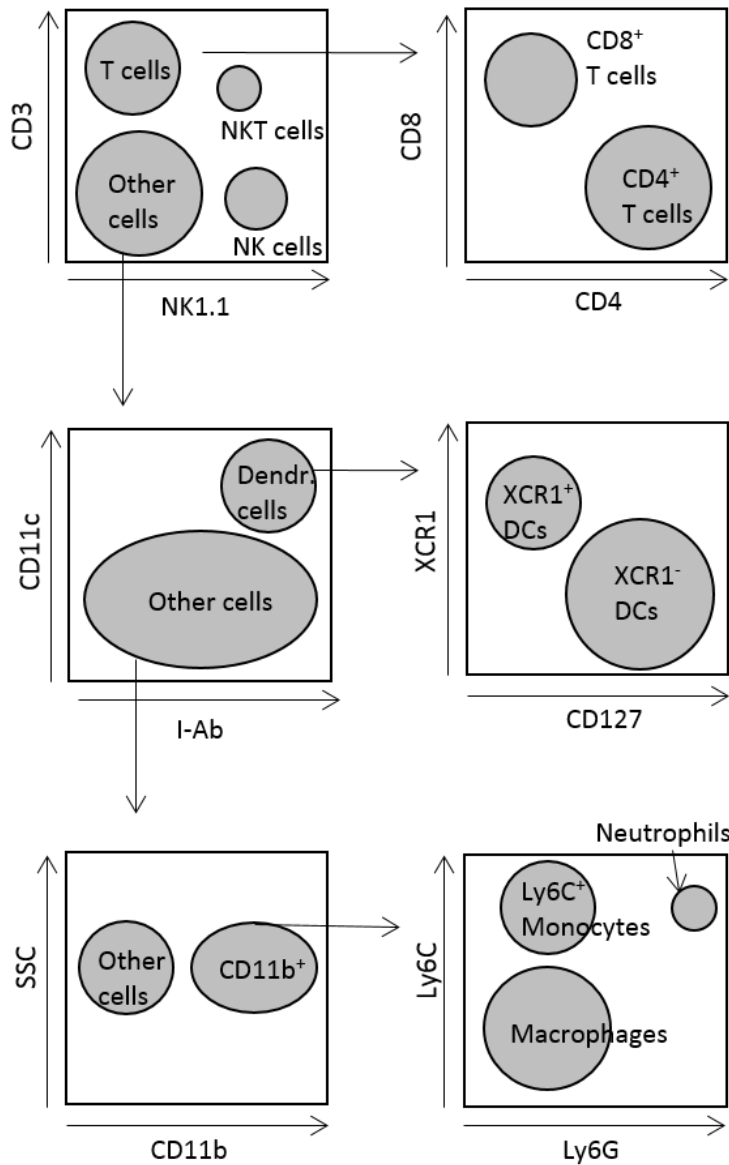


Figure 3.9: **FACS gating scheme for spleen cells.** Schematic drawn to show the gating strategy for spleen cells that were isolated from naive and PbA-infected mice. Cells were stained for CD3 and NK1.1 to differentiate between T cells ($CD3^+NK1.1^-$), NKT cells ($CD3^+NK1.1^+$) and NK cells ($CD3^-NK1.1^+$). $CD3^+$ cells were separated into $CD8^+$ and $CD4^+$ T cells. Cells negative for CD3 and NK1.1 were gated for $CD11c^+I\text{-Ab}^+$ (dendritic cells), which were further differentiated into $XCR1^+$ and $XCR1^-$ DCs. Other cells were analyzed for the expression of CD11b and were further separated into macrophages ($Ly6C^-Ly6G^-$), $Ly6C^+$ monocytes ($Ly6C^+Ly6G^-$) and neutrophils ($Ly6C^+Ly6G^+$).

differentiated into $CD3^+NK1.1^-$ (T cells), $CD3^+NK1.1^+$ (NKT cells), $CD3^-NK1.1^+$ (NK cells) and $CD3^-NK1.1^-$ (other subsets that need further discrimination). Then, $CD4^+$ T cells were separated from $CD8^+$ T cells.

3.1. *Batf3*^{-/-} MICE WERE PROTECTED FROM EXPERIMENTAL CEREBRAL MALARIA AFTER PBA-INFECTION

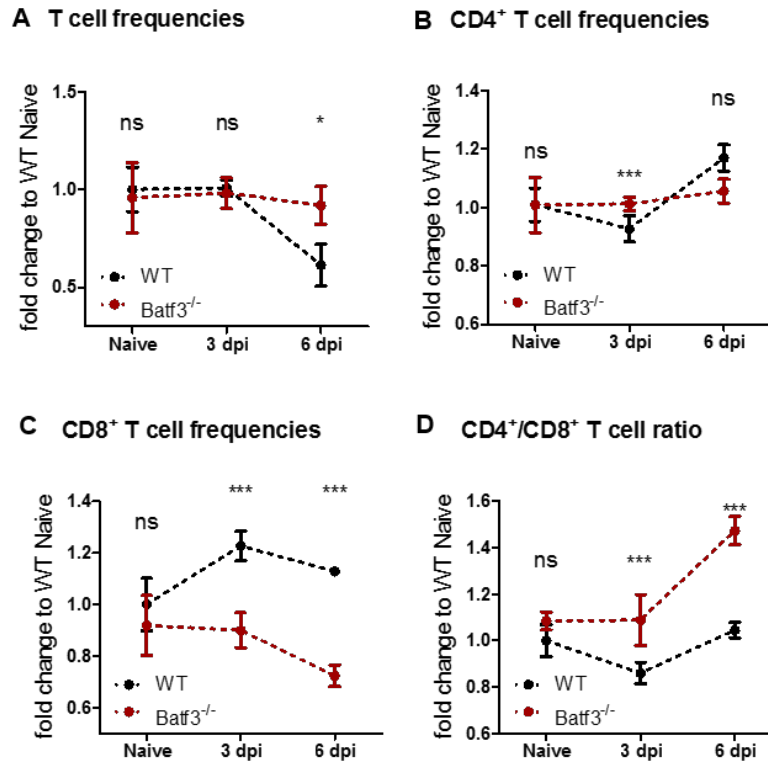


Figure 3.10: **Increased CD4⁺ vs. CD8⁺ T cell ratios in spleens of *Batf3*^{-/-} mice at all tested time points after PbA-infection.** (A) T cell frequencies of d+3 or d+6 PbA-infected mice (n=5-6) and naive controls (n=3-4) were identified by surface marker CD3. CD3⁺ T cells were further differentiated into CD4⁺ (B) and CD8⁺ (C) T cells (both calculated from frequency from CD3⁺ cells). (D) The ratio between CD4⁺ and CD8⁺ T cells was calculated. Values from different time points of analysis are presented as mean fold change (\pm SD) to naive WT mice. Dashed lines are shown for better visualization but time points were analyzed in different mice. Differences were tested separately with ANOVA followed by the Tukey post-test; p values below 0.05 were considered significant (* = $p < 0.05$, ** = $p < 0.01$, *** = $p < 0.001$).

The analysis of CD3 positive T cells did not reveal any significant differences in frequencies of this cell subset between naive and d+3 PbA-infected WT, as well as naive and d+3 infected *Batf3*^{-/-} mice (fold change to "WT Naive": "WT PbA" 1.01, "*Batf3*^{-/-} Naive" 0.96, "*Batf3*^{-/-} PbA" 0.98; Fig. 3.10A). Six days after infection, T cells frequencies were decreased in PbA-infected WT mice, but not in the *Batf3*^{-/-} group (fold change to "WT Naive": "WT PbA" 0.61, "*Batf3*^{-/-} PbA" 0.92; Fig. 3.10A). The higher numbers of total splenocytes that was observed in d+6 PbA-infected *Batf3*^{-/-} mice (Fig. 3.8), magnified the difference in total T cell counts compared to splenic T cells from d+6 PbA-infected WT mice (Fig. S5).

In both naive groups, the frequencies of CD4⁺ and CD8⁺ T cells were similar (CD4⁺ T cells: "*Batf3*^{-/-} Naive" 1.02-fold change to "WT Naive", CD8⁺ T cells: "*Batf3*^{-/-} Naive"

0.92-fold change to "WT Naive"; Fig. 3.10B, C). PbA-infection in WT mice did not influence CD4⁺ frequencies significantly, albeit we saw a small increase on 6 dpi (3 dpi: 0.91-fold change to "WT Naive", $p < 0.01$; 6 dpi: 1.18-fold change to "WT Naive", not significant). In contrast, in *Batf3*^{-/-} mice, splenic CD4⁺ T cell frequencies did not change significantly at any of the analyzed time points after PbA-infection (fold change to "WT Naive" on 3 dpi: 1.01; on 6 dpi 1.07). The difference between WT and *Batf3*^{-/-} mice was significant on 3 dpi (less CD4⁺ cells in WT) but the increase in CD4⁺ in WT mice 6 days after PbA-infection remained a trend (Fig. 3.10B).

Importantly, we observed an early expansion of CD8⁺ T cells in PbA-infected WT mice on day 3 p.i., which slightly decreased on 6 dpi. In contrast, the analysis of spleens from PbA-infected *Batf3*^{-/-} mice revealed decreased frequencies of CD8⁺ T cells, which were significantly different to CD8⁺ T cell frequencies in PbA-infected WT mice (fold change to "WT Naive" on 3 dpi: "WT PbA" 1.23 vs. "*Batf3*^{-/-} PbA" 0.90, $p < 0.001$; on 6 dpi: "WT PbA" 1.13 vs. "*Batf3*^{-/-} PbA" 0.27, $p < 0.001$; Fig. 3.10C).

Calculation of CD4⁺/CD8⁺ T cell ratios mirrored the strong drop of splenic CD8⁺ T cells in PbA-infected *Batf3*^{-/-} mice in comparison to infected WT mice, in particular at 6 dpi, while the ratios did not differ between naive mice from both strains (Fig. 3.10D). PbA-infected WT mice presented a significantly lower CD4⁺/CD8⁺ T cell ratio compared to *Batf3*^{-/-} mice on both analyzed time points after infection (fold change to "WT Naive" on 3 dpi: "WT PbA" 0.86 vs. "*Batf3*^{-/-} PbA" 1.09, $p < 0.001$; on 6 dpi: "WT PbA" 1.05 vs. "*Batf3*^{-/-} PbA" 1.47, $p < 0.001$; Fig. 3.10D).

Taken together, these data showed an early expansion of splenic CD8⁺ T cell upon PbA-infection in WT mice, but not in spleens of infected *Batf3*^{-/-} mice on 3 dpi. Over the time course of infection, the CD4⁺/CD8⁺ T cell ratio was always significantly lower in WT animals than in *Batf3*^{-/-} mice.

3.1.3.2 Cytotoxicity and activation of splenic CD8⁺ T cells was reduced in PbA-infected *Batf3*^{-/-} mice on dpi 6

Even more important than the size of a certain cell subset is its activation status. The presence and ability of cytotoxic T cells to release pro-inflammatory cytokines and to kill specifically (infected) cells that might endanger the health of the host organism is essential for effective immune functions. However, in the case of cerebral malaria, an

excessive activation of T cells can be detrimental in those cases when host tissue is also affected.

Building on preliminary data from our lab on T cell activity on 6 dpi, which revealed an impaired ability of CTLs from *Batf3*^{-/-} mice to lyse antigen-specific target cells (Schumak et al., unpublished data: Fig. 1.2F), we analyzed spleens from PbA-infected WT and *Batf3*^{-/-} mice on both 3 and 6 dpi more detailed for their immune effector activity in comparison to their naive controls. The cytotoxicity of splenocytes from our experimental groups was determined by measurement of cytokines release (granzyme B, IFN γ) of cultured spleen cells. Cytokines were analyzed by ELISA in supernatants of spleen cells which were obtained from d+6 PbA-infected mice and cultured for 24h. IFN γ was measured also in serum of all experimental groups. Furthermore, splenic CD8⁺ T cells from all groups were examined by flow cytometry for their expression profile of surface marker ICAM-1, an adhesion molecule that is associated with T cell activation. In all experiments naive mice served as controls.

Splenocyte single cell suspensions from naive animals of WT and *Batf3*^{-/-} mice showed similar granzyme B release, which increased in both groups after PbA-infection (Fig. 3.11A). Three days after PbA-infection, splenocytes from WT mice released more granzyme B compared to *Batf3*^{-/-} mice as shown by significant differences in fold change to naive WT mice for both groups (fold change to "WT Naive" on 3 dpi: "WT PbA" 2.11 vs. "*Batf3*^{-/-} PbA" 1.10, $p < 0.01$). In the late phase of infection, granzyme B release from both strains was strongly increased, but again, splenocytes from WT mice produced significantly more granzyme B than those from *Batf3*^{-/-} mice and this difference was even bigger compared to 3 dpi (fold change to "WT Naive" on 6 dpi: "WT PbA" 33.32 vs. "*Batf3*^{-/-} PbA" 11.82, $p < 0.01$; Fig. 3.11A).

We measured increased IFN γ levels in supernatants of spleen cells from d+3 PbA-infected WT mice to uninfected WT and found similarly elevated levels of IFN γ in splenocyte cultures from d+3 PbA-infected *Batf3*^{-/-} mice (fold change to "WT Naive" on 3 dpi: "WT PbA" 3.84 vs. "*Batf3*^{-/-} PbA" 3.05, not significant; Fig. 3.11B). Similar to granzyme B release, the IFN γ production from cultured splenocytes increased strongly on 6 dpi in both infected groups. However, splenocytes from PbA-infected WT mice produced significantly more cytokines than those from *Batf3*^{-/-} mice (fold change to "WT Naive" on 6 dpi: "WT PbA" 32.46 vs. "*Batf3*^{-/-} PbA" 21.37, $p < 0.001$; Fig. 3.11B).

In agreement with the cytokine production from spleen cell culture, more IFN γ was detected in serum from d+3 PbA-infected WT mice than in plasma from naive WT

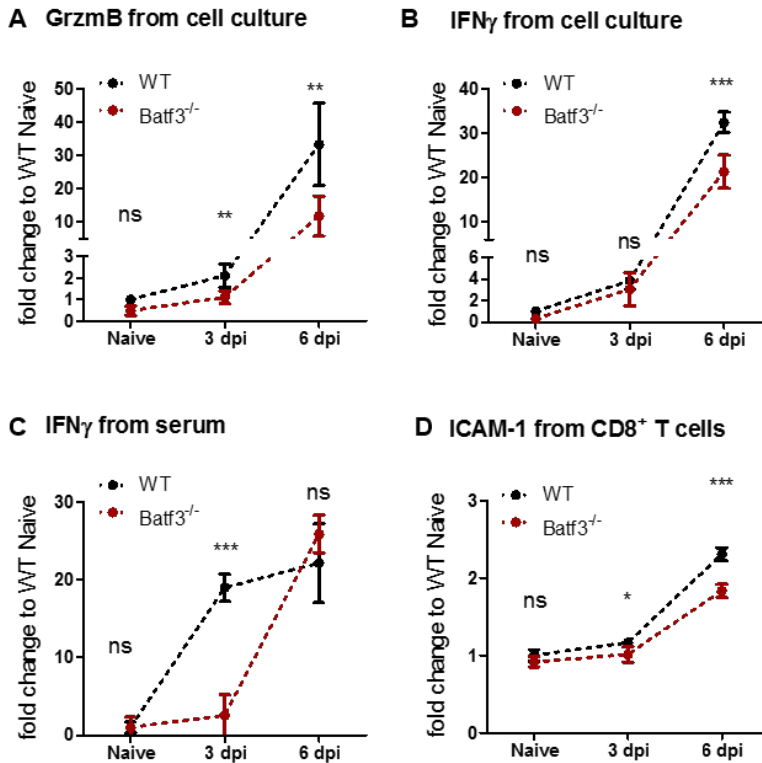


Figure 3.11: Cytotoxicity was reduced in spleens of *Batf3*^{-/-} mice. PbA-infected WT and *Batf3*^{-/-} mice were analyzed on 3 and 6 dpi together with naive control mice (n=3-5). A and B: Granzyme B (GrzmB) and IFN γ were measured by ELISA in supernatant of 24h splenocyte culture. C: IFN γ was determined by ELISA in serum of all experimental animals. D: Presence of surface marker ICAM-1 on CD8⁺ T cells was analyzed by flow cytometry. Values from different time points of analysis are presented as mean fold change (\pm SD) to naive WT mice. Dashed lines are shown for better visualization but time points were analyzed in different mice. Differences were tested separately with ANOVA followed by the Tukey post-test; p values below 0.05 were considered significant (* = p < 0.05, ** = p < 0.01, *** = p < 0.001).

mice. Serum levels of IFN γ from *Batf3*^{-/-} mice were slightly increased on 3 dpi but were significantly lower compared to infected WT controls (fold change to "WT Naive" on 3 dpi: "WT PbA" 18.96 vs. "*Batf3*^{-/-} PbA" 2.56, p < 0.001; Fig. 3.11C). Interestingly, IFN γ in the serum of d+6 PbA-infected mice was at similar high levels in both WT and *Batf3*^{-/-} mice (fold change to "WT Naive" on 6 dpi: "WT PbA" 22.13 vs. "*Batf3*^{-/-} PbA" 25.87, not significant; Fig. 3.11C).

The analysis for surface marker ICAM-1 on CD8⁺ T cells revealed a small, but significant reduction in expression of this adhesion molecule in *Batf3*^{-/-} mice compared to WT controls 3 days after infection (fold change to "WT Naive" on 3 dpi: "WT PbA" 1.17 vs. "*Batf3*^{-/-} PbA" 1.01, not significant; Fig. 3.11D). Six days after PbA-infection, ICAM-1 expression was increased in both infected groups when compared to naive controls, but

3.1. *Batf3*^{-/-} MICE WERE PROTECTED FROM EXPERIMENTAL CEREBRAL MALARIA AFTER PBA-INFECTION

CD8⁺ T cells from *Batf3*^{-/-} mice expressed significantly less ICAM-1 when compared to the WT infection controls (fold change to "WT Naive" on 6 dpi: "WT PbA" 2.30 vs. "*Batf3*^{-/-} PbA" 1.83, $p < 0.001$; Fig. 3.11D).

In summary, peripheral production of inflammation-associated cytokines and ICAM-1 expression on CD8⁺ T cells was elevated in WT mice but not in *Batf3*^{-/-} mice in early and late phases of PbA-infection.

In addition to the previously shown results we analyzed CD8⁺ T cells in more detail on 6 dpi. Analysis of T cell activation markers was performed via flow cytometry analysis on CD8⁺ T cells for intracellular cytokine production (granzyme B and IFN γ) and extracellular expression of CD11c, which is an accepted marker of T cell activation.

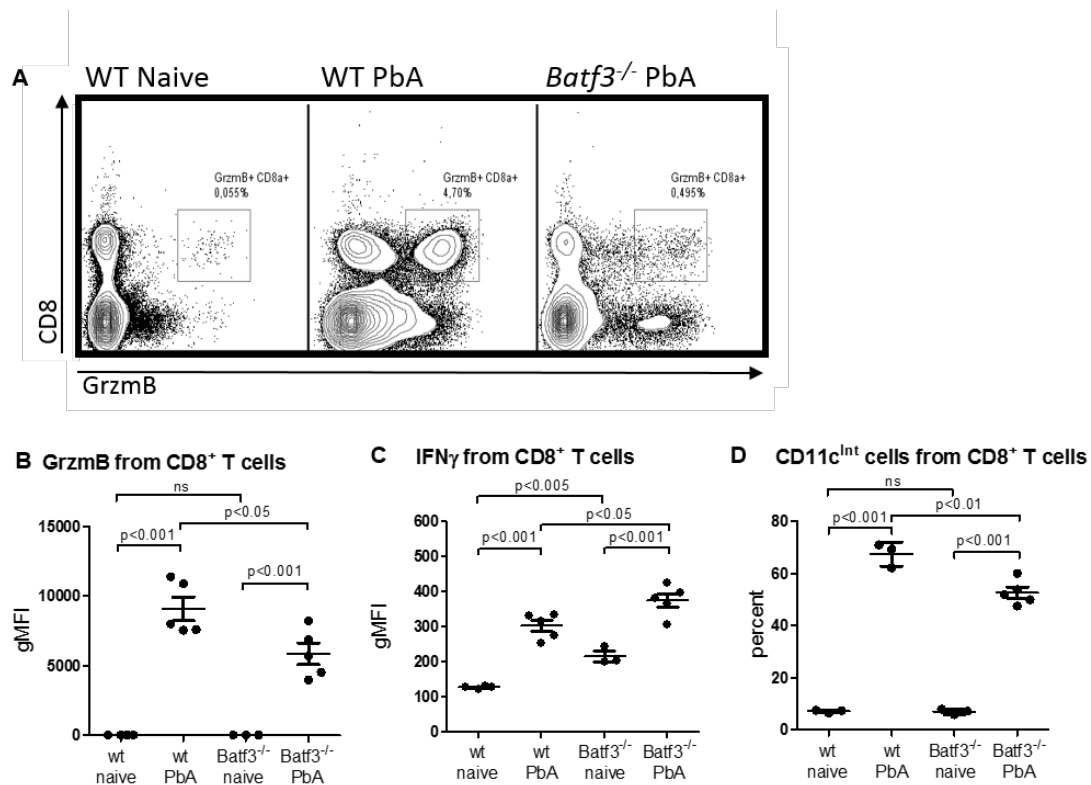


Figure 3.12: **Impaired cytotoxicity in spleens of PbA-infected *Batf3*^{-/-} mice on 6 dpi.** WT and *Batf3*^{-/-} mice were analyzed 6 days after PbA-infection and compared with naive control mice of both strains. CD8⁺ T cells were gated in flow cytometry analysis as described before. We further analyzed this population for different intra- and extracellular activation markers: granzyme B (A: dot plot from spleen cells, B: gMFI), IFN γ (C: gMFI) and CD11c intermediate population (D: frequency). All data are presented as mean (\pm SEM (standard error of mean)) and were analyzed for significance with ANOVA and Tukey correction. p values smaller than 0.05 were considered significant.

On day 6 after PbA-infection, we measured high levels of granzyme B in splenic CD8⁺ T cells from WT and *Batf3*^{-/-} mice which was seen in FACS dot plot as frequencies (Fig. 3.12) and measured as geometric mean fluorescence intensity ("WT PbA": gMFI 9093, "*Batf3*^{-/-} PbA": gMFI 5862), compared to baseline levels in both naive groups ("WT Naive": gMFI 16; "*Batf3*^{-/-} Naive": gMFI 18; $p < 0.001$ compared to PbA-infected mice). However, the increase in granzyme B expression in *Batf3*^{-/-} mice was significantly lower than in infected WT mice ($p < 0.05$; 3.12B). We also determined increased production of intracellular IFN γ in splenic CD8⁺ T cells from PbA-infected WT mice compared to weak baseline levels in naive mice ("WT PbA": gMFI 303, "WT Naive": gMFI 127, $p < 0.001$; Fig. 3.12C). Interestingly, T cells from *Batf3*^{-/-} mice showed an enhanced IFN γ level already in the naive status (gMFI 199, $p < 0.05$ to "WT Naive") that was further increased after PbA-infection (gMFI 374, $p < 0.001$ to "*Batf3*^{-/-} Naive") and was significantly ($p < 0.05$) higher than the gMFI of IFN γ in PbA-infected WT mice.

CD11c is expressed on regulatory and effector CD8⁺ T cells, but in different intensities: high CD11c expression is found on regulatory cells, intermediate expression is a sign for effector cells [Vinay and Kim, 2009]. Therefore the analysis of the mean intensity is not possible for this marker, but the frequency of CD8⁺ T cells expressing intermediate CD11c could be determined. Similar to the other results, we found more CD11c^{Int} CD8⁺ T cells in spleens of mice that had been infected with PbA before compared to naive mice ("WT Naive": 7.1%, "WT PbA": 67.4%, "*Batf3*^{-/-} Naive": 6.9%, "*Batf3*^{-/-} PbA": 52.6%; 3.12D). We could not see any difference between naive mice of both strains regarding their frequencies of CD11c^{Int} cells of CD8⁺ T cells, but in spleens of PbA-infected *Batf3*^{-/-} mice significantly less T cells expressed CD11c^{Int} compared to T cells from in WT mice ($p < 0.01$).

Taken together, these results show that the pro-inflammatory environment in the spleen and especially the activation of cytotoxic T cells was markedly impaired in PbA-infected *Batf3*^{-/-} mice. However, we could not differentiate between different cell types in the spleen cell culture. It is likely that also other cells, such as CD4⁺ T Cells, natural killer cells (NK cells) and natural killer T cells (NKT cells) have contributed to cytokine levels and also to immune responses in PbA-infected mice. However, activation markers in CD4⁺ cells were similar to those seen in CD8⁺ T cells (Fig. S7).

3.1.3.3 NK cells were more activated in the spleens of PbA-infected *Batf3*^{-/-} mice on dpi 6

In addition to T cells, also natural killer (NK) and natural killer T (NKT) cells can contribute to a pro-inflammatory immune responses and fighting an infection by production of IFN γ and granzyme B [Hansen et al., 2007]. In *Plasmodium* infection, NK cells are mainly described to be involved in the first line defense as part of the innate immune system [Roetynck et al., 2006]. Even though, NK cells are probably not the main cytotoxic effector cells in cerebral malaria, a change of cell numbers or NK / NKT cell activation might contribute to the high levels of IFN γ and granzyme B in whole spleen cell cultures.

To address the role of NK cells in our PbA-mouse model, spleens from d+3 and d+6 PbA-infected WT and *Batf3*^{-/-} mice were processed for FACS staining as described before and surface markers CD3 and NK1.1 were used to differentiate between NK cells (CD3⁻NK1.1⁺) and NKT cells (CD3⁺NK1.1⁺). Additionally we purified NK and NKT cells via MACS separation using magnetic antibodies coupled to DX5, which is present on NK and NKT cells. These enriched cells were cultured with IL-2 for stimulation and WT BMDCs, BMDCs derived from *Batf3*^{-/-} mice or without any BMDCs. The generated cell culture supernatant was collected after 24h and analyzed by ELISA for granzyme B and IFN γ .

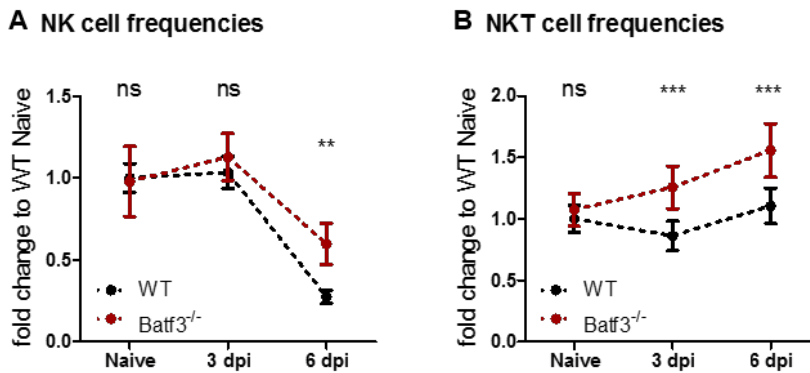


Figure 3.13: NK and NKT cells were elevated in spleens of *Batf3*^{-/-} mice after PbA-infection, compared to infected WT mice. Spleens of d+3 and d+6 PbA-infected WT and *Batf3*^{-/-} mice (n=5-6) as well as naive controls (n=3-4) were processed for FACS analysis and stained with surface markers CD3 and NK1.1 to identify NK cells (CD3⁻NK1.1⁺; A) and NKT cells (CD3⁺NK1.1⁺; B). Values from different time points of analysis are presented as mean fold change (\pm SD) to naive WT mice. Dashed lines are shown for better visualization but time points were analyzed in different mice. Differences were tested separately with ANOVA followed by the Tukey post-test; p values below 0.05 were considered significant (* = p < 0.05, ** = p < 0.01, *** = p < 0.001).

We observed no differences in the percentage of splenic NK cells on day 3 after PbA-infection, but a strong decrease in this cell population on 6 dpi in WT and *Batf3*^{-/-} mice (fold change to "WT Naive" on 3 dpi: "WT PbA" 1.03 vs. "*Batf3*^{-/-} PbA" 1.13, not significant; on 6 dpi: "WT PbA" 0.27 vs. "*Batf3*^{-/-} PbA" 0.60, $p < 0.001$; Fig. 3.13A). Interestingly, spleens of *Batf3*^{-/-} mice at 6 dpi contained more NK cells compared to WT controls at the same day.

In contrast to NK cells, NKT cell frequencies did not drop during the course of infection. Spleens of PbA-infected WT mice contained similar frequencies of NKT cells on 3 and 6 dpi (fold change to "WT Naive" on 3 dpi: "WT PbA" 0.86, on 6 dpi: "WT PbA" 1.11; Fig. 3.13B). Uninfected *Batf3*^{-/-} mice contained similar frequencies of NK cells in their spleens, but this cell population increased upon PbA-infection and led to significantly ($p < 0.001$) more splenic NKT cells in *Batf3*^{-/-} mice at 3 and 6 dpi (fold change to "WT Naive" in "*Batf3*^{-/-} Naive": 1.07, on 3 dpi: 1.26, on 6 dpi: 1.56; Fig. 3.13B).

Taken together, PbA-infected *Batf3*^{-/-} mice contained more NK and NKT cells in their spleens compared to their WT infection-controls.

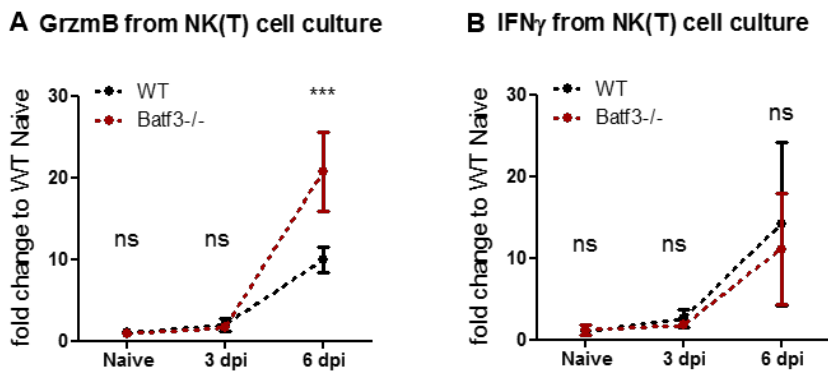


Figure 3.14: NK and NKT cells from spleens of *Batf3*^{-/-} mice produced significantly more granzyme B after PbA-infection than infected WT mice. NK and NKT cells from all experimental groups ($n=3-5$; 3 and 6 dpi for PbA-infected mice) were sorted via MACS sorting after labeling with magnetic beads coupled to DX-5 antibody. Sorted cells were incubated with IL-2 and BMDCs from naive WT donor mice that were cultured with GM-CSF for a week prior to the experiment. Supernatant was collected the next day and subjected to sandwich-ELISAs for granzyme B (A) and IFN γ (B). Values from different time points of analysis are presented as mean fold change (\pm SD) to naive WT mice. Dashed lines are shown for better visualization but time points were analyzed in different mice. Differences were tested separately with ANOVA followed by the Tukey post-test; p values below 0.05 were considered significant (* = $p < 0.05$, ** = $p < 0.01$, *** = $p < 0.001$).

Production of granzyme B and IFN γ from DX-5 sorted NK and NKT cells was similarly low in both naive groups and increased around 2-fold in both infected groups at 3 dpi (granzyme B fold change to "WT Naive" on 3 dpi: "WT PbA" 1.97 vs. "*Batf3*^{-/-}

PbA” 1.64, not significant; IFN γ on 3 dpi: ”WT PbA” 2.58 vs. ”*Batf3*^{-/-} PbA” 1.77, not significant; Fig. 3.14A, B). Cells purified from spleens of d+6 PbA-infected mice of both strains produced more than 10-fold more granzyme B and IFN γ than naive controls (granzyme B fold change to ”WT Naive” on 6 dpi: ”WT PbA” 9.91 vs. ”*Batf3*^{-/-} PbA” 20.72, $p < 0.001$; IFN γ on 3 dpi: ”WT PbA” 14.17 vs. ”*Batf3*^{-/-} PbA” 11.08, not significant; Fig. 3.14A, B). Importantly, NK and NKT cells from d+6 PbA-infected *Batf3*^{-/-} mice produced significantly more granzyme B than cells from infected WT mice ($p < 0.001$).

Additionally to culturing the DX55 sorted cells with BMDCs from naive WT mice, we performed another two approaches. Here, splenic DX5-sorted NK/T cells were either incubated with BMDCs from naive *Batf3*^{-/-} mice or without any BMDCs. Culturing with BMDCs from *Batf3*^{-/-} mice did not show any difference in levels of cytokine production for IFN γ and granzyme B. When cells were incubated without BMDCs, they were still able to produce cytokines, but at a reduced level (10-fold less). Interestingly, the differences between the experimental groups remained the same.

Additionally, we examined the NK/T cells of d+6 PbA-infected WT and *Batf3*^{-/-} mice by flow cytometry for signs of activation such as changes in intracellular cytokine production and surface markers. We analyzed the expression of intracellular granzyme B and IFN γ and extracellular surface markers which are associated with inflammation such as ICAM-1 and CD107a.

While the analysis of NKT cells did not reveal any differences between all PbA-infected WT and *Batf3*^{-/-} mice (exception CD107a, Fig. S10), we observed significant differences in NK cells from PbA-infected WT and *Batf3*^{-/-} mice (Fig. 3.15). The analysis of granzyme B in splenic NK cells revealed a strong increase in cytokine production after PbA-infection. While naive mice from both strains had almost no detectable granzyme B (gMFI WT: 357, gMFI *Batf3*^{-/-}: 284), granzyme B expression was increased in PbA-infected WT mice ($p < 0.05$ to ”WT Naive”) and in infected *Batf3*^{-/-} mice ($p < 0.01$ to ”*Batf3*^{-/-} Naive”, Fig. 3.15A). The higher level of granzyme B in infected *Batf3*^{-/-} mice was not significantly different compared to the values of the ”WT PbA” groups, possibly also due to the high standard deviation in the latter group.

In these splenic NK cells, IFN γ levels were very low in general, however, we detected a significant ($p < 0.05$) reduction of IFN γ expression in NK cells from PbA-infected *Batf3*^{-/-} mice compared to infected WT controls (gMFIs of ”WT Naive”: 240, ”WT PbA”: 226, ”*Batf3*^{-/-} Naive”: 219, ”*Batf3*^{-/-} PbA”: 179; Fig. 3.15B).

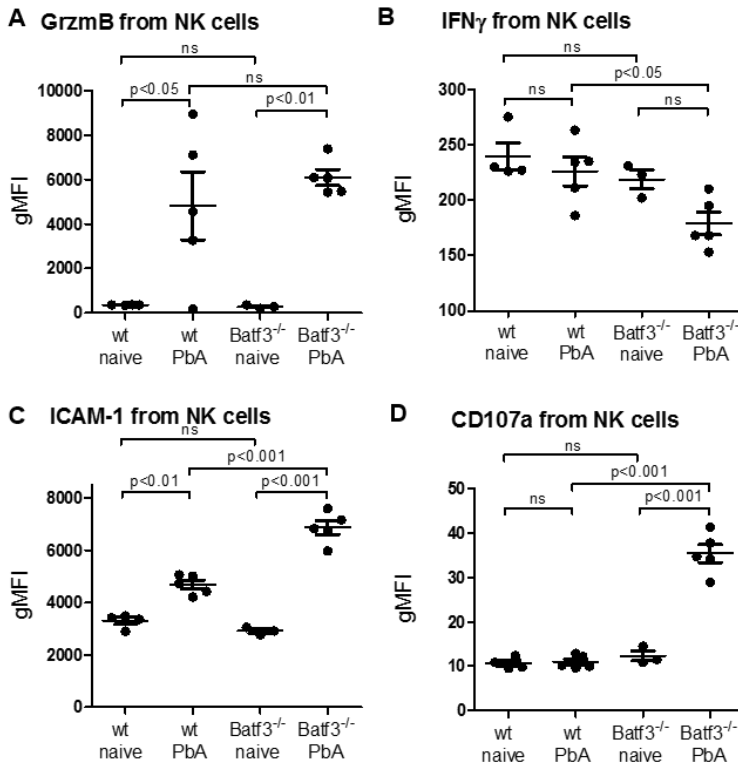


Figure 3.15: NK cells from spleens of d+6 PbA-infected *Batf3*^{-/-} mice displayed enhanced activity in both, cytotoxic and regulatory markers. NK cells from spleens of PbA-infected and naive mice of WT and *Batf3*^{-/-} strains (n=3-5) were defined as described before. Cells were then analyzed via flow cytometry for intracellular cytokines granzyme B (A) and IFN γ (B) and surface markers ICAM-1 (C) and CD107a (D). Results are shown as mean (\pm SEM) and were tested for statistical significance with ANOVA and Tukey post test. p values below 0.05 were considered significant.

Six days after PbA-infection, the surface expression of ICAM-1 on splenic NK cells were significantly changed in WT mice (naive: gMFI 3297, gMFI infected: 4687, $p < 0.01$; Fig. 3.15C). Uninfected *Batf3*^{-/-} mice had similar ICAM-1 expression as their WT counterparts (gMFI 2769), but NK cells from PbA-infected *Batf3*^{-/-} mice expressed significantly ($p < 0.001$) more ICAM-1 on their surface (gMFI 6759) compared to their naive controls but also to PbA-infected WT mice ($p < 0.001$; Fig. 3.15C).

CD107a is an activation marker that is used to identify degranulating cells and was only expressed at very low levels in NK cells from WT mice and naive *Batf3*^{-/-} mice ("WT Naive": gMFI 11, "WT PbA": gMFI 10, "*Batf3*^{-/-} Naive": gMFI 12). Interestingly, in PbA-infected *Batf3*^{-/-} mice, the surface expression of CD107a on splenic NK cells was significantly increased (gMFI 35, $p < 0.001$; Fig. 3.15D). Analysis of splenic NKT cells revealed similar results for expression of CD107a (Fig. S10D). However, this expression

level was still very low in general.

All together, PbA-infected *Batf3*^{-/-} mice had more NK and NKT cells in their spleens and these cells were found to produce more cytokines and express more pro-inflammatory markers than cells from PbA-infected WT mice.

3.1.3.4 CD4⁺ dendritic cells from *Batf3*^{-/-} mice expressed more CD40 on their surface after PbA-infection

Dendritic cells represent a link between innate and adaptive immunity by presenting antigen to effector cells. As *Batf3*^{-/-} mice genetically lack cross-presenting dendritic cells (defined as XCR1⁺), which are important in generation of the cytotoxic CD8⁺ T cell response, we were interested if XCR1⁻ dendritic cells would be more activated to compensate for this lack.

To address this question, we sacrificed PbA-infected WT and *Batf3*^{-/-} mice 3 and 6 days p.i. as well as naive mice from both strains and prepared their spleens for flow cytometry analysis as described before. After excluding CD3⁺, NK1.1⁺ and B220⁺ cells from analysis, dendritic cells were defined as CD11c⁺I-Ab⁺. Dendritic cells were further divided into XCR1⁺ and CD4⁺ subsets, with the first being cross-presenting DCs (which are lacking in *Batf3*^{-/-} mice) and the latter being conventional DCs.

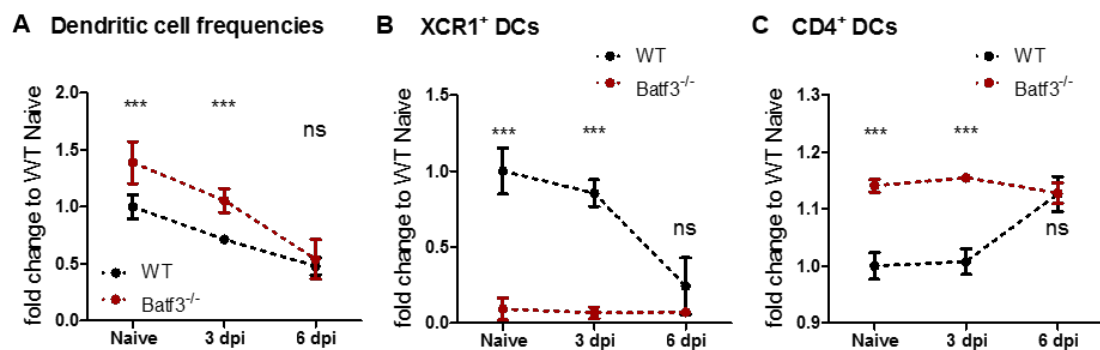


Figure 3.16: Dendritic cell numbers decreased in spleens of PbA-infected WT and *Batf3*^{-/-} mice. Spleens of d+3 and d+6 PbA-infected WT and *Batf3*^{-/-} mice and their respective naive controls were processed for FACS staining (n=3-6). A: Dendritic cells were defined as CD11c⁺I-Ab⁺ from CD3⁻NK1.1⁻B220⁻ cells. Dendritic cells were further subdivided into XCR1⁺ DCs (B) and CD4⁺ DCs (C). Values from different time points of analysis are presented as mean fold change (\pm SD) to naive WT mice. Dashed lines are shown for better visualization but time points were analyzed in different mice. Differences were tested separately with ANOVA followed by the Tukey post-test; p values below 0.05 were considered significant (* = p < 0.05, ** = p < 0.01, *** = p < 0.001).

The results of dendritic cell staining indicated that uninfected *Batf3*^{-/-} mice contained significantly more DCs in their spleens compared to WT mice (fold change to "WT Naive" 1.39, $p < 0.001$; Fig. 3.16A). Compared to their respective naive controls, PbA-infected mice of both experimental groups contained reduced DC frequencies in spleens from 3 dpi on, which further declined on 6 dpi. The higher frequency of dendritic cells in *Batf3*^{-/-} mice compared to WT controls seen in naive mice remained visible on 3 dpi, but was no longer seen 6 days after infection (fold change to "WT Naive" on 3 dpi: "WT PbA" 0.71 vs. "*Batf3*^{-/-} PbA" 1.06, $p < 0.001$; on 6 dpi: "WT PbA" 0.48 vs. "*Batf3*^{-/-} PbA" 0.54, not significant; Fig. 3.16A).

As expected, we confirmed the genetic deficiency of cross-presenting DCs, as in *Batf3*^{-/-} mice almost no XCR1⁺ DCs were found (fold change to "WT Naive": naive 0.09, on 3 dpi 0.07, on 6 dpi 0.07; Fig.3.16B) and the vast majority of DCs were CD4⁺ (fold change to "WT Naive": naive 1.14, on 3 dpi 1.15, on 6 dpi 1.13; Fig.3.16C). Interestingly, in spleens of WT mice frequencies of cross-presenting DCs, identified by XCR1, decreased 3 day after PbA-infection and further declined in the course of infection till 6 dpi (fold change to "WT Naive": on 3 dpi 0.86, on 6 dpi 0.24; Fig.3.16B). Accordingly, the number of CD4⁺ (XCR1⁻) dendritic cells increased in WT mice till 6 days after PbA-infection (fold change to "WT Naive": on 3 dpi 1.01, on 6 dpi 1.13; Fig.3.16B). Differences in DC subsets between both strains were found to be significant in naive mice and on 3 dpi ($p < 0.001$), but no longer on 6 dpi were almost no XCR1⁺ DCs were found in PbA-infected WT mice.

Additionally to the regulations in cell frequencies, we were also interested in the activation status of the dendritic cells. The lack of XCR1⁺ DCs in *Batf3*^{-/-} mice could lead to a regulation of the remaining DCs in order to compensate for the missing subset. Therefore, CD4⁺ DCs were stained for CD40, CD80 or CD86 and CCR7, which enhance the interactions of dendritic cells with T cells but also B cells and regulate their functions.

Surface expression of CD40 on CD4⁺ dendritic cells found in the spleens of d+6 PbA-infected WT mice was slightly increased on 3 dpi in both, WT and *Batf3*^{-/-} mice, compared to CD40 levels in naive WT mice (fold change to "WT Naive" on 3 dpi: "WT PbA" 1.41 vs. "*Batf3*^{-/-} PbA" 1.54, not significant; Fig. 3.17A). However, splenic DCs of naive and d+3 PbA-infected *Batf3*^{-/-} mice did not differ from those of WT control mice in their CD40 expression. After 6 days of PbA-infection, the surface expression of CD40 on CD4⁺ dendritic cells increased in both groups, but significantly more so in *Batf3*^{-/-} mice (fold change to "WT Naive" on 6 dpi: "WT PbA" 2.35 vs. "*Batf3*^{-/-} PbA" 3.76, $p < 0.001$;

3.1. *Batf3*^{-/-} MICE WERE PROTECTED FROM EXPERIMENTAL CEREBRAL MALARIA AFTER PBA-INFECTION

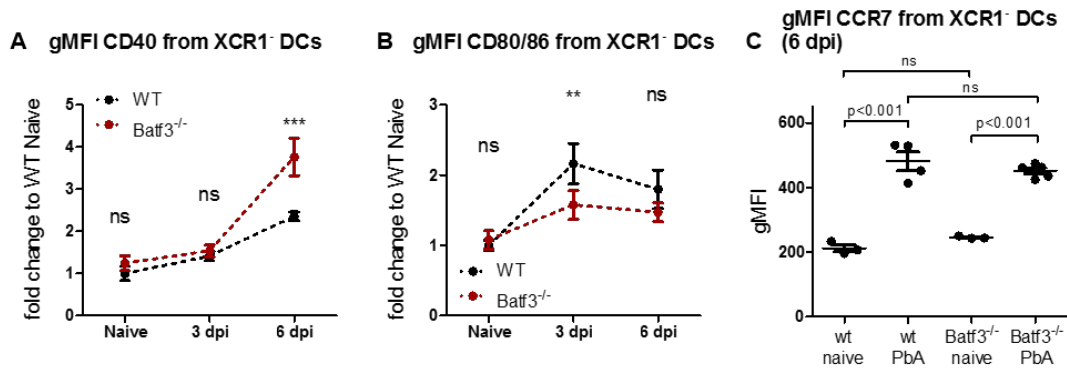


Figure 3.17: CD40 was increased on splenic DCs in d+6 PbA-infected *Batf3*^{-/-} mice. CD4⁺ dendritic cells that were identified from spleens of d+3 and d+6 PbA-infected *Batf3*^{-/-} and WT mice and their respective uninfected controls (Fig. 3.16), were analyzed for expression of surface marker CD40 (A), CD80/CD86 (B) and CCR7 (C, 6 dpi only) by flow cytometry (n=3-6). Values from different time points of analysis are presented as mean fold change (±SD) to naive WT mice. Dashed lines are shown for better visualization but time points were analyzed in different mice. Values from 6 dpi are presented as mean ± SEM. Differences were tested separately with ANOVA followed by the Tukey post-test; p values below 0.05 were considered significant (* = p < 0.05, ** = p < 0.01, *** = p < 0.001).

Fig. 3.17A).

Unlike for CD40, we could not detect an increase of CD80 expression on non-cross-presenting DCs in spleens of PbA-infected *Batf3*^{-/-} mice compared to the WT infection control, but rather a small down-regulation on 3 dpi, which was resolved by 6 dpi (fold change to "WT Naive" on 3 dpi: "WT PbA" 2.16 vs. "*Batf3*^{-/-} PbA" 1.58, p < 0.01; on 6 dpi: "WT PbA" 1.80 vs. "*Batf3*^{-/-} PbA" 1.47, not significant; Fig. 3.17B).

The expression of CCR7, a receptor that is involved in T_{reg} regulation by DCs, was significantly increased in both infected groups on 6 dpi (p < 0.001) with no differences between WT and *Batf3*^{-/-} mice ("WT Naive": gMFI 212, "WT PbA": gMFI 481, "*Batf3*^{-/-} Naive": gMFI 246, "*Batf3*^{-/-} PbA" gMFI 451, ; Fig. 3.17C).

In summary, frequencies of dendritic cells were higher in uninfected *Batf3*^{-/-} mice and in early infection but did not differ between d+6 PbA-infected *Batf3*^{-/-} and WT mice. Six days after PbA-infection, splenic CD4⁺ DCs from knock-out animals had a stronger upregulation of CD40 on their surface, but this observation was not consistent throughout all experiments.

3.1.3.5 Antigen-presenting cells in *Batf3*^{-/-} mice showed a reduced pro-inflammatory milieu on 3 dpi, compared to WT controls

Not only dendritic cells but also other antigen-presenting and phagocytic cells like neutrophils, Ly6C⁺ monocytes and macrophages help to fight an infection as part of the innate immune response but also for initiation and support for the adaptive immune response.

First, we were interested if frequencies of neutrophils, Ly6C⁺ monocytes or macrophages would change differently in *Batf3*^{-/-} and WT mice upon PbA-infection. Therefore spleens were harvested from those mice 6 days after PbA-infection and analyzed for these cell types by flow cytometry. Spleens of infected and naive mice of both strains were prepared as usual. After exclusion of T cells, NK cells, NKT cells, B cells and dendritic cells, the remaining cells were gated for CD11b before differentiation into Ly6C⁺Ly6G⁺ (neutrophils), Ly6C⁺Ly6G⁻ (Ly6C⁺ monocytes) or Ly6C⁻Ly6G⁻ (macrophages) subsets.

The flow cytometric analysis did not reveal any differences in CD11b⁺ frequency in d+3 PbA-infected WT mice compared to their naive controls, but a significant increase of these cells in d+3 PbA-infected *Batf3*^{-/-} mice compared to their WT infection controls (fold change to "WT Naive" on 3 dpi: "WT PbA" 1.03 vs. "*Batf3*^{-/-} PbA" 1.43, $p < 0.01$; Fig. 3.18A). Six days after infection, the frequencies of CD11b⁺ cells in spleens of PbA-infected mice dropped in both groups and the difference seen on 3 dpi was no longer significant (fold change to "WT Naive" on 6 dpi: "WT PbA" 0.31 vs. "*Batf3*^{-/-} PbA" 0.54, not significant; Fig. 3.18A).

CD11b⁺ cells were then gated for Ly6C and Ly6G to distinguish between neutrophils (Fig. 3.18B), Ly6C⁺ monocytes (fig, 3.18C) and other macrophages (Fig. 3.18D). When analyzing neutrophils we did observe a small decrease of neutrophil frequencies on 3 dpi, followed by a strong increase in frequencies on 6 dpi in both PbA-infected groups. Differences between WT and *Batf3*^{-/-} mice were very small and only 3 dpi revealed significant differences ($p < 0.05$, as spleens of *Batf3*^{-/-} mice contained slightly more neutrophils among CD11b⁺ cells (fold change to "WT Naive" on 3 dpi: "WT PbA" 0.63 vs. "*Batf3*^{-/-} PbA" 0.75, not significant; on 6 dpi: "WT PbA" 1.90 vs. "*Batf3*^{-/-} PbA" 1.89, not significant; Fig. 3.18B).

While there was also no difference between naive WT and *Batf3*^{-/-} mice in the percentage of Ly6C⁺ monocytes (fold change to "WT Naive" 0.99), the analysis of d+3 infected mice revealed a significant increase of Ly6C⁺ monocytes in spleens of WT mice but not in *Batf3*^{-/-} mice (fold change to "WT Naive" on 3 dpi: "WT PbA" 1.43 vs. "*Batf3*^{-/-}

3.1. *Batf3*^{-/-} MICE WERE PROTECTED FROM EXPERIMENTAL CEREBRAL MALARIA AFTER PBA-INFECTION

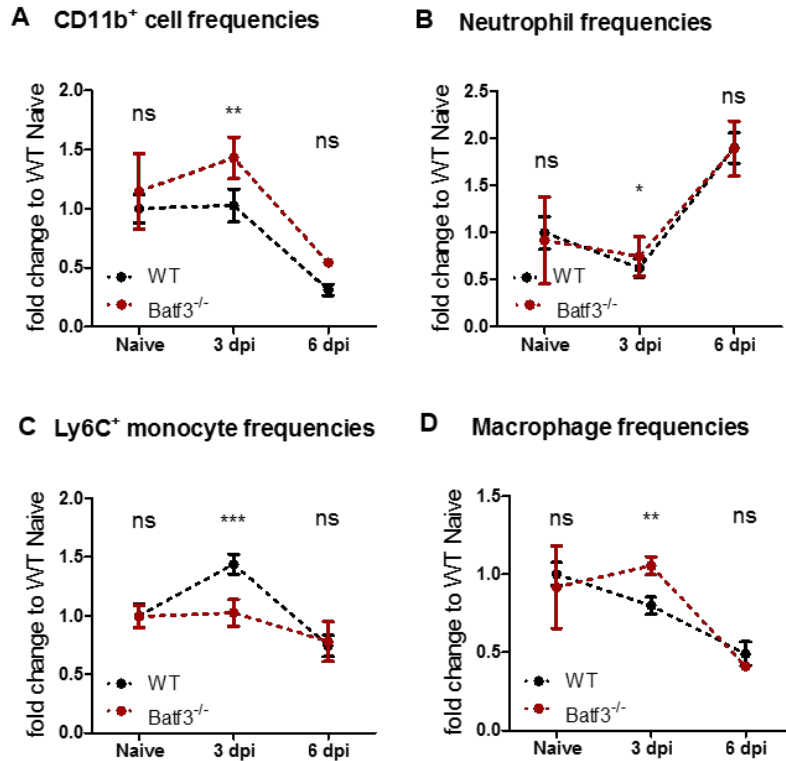


Figure 3.18: **Inflammatory monocytes were not increased in spleens of *Batf3*^{-/-} but in WT mice on dpi 3.** Spleens of PbA-infected (3 and 6 dpi) and naive WT and *Batf3*^{-/-} mice (n=3-6) were analyzed for CD11b⁺ cells by FACS (A), after exclusion of other cell subsets and further differentiated into neutrophils (Ly6C⁺Ly6G⁺, B), Ly6C⁺ monocytes (Ly6C⁺Ly6G⁻, C) or macrophages (Ly6C⁻Ly6G⁻, D). Values from different time points of analysis are presented as mean fold change (\pm SD) to naive WT mice. Dashed lines are shown for better visualization but time points were analyzed in different mice. Differences were tested separately with ANOVA followed by the Tukey post-test; p values below 0.05 were considered significant (* = p < 0.05, ** = p < 0.01, *** = p < 0.001).

PbA” 1.02, p < 0.001; Fig. 3.18C). Accordingly, the amount of other macrophages was significantly reduced in PbA-infected WT mice on 3 dpi when compared to synchronistic infected *Batf3*^{-/-} mice (fold change to ”WT Naive” on 3 dpi: ”WT PbA” 0.80 vs. ”*Batf3*^{-/-} PbA” 1.05, p < 0.01; Fig. 3.18D).

Interestingly, we observed a reduction in Ly6C⁺ monocytes and other macrophage populations in d+6 PbA-infected WT and *Batf3*^{-/-} mice, but no differences between both strains in the late phase of infection (fold change to ”WT Naive” in Ly6C⁺ monocytes: ”WT PbA” 0.74 vs. ”*Batf3*^{-/-} PbA” 0.78, not significant; in other macrophages: ”WT PbA” 0.49 vs. ”*Batf3*^{-/-} PbA” 0.41, not significant; Fig. 3.18C, D).

Overall we saw a shift to more Ly6C⁺ monocytes in splenic CD11b⁺ cells in WT mice but not in *Batf3*^{-/-} mice on 3 dpi. Analyses on 6 dpi did not reveal any differences in

CD11b+ cells and defined subsets.

Additionally to surface markers on dendritic cells, we checked for cytokines like TNF and CCL2 that are produced by antigen-presenting cells, in supernatants of cultured splenocytes, that were isolated from d+3 PbA-infected WT and *Batf3*^{-/-} mice or their respective controls and incubated for 24h.

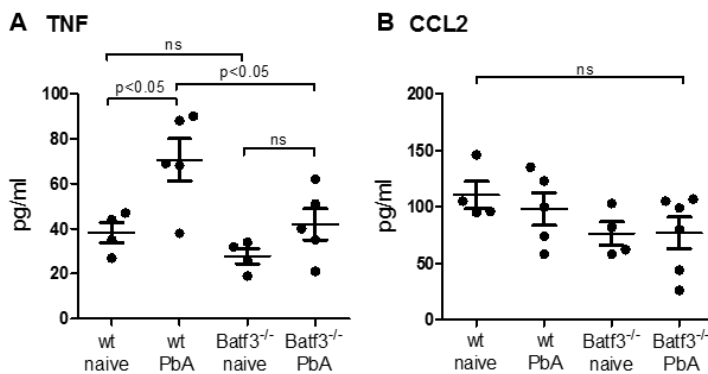


Figure 3.19: **TNF production in the spleen was increased 3 days after PbA-infection, but CCL2 levels remained unchanged.** Cytokine production for TNF (A) and CCL2 (B) was measured in spleen cells harvested 3 days after PbA-infection and uninfected animals (WT and *Batf3*^{-/-}; n=4-6). Cells supernatant was collected after 24h and subjected to an ELISA assay. Results are shown as mean (\pm SEM). Statistical differences with $p < 0.05$ calculated with ANOVA + Tukey were considered significant.

TNF was similar in supernatants of naive mice from both strains (WT: 38.3 pg/ml, *Batf3*^{-/-}: 27.8 pg/ml) and increased upon PbA-infection (3 dpi) (WT: 68.0 pg/ml, *Batf3*^{-/-}: 41.8 pg/ml; Fig. 3.19A). Importantly, splenocyte cultures of PbA-infected WT mice produced significantly more TNF than PbA-infected *Batf3*^{-/-} mice and also naive WT controls ($p < 0.05$). CCL2 production of splenocytes did not differ between all analyzed groups (76-110 pg/ml; Fig. 3.19B)

In summary, we observed a significantly reduced TNF production from splenocytes of PbA-infected *Batf3*^{-/-} mice when compared to infected WT mice, but CCL2 levels remained unchanged in all groups.

3.1.3.6 Phagocytic capacity of CD11b⁺ cells from PbA-infected *Batf3*^{-/-} mice was reduced on 6 dpi compared to WT mice

Antigen-presentation is indispensable for initiation of the adaptive immune response. Antigen uptake (phagocytosis) is an important first step to its later presentation by MHC class II molecules, which leads to activation of CD4⁺ T cells. As *Batf3*^{-/-} mice lack cross-presenting dendritic cells we were interested to see if other classical antigen-presenting cells would differ in their ability to take up antigen. To answer this question we set up a phagocytosis assay where spleen cells from uninfected and PbA-infected mice (6 dpi, WT and *Batf3*^{-/-}) were first MACS-sorted for CD11b. Sorted cells were then incubated with opsonized, fluorescent labeled beads for one hour to give cells time to take up the beads. For opsonation beads were incubated with pooled plasma from naive and infected mice of both strains.

Combination of serum opsonized beads and cells (see also Table 2.1)

Cells*:	Plasma**:	WT Naive	WT PbA	<i>Batf3</i> ^{-/-} Naive	<i>Batf3</i> ^{-/-} PbA
CD11b ⁺ WT Naive		X	X	X	X
CD11b ⁺ WT PbA		X	X	X	X
CD11b ⁺ <i>Batf3</i> ^{-/-} Naive		X	X	X	X
CD11b ⁺ <i>Batf3</i> ^{-/-} PbA		X	X	X	X

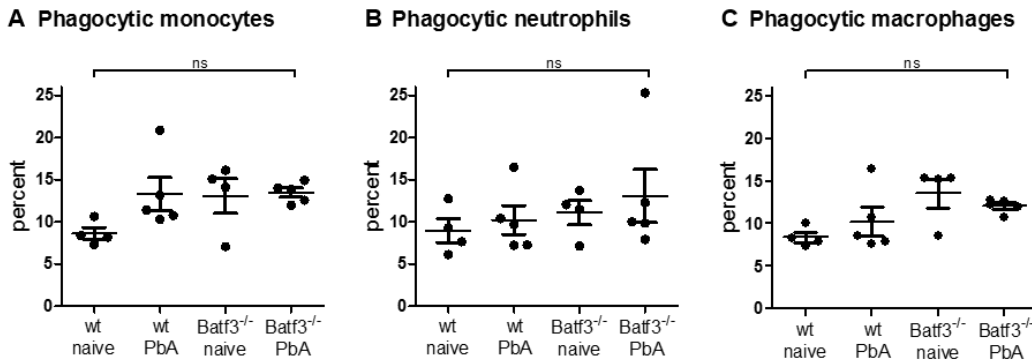
*Source of potential phagocytosing cells; single approaches for all animals per group

** Source of plasma for bead opsonation; pooled plasma from all animals in one group

We first compared the phagocytic activity in CD11b⁺ cells after PbA-infection separately for Ly6C⁺ monocytes (Ly6C⁺Ly6G⁻), neutrophils (Ly6C⁺Ly6G⁺) and macrophages (Ly6C⁻Ly6G⁻) on 3 dpi. Overall around 10% of CD11b⁺ cells were able to phagocytose the beads opsonized with serum from the corresponding groups ("matched approach", Fig. 3.20). However, we could neither observe any difference between the two different mouse strains nor between d+3 PbA-infected mice and their uninfected controls. Incubating cells from uninfected mice with beads opsonized with serum from infected mice and vice versa did not alter these findings.

When we analyzed the phagocytic capacity 6 days after PbA-infection, the frequency of phagocytic splenic monocytes was significantly increased in WT mice as compared to

3 dpi



6 dpi

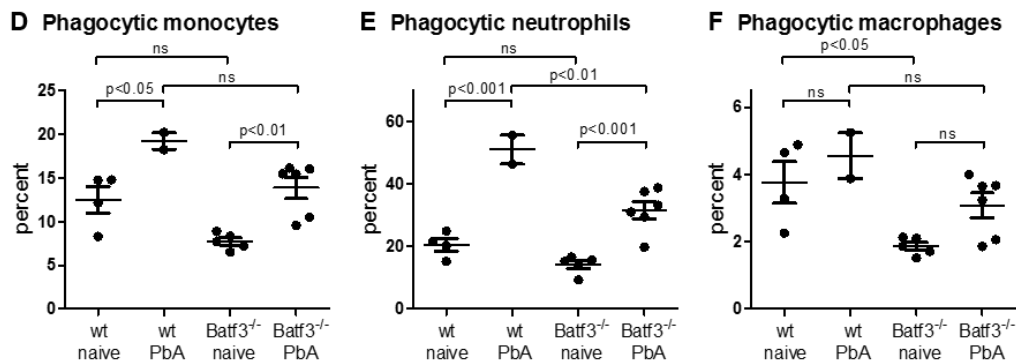


Figure 3.20: **Phagocytosis of APCs in the spleen was impaired in *Batf3*^{-/-} mice on 6 dpi but not changed in early PbA-infection (3 dpi).** Phagocytic activity was tested with a bead-uptake-assay 3 and 6 days after PbA-infection in WT (n=2-5) and *Batf3*^{-/-} mice (n=5-6) and their respective naive controls (n=4-5). For enhancement of bead uptake, beads were opsonized with plasma from the corresponding groups. Graphs show the percentage of different CD11b⁺ cell subsets that were able to take up beads during one hour incubation. Cell subsets were differentiated via FACS staining into Ly6C⁺ monocytes (CD11b⁺Ly6C⁺Ly6G⁻; A: 3 dpi, D 6 dpi), neutrophils (CD11b⁺Ly6C⁺Ly6G⁺; B: 3 dpi, E 6 dpi) and macrophages (CD11b⁺Ly6C⁻Ly6G⁻; C: 3 dpi, F 6 dpi). Data is shown as mean (\pm SEM), statistical significance was tested with ANOVA followed by Tukey post test. p values less than 0.05 were considered significant.

samples from naive WT controls ("WT Naive": 12.1%, "WT PbA": 19.2%, "p < 0.05; 3.20D). This was also observed in samples from *Batf3*^{-/-} mice when we compared naive and PbA-infected mice (7.7% in naive to 13.9% in infected animals, p < 0.05). Similar to analysis on 3 dpi, phagocytosis in naive *Batf3*^{-/-} mice did not differ significantly to WT mice).

Similarly, in splenic neutrophils from WT and *Batf3*^{-/-} mice the capacity to phagocytose beads increased significantly in both strains upon in PbA-infection ("WT Naive":

20.5%, "WT PbA": 51%, "*Batf3*^{-/-} Naive": 14.2%, "*Batf3*^{-/-} PbA": 32.6%, $p < 0.001$; Fig. 3.20E). Importantly, while the phagocytic capacity increased in both strains after PbA-infection, splenic neutrophils from *Batf3*^{-/-} mice took up significantly less beads than neutrophils from WT mice ($p < 0.01$). Again, no significant difference between naive mice from both strains were observed.

Analysis of macrophages showed that only few cells of this subtype were able to phagocytose the beads in this experiment (1.5-5.2%); 3.20F. However, a trend to more phagocytosis in infected animals of both strains remained (WT 3.8 vs. 4.6%, *Batf3*^{-/-} 1.9% vs. 3.1%). In this experiment cells isolated from naive *Batf3*^{-/-} mice showed a small decrease in phagocytic activity when compared to naive WT animals ($p < 0.05$).

Additionally to the described "matched" setup (beads were opsonized with plasma from one group and then incubated with CD11b⁺ cells from the same group), we also performed "mixed approaches" (incubation of beads that were opsonized with plasma from naive WT and PbA-infected mice and then incubated with CD11b⁺ cells from all groups; see Chapter 2.2.9). First, we observed that more cells from naive mice of both strains ingested beads which were opsonized with plasma from PbA-infected WT mice (compared to uptake of bead opsonized with naive plasma). On the other hand, less WT PbA-CD11b⁺ cells were able to phagocytose beads that were incubated with naive plasma compared to opsonation with PbA-plasma.

In summary, phagocytic activity was not changed in any CD11b⁺ cell subset in early PbA-infection (3 dpi) in neither WT nor *Batf3*^{-/-} mice and no differences between both strains were seen. Six days after infection, we observed an increase in phagocytic activity in both mouse strains after PbA-infection, but this increase was less in *Batf3*^{-/-} mice. Interestingly, our "mixed approach" showed that the plasma that was used to opsonize the beads was also influencing the number of beads that were taken up by CD11b⁺ cells.

3.1.3.7 Immune regulatory mechanisms in PbA-infected *Batf3*^{-/-} mice were elevated on 6 dpi

Pro-inflammatory immune responses need regulatory mechanisms to prevent damage to healthy cells by undesired side effects of the immune response. As cerebral malaria is partly caused by an overwhelming immune response to the parasite, the role of regulatory immune mechanisms in *Plasmodium* infections have to be considered. The analyses of

PbA-infected *Batf3*^{-/-} mice revealed complete protection from ECM in these mice and an impaired cytotoxic activity in CD8⁺ T cells. We were now interested whether the protection from ECM in *Batf3*^{-/-} mice was caused not only by attenuated cytotoxicity in T cells but also by active regulatory mechanism. As regulatory functions are described to take also place early in infection [Mitchell et al., 2005], we compared spleens of PbA-infected WT and *Batf3*^{-/-} mice on 3 and 6 dpi with naive animals serving as controls.

First, we analyzed the capability of splenocytes to produce the regulatory cytokine IL-10 in whole spleen cell cultures from all experimental groups on 3 and 6 dpi. Therefore, single cell suspensions were generated from harvested spleens and cultured for 24h.

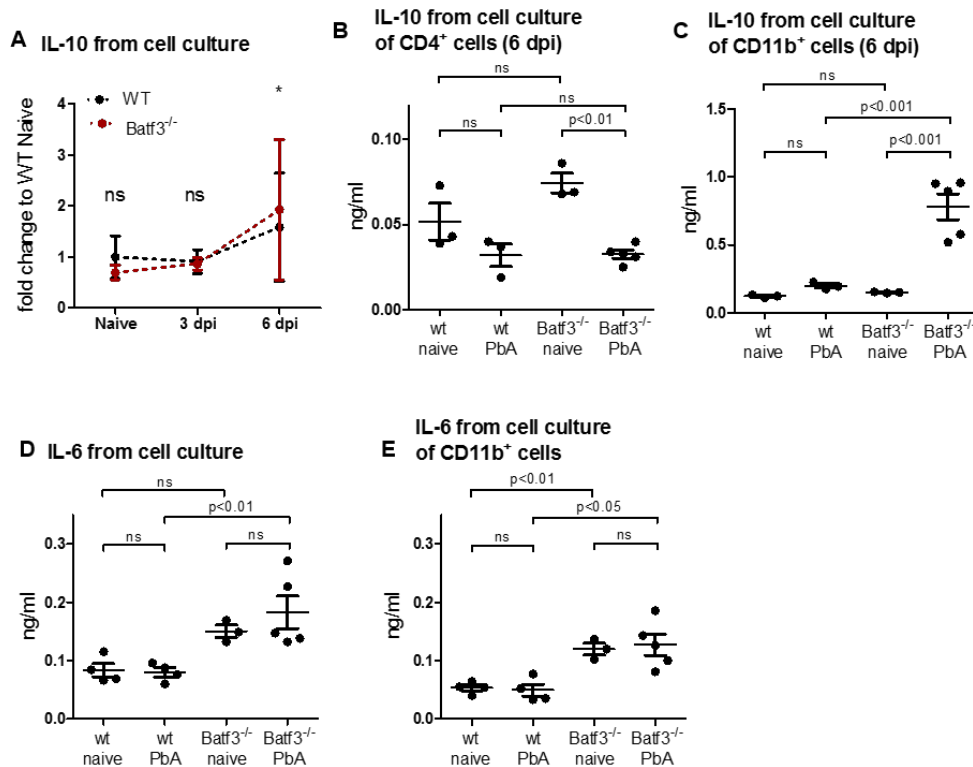


Figure 3.21: **IL-10 and IL-6 production from splenic CD11b⁺ cells was increased in PbA-infected *Batf3*^{-/-} mice.** WT and *Batf3*^{-/-} mice were infected with PbA (n=3-5) and spleens were analyzed 3 and 6 days later. Naive mice (n=3) served as controls. IL-10 was measured in supernatant of 24h incubated splenocyte culture with whole spleen cell suspension (A) or cells sorted for CD4 (B) or CD11b (C). IL-6- was measured in supernatants of whole splenocytes cultures (D) and cultured CD11b MACS-sorted cells (E) that were obtained from d+6 PbA-infected and naive mice. Results from 6 dpi are presented as mean (\pm SEM). Values from different time points of analysis are presented as mean fold change (\pm SD) to naive WT mice. Dashed lines are shown for better visualization but time points were analyzed in different mice. All differences were tested separately with ANOVA followed by the Tukey post-test; p values below 0.05 were considered significant (* = p < 0.05, ** = p < 0.01, *** = p < 0.001).

The ELISA of samples from whole splenocyte cultures did not show any significant difference in all experimental groups without PbA-infection and on 3 dpi, however we observed increased IL-10 production at 6 dpi in both groups with more IL-10 in supernatants of splenocyte culture from *Batf3*^{-/-} mice (fold change to "WT Naive" on 3 dpi: "WT PbA" 0.91 vs. "*Batf3*^{-/-} PbA" 0.87, not significant; on 6 dpi: "WT PbA" 1.59 vs. "*Batf3*^{-/-} PbA" 1.93, $p < 0.05$; Fig. 3.21A). Repetition experiments showed similar trends, but not all reached significance with this number of experimental animals per group.

We observed increased IL-10 levels in splenocyte cultures from *Batf3*^{-/-} mice on 6 dpi and therefore, asked which cell type could be the source of the measured IL-10, as it can be produced by different immune cells with regulatory functions like CD4⁺ T cells, M2 Macrophages, CD11b⁺ dendritic cells but also by B cells. We analyzed IL-10 in supernatant of MACS-purified CD4⁺ (mainly T cells) and CD11b⁺ (macrophages, dendritic cells) cells which were cultured separately to gain insight in the source of IL-10 production. As also IL-6 can be produced by M2 macrophages, we measured this interleukin in CD11b⁺ cell culture.

IL-10 production from in CD4⁺ sorted spleen cells was rather low in general (around 6-fold less compared to total spleen cell culture) and PbA-infection further reduced IL-10 production in both strains ("WT Naive": 0.05 ng/ml, "WT PbA": 0.03 ng/ml, "*Batf3*^{-/-} Naive": 0.07 ng/ml, "*Batf3*^{-/-} PbA": 0.03 ng/ml; Fig. 3.21B). The difference between naive and infected *Batf3*^{-/-} mice was big enough to reach statistical significance ($p < 0.01$) which was not the case in the WT groups. Interestingly, CD11b⁺ cells from naive mice of both groups but also PbA-infected WT mice produced only low levels of IL-10 while production of this cytokine was markedly increased in PbA-infected *Batf3*^{-/-} mice ("WT Naive": 0.12ng/ml, "WT PbA": 0.20 ng/ml, "*Batf3*^{-/-} Naive": 0.15 ng/ml, "*Batf3*^{-/-} PbA": 0.78 ng/ml, $p < 0.001$; Fig. 3.21C).

IL-6 levels in supernatants of whole spleen cell cultures and in MACS-sorted CD11b⁺ splenocytes cultures were generally higher in *Batf3*^{-/-} mice compared to WT mice, independent of the infection status, but interestingly, IL-6 production did not change significantly in either group upon PbA-infection. (whole splenocyte culture: "WT Naive": 0.08 ng/ml, "WT PbA": 0.08 ng/ml, "*Batf3*^{-/-} Naive": 0.15 ng/ml, "*Batf3*^{-/-} PbA": 0.18 ng/ml, $p < 0.05$; CD11b⁺ cell culture: "WT Naive": 0.05 ng/ml, "WT PbA": 0.05 ng/ml, "*Batf3*^{-/-} Naive": 0.12 ng/ml, "*Batf3*^{-/-} PbA": 0.13 ng/ml, $p < 0.05$; Fig. 3.21D,E).

In summary, we observed higher levels of IL-10 in spleen cell culture supernatant from d+6 PbA-infected *Batf3*^{-/-} mice, especially in cultures containing CD11b⁺ cells, which also produced more IL-6.

After detection of increased IL-10 production in *Batf3*^{-/-} mice, we investigated possibly regulatory cell types, which could be the source of IL-10, in more detail. CD4⁺ T cells did not produced more IL-10 in cell culture, but a change in cell number could alter the regulatory milieu in *Batf3*^{-/-} mice after PbA-infection. In the previous experiments we discovered an expanded CD4⁺ T cell population in PbA-infected *Batf3*^{-/-} mice 3 and 6 days p.i. (increased CD4⁺ vs. CD8⁺ T cell ratio, 3.10B). Therefore we first analyzed CD4⁺ and CD8⁺ T cells for common markers of regulatory T cells (*T_{reg}*), FoxP3 (intracellular) and CD25, but also for the programmed death protein 1 (PD-1) which has immune regulatory functions and is found on the surface of T cells. PD-1 has been shown to be involved in T cell exhaustion in a mouse model of chronic malaria [Horne-Debets et al., 2013].

Analyses of *T_{regs}* (FoxP3⁺CD25⁺) in spleens of experimental animals revealed significantly higher *T_{reg}* frequencies in naive *Batf3*^{-/-} mice compared to naive WT mice (fold change 1.30, $p < 0.001$, Fig. 3.22A). However, after a small increase on 3 dpi, the *T_{reg}* frequencies in PbA-infected *Batf3*^{-/-} dropped again to similar levels on 6 dpi as in naive mice, while in WT mice the *T_{reg}* frequencies increased steadily throughout infection. These different progresses in *T_{reg}* populations led to more *T_{regs}* in *Batf3*^{-/-} mice on 3 dpi, but less on 6 dpi (fold change to "WT Naive" on 3 dpi: "WT PbA" 1.35 vs. "*Batf3*^{-/-} PbA" 1.54, $p < 0.01$; on 6 dpi: "WT PbA" 1.65 vs. "*Batf3*^{-/-} PbA" 1.25, $p < 0.05$; Fig. 3.22A).

Interestingly, the increase in CD4⁺ vs CD8⁺ T cell ratio in PbA-infected *Batf3*^{-/-} mice did not have an impact on *T_{reg}* populations. A calculation of frequencies of all T cells revealed that naive *Batf3*^{-/-} mice contained more FoxP3⁺CD25⁺ cells in their spleens compared to uninfected WT mice (WT: 5.8%, *Batf3*^{-/-} 3: 7.9%, $p < 0.05$). The *T_{reg}* percentages increased in WT mice 6 days after infection (9.6%, $p < 0.001$) but did not change in PbA-infected *Batf3*^{-/-} mice (7.3%; Fig. 3.22B). Comparing the frequencies of regulatory T cells in the "WT PbA"-group and the "*Batf3*^{-/-} PbA"-group, revealed a significant ($p < 0.01$) decrease of FoxP3⁺CD25⁺ cells in the knock-out animals. However, when calculating against the total spleen cell number, which was higher in PbA-infected *Batf3*^{-/-} mice, these differences were reversed. The total number of *T_{regs}* in spleens of *Batf3*^{-/-} mice was significantly higher than in their WT infection controls ($p < 0.001$) and

3.1. *Batf3*^{-/-} MICE WERE PROTECTED FROM EXPERIMENTAL CEREBRAL MALARIA AFTER PBA-INFECTION

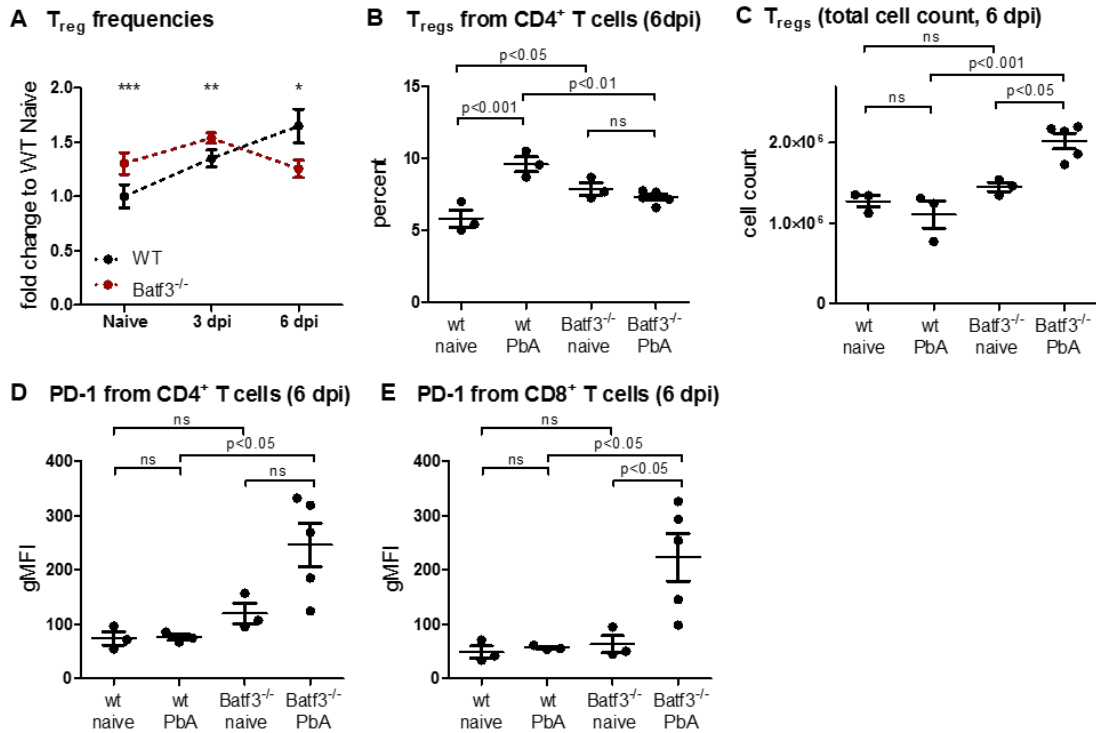


Figure 3.22: The total amount of T_{regs} was increased in spleens of PbA-infected *Batf3*^{-/-} mice on 6 dpi. WT and *Batf3*^{-/-} mice were infected with PbA (n=3-6) and spleens were analyzed at 3 and 6 dpi. Naive mice (n=3-4) were used as controls. A: T cells were identified via FACS as described before and CD4⁺ cells were analyzed via flow cytometry for CD25 and FoxP3 double positive cells (T_{regs}). Fractions were calculated to present the percentage of T_{regs} from all T cells. B and C: T_{regs} at dpi are shown separately in frequency and total cell count. D and E: PD-1 expression was analyzed on CD4⁺ and CD8⁺ T cells by calculation of the geometrical mean fluorescence intensity. Results from 6 dpi are presented as mean (±SEM). Values from different time points of analysis are presented as mean fold change (±SD) to naive WT mice. Dashed lines are shown for better visualization but time points were analyzed in different mice. All differences were tested separately with ANOVA followed by the Tukey post-test; p values below 0.05 were considered significant (* = p < 0.05, ** = p < 0.01, *** = p < 0.001).

naive *Batf3*^{-/-} mice (p < 0.05). Naive mice from both groups did not differ in their total amount of T_{regs} in their spleens and the relative increase seen in FoxP3⁺CD25⁺ cells among CD4⁺ T cells from PbA-infected WT mice compared to their naive controls was no longer observed in the total cell amount ("WT Naive": 1.3e6 cells, "WT PbA": 1.1e6 cells, "*Batf3*^{-/-} Naive": 1.4e6 cells, "*Batf3*^{-/-} PbA": 2.0e6 cells; Fig. 3.22C).

PD-1 expression was low on both CD4⁺ and CD8⁺ T cells in WT mice, independent of their infection status ("WT Naive": gMFI on CD4⁺ 74, gMFI on CD8⁺ 49, "WT PbA": gMFI on CD4⁺ 75, gMFI on CD8⁺ 57; Fig. 3.22D, E). Naive *Batf3*^{-/-} showed similar expression patterns, but PbA-infection led to a significant (p < 0.05) increase of PD-1

on T cells in *Batf3*^{-/-} mice ("Batf3^{-/-} Naive": gMFI on CD4⁺ 120, gMFI on CD8⁺ 63, "Batf3^{-/-} PbA": gMFI on CD4⁺ 246, gMFI on CD8⁺ 223; Fig. 3.22D, E). However, the increased PD-1 expression on cells from infected *Batf3*^{-/-} mice was less prominent in other experiments. Further experiments are required to draw final conclusions.

Splenic NK cells, which can also contribute to regulatory mechanisms, showed similar increased expression of PD-1 in d+6 PbA-infected *Batf3*^{-/-} mice, comparable to the results from T cell analysis and additional increased CTLA-4 expression (Fig. S16). Both surface markers have been shown to down-regulate IFN γ production in NK cells [Stojanovic et al., 2014, Alvarez et al., 2010].

We did not observe an expansion of T_{reg} frequencies but a higher number of total T_{regs} in *Batf3*^{-/-} mice on 6 dpi and higher PD-1 levels in CD4⁺ and CD8⁺ T cells from d+6 infected *Batf3*^{-/-} mice.

Alternatively activated macrophages (AAM) are another type of regulatory immune cells, which could play a role in the development of cerebral malaria [Besnard et al., 2015]. As we observed increased levels of IL-10 and IL-6 in supernatants of cultured CD11b⁺ cells, we analyzed spleens of PbA-infected WT and *Batf3*^{-/-} for the presence of AAM. Therefore, splenocytes were prepared for analysis as described before and AAMs were identified from CD11b⁺ cells as F4/80^{hi}Relm α ^{hi}Ly6C^{lo}Ly6G^{int}.

Flow cytometry analysis of CD11b⁺ cells for alternatively activated macrophages showed different cell populations that were differentiated into AAMs (F4/80^{hi}Relm α ^{hi}Ly6C^{lo}Ly6G^{int}; dark green), neutrophils (F4/80^{neg}Relm α ^{neg}Ly6C^{int}Ly6G^{hi}; light green) and monocytes (F4/80^{int}Relm α ^{neg}Ly6C^{hi}Ly6G^{neg}; light blue). An overlay of these population is shown in Fig. 3.23A. On average, 6.8% of CD11b⁺ splenocytes were identified as AAMs in uninfected WT and *Batf3*^{-/-} mice. Six days after PbA-infection, the frequencies of AAMs among CD11b⁺ cells decreased in spleens of both strains ("WT PbA": 1.0%, "Batf3^{-/-} PbA": 2.1%, p < 0.001 to naive controls; Fig. 3.23B). Despite the decrease of AAMs after infection, spleens of PbA-infected *Batf3*^{-/-} mice contained a significantly (p < 0.001) higher frequency of AAMs in their spleens when compared to WT infection-controls. This difference was even more prominent in total cell counts, as splenocytes counts (Fig. 3.8C) and CD11b⁺ cells (Fig. 3.18A) were higher in d+6-infected *Batf3*^{-/-} mice: spleens from both naive groups contained more AAMs than their infected counterparts, but PbA-infected *Batf3*^{-/-} mice showed almost 5-fold more AAMs than infected WT controls ("WT Naive": 3,406e5 cells, "WT PbA": 6,359e4 cells, "Batf3^{-/-} Naive": 4,971e5

3.1. *Batf3*^{-/-} MICE WERE PROTECTED FROM EXPERIMENTAL CEREBRAL MALARIA AFTER PBA-INFECTION

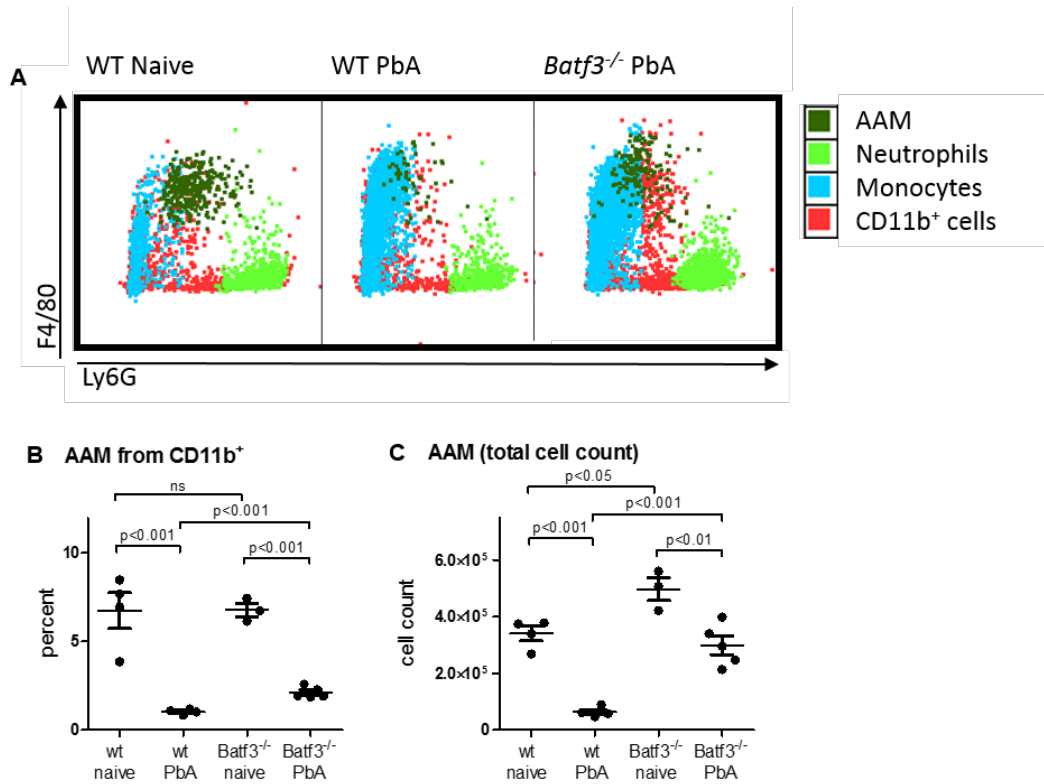


Figure 3.23: Splenic CD11b⁺ cells from d+6 PbA-infected *Batf3*^{-/-} mice contained higher frequencies of alternatively activated macrophages. WT and *Batf3*^{-/-} mice were infected with PbA and spleens were analyzed 6 days later with spleens from naive mice serving as controls (all n = 3-5). A: Representative dot plot of CD11b⁺ cells (red in dot plot, prepared and identified as before) from naive WT mice compared to PbA-infected WT and *Batf3*^{-/-} mice. Ly6C, Ly6G, F4/80 and Relm α were used to distinguish between AAMs (F4/80^{hi}Relm α ^{hi}Ly6C^{lo}Ly6G^{int}; dark green), neutrophils (F4/80^{neg}Relm α ^{neg}Ly6C^{int}Ly6G^{hi}; light green) and monocytes (F4/80^{int}Relm α ^{neg}Ly6C^{hi}Ly6G^{neg}; light blue). Relative amount of AAMs among CD11b⁺ splenocytes (B) and total AAM count (C) are shown for all experimental groups. Results are presented as mean (\pm SEM). After confirmation of overall statistical significance with ANOVA paired with Tukey post test, differences between two groups were tested additionally with an unpaired t-test; p < 0.05 was considered significant.

cells, " *Batf3*^{-/-} PbA": 2,992e5, "WT PbA" vs. " *Batf3*^{-/-} PbA" p < 0.001; Fig. 3.23C).

In summary, these results showed that spleens of *Batf3*^{-/-} mice show a more immune regulatory phenotype when compared to WT mice after PbA-infection. We observed higher levels of regulatory cytokine IL-10 and elevated total amounts of T_{regs} and alternatively activated macrophages in spleens of PbA-infected *Batf3*^{-/-} mice. Additionally, the expression of regulatory PD-1 was increased in *Batf3*^{-/-} mice after PbA-infection on T cells and NK cells.

3.2 ECM development after doxycycline administration from 4 dpi

An artemisinin-based combination therapy (ACT) is the standard treatment in human malaria in order to achieve rapid parasite elimination [WHO, 2015]. The tetracycline derivate doxycycline, that was initially developed as a broad-spectrum antibiotic, is available as follow-up treatment and prophylaxis but no longer in the treatment guidelines as first line treatment [WHO, 2015], because of its slow anti-plasmodial effect. Nevertheless, we found this drug to be interesting because of its described additional anti-inflammatory properties [Krakauer and Buckley, 2003, Griffin et al., 2011], which prompted us to investigate a possible use of doxycycline not only as an anti-parasitic drug but in the control of the *Plasmodium* infection induced inflammatory processes in the brain that are associated with cerebral malaria. This first chapter will summarize our preliminary data that provided the background for further studies.

We made use of the standard murine CM model with experimental *P. berghei* ANKA infection of C57Bl/6 mice that are susceptible to experimental cerebral malaria (ECM, [Li et al., 2001]). In initial experiments we compared different routes of doxycycline administration in PbA-infected mice in order to find a treatment regimen that would prevent ECM in C57Bl/6 mice. Therefore, Bl/6 mice were infected with a standard dose of 5×10^4 iRBCs and subjected to different treatment regimens. Two groups received different doses (80 mg/kg/d or 250 mg/kg/d) of the drug orally (p.o.) and one group was injected intravenously (i.v.) with 80 mg/kg/d doxycycline. We determined the doses due to pharmacokinetic studies conducted by Prall et al. [Prall et al., 2002]. In this study, they compared plasma levels of doxycycline in mice and human after oral administration and found that 200 mg/d doxycycline in human, which is also the standard dose in malaria treatment [Lalloo et al., 2007], resembled a dose of 50-100 mg/kg/d given to mice in drinking water. We treated all groups once daily with their respective dose from 4 to 7 dpi. Untreated PbA-infected mice served as control. All mice were monitored for survival, disease score and parasitemia from 4 dpi on until the end of the experiment.

While untreated control mice developed ECM, as expected, between 6 and 8 dpi, we observed that all PbA-infected mice that received 80 mg/kg/d doxycycline i.v. were protected from ECM. In contrast, only 20-30% of the mice receiving oral doxycycline were protected from developing ECM (Fig. 3.24A). Thus, among the different approaches, only i.v. injection of 80 mg/kg/day doxycycline from 4 dpi was effective in ECM prevention

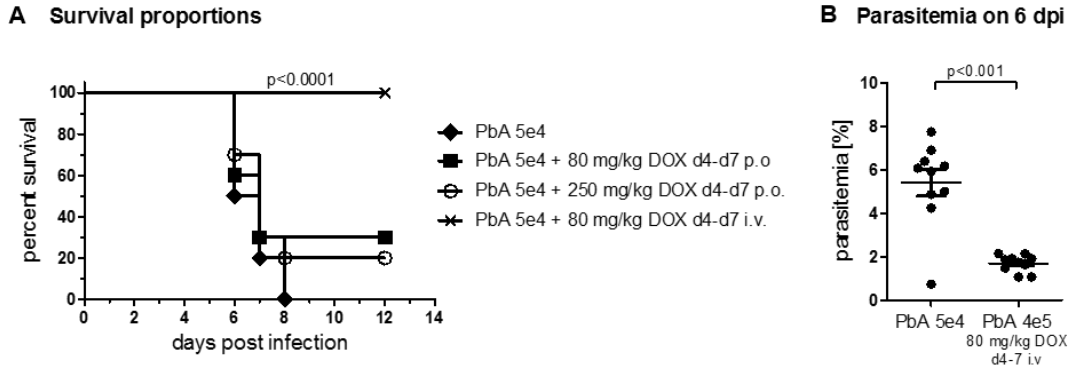


Figure 3.24: **Intravenous doxycycline prevented ECM when given from 4 dpi.** A: Survival was analyzed in mice that were infected with a dose of 5e4 PbA-infected RBCs. Groups of 10 mice each received doxycycline in oral form at 80 mg/kg/d (filled square) or 250 mg/kg/d (X) or an i.v. dose of 80 mg/kg/d (empty circle). One group was left untreated as infection control (filled diamond). B: Parasitemia was counted from blood smears of untreated PbA-infected mice and mice treated i.v. with doxycycline at 6 dpi, shortly before death of the untreated control group. Differences in survival were tested for significance with log-rank test. Statistical significance between the two groups for parasitemia were analyzed by t-test. p values below 0.05 were considered significant.

in PbA-infected Bl/6 mice, which was therefore used for the following experiments. Furthermore, we found that treatment for 3 days (4-6 dpi) was sufficient to prevent ECM.

Importantly, peripheral parasitemia was strongly reduced on 6 dpi in DOX treated mice when compared to untreated infection controls (Fig. 3.24B).

In order to analyze the anti-inflammatory effects of doxycycline treatment after *Plasmodium* infection, we characterized disease hallmarks like BBB disruption and immunological features of doxycycline-treated PbA-infected mice versus control-infected mice and naive controls. Both infected groups were inoculated i.v. with 5e4 iRBC and the treatment group received i.v. injections of 80 mg/kg/d doxycycline from 4 dpi on. Mice were sacrificed 6 days post infection and perfused with PBS before isolation of spleens and brains for various analyses.

Doxycycline-treated mice showed a stable blood-brain barrier, as seen in an Evans blue Assay (13.4 μg Evans blue / g brain in "PbA 5e4 + DOX": versus 80.8 μg Evans blue / g brain in untreated PbA-mice, $p < 0.05$, Fig. 3.25A) and reduced infiltration of peripheral immune cells into the brain (1.62e5 cells / brain in "PbA 5e4 + DOX": versus 4.64e5 cells / brain in "PbA 5e4", $p < 0.001$, Fig. 3.25B). Next we isolated mRNA from brain tissue from PbA-infected mice \pm DOX treatment on 6 dpi to analyze differences in gene expression in a PCR array. Brain tissue of DOX-treated mice revealed a significant reduction of cell adhesion molecules L- and P-selectin and cytokines CCL2, CCL5 and CXCL2 as

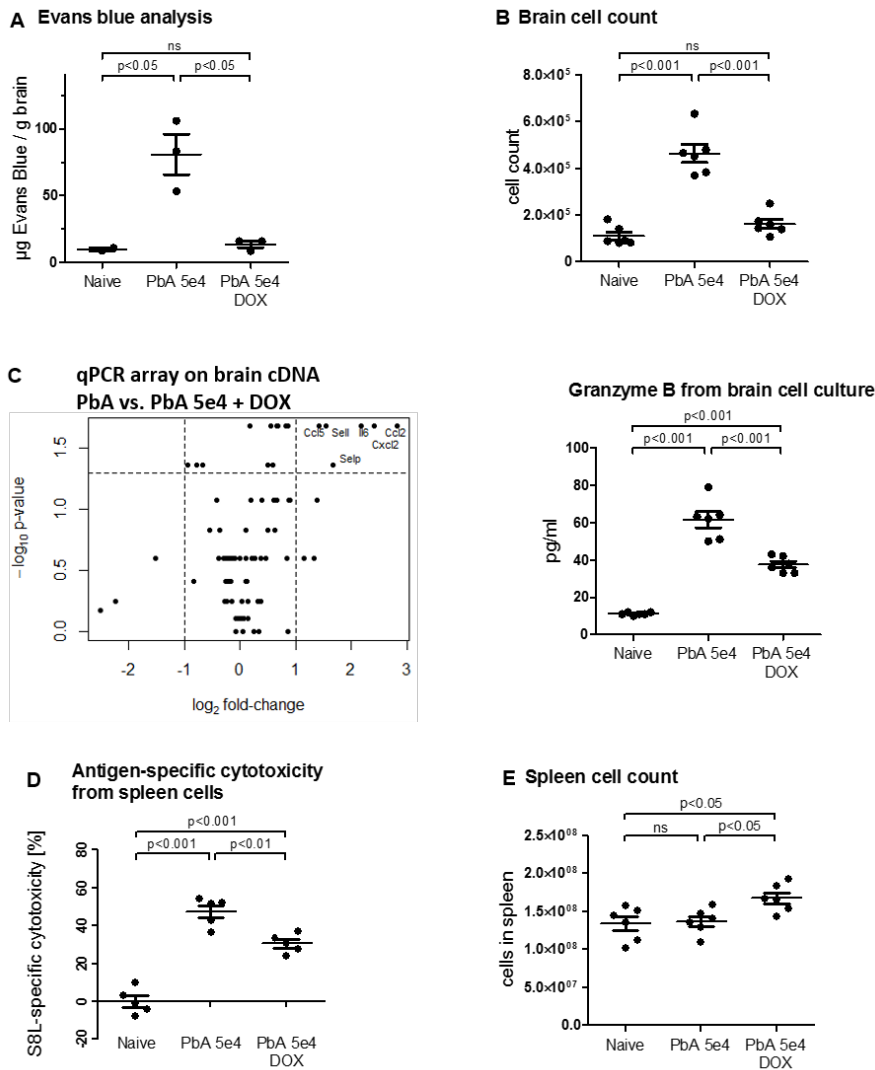


Figure 3.25: **Doxycycline treatment from 4 dpi led to a stable BBB and reduced cytotoxicity in PbA-infected mice.** Mice were infected with 5e4 iRBC and either treated with doxycycline (80 mg/kg/d i.v. from 4 dpi, "PbA 5e4 + DOX", n=3-6) or left untreated ("PbA 5e4", n=3-6). Naive mice served as controls ("Naive", n=3-6). All analyses were performed 6 days p.i. when untreated mice showed symptoms of neuro-specific symptoms. A: Mice were injected with 2% Evans blue dye i.v. and sacrificed after one hour. Brains were removed and EB was extracted by incubation in formamide for 2 days. Results are displayed as mean of Evans blue per gram brain. B: Lymphocytes were enriched with a percoll gradient after perfusion of d+6 infected mice. Total number of purified cells was counted. C: RNA was extracted from mice brains on 6 dpi, transcribed to cDNA and subjected to an PCR array. The dot plot graph shows differences in expression level of genes between PbA-infected mice versus PbA-infected mice that were treated with doxycycline. Values for \log_2 fold change and $-\log_{10}$ p-value are plotted against each other. The upper right corner represents genes that were considerably changed in their expression (fold change > 2) and their p-value considered significant ($p < 0.05$). D: Antigen-specific cytotoxicity was tested in an *in vivo* kill using peptide loaded target cells that were injected to mice on 5 dpi and the analyzed 18h later. E: Total number of spleen cells. Statistical analysis in A, B, D and E was performed with ANOVA, followed by Tukey post-test. Statistical analysis of the PCR-array (C) was done with the Mann-Whitney test and Benjamini-Hochberg correction. p values below 0.05 were considered significant.

well as IL-6, which are all associated with inflammatory processes, when compared to untreated PbA-infected mice (Fig. 3.25C). In addition to these results, that point to reduced inflammation in brains of doxycycline treated mice, we measured reduced parasite-specific cytotoxicity in spleens of DOX-treated mice compared to control-infected mice (30.5% lytic activity in "PbA 5e4+ DOX": versus 4.74 % lytic activity in "PbA 5e4", $p < 0.01$, Fig. 3.25D). Interestingly, we could observe an increase in total spleen cell numbers in DOX-treated mice compared to untreated infection controls and naive mice ("PbA 5e4 + DOX": 1.67e8 cells / spleen vs. "PbA 5e4": 1.37e8 cells and "Naive": 1.34e8 cells, $p < 0.05$; Fig. 3.25E). Naive and untreated PbA-infected mice did not differ significantly, but showed a small increase in infected mice in some experiments; however, the total splenocyte number was always higher in DOX-treated mice compared to all other groups.

The results that are summarized above (Fig. 3.24 and 3.25) were acquired during my diploma thesis. These data raised the question whether anti-inflammatory effects might have contributed to the protection from ECM, in addition to the well-described anti-parasitic effect of doxycycline. While parasite elimination is doubtless helpful in treatment of *Plasmodium* infection, it makes it difficult to distinguish between anti-inflammatory effects and decreases in inflammation due to reduced parasite load. The following experiments aim to overcome this problem and to study the anti-inflammatory features of doxycycline.

3.2.1 Increased splenocyte numbers in doxycycline treated mice was neither caused by altered migration patterns nor by increased proliferation

The observed low cell numbers in brains of doxycycline-treated, PbA-infected mice (Fig. 3.25B) and the concurrent increase in total spleen cell numbers (Fig. 3.25E) made us question whether doxycycline treatment resulted in a hampered ability of splenocytes from the treated group to migrate to the brains of infected animals. To address this question, we designed a migration assay where brain cells from d+6 PbA-infected mice were cultured in the bottom of a transwell plate together with FarRed labeled splenocytes in the upper well (see Fig. 2.2) The pores of the upper chamber were small enough to allow mainly active migration in contrast to cells falling through the pores. We expected the brain cells to produce cytokines which should attract cells from the upper chamber, which could give

us a hint about the *in vivo* situation. As cells have already reached the brain in untreated PbA-infected mice on 6 dpi, we decided to perform our experiment one day earlier, when migration occurs.

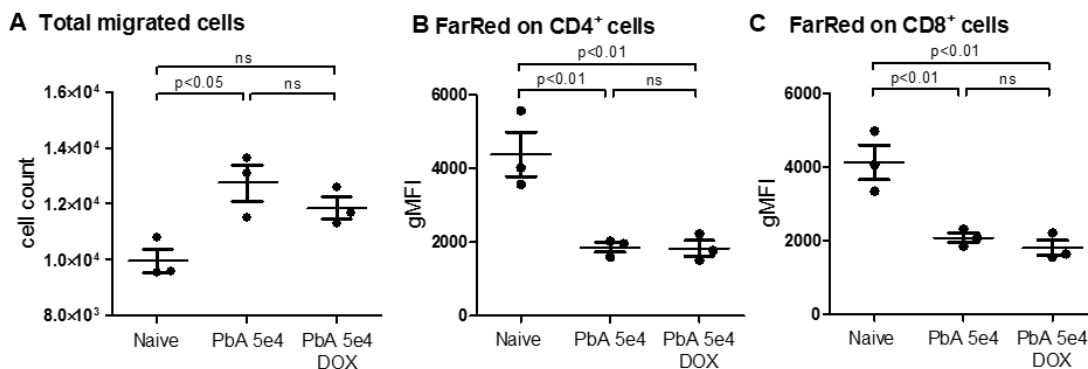


Figure 3.26: **Migration of spleen cells towards *in vitro* cultured brain cells was not altered in samples from doxycycline-treated mice.** Mice were intravenously injected with 80 mg/kg doxycycline daily from 4 dpi on. Brains and spleens were removed from these animals on 5 dpi and cultured for 6h in a transwell plate as with brain cells in the lower and fluorescently (FarRed) labeled spleen cells in the upper chamber, as depicted in Fig. 2.2. After this incubation period, cells in the lower chamber were analyzed for the presence of spleen cells (A, shown as total cells from 3e4 analyzed cells) and those spleen cells were further differentiated for CD4 and CD8, which were analyzed for their geometric mean fluorescent intensity of the FarRed labeling (B, C). Statistical analysis was performed with ANOVA, followed by Tukey post-test. p values below 0.05 were considered significant.

Analysis of the lower chamber of our transwell plate after 6 hours showed a background of 9.98×10^3 FarRed labeled cell in the 3×10^4 cells analyzed per well (Fig. 3.26A). After PbA-infection, the number of splenocytes among the analyzed cells increased significantly in untreated mice ($p < 0.05$), but not in doxycycline-treated animals ("PbA 5e4": 1.28×10^4 cells, "PbA 5e4+ DOX": 1.19×10^4 cells). However, the difference between doxycycline-treated and untreated mice after PbA-infection was only small and not significant. Additionally, we stained the cells from the lower well for CD4 and CD8 (mainly T cells of the respective subset) to be able to analyze especially the behavior of T cells in this assay. While there were no differences between CD4⁺, CD8⁺ and double negative cells in their migration pattern, we came across another interesting finding: CD4⁺ and CD8⁺ cells from PbA-infected mice had a lower mean fluorescence intensity of the FarRed label than cells from naive animals (gMFI FarRed on CD4⁺ cells: "Naive": 4378, "PbA 5e4": 1859, "PbA 5e4 + DOX": 1834, $p < 0.01$; gMFI FarRed on CD8⁺ cells: "Naive": 4129, "PbA 5e4": 2087, "PbA 5e4 + DOX": 1809, $p < 0.01$; Fig. 3.26B, C). These observations could be a sign of proliferation of these cells on PbA-infected mice. Again, we could not find a difference between PbA-infected mice with or without DOX treatment.

All together, we concluded, that doxycycline did not alter the migration pattern in this assay. However, improvement of the assay might provide more insights to this subject.

We further asked ourselves whether different proliferation activity of spleen cells in doxycycline treated PbA-infected mice could explain the higher splenocyte cell count in this group. BrdU is a synthetic nucleoside that is inserted in newly synthesized DNA instead of thymidine and can therefore be detected in proliferating cells. To analyze proliferation in our model, mice were given oral BrdU 2 days before splenocytes were isolated and stained for living cells with 7AAD followed by intracellular staining of BrdU. We analyzed the mice on 5 dpi and 6 dpi to get a picture shortly after treatment start and just before ECM onset in untreated controls.

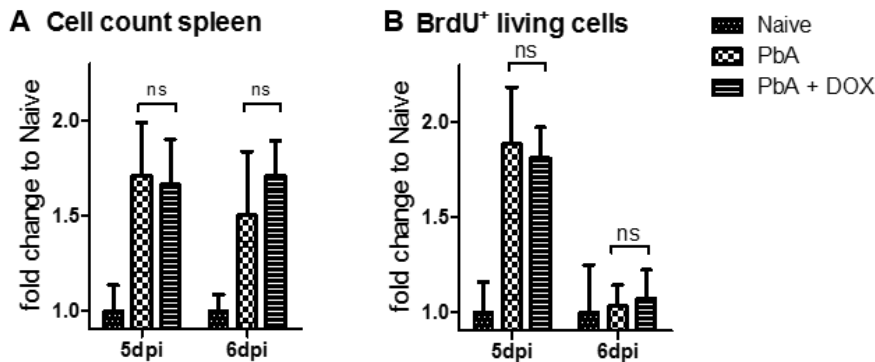


Figure 3.27: **Splenocytes from doxycycline-treated mice had a similar proliferation rate as untreated mice on 5 dpi.** Mice from all groups received BrdU 2, 1.5 and 0.5 days before analysis on 5 or 6 dpi. Animals in the "PbA + DOX" group were intravenously injected with 80 mg/kg doxycycline daily from 4 dpi on. Spleens were removed from all animal on 5 and 6 dpi (n = 4 / day / group). A: The total splenocyte count was determined with the help of a cell counter. B: Living cells were identified by flow cytometry analysis of 7AAD followed by intracellular BrdU staining as an indicator for proliferating cells. Mean results are presented as bars with SD. Statical analysis was performed with ANOVA, followed by Tukey post-test. p values below 0.05 were considered significant.

The total amount of spleen cells, counted from a single cell suspension with a cell counter, was already increased in both PbA-infected groups on 5 dpi when compared to naive mice (fold change to "Naive" on 5 dpi "PbA": 1.71, "PbA + DOX": 1.61) and remained at similar levels at 6 dpi (fold change to "Naive" on 6 dpi "PbA": 1.50, "PbA + DOX": 1.71; Fig. 3.27A). While differences in this experiment were not significant between both infected groups (\pm DOX) on 6 dpi, the trend of higher splenocyte counts in "PbA + DOX" mice remained. Interestingly, untreated mice showed a small decrease in cell numbers from 5 to 6 dpi, but the splenocyte count increased slightly in doxycycline

treated mice in the same time frame.

We detected an increase in proliferation in the spleens from d+5 PbA-infected mice (\pm DOX), as shown by higher frequencies of BrdU positive cells among living spleen cells, but no differences between both infected groups (fold change to "Naive" on 5 dpi "PbA": 1.88, "PbA + DOX": 1.81; Fig. 3.27B). Interestingly, proliferation was similar in all groups on 6 dpi (fold change to "Naive" on 6 dpi "PbA": 1.03, "PbA + DOX": 1.07; Fig. 3.27B).

These results showed, that the higher splenocyte counts from PbA-infected mice after doxycycline treatment compared to untreated controls was not caused by increased proliferation in the treated animals.

3.2.2 Higher infective dose in doxycycline treated animals allowed the comparison between treated and untreated animals with similar parasite loads

We next addressed the question whether mice with an increased parasite infectious load would still be protected from ECM and whether this approach could help to distinguish between DOX-induced anti-inflammatory effects and reduced inflammation due to anti-parasitic properties. Therefore, we infected the groups of mice that would receive doxycycline treatment with a higher initial dose of parasites in order to achieve the same blood parasitemia that is observed in untreated mice on 6 dpi, when they show first symptoms of ECM. We decided to infect mice intravenously with $1e6$ iRBCs in comparison to the infectious standard dose of $5e4$ iRBC that was used before and from each infection group, half of the infected animals were left untreated and the other half received the dose of doxycycline that was established before (80 mg/kg/d, 4-6 dpi). The groups were named "PbA $5e4$ \pm DOX" and "PbA $1e6$ \pm DOX".

Consistently with previous findings, the control group "PbA $5e4$ + DOX" survived PbA-infection past the time point of 20 dpi without any signs of ECM while untreated mice ("PbA $5e4$) developed severe neurological symptoms between 6-8 dpi and died from ECM (Fig. 3.28A+B). The group of mice that had been infected with an elevated dose of PbA iRBCs ("PbA $1e6$ ") also developed ECM and showed a similar survival (80% died before 10 dpi, Fig. 3.28A) and ECM score (Fig. 3.28B) as compared to $5e4$ infected mice.

Doxycycline treatment of mice infected with $1e6$ iRBC resulted in a similar protection from ECM and survival as we had observed before in doxycycline treatment of mice

3.2. ECM DEVELOPMENT AFTER DOXYCYCLINE ADMINISTRATION FROM 4 DPI

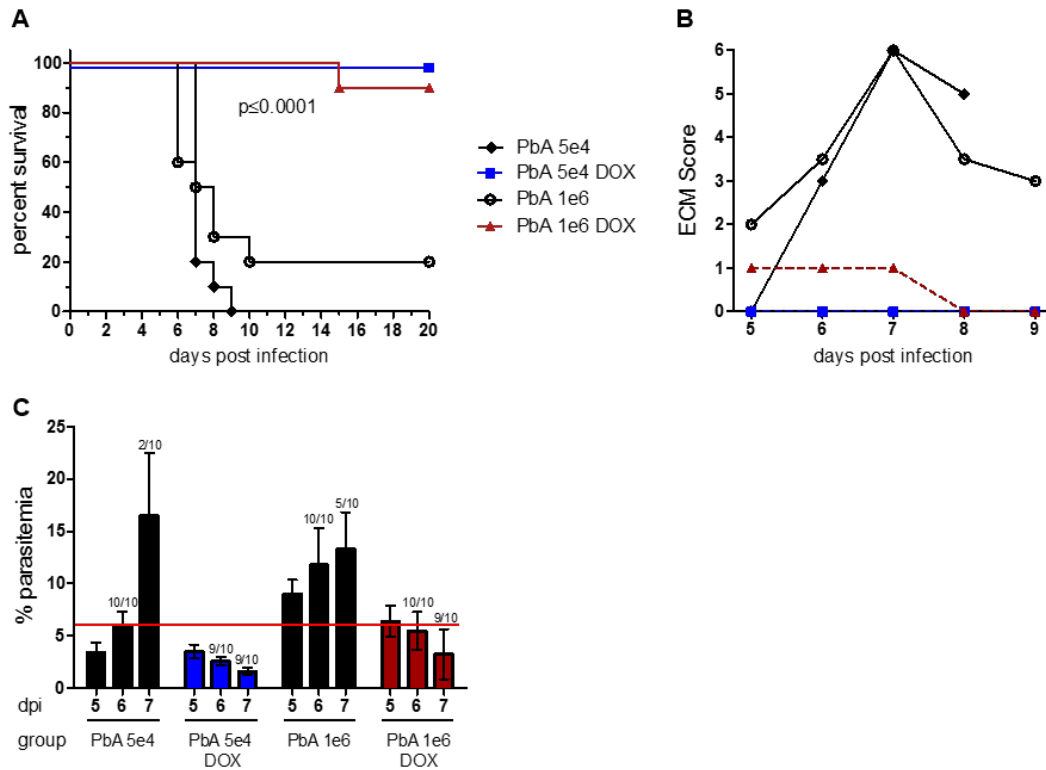


Figure 3.28: **ECM was prevented in mice infected with high parasite load and treated with doxycycline.** Mice were infected with 5e4 or 1e6 iRBC i.v. and either treated with 80 mg/kg/d doxycycline (4-6 dpi) or not (all groups n = 10). All groups were analyzed for survival (A), ECM score (B, displayed as median). C: Mean parasitemia is shown from 5 to 7 dpi. Small numbers above the bars indicate how many mice were still alive and considered for analysis. At 5 dpi all mice were alive and analyzed for parasitemia. Differences in survival were tested for significance with log-rank test. Significance for parasitemia was tested with ANOVA followed by Tukey post test. p values below 0.05 were considered significant.

infected with the standard dose of 5e4 iRBCs. Both doxycycline-treated group survived past 20 dpi (Fig. 3.28A) with only unspecific symptoms of illness around the critical phase (6-8 dpi), which were completely reversible (Fig. 3.28B).

Doxycycline targets the apicoplast genome in *Plasmodium* parasites which leads to impaired apicoplast function in daughter merozoites and a noticeable drop in parasitemia 2 days after treatment start [Dahl et al., 2006]. Therefore, one day after treatment start (5 dpi), the parasitemia was not changed significantly between doxycycline treated mice and the control-infected animals but higher in 1e6 iRBC infected animals ("PbA 1e6": 9.0%, "PbA 1e6 + DOX": 6.4%) when compared to their respective groups that were inoculated with 5e4 iRBCs ("PbA 5e4": 3.5%, "PbA 5e4 + DOX": 3.4%, Fig. 3.28C). In untreated groups, parasitemia increased throughout the analyzed time frame ("PbA 5e4"

3.4 to 16.5%, "PbA 1e6" 9.0 to 13.3%), while parasitemia declined in doxycycline treated mice ("PbA 5e4 + DOX" 3.5 to 1.6%, "PbA 1e6 + DOX" 6.4 to 3.3%). Importantly, when we compared untreated 5e4 iRBC infected mice to the "PbA 1e6 + DOX" group, we did not find any differences in parasitemia on day 6 post infection ("PbA 5e4" 6.0%, "PbA 1e6 + DOX" 5.5%), but significant differences in survival of both groups (Fig. 3.28A).

These results show, that we could establish a model to compare untreated mice with doxycycline treated mice at 6 dpi with a similar parasitemia. In the following experiments we compared these two groups with the same parasitemia ("PbA 5e4" and "PbA 1e6 + DOX") with naive control mice in order to investigate the anti-inflammatory effects of doxycycline in the mouse model of cerebral malaria.

3.2.3 Blood-brain barrier remained stable after doxycycline treatment despite high parasitemia

The first step in characterizing the anti-inflammatory effects of doxycycline in ECM was the analysis of the blood-brain barrier. As described before, the opening of the BBB is a hallmark in ECM and can be easily tested with an Evans blue assay. Therefore, we infected one group of mice with 5e4 iRBCs ("PbA 5e4") and one group with 1e6 iRBCs, which was treated with doxycycline ("PbA 1e6 + DOX"). Both groups were subjected to the Evans blue assay and compared to naive mice on 6 dpi. In addition, we were also interested in the progression of the BBB stability in "PbA 1e6 + DOX" mice. Therefore some mice of this group were analyzed on 7, 8 and 9 dpi. As untreated mice succumb to ECM after 6 dpi, "PbA 1e6 + DOX" mice were only compared to naive mice.

The blood-brain barrier in mice that were infected with 5e4 iRBC but not treated with doxycycline was clearly destroyed, indicated by the blue color of the brain, which was in sharp contrast to almost unstained brains of naive and doxycycline treated mice (Fig. 3.29A). These findings were also quantified by formamide extraction of the extravasated dye. Brain samples from untreated PbA-infected mice contained significantly more Evans blue dye when compared to naive mice (7.5 fold change to naive mice; Fig. 3.29B) and doxycycline treated mice (2.3 fold change to naive, $p < 0.01$ to "PbA 5e4").

On all days the difference between naive mice and "PbA 1e6 + DOX" mice was not significant, but we could detect a slightly higher EB leakage in brains of PbA-infected, doxycycline treated mice on 6 dpi, which clearly reduced in the following days (Fig. 3.29D

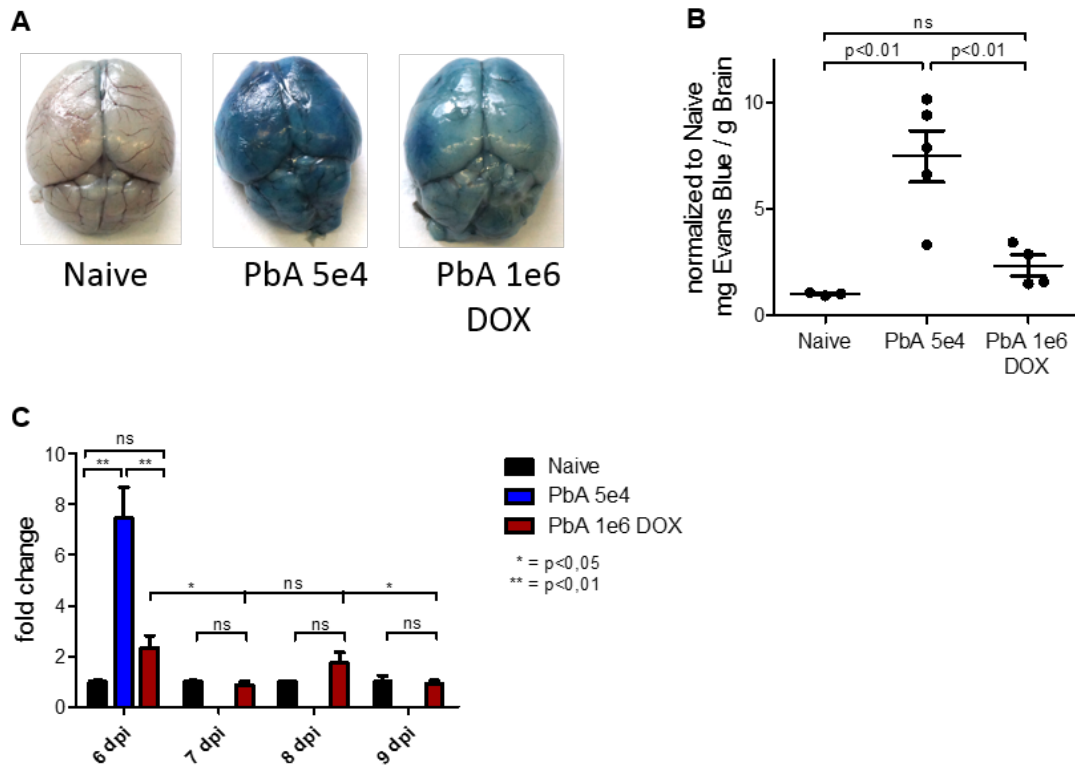


Figure 3.29: **Stable Blood-brain barrier in 1e6 iRBC infected mice after doxycycline treatment.** An Evans blue assay was performed with mice that were either infected with 1e6 iRBCs and treated with doxycycline (n=5 / day) or infected with 5e4 iRBC and left untreated (n=5). Naive mice served as controls (n=3 / day). On 6 dpi all groups were compared to each other, the following days only "PbA 1e6 + DOX" mice and naive controls were analyzed. A: Photographs of one exemplary brain from each group on 6 dpi. B: Dot plot for Evans blue dye that was extracted from brains after EB injection on 6 dpi. Data is presented as mg EB per g brain. C: Amount of Evans blue that was extracted from brains of the described groups. All values were normalized to the naive mice from the respective day. Bars represent means. Significance for results from Evans blue assay was calculated with ANOVA following Tukey post test. p values less than 0.05 were considered significant.

presents fold changes of "PbA 1e6 + DOX" to naive: 6 dpi: 2.3, 7 dpi: 0.9, 8 dpi: 1.7, 9 dpi: 0.9)

In summary we observed a stable blood-brain barrier "PbA 1e6 + DOX" mice whereas untreated mice that were infected with 5e4 iRBCs displayed a severely ruptured BBB despite a similar parasitemia.

3.2.4 Immune cell infiltration and activation was reduced in brains of doxycycline treated mice

The opening of the blood-brain barrier is often attended by an infiltration of immune cells from the periphery into the brain. Especially in cerebral malaria the infiltration of immune

cells that were primed in the periphery (mainly spleen) is of great interest and probably the main factor driving the disease [Engwerda et al., 2005]. Therefore, we isolated immune cells that were present in the brains of mice that were either infected with $5e4$ PbA-iRBCs and left untreated or were injected with $1e6$ PbA-iRBCs and treated daily with 80 mg/kg doxycycline from 4 dpi on. Naive mice served as controls. The cells were harvested from PBS-perfused animals and purified via a percoll-gradient to enrich leukocytes. These cells were then stained for different extra- and intracellular markers and analyzed with a flow cytometer.

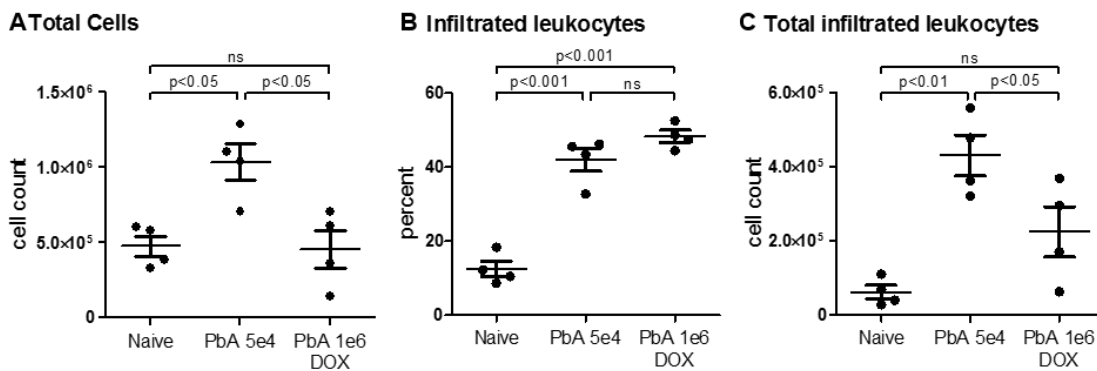


Figure 3.30: **The total number of brain infiltrated cells was reduced after doxycycline treatment.** Brains of d+6 $5e4$ iRBC infected ($n=4$) and d+6 $1e6$ iRBC infected doxycycline treated mice ($n=4$) were analyzed for cellular infiltrates by counting cells after leukocyte enrichment and identification of infiltrated cells by CD45 in flow cytometry. Naive mice ($n=4$) served as control. A: Total number of cells purified from brains of the respective groups, counted with a cell counter. B / C: Percentage and total amount of CD45^{hi} cells from these cells. Results were tested for significance with ANOVA, followed by Tukey post-test. p values below 0.05 were considered significant.

The total amount of cells from homogenized brains of PBS-perfused mice was counted after a percoll gradient. Mice infected with $5e4$ PbA-infected erythrocytes contained significantly more cells in their purified brain fractions than samples from naive mice ("PbA 5e4": $1.04e6$ cells/brain vs. "Naive": $4.75e5$ cells/brain, $p < 0.05$; Fig. 3.30A). Mice that were infected with the higher amount of iRBCs ($1e6$) and treated with doxycycline did not show an increase in total cell numbers ($4.55e5$ cells/brain; $p < 0.05$ to "PbA 5e4", not significant different to "Naive").

These purified cells were further analyzed for the hematopoietic cell surface marker CD45 via flow cytometry to differentiate between infiltrated immune cells (CD45^{hi}), microglia (CD45^{lo}) and other cerebral cells or cell debris that were not culled out in the gradient. In both groups of infected mice (\pm DOX) the frequencies of CD45^{hi} cells were signifi-

cantly increased ("PbA 5e4": 41.9%, "PbA 1e6 + DOX": 48.2%) when compared to naive mice (12.4%, $p < 0.001$ against both PbA groups, Fig. 3.30B). However, while frequencies of CD45^{hi} cells did not differ between doxycycline treated mice ("PbA 1e6 + DOX") and untreated mice ("PbA 5e4"), the total amount of infiltrating CD45^{hi} cells per brain was significantly reduced in doxycycline treated animals ($p < 0.05$, Fig. 3.30C). With an average of 2.25e5 CD45^{hi} cells per brain in doxycycline treated mice ("PbA 1e6 + DOX") this group contained more cellular infiltrates than naive mice (6.36e4 cells/brain), but this difference was not significant. We found significantly more CD45^{hi} cells in brains of PbA-infected, untreated mice than in those from naive mice ("PbA 5e4": 6.36e4 cells/brain vs. "Naive": 4.31e5 cells/brain, $p < 0.05$) and almost twice as many cells as doxycycline treated mice.

Taken together, mice that were infected with 1e6 iRBC and treated with doxycycline contained less cellular infiltrates in their brains compared to untreated mice with a lower infectious dose.

3.2.4.1 Brain infiltrated T cell were less activated but did not differ in frequencies after doxycycline treatment

As mentioned before, the host immune response - especially driven by T cells - is important in the development of cerebral malaria. Therefore, we analyzed the infiltrated cells from PbA-infected mice with or without doxycycline treatment regarding their phenotype and activation status in more detail. For this purpose we isolated brains from the three different groups of mice ("Naive", "PbA 5e4", "PbA 1e6 + DOX"). The organs were prepared as described before and analyzed with flow cytometry. We gated the cells according to their CD45 expression and from CD45^{hi} cells we separated into different cell subtypes, such as CD3⁺ T cells, CD11c⁺ dendritic cells and CD11b⁺ mononuclear cells. CD3⁺ T cells from CD45^{hi} cells were further differentiated into CD4⁺ and CD8⁺ T cells.

On 6 dpi, brains of PbA-infected mice showed a significant increase of CD3⁺ T cells compared to naive mice ("PbA 5e4": 58.6% vs. "Naive": 17.9%; $p < 0.001$), which was interestingly also observed in doxycycline treated mice (68.4%, $p < 0.001$; Fig. 3.31A). The difference between both infected group was not significant.

Further analysis of T cell subsets showed that almost no CD4⁺ were present in the brains of the experimental animals ("Naive" 3.3%, "PbA 5e4" 1.6%, "PbA 1e6 + DOX" 1.4%; Fig. 3.31B) and CD8⁺ T cells were the majority of infiltrated T cells in all groups

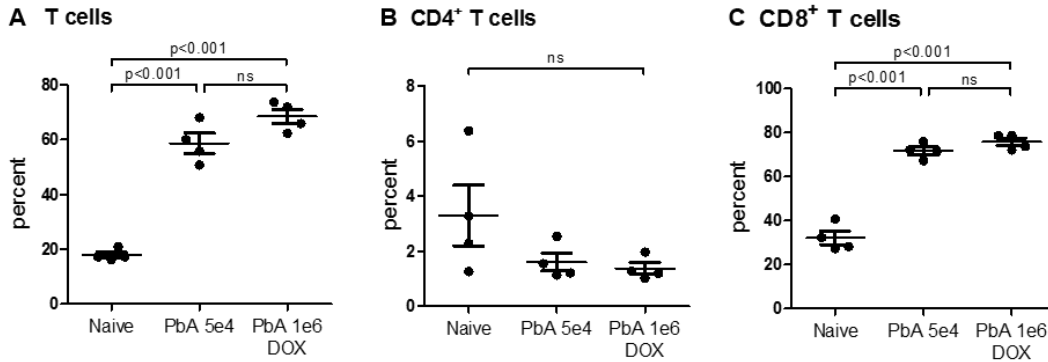


Figure 3.31: **T cells in the brains of PbA-infected mice showed no alteration in their frequencies after doxycycline treatment.** T cells were identified from CD45^{hi} cells of naive, d+6 "PbA 5e4" and "PbA 1e6 + DOX" mice (all n=4) by CD3 and further differentiated into CD4⁺ and CD8⁺ T cells. A: Percentage of CD3⁺ cells from all CD45^{hi} cells. B / C: Percentages of CD4⁺ and CD8⁺ T cells from CD3⁺. Statistical significance was tested with ANOVA and Tukey; $p < 0.05$ was considered significant.

of mice. Importantly, the analysis of CD8 between the different groups revealed a significant increase in CD8⁺ T cell frequencies after PbA-infection ($p < 0.001$), irrespective of doxycycline treatment ("Naive" 32.0%, "PbA 5e4" 71.6%, "PbA 1e6 + DOX" 75.6%; Fig. 3.31C).

Since we calculated similar T cell frequencies in PbA-infected mice with or without doxycycline treatment, we addressed the question whether these T cells displayed different activation profiles which could result in the protection of doxycycline treated mice from the development of cerebral malaria. Therefore, these cell populations were evaluated for the expression of molecules that are well-known to play a role in cerebral malaria development: granzyme B (Grzm B, an intracellular cytotoxic serine protease) and ICAM-1 (CD54, a surface adhesion molecule). The expression of these activation markers on T cells was evaluated via the average geometric fluorescent mean intensity (gMFI).

Granzyme B was almost absent on CD8⁺ T cells analyzed from brains of naive mice but was significantly increased in the untreated "PbA 5e4" group and the doxycycline treated group ("Naive": gMFI 1449 vs. "PbA 5e4": gMFI 24,372 vs. "PbA 1e6 + DOX": gMFI 17,766; $p < 0.001$; Fig. 3.32A). Importantly, we observed a statistically significant reduction of granzyme B expression in CD8⁺ T cells from brains of doxycycline treated animals ($p < 0.05$). The analysis of adhesion molecule ICAM-1 on the surface of T cells showed significant differences between PbA-infected mice depending on their treatment regimen ($p < 0.01$; Fig. 3.32B). While T cells from untreated PbA-infected mice showed

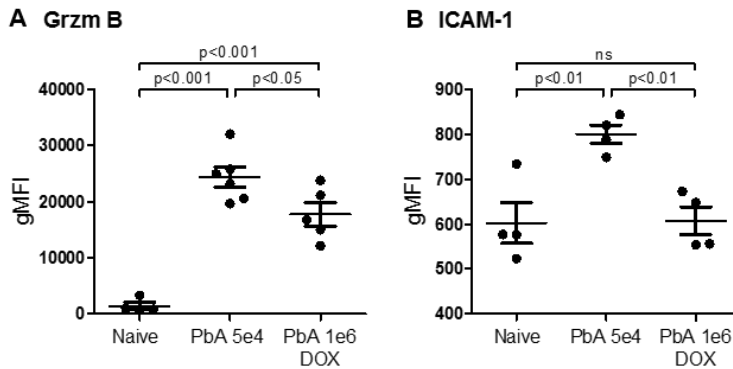


Figure 3.32: **CD8⁺ T cells found in the brains of PbA-infected mice were less activated after doxycycline treatment.** CD8⁺ T cells from brains of doxycycline treated (PbA 1e6), untreated (PbA 5e4) and naive animals (n=4) were analyzed for different activation markers by flow cytometry. A: intracellular granzyme B staining, B: surface staining for ICAM-1. Statistics were performed with ANOVA and Tukey post-test with $p < 0.05$ considered significant.

an enhanced expression of ICAM-1 compared to naive control animals ("PbA 5e4": 800 vs. "Naive": gMFI 603; $p < 0.01$), this up-regulation was not observed in samples from doxycycline treated PbA-infected mice (gMFI 608).

Taken together, the frequencies of brain infiltrating T cells were comparable between doxycycline treated and untreated mice 6 days after PbA-infection. However, total CD8⁺ T cell numbers were reduced after treatment and these cells showed decreased activity in doxycycline treated animals that were protected from ECM in comparison to untreated PbA-infected controls which were suffering from ECM. We found a similar activity profile in CD4⁺ T cells (Fig. S17).

3.2.4.2 Antigen presenting cell frequencies were not altered in brains of doxycycline treated mice, but they expressed less activation markers

Antigen-presenting cells are required to prime and activate T cells and therefore contribute to ECM development. Next to infiltration of APCs from the periphery, like dendritic cells or mononuclear cells, also microglia and endothelial cells play a role in ECM development [Medana et al., 1997, Howland et al., 2015].

In order to characterize antigen-presenting cells from our experimental groups of interest, we prepared brain infiltrates from naive mice ("Naive"), mice infected with 5e4 iRBCs 6 days before analysis ("PbA 5e4") and animals infected with 1e6 iRBCs and treated with doxycycline from 4 dpi ("PbA 1e6 + DOX"). Infiltrates were gated for CD45^{hi} as described before. From CD3⁻ cells we gated for CD11c⁺I-Ab⁺ cells which are defined as

dendritic cells (DCs). These DCs were also checked for changes in activation markers such as ICAM-1.

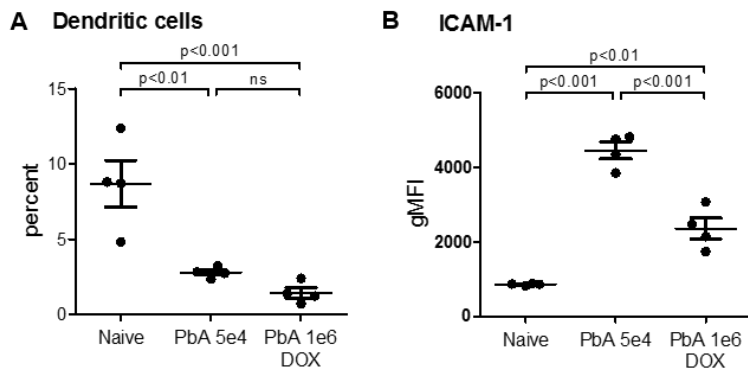


Figure 3.33: **Dendritic cells in the brain expressed less ICAM-1 after doxycycline treatment in PbA-infection.** Dendritic cells among brain infiltrated cells from the respective groups (Naive, PbA 5e4, PbA 1e6 + DOX; n=4) were identified by flow cytometry analysis for surface markers CD11c and I-Ab (A, percent of total CD45^{hi} cells). Activation of these cells was investigated by changes in surface expression of ICAM-1 (B, gMFI). Results were statistically analyzed by ANOVA followed by Tukey post test; $p < 0.05$ was considered significant.

We found markedly decreased dendritic cell frequencies in brains of mice after PbA-infection (\pm DOX treatment; Fig. 3.33A). From 8.7% in naive mice, the frequency of DCs dropped significantly ($p < 0.01$) on 6 dpi to 2.9% in "PbA 5e4" mice and 1.4% in PbA-infected mice of the DOX-group ("1e6 + DOX"). The small difference between both PbA-infected groups (\pm DOX treatment) was not significant. It is of note that even though the percentage of dendritic cells was higher in naive mice, they have a low cell count regarding the total number of infiltrated cells and therefore the total amount of DCs was smaller than in PbA-infected mice without doxycycline treatment. Accordingly, dendritic cells numbers in brain samples from untreated mice will be higher than in "PbA 1e6 + DOX" mice due to the difference in total infiltrated cells.

Next, we evaluated the expression of adhesion molecule ICAM-1 on brain infiltrated DCs from the different groups. We found increased levels of ICAM-1 on DCs from both PbA infected groups compared to cells from naive animals ("PbA 5e4" gMFI 2,350, "PbA 1e6 + DOX" 4,436", Naive": gMFI 854, $p < 0.01$; Fig. 3.33B). Interestingly, dendritic cells expressed less ICAM-1 on their surfaces in mice that were infected with 1e6 iRBCs and treated with doxycycline compared to mice that were infected with 5e4 iRBCs but were left untreated ($p < 0.001$).

CD11b⁺ cells comprise several groups of antigen-presenting cells including macrophages,

monocytes, neutrophils but also a dendritic cell subset. For flow cytometry analysis, we first excluded microglia, T cells and CD11c⁺ cells that were analyzed separately. After defining the group of antigen-presenting CD11b⁺ cells, they were analyzed for different markers of activation.

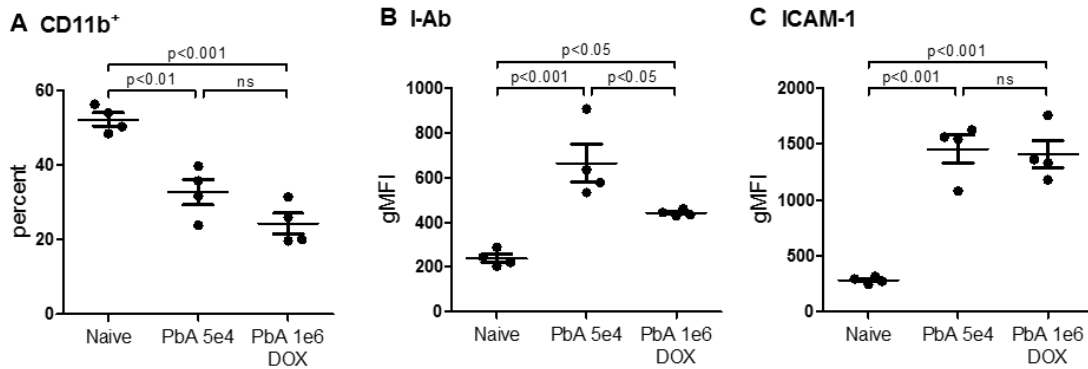


Figure 3.34: **CD11b⁺ cells in the brain were less activated in PbA-infected mice after doxycycline treatment.** CD45^{hi} cells that were derived from brains of PbA-infected (5e4 iRBC or 1e6 iRBC + DOX) and naive mice (all n=4) were gated for CD11b expression and the presence of activation markers. A: Percentage of CD11b⁺ cells from CD45^{hi} cells. B-C: gMFI of I-Ab and ICAM-1 from flow cytometry analysis. Significance was tested with ANOVA and Tukey post-test; $p < 0.05$ was considered significant.

The frequency of CD11b⁺ cells in the brain was reduced after PbA-infection in both infected groups which had significantly less CD11b⁺ cells ("PbA 5e4" 32.7%, "PbA 1e6 + DOX" 24.3%; Fig. 3.34A) than uninfected animals ("Naive" 52.2%, $p < 0.01$). The small decrease of CD11b⁺ cells in brains of doxycycline treated mice compared to the untreated group was not significant but we observed differences in expression of activation markers. Expression of I-Ab increased from a gMFI of 240 in naive mice to gMFI 663 in untreated 5e4 iRBC infected mice ($p < 0.001$; Fig.3.34B). Brain CD11b⁺ cells from DOX-treated mice showed significantly reduced expression of I-Ab compared to untreated mice ("PbA 1e6 + DOX": gMFI 430, $p < 0.05$) but the gMFI was still a bit higher compared to naive controls ($p < 0.05$). ICAM-1 expression on brain infiltrated CD11b⁺ cells, did not differ between PbA-infected animals with or without doxycycline treatment ("PbA 5e4" gMFI 1,453, "PbA 1e6 + DOX" gMFI 1,408; Fig.3.34C). However, as seen for the other markers, CD11b⁺ cells in brains from naive mice had significantly less ICAM-1 expression on their surface compared to both infected groups (gMFI 283, $p < 0.001$).

Similar to the results from dendritic cells we could not observe a difference in the frequencies of CD11b⁺ cells, but cells from doxycycline treated mice were generally less

activated as shown by MHC class II expression.

Taken together, we frequencies of CD11c⁺ and CD11b⁺ cells in brains of PbA-infected mice did not change after doxycycline treatment. However, their activation was slightly reduced.

3.2.4.3 Microglia showed reduced expression of MHC class II molecules in doxycycline-treated PbA-infected mice

Besides infiltrating immune cells that were primed and activated in the periphery, microglia, brain resident APCs, could also contribute to the development of cerebral malaria. As microglia are present in brains of healthy and diseased mice, we were especially interested in changes in activation of these cells in PbA-infected \pm DOX-treated mice. The percoll gradient that we used to enrich leukocytes does includes microglia. Therefore, we used this approach to harvest microglia before staining them for surface markers to distinguish them from other immune cells and to check their activation.

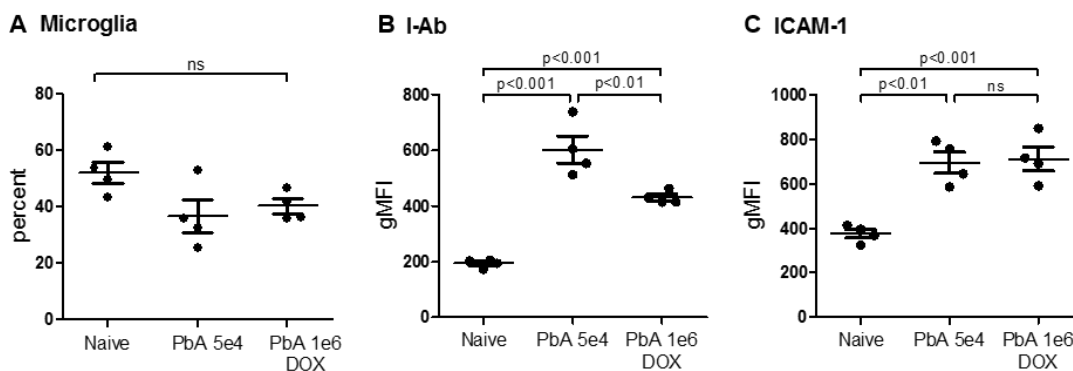


Figure 3.35: **Microglia expressed less I-Ab in PbA-infected mice after doxycycline treatment.** Microglia were defined as CD45^{lo}CD11b⁺ cells that were derived from brains of PbA-infected (5e4 iRBC or 1e6 iRBC + DOX) and naive mice (all n=4) these microglia were then analyzed for changes in expression of activation markers. A: Percentage of microglia (CD45^{lo}CD11b⁺) from total cells after gradient. B-C: gMFI of I-Ab and ICAM-1 from flow cytometry analysis. Significance was tested with ANOVA and Tukey post-test; p < 0.05 was considered significant.

The frequencies of microglia did not differ significantly between both experimental groups and naive control mice ("Naive": 51.9%, "PbA 5e4": 36.7%, "PbA 1e6 + DOX": 40.2%; Fig. 3.35A). We further checked these cells for I-Ab and ICAM-1 expression, which could be both upregulated upon activation. I-Ab expression on microglia was significantly upregulated in PbA-infected mice ("PbA 5e4" gMFI 603, "PbA 1e6 + DOX" gMFI 430) compared to naive controls (gMFI 194, p < 0.001; Fig.3.35B). While an increase in I-Ab

was seen in both groups of mice with and without doxycycline treatment, the upregulation was significantly ($p < 0.01$) reduced in the treated mice. Expression of adhesion molecule ICAM-1 was also significantly increased on microglia from both infected groups ("PbA 5e4" gMFI 695, "PbA 1e6 + DOX" gMFI 712) in comparison to naive mice (gMFI 375, $p < 0.01$; Fig.3.35C), but we could not observe any differences with or without doxycycline treatment.

In general we could see a reduced I-Ab expression in microglia after doxycycline, comparable to our findings in brain infiltrated APCs.

3.2.4.4 Cytokine production was reduced in brains of mice treated with doxycycline

Not only expression of activation markers but also local cytokine production from resident and infiltrated brain cells could explain differences in disease development between PbA-infected mice with or without doxycycline treatment. As cytokines could be either produced by infiltrated immune cells or by brain resident cells, and we were interested in characterizing the local cytokine milieu in the brains, we decided to culture whole brain homogenate samples from d+6 infected animals that were either inoculated with 5e4 iRBCs and left untreated ("PbA 5e4") or received 1e6 iRBCs and were treated from 4 dpi with doxycycline ("PbA 1e6 + DOX"). Brains from naive mice were included as controls for not inflamed brains. Supernatants from over night-incubated brain cell cultures were analyzed by ELISA for the presence of the acute-phase protein TNF and chemokine CCL5 that are both associated with the development of cerebral malaria.

TNF production by brain tissue from PbA-infected, untreated mice was significantly increased compared to samples from naive control mice ("PbA 5e4": 19.5 pg/ml, "Naive": 0.8 pg/ml, $p < 0.05$; Fig. 3.36A). We also measured increased levels of TNF in samples from doxycycline-treated mice (6.3 pg/ml), however, differences to both other groups were not significant, probably due to the small number of mice and an outlier in the "PbA 5e4" group. We gained similar results for CCL5: brain cells extracted from "PbA 5e4" mice produced significantly more CCL5 compared to naive controls ("Naive" 6.3 pg/ml, "PbA 5e4" 103.5 pg/ml, $p < 0.05$; Fig. 3.36B). With an average of 66.7 pg/ml CCL5 in brain cell supernatant, doxycycline treated mice produced more of this chemokine than naive mice but less compared to untreated mice. However, these differences did not reach statistical significance.

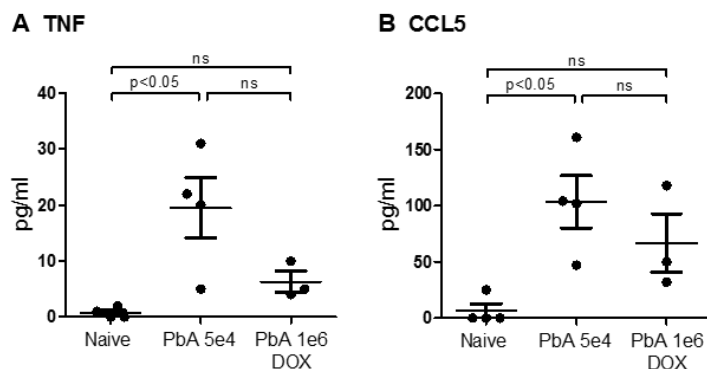


Figure 3.36: **TNF and CCL5 release were slightly downregulated in brains of "PbA 1e6 + DOX" mice compared to untreated "PbA 5e4" mice.** Cytokine release was measured in brain homogenates (before percoll gradient) of 5e4 iRBC-infected mice compared to 1e6 iRBC-infected mice that were treated with doxycycline and also to naive mice (n=4). Brain cell homogenates were cultured in RPMI medium and after over night incubation, supernatants were subjected to an ELISA for TNF (A) and CCL5 (B). Statistical significance ($p < 0.05$) was tested with ANOVA followed by Tukey post-test.

In summary we saw a small trend to less cytokine production in brains of doxycycline treated mice compared to their uninfected counterparts.

3.2.4.5 Cross-presentation by brain microvessels was not altered after doxycycline treatment

It has been shown recently, that cross-presentation of parasite-specific antigen to $CD8^+$ T cells by activated endothelial cells in brain microvessels is a hallmark of experimental cerebral malaria [Howland et al., 2013, Howland et al., 2015]. To test whether doxycycline treatment of PbA-infected mice would alter the cross-presentation in these cerebral vessels, our collaborators S. Howland and L. Rénia analyzed our experimental groups with their established brain microvessel cross-presentation assay [Howland et al., 2013]. In this assay microvessel fragments were isolated from all mice and incubated with NFAT-lacZ reporter cells that were transduced with a T cell receptor (TCR) recognizing the S_QL_L-N_AK_YL epitope and interaction was analyzed by β -galactosidase staining after over-night culture. The presence of PbA antigen in the brains of PbA-infected mice with or without doxycycline treatment was determined by qRT-PCR measurement of PbA 18srRNA in cDNA that was transcribed from brains of all experimental groups.

Analysis of cross-presentation for the S_QL_LN_AK_YL epitope revealed a background of 5 blue spots in samples from naive animals and a significant increase in blue spots per brain in both PbA-infected groups (\pm DOX, $p < 0.05$). The small decrease in cross-

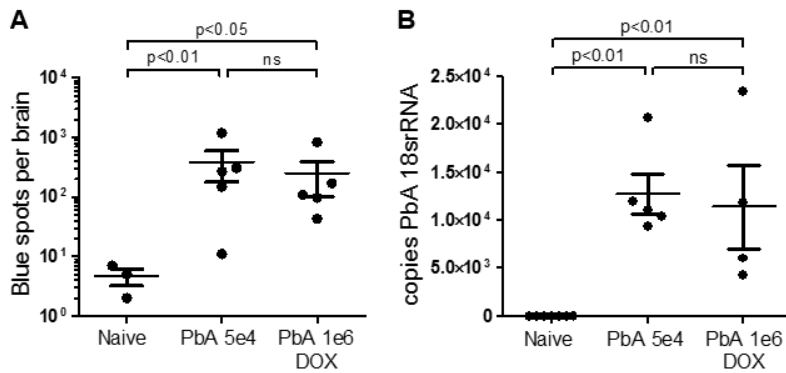


Figure 3.37: **Brain microvessels of doxycycline treated PbA-infected mice were able to cross-present antigen.** A: Brain microvessels were isolated from 5e4 iRBC PbA-infected Bl/6 mice and 1e6 iRBC PbA-infected mice that received doxycycline treatment from 4 dpi (both n=5). Naive mice were included as controls (n=3). Isolated cells were incubated over night with TCR-transduced NFAT-lacZ reporter cells and cross-presentation was measured after beta-galactosidase staining as blue spot per brain. B: Parasite load in brains of all experimental groups was determined by qRT-PCR. Results were tested for significance with ANOVA and Tukey's post-test. P-values below 0.05 were considered significant.

presentation in doxycycline-treated mice was not significantly different to ECM-positive mice that were left untreated ("PbA 5e4": 384 blue spots per brain, "PbA 1e6 + DOX": 249 blue spots per brain; Fig. 3.37A).

We were able to detect an increased parasite load in brains of PbA-infected mice on 6 dpi. However, no significant differences were found in mice with or without doxycycline treatment ("PbA 5e4": 1.27e4 copies of 18srRNA, "PbA 1e6 + DOX": 1.14e4 copies of 18srRNA, Fig. 3.37B).

Taken together, cross-presentation in cerebral microvessels from PbA-infected mice was not affected by doxycycline treatment and the parasite load (= antigen levels) was also comparable in both groups.

3.2.5 Cytotoxicity in the spleen was reduced after doxycycline treatment

The results from the described brain analyses suggested that doxycycline treatment interferes with the generation or amplification of the harmful immune response in the brain in our model of experimental cerebral malaria. As the immune reaction in the brain is initiated in the spleen (described before), we were interested in the question whether the observed effects were local impacts in the brain or if the peripheral immune response was also affected.

Therefore, we analyzed spleens of mice that were either infected with 5×10^4 PbA-infected iRBCs ("PbA 5×10^4 ") or with 1×10^6 iRBCs and treated daily with doxycycline from 4 dpi on ("PbA 1×10^6 + DOX"). Both infected groups were sacrificed 6 days p.i. when untreated mice showed first neuro-specific disease symptoms. Naive mice of the same strain ("Naive") were included as uninfected controls.

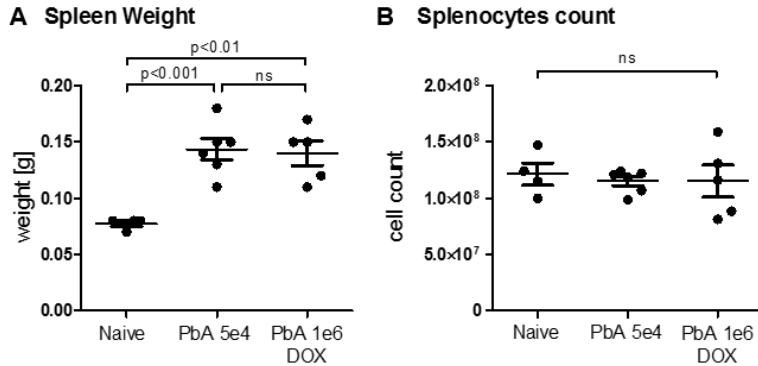


Figure 3.38: **Total number of spleen cells did not differ between doxycycline treated and untreated mice.** Mice were infected with PbA (5×10^4 or 1×10^6 iRBC, as indicated, $n=4$) and sacrificed six days later. One group was treated with doxycycline from 4 dpi ("1e6 iRBC + DOX"). Naive mice were included as controls ($n=4$). Spleens were removed after PBS-perfusion, weighed (A) and digested in collagenase before the total cell count per spleen was measured with a cell counter (B). Statistical significance was tested with ANOVA, followed by Tukey post-test; $p < 0.05$ was considered significant.

After perfusion and removal of organs we first weighed the spleens of all experimental groups to examine splenomegaly in PbA-infected mice with or without doxycycline treatment. We found that PbA-infection led to heavier spleens in both infected groups but no difference between treated and untreated mice ("Naive": 0.08g, "PbA 5×10^4 ": 0.14g, "PbA 1×10^6 + DOX": 0.14g cells, $p < 0.01$ to "Naive"; Fig. 3.38A).

Afterwards we generated single cell suspensions, counted the cells with a cell counter and calculated the total number of cells per spleen. The total splenocyte numbers did not differ between all experimental groups ("Naive": 1.36×10^8 cells, "PbA 5×10^4 ": 1.53×10^8 cells, "PbA 1×10^6 + DOX": 1.33×10^8 cells; Fig. 3.38B).

3.2.5.1 T cell numbers did not differ in spleens of doxycycline treated mice, but their cytotoxicity was significantly reduced

In experimental cerebral malaria cytotoxic $CD8^+$ T cells are thought to contribute most to the ECM disease development. Therefore, we investigated T cell populations and their activity in the spleens of our experimental groups ("Naive", "PbA 5×10^4 ", "PbA 1×10^6

+ DOX”) 6 days after PbA-infection. We analyzed T cell populations ($CD3^+$, divided into $CD4^+$ and $CD8^+$) and different activation markers via flow cytometry and measured cytokine production in supernatants of over night-incubated spleen cells. Additionally, we performed an *in vivo* cytotoxicity assay to evaluate the lytic activity of antigen-specific cytotoxic T cells.

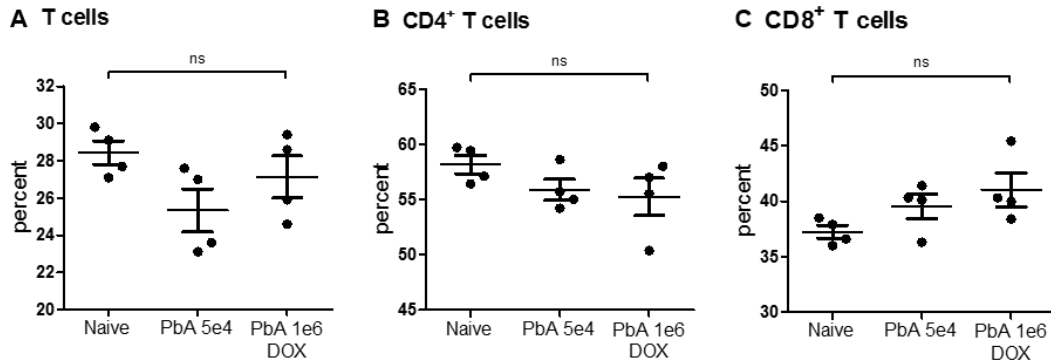


Figure 3.39: **T cell numbers in the spleen did not differ after doxycycline treatment of PbA-infected mice.** Splens of naive, 5e4 iRBC-infected and 1e6 iRBC-infected mice that were treated with doxycycline were harvested on 6 dpi and prepared for FACS staining (n=4). Cells were stained for CD3 (A) and further differentiated into $CD4^+$ T cells (B) and $CD8^+$ T cells (C); shown as frequency from $CD3^+$ cells. Graphs show mean percentages of the indicated marker. Results were tested for significance with ANOVA and Tukey post-test; $p < 0.05$ was considered significant.

The frequency of $CD3^+$ cells in the spleen did not differ significantly between d+6 PbA-infected mice without treatment (“PbA 5e4”: 25.3%) and doxycycline treated animals (“PbA 1e6 + DOX”: 27.2%; Fig. 3.39A). Both infected groups had comparable T cell numbers in their spleens in regard to the naive control group (28.4%). The analysis of $CD4^+$ and $CD8^+$ T cell subpopulations did also not reveal any significant differences between all experimental groups. Naive mice had a $CD4^+$ T cells proportion of 58.3% compared to 55.9% in “PbA 5e4” mice and 55.2% in the “PbA 1e6 + DOX” group (Fig. 3.39B). Accordingly, the percentages of $CD8^+$ cells among the T cell population were also similar in all experimental groups (“Naive”: 37.3%, “PbA 5e4”: 39.5%, “PbA 1e6 + DOX”: 41.0%; Fig. 3.39C).

As we did not observe any differences in T cell frequencies we were wondering if T cells from doxycycline treated mice (“1e6 PbA + DOX”) showed any changes regarding their activity as compared to untreated, PbA-infected mice (“PbA 5e4”). Therefore, we first evaluated the expression of activation markers with the help of flow cytometry on 6 dpi in spleen samples from infected mice \pm DOX treatment.

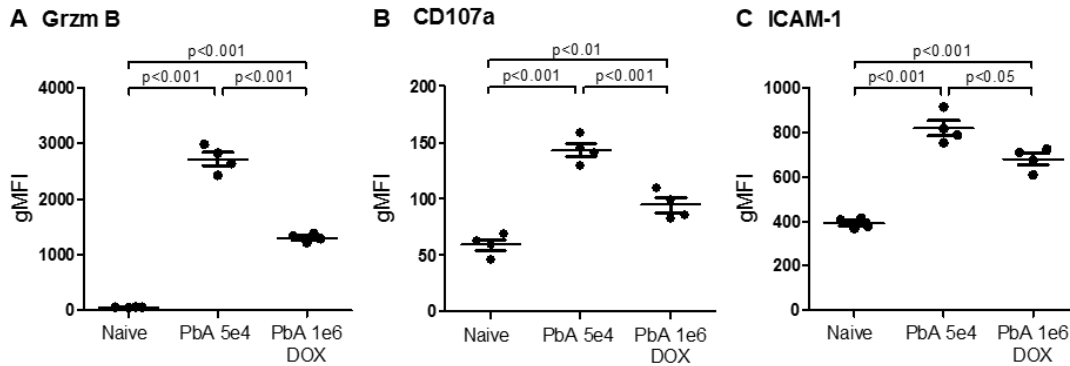


Figure 3.40: **Activation markers were decreased in splenic CD8⁺ T cells from doxycycline treated, PbA-infected mice.** CD8⁺ T cells from spleens of 5e4 iRBC-infected, 1e6 iRBC-infected, doxycycline treated mice and naive controls (n=4) were analyzed for different activation markers. The geometric mean fluorescence intensity of granzyme B (A), CD107a (B) and ICAM-1 (C) was determined by flow cytometry. Statistical differences were evaluated with ANOVA and Tukey post-test. p values below 0.05 were considered to be significant.

Granzyme B is an effector molecule released from cytotoxic T cells upon activation. Splenic CD8⁺ T cells from PbA-infected mice (\pm DOX) showed a vast increase in intracellular granzyme B compared to samples from naive controls, which were almost negative ("PbA 5e4": gMFI 2,722, "PbA 1e6 + DOX": gMFI 1,217, "Naive"; gMFI 58, $p < 0.001$; Fig. 3.40A). Importantly, splenic CD8⁺ T cells from doxycycline treated, 1e6 iRBC-infected mice had significantly less granzyme B stored compared to untreated, 5e4 iRBC-infected mice ($p < 0.001$).

Analysis of CD107a, a marker for degranulation, supported the decreased cytotoxicity in T cells from DOX-treated mice: infection of Bl/6 mice with PbA induced a significant increase in the surface expression of CD107a on CD8⁺ T cells compared to a weak expression in T cells from naive mice to mean gMFI of 144 in "PbA 5e4"-mice and gMFI 95 in doxycycline treated mice ("PbA 5e4": gMFI 144, "PbA 1e6 + DOX": gMFI 95, "Naive"; gMFI 60, $p < 0.001$; Fig. 3.40B), whereas splenic T cells from doxycycline-treated mice showed less CD107a expression than cells from untreated PbA-infected animals ("PbA 1e6 + DOX": gMFI 95, $p < 0.001$; Fig. 3.40B).

CD8⁺ T cells from PbA-infected mice expressed more ICAM-1 than the T cells from naive controls, however, similar to granzyme B and CD107a, CD8⁺ T cells from doxycycline-treated mice expressed less ICAM-1 compared to untreated "PbA 5e4" mice ("Naive": gMFI 392, $p < 0.001$; "PbA 5e4": gMFI 818 vs. "PbA 1e6 + DOX": gMFI 679, $p < 0.05$; Fig. 3.40C).

Similar results were seen in flow cytometry analysis of CD4⁺ T cells.

In addition, we evaluated the cytotoxic activity and general cytokine production of splenocytes from PbA-infected mice with and without doxycycline treatment. Therefore, we analyzed the supernatants from splenocyte *ex vivo* cultures for the presence of pro- and anti-inflammatory mediators via ELISA.

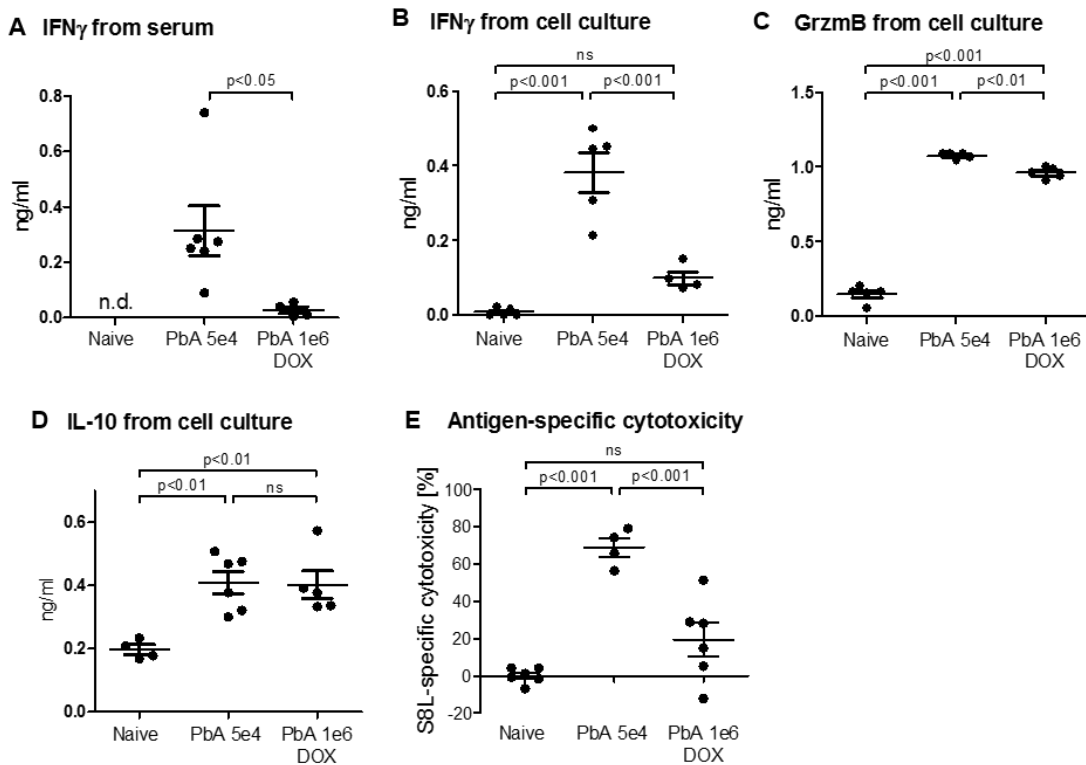


Figure 3.41: **Cytotoxicity was reduced in spleens and serum of PbA-infected mice after doxycycline treatment.** Cytotoxicity in PbA-infected mice with ("PbA 1e6 + DOX") or without ("PbA 5e4") doxycycline treatment and naive controls (n=4) was investigated by ELISA in serum and spleen and an *in vivo* kill. Serum (A) and cell culture supernatant (B) from over night incubated spleen cells were analyzed for IFN γ by ELISA. Splenocyte cell culture supernatant was additionally analyzed by ELISA for granzyme B (C) and IL-10 (D). Antigen-specific cytotoxicity was measured with an *in vivo* kill (E). Statistical significance was calculated with ANOVA followed by Tukey post-test; $p < 0.05$ was considered significant.

Production of IFN γ , a cytotoxic mediator, was not detectable in naive controls but strongly increased in serum of untreated PbA-infected mice ("PbA 5e4": 0.31 ng/ml; Fig. 3.41A). Doxycycline treated mice that had been infected with 1e6 iRBCs, contained significantly lower IFN γ level in their blood compared to untreated mice that had received 5e4 iRBCs ("PbA 1e6 + DOX": 0.03 ng/ml, $p < 0.05$).

Similarly to serum levels, spleen cell supernatant from naive mice contained almost no IFN γ and we detected a significant increase in the "PbA 5e4" group ("Naive": 0.01 ng/ml,

"PbA 5e4": 0.38 ng/ml, $p < 0.001$; Fig. 3.41B). Splenocyte cultures from doxycycline-treated mice contained 4-fold less IFN γ than samples from PbA-infected control mice ("PbA 1e6 + DOX": 0.1 ng/ml, $p < 0.001$).

Cultured spleen cells from both infected groups, harvested on 6 dpi, produced significantly more granzyme B than uninfected control mice (0.15 ng/ml, $p < 0.001$; Fig. 3.41C). Doxycycline treatment after PbA-infection (1e6 iRBC) led to small but significant reduction of granzyme B production in the splenocyte cultures compared to samples from untreated PbA-infected control mice ("PbA 1e6 + DOX": 0.91 ng/ml, "PbA 5e4": 1.08 ng/ml, $p < 0.01$; Fig. 3.41C).

We found significantly increased production of IL-10 in supernatant from cultured splenocytes 6 days after PbA-infection ($p < 0.01$), but no difference between doxycycline treated and untreated mice was observed ("Naive": 0.20 ng/ml, "PbA 5e4": 0.41 ng/ml, "PbA 1e6 + DOX": 0.40 ng/ml; Fig. 3.41D).

Next, we performed an *in vivo* CTL assay. Here, infected mice and controls received peptide-pulsed, CFSE-labeled target cells from syngenic donors i.v. in order to determine the cytotoxicity of antigen-specific T cells in the recipient animals on 6 dpi.

We measured a reduced antigen-specific CTL response in the spleens of DOX-treated mice on 6 dpi (Fig. 3.41E). The minor unspecific loss of labeled target cells in naive mice was defined as background, as those mice could not have any target-specific active T cells. Compared to the uninfected mice, PbA-infected mice generated a significant lytic activity ("PbA 5e4": 68.8%, $p < 0.001$), whereas doxycycline treatment dampened this response markedly: we measured a 3.5-fold reduction of lytic activity in spleens from doxycycline-treated mice ("PbA 1e6 + DOX": 19.3%, $p < 0.001$).

These results are in agreement with the attenuated expression of activation markers we had observed in splenic T cells from DOX-treated mice as well as impaired production of inflammatory mediators in serum and from spleen cell cultures (Fig. 3.40, 3.41A-C).

In summary, doxycycline treatment in PbA-infected mice did not change the T cell numbers and frequencies, but splenic CD8⁺ T cells showed impaired activity and levels of pro-inflammatory cytokines were reduced.

3.2.5.2 Antigen presenting cells were less activated in doxycycline treated mice

The analysis of T cells in doxycycline treated mice that were infected with PbA 6 days prior to analysis showed a marked impairment of activation in this cell type. Extending our investigation to antigen-presenting cells should help to answer the question whether doxycycline had a direct effect on T cell activity or if our findings could be a consequence of hampered APC function.

Analysis of splenic APCs was performed on spleen cells that were harvested from d+6 PbA-infected mice with doxycycline treatment ("PbA 1e6 + DOX") or without treatment ("PbA 5e4") and naive control animals. Spleens were processed as describe before and stained for flow cytometry analysis. CD3 was used to exclude T cells before other cells were split into dendritic cells (CD11c⁺I-Ab⁺) and CD11b⁺ cells (from cells that were not DCs) that include macrophages, monocytes and neutrophils. All cell subsets were further analyzed for signs of activation by expression of ICAM-1, MHC I upregulation and expression level of I-Ab in CD11b⁺ cells.

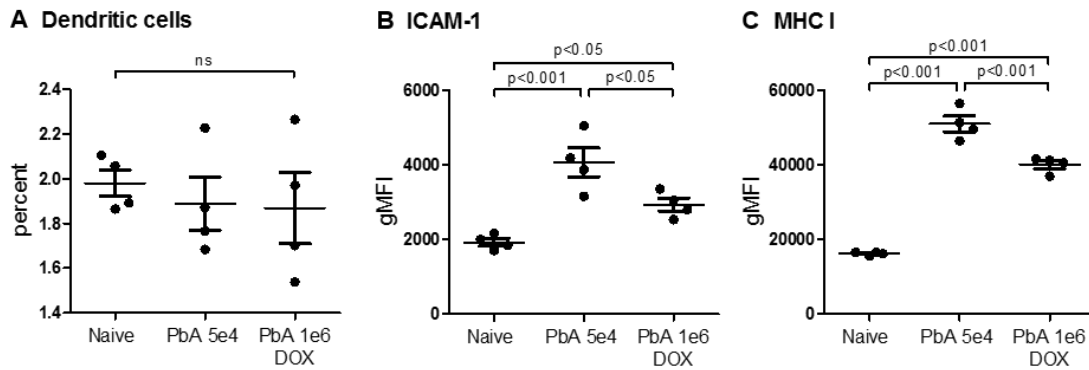


Figure 3.42: **Activation markers on splenic dendritic cells were reduced in doxycycline treated, PbA-infected mice.** Spleen cells were isolated from naive mice and PbA-infected animals with or without doxycycline treatment (n=4) and analyzed by flow cytometry. Dendritic cells were defined as CD3⁻CD11c⁺I-Ab⁺ (A, percentage of total cells) and further analyzed for changes in surface markers ICAM-1 (B, gMFI) and MHC I molecules (C, gMFI). Results were tested for significance between two groups with an unpaired t-test and between three groups with ANOVA and Tukey post-test; p < 0.05 was considered significant.

Dendritic cells frequencies (CD11c⁺I-Ab⁺) in spleens of PbA-infected, doxycycline treated mice ("PbA 1e6 + DOX": 1.87% of total spleen cells) did not differ significantly from untreated, infected ("PbA 5e4": 1.87%) and uninfected mice ("Naive": 1.98%; Fig. 3.42A). However, the analysis of ICAM-1 and MHC I molecules on the surface of

DCs revealed a diminished activation in doxycycline treated mice. ICAM-1 expression on DCs was significantly increased in untreated, PbA-infected mice (gMFI 4066) compared to uninfected controls (gMFI 1709, $p < 0.001$). A smaller increase of ICAM-1 expression was found on splenic DCs from doxycycline treated mice (gMFI 2938), which was significantly less than in untreated animals, but higher compared to naive controls ($p < 0.05$; Fig. 3.42B). MHC I expression revealed a similar picture (Fig. 3.42C): we observed a significant upregulation of MHC I in PbA-infected mice ("PbA 5e4" gMFI: 50,962) compared to naive controls ("Naive" gMFI 16,263, $p < 0.001$). This increase was also seen in doxycycline treated mice ("PbA 1e6 + DOX" gMFI: 40,110, $p < 0.001$ against "Naive") but significantly reduced compared to the untreated group ($p < 0.001$).

CD11b⁺ cells from all experimental groups were gated from the CD3⁻ cells that were not DCs and also analyzed for activation markers.

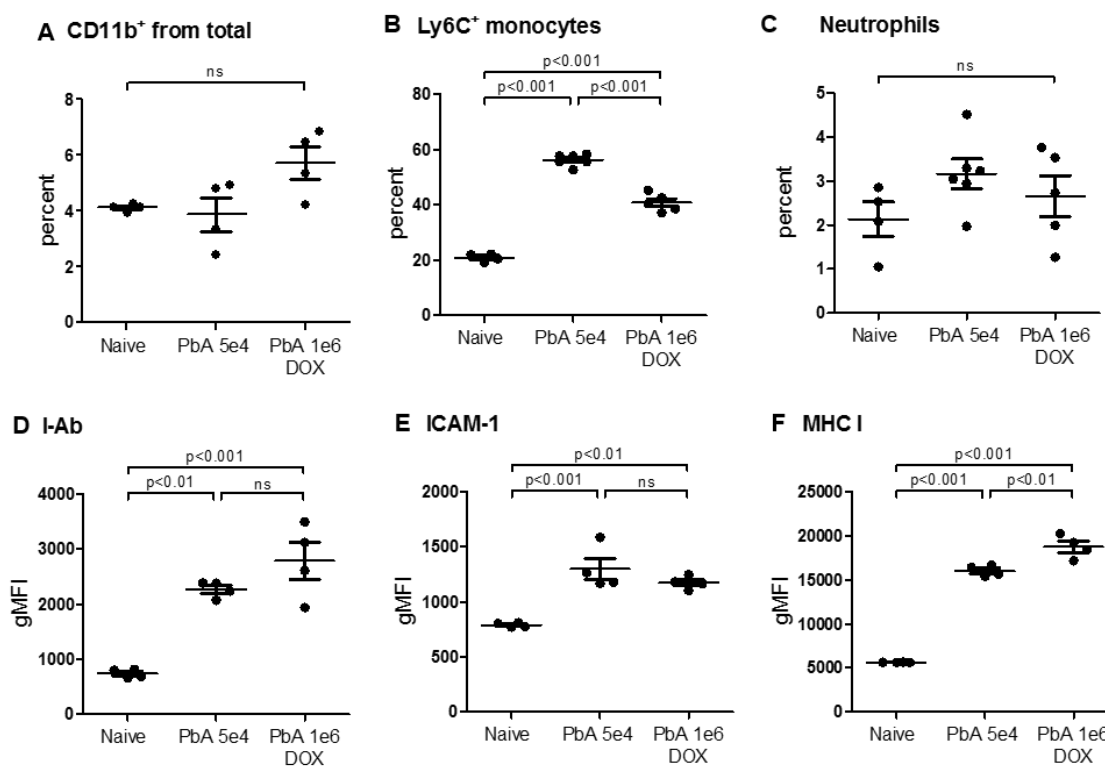


Figure 3.43: **Less Ly6C⁺ monocytes in spleens of doxycycline treated mice but similar activation in CD11b⁺ cells in general, compared to untreated mice.** Spleens of PbA-infected mice (with or without doxycycline treatment, $n=4$) and naive controls ($n=4$) were analyzed at 6 dpi for changes in CD11b⁺ cell frequencies (CD3⁻, no dendritic cells) by flow cytometry (A), and were further differentiated into Ly6C⁺ monocytes (B, Ly6C⁺Ly6G⁻) and neutrophils (C, Ly6C^{int}Ly6G⁺). Furthermore, the gMFI of I-Ab (D), ICAM-1 (E) and MHC I (F) was determined in this cell population. Statistical analysis were done with ANOVA followed by Tukey post-test with $p < 0.05$ considered to be significant.

Spleens of doxycycline treated mice ("PbA 1e6 + DOX") showed a small, but insignificant increase in CD11b⁺ cells (5.7%) compared to untreated PbA-infected mice ("PbA 5e4": 3.9%) and naive controls (4.1%; Fig. 3.43A). Further differentiation of CD11b⁺ cells revealed an increase in Ly6C⁺ monocytes in both PbA-infected groups with significantly more Ly6C⁺ monocytes among the CD11b⁺ splenocytes in untreated 5e4 iRBC-infected mice compared to doxycycline treated, 1e6 iRBC-infected animals ("Naive": 20.9%, "PbA 5e4": 56.3%, "PbA 1e6 + DOX": 40.7%, $p < 0.001$; 3.43B). Analysis of neutrophils among splenic CD11b⁺ cells showed no differences in our experimental groups ("Naive": 2.1%, "PbA 5e4": 3.2%, "PbA 1e6 + DOX": 2.7%; 3.43C).

I-Ab expression on CD11b⁺ cells significantly increased ($p < 0.001$) from a gMFI of 743 in naive mice to gMFI 2,269 in untreated, PbA-infected mice and even more to a gMFI value of 2,791 after doxycycline treatment (Fig. 3.43D). Despite being a small trend, the difference between doxycycline treated and untreated mice was not significant. A similar pattern was observed in ICAM-1 expression on CD11b⁺ cells: it significantly ($p < 0.01$) increased from gMFI 790 in naive mice to 1,299 in the "PbA 5e4" group and to 1,175 in the doxycycline treated group. No significant differences were found between PbA-infected mice, regardless of doxycycline treatment (Fig. 3.43E). MHCII expression was the only analyzed surface marker that differed between both PbA-infected groups. Interestingly, CD11b⁺ cells from doxycycline treated animals expressed significantly more MHCII than untreated mice ("PbA 1e6 + DOX" gMFI: 18,770, "PbA 5e4" gMFI: 16,024, $p < 0.01$). Again, cells from both PbA-infected groups expressed more MHCII than naive mice (gMFI 5636, $p < 0.001$; Fig. 3.43F).

All together, analysis of antigen-presenting cells in spleens of d+6 infected mice showed no differences in cell frequencies depending on doxycycline treatment. Dendritic cells from doxycycline treated mice expressed less surface markers that are associated with cell activation compared to untreated mice, while the analysis of CD11b⁺ cells revealed no differences between both groups.

3.2.6 Reduction of doxycycline dose to sub-antimicrobial doses still improved survival independent of parasite killing

Some studies showed, that the anti-inflammatory properties of antibiotics from the tetracycline group were still maintained when the drugs were given in sub-antimicrobial doses, i.e. a concentration that does not affect bacteria [Brown et al., 2004]. Based on these

findings, we were interested whether we could find a sub-antimicrobial dose that would not affect parasite growth but still work anti-inflammatory to overcome the difficulty of differentiating between direct anti-inflammatory effects and the effects caused by a reduced parasitemia.

To address this idea, C57Bl/6 mice were infected with 5×10^4 PbA-infected RBCs and either left untreated ("PbA 5×10^4 ", infection control group) or divided into one of four groups that received different concentrations of doxycycline intravenously. Starting from the already established 80 mg/kg/day (group "PbA 5×10^4 + DOX 80") we decided to reduce the concentration of doxycycline to 32 mg/kg/day ("PbA 5×10^4 + DOX 32"), 16 mg/kg/day ("PbA 5×10^4 + DOX 16") and 8 mg/kg/day ("PbA 5×10^4 + DOX 8"). All treated groups received doxycycline intravenously from day 4 post infection (p.i).

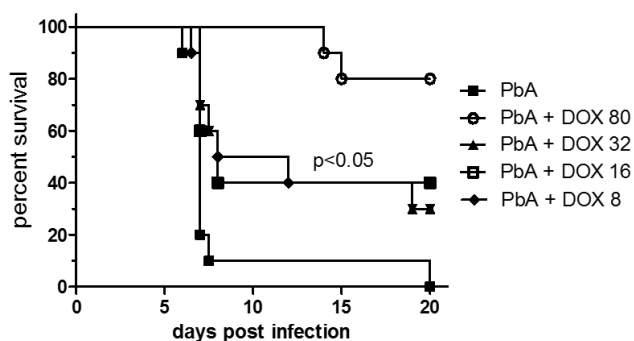


Figure 3.44: Mice treated with different doses of doxycycline showed better survival compared to untreated mice. Mice were intravenously injected with their respective dose of doxycycline daily from 4 dpi on. Differences in survival were tested for significance with log-rank test. p values below 0.05 were considered significant.

Analysis of survival confirmed our previous findings that treatment with our established doxycycline dose of 80 mg/kg/d from 4-6 dpi led to a 100% protection from ECM in PbA-infected mice, whereas almost all control-infected mice died from cerebral malaria between 6-8 dpi (Survival 10% at 10 dpi, Fig. 3.44). First mice of the DOX-treated group died after 14 dpi due to other complications like anemia, as the short treatment time was not sufficient to clear all parasites from the blood. Other groups with lower doses of doxycycline (32, 16, 8 mg/kg/d; 4-6 dpi) showed significantly better survival compared to untreated mice (40-50% DOX-treated vs. 10% in untreated; $p < 0.05$), but the protection was not as good as in the "PbA 5×10^4 + DOX 80" group, as only about half of the mice remained ECM free. However, we were also interested how the reduced doses would affect parasitemia, especially in surviving mice of the low dose doxycycline groups.

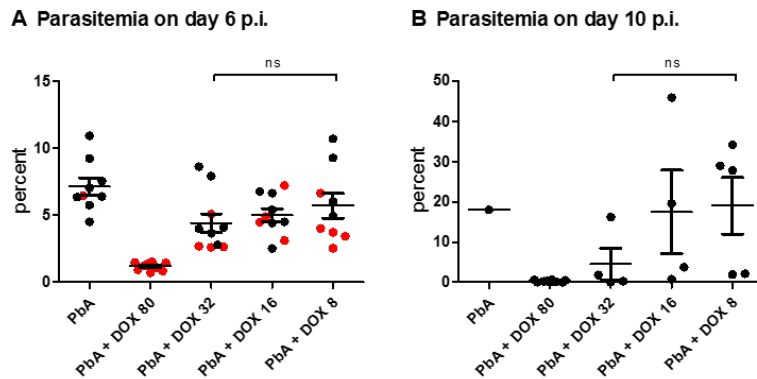


Figure 3.45: **Doxycycline was able to protect mice from ECM without affecting parasitemia.** PbA-infected mice were intravenously injected with their respective dose of doxycycline daily from 4 dpi on. Parasitemia was determined in Giemsa stained thin bloods smears, graphs are shown for 6 dpi (onset of disease in untreated mice) and 10 dpi (time point after ECM phase). Red dots in A represent mice that survived till 10 dpi and are shown in B. Statistical significance was tested with ANOVA paired with Tukey post test; $p < 0.05$ was considered significant.

We evaluated the parasite load on 6 dpi, the typical time point of ECM onset and appearance of neuro-specific symptoms in PbA-infected mice. At this time point PbA-infected control mice had a peripheral parasitemia of 7.1% whereas "PbA + DOX 80" mice had a significantly reduced parasite load of 1.2% ($p < 0.001$; Fig. 3.45A). Groups that were treated with 32, 16 or 8 mg/kg had similar intermediate parasite counts (4.4%, 5.0% and 5.7% respectively). When we analyzed the parasitemia on 10 dpi, which is a time point already after the critical ECM phase, one surviving mouse of the untreated controls had a blood parasitemia of 18.0% and mice treated with our previous established doxycycline dose of 80 mg/kg/d had a mean parasitemia of only 0.28% (Fig. 3.45B). We observed a wide range of parasitemia (0-45.8%) in the groups that received lower doses of doxycycline (32mg/kg, 16mg/kg, 8mg/kg; Fig. 3.45B). We found mice with almost not detectable parasitemia (0.0%; but still few parasites found in the whole slide) and animals with rather high parasite load (up to 45.8%; Fig. 3.45B) in all groups with reduced doxycycline doses (compared to the 80 mg/kg control group).

These results showed that some PbA-infected mice that had received reduced doses of doxycycline (32mg/kg or less), were still protected from developing ECM, despite an increasing parasitemia.

Chapter 4

Discussion

The mechanisms that form the basis of cerebral malaria are multi-factorial and have not yet been understood completely. Mechanical obstruction of cerebral blood vessels and subsequent shortage of nutrition in the brain caused by intravascular sequestration of infected red blood cells were assumed to be major factors contributing to the disease. However, detection of strong inflammatory responses in CM patients brought focus on the host's immune responses, which could be confirmed in experimental models of CM. With the help of well-established and accepted mouse models, inflammatory cytokines and CD8⁺ T cells were identified as indispensable components in the development of ECM malaria and so far, several factors could be validated in human studies, linking CM development to strong inflammation.

Using the PbA infection model in mice, we addressed the question, how the genetic lack of cross-presenting DCs - a key cell population in the induction of a strong CD8⁺ T cell-associated T_H1 response - affects the development of ECM and the involved immune responses and secondly, whether and how an experimental treatment with doxycycline was able to interfere with the already primed effector immune responses and survival in PbA-infected mice.

In the first part of this study, we analyzed PbA-infected *Batf3*^{-/-} mice that are deficient of cross-presenting DCs and that are completely protected from ECM. This protection was associated with the complete absence of cerebral inflammation, which was in sharp contrast to infected WT controls that suffered from ECM, characterized by severe brain inflam-

mation. Importantly, whereas PbA-infected WT mice generated a strong inflammatory immune-response in the periphery, we found weak, but still detectable cytotoxic immune responses and a rather regulatory milieu in infected *Batf3*^{-/-} mice. These findings included reduced cytotoxic activity and increased presence of regulatory cells (T_{regs} , AAMs) and cytokines (IL-10) in spleens of the infected knock-out mice. Thus, the genetic ablation of cross-presenting dendritic cells, prevented the generation of excessive inflammatory responses and rather enabled the development of a balanced milieu, resulting in protection from fatal ECM.

The second part of this thesis addressed the question whether a late therapeutic intervention after PbA-infection of Bl/6 WT mice was able to interfere with the usually fatal disease progression. We showed that doxycycline treatment successfully prevented ECM development in infected mice when given from day four p.i., which is just before first specific neurological symptoms usually manifest, but the infection is already established (although not yet with neuro-pathological symptoms). Doxycycline-treated mice contained less cellular infiltrates in their brains and showed strongly reduced activation of T cells and also antigen-presenting cells, which added up to a complete ECM-protection in otherwise susceptible mice. Importantly, we could show, that in addition to the well-known anti-parasitic properties of doxycycline, the anti-inflammatory effect is strongly contributing to ECM protection.

4.1 Cross-presenting dendritic cells were required for development of ECM in a PbA mouse model

Batf3^{-/-} mice, which genetically lack cross-presenting dendritic cells, were not susceptible to cerebral malaria (100% survival), in contrast to PbA-infected WT mice (Fig. 1.2A, B), which is in line with the observations from others in *Batf3*^{-/-} mice [Zhao et al., 2014] or in mice that were depleted from CD11c^{hi}CD8a⁺ or all conventional DCs early in infection [Piva et al., 2012, DeWalick et al., 2007]. Interestingly, Zhao et al., using *Batf3*^{-/-} mice, described a lower survival rate of only around 50%, which might be explained by the different infectious doses that were used. We routinely use 5e4 iRBCs (injected i.v.), while Zhao et al. infected mice i.v. with 1e6 iRBCs. As injection of iRBC is done by whole blood transfer from PbA-infected donor mice, this does not only mean that a higher

parasite load but also more competent immune cells are injected, which could trigger a stronger immune response leading to ECM.

Importantly, we observed that the lack of cross-presenting dendritic cells did not only prevent ECM after blood-stage infection but also after sporozoite injection (Fig. 3.1A, B). Sporozoites undergo a liver stage before they develop to merozoites that re-enter the blood stream, resulting in a delay of 1-2 days for disease onset. Research models that infect with blood-stage parasites bypass the liver phase, which might trigger different immune responses against the pathogen. We are aware of this possibility, but since both routes of infection resulted in the same outcome, we focused on the blood-stage infection.

A relevant finding was that blood parasitemia of WT and *Batf3*^{-/-} mice after infection with either iRBCs or sporozoites was comparable (Fig. 1.2C, 3.1C), which is in agreement with the results from others that depleted cDCs and cross-presenting DCs in [Piva et al., 2012, DeWalick et al., 2007]. This indicated that the ECM-protection of PbA-infected *Batf3*^{-/-} mice was not caused by a reduction of the parasite load but by other unknown mechanisms and that the lack of cross-presenting dendritic cells neither impaired the ability of the parasites to replicate nor did it interfere with the immune systems capability to fight the parasites. However, infection of *Batf3*^{-/-} mice with murine *Plasmodium* strains like *P. chabaudi chabaudi* which are not lethal in C57Bl/6 mice and can be controlled by the animals [Li et al., 2001], would further help to characterize the role of cross-presenting DCs in replication control of *Plasmodium* parasites.

4.1.1 PbA-infected *Batf3*^{-/-} mice maintained a stable blood-brain barrier and lacked infiltration of effector T cells into the brain

In addition to sequestration of blood cells in the brain, the breakdown of the blood-brain barrier is a hallmark of experimental cerebral malaria and has also been described in human CM. However, the situation in human patients is less clear and until today there is no evidence that cerebral malaria is strictly linked to a damaged blood-brain barrier in humans. Interestingly, the link between CM and a destructed BBB were dependent on age and origin of the patients [Renia et al., 2012].

C57Bl/6 mice that are infected with *P. berghei* ANKA usually die between 6 and 8 dpi, shortly after displaying neurological symptoms of disease like limb paralysis and convulsions. The rapid disease progression that leads to death within hours after first

symptoms is closely related to the destruction of the blood-brain barrier, which starts at the olfactory bulb on 5 dpi, a few hours before ECM onset [Zhao et al., 2014]. We observed a massive BBB disruption in PbA-infected WT mice, but not in *Batf3*^{-/-} mice, which were free of disease symptoms and completely protected from ECM (Fig. 1.2D,E).

This finding was also mirrored by the low number of cellular infiltrates found in brains of PbA-infected *Batf3*^{-/-} mice and naive mice, in contrast to samples from infected WT mice containing significantly increased cell numbers (Fig. 3.3). Reduced cellular brain infiltration was also described in other studies of PbA-infected mice that were depleted of cross-presenting DCs [Piva et al., 2012]. However, recovered cells from brains of experimental animals have not necessarily passed the blood-brain barrier but could also be attached to cerebral blood vessels strong enough to circumvent removal by perfusion of the animals. Therefore, BBB breakdown and detection of peripheral immune cells in brain samples by flow cytometry do not describe the same phenomenon; but it is likely, that adhesion and activation of immune cells in the brain after *Plasmodium* infection strongly contribute to the disruption of the blood-brain barrier.

In ECM, CD8⁺ T cells were clearly identified as primarily responsible effector lymphocytes by using transgenic mouse models and depleting antibodies [Belnoue et al., 2002, Rénia et al., 2006]. In contrast, the role of CD4⁺ T cells is less clear and studies on this cell subset have shown inconsistent data regarding their importance [Belnoue et al., 2002].

In brain samples of d+6 PbA-infected Bl/6 mice that suffered from ECM, we found a clear increase of CD8⁺ T cells and Ly6C⁺ monocytes. In contrast, in brains of PbA-infected *Batf3*^{-/-} mice, which were ECM-free, we detected only minor amounts of peripheral immune cells and the cell count and cellular composition in the digested brain samples did not differ to that from naive animals (Fig. 3.4, 3.5).

These findings suggested that in addition to a general reduced cellular infiltration in the brains of *Batf3*^{-/-} mice compared to WT mice, the frequencies and absolute cell counts of certain effector cell subsets were only in ECM-susceptible mice significantly altered. These changes resulted in a prevalence of cells promoting inflammation, which supports the general idea that cerebral malaria is the result of overwhelming immune responses. These alterations in brain infiltrated cells might also emerge from differences in the cellular composition and activation in the spleen - where the infiltrated cell have been primed - and will be discussed later.

4.1.2 ECM-protected *Batf3*^{-/-} mice showed no signs of cerebral inflammation 6 days after PbA-infection

The migration of immune effector cells - especially of T lymphocytes - to the brain is necessary but not sufficient for the development of experimental cerebral malaria. Further important factors are effector molecules that are associated with strong inflammation and ECM, such as granzyme B, IFN γ and members of the TNF family, which are well described in PbA-infected WT mice and were also detected in our experiments. In contrast, we found significantly less of these mediators and also impaired expression of activation markers on infiltrated immune cells in brain samples from *Batf3*^{-/-} mice, thereby confirming diminished cerebral inflammation.

4.1.2.1 Cells in brains of PbA-infected *Batf3*^{-/-} mice produced less effector molecules

Cytotoxic T cells that come to the brain have to be previously activated in the periphery but require a certain local parasite (= antigen) threshold to be fully functional [Haque et al., 2011]. Granzyme B is one of the important molecules that account for the activity of cytotoxic T cells and was identified as a requirement for ECM development [Haque et al., 2011].

For a thorough analysis of activation markers relevant in ECM, we need to differentiate between a cell's capability to produce cytotoxic or immune regulatory mediators versus their actual release, *in* or *ex vivo*. In our study, brain samples of PbA-infected WT mice contained strongly elevated amounts of granzyme B on protein level in CD8⁺ T cells as measured by intracellular FACS as well in supernatant of whole brain cell culture by ELISA and also on mRNA level via qRT-PCR. In contrast, we detected significantly reduced granzyme B expression in brains of PbA-infected *Batf3*^{-/-} mice (Fig. 3.6A-C). These data fitted with reduced parasite loads in PbA-infected *Batf3*^{-/-} mice in contrast to high parasite infiltration in infected WT mice (preliminary data not shown).

All data clearly demonstrated reduced cytotoxicity of the few CD8⁺ T cells that were found in the brains of *Batf3*^{-/-} mice after PbA-infection, which might be also linked to the lower parasite load in the brain. While the pure presence of granzyme B⁺ T cells in brains was not sufficient to induce ECM [Shaw et al., 2015], the absence of this cytotoxic cells are clearly an advantage for the infected *Batf3*^{-/-} mice, as mice lacking granzyme B have been shown to be protected from ECM [Haque et al., 2011].

In addition to elevated levels of granzyme B, we measured significantly more TNF production in brain samples of ECM positive WT mice, but not in samples from ECM-negative *Batf3*^{-/-} mice (Fig. 3.6E). TNF can be released by many cell types, such as blood-borne macrophages and Ly6C⁺ monocytes, which were found in increased numbers in brains of PbA-infected WT mice but not in infected *Batf3*^{-/-} mice (Fig. 3.5), but also from brain resident microglia and even astrocytes [Renno et al., 1995, Lieberman et al., 1989]. Initially, TNF was shown to be necessary for ECM development, as depletion by anti-TNF antibodies resulted in ECM protection in mice [Grau et al., 1987], however trials in human CM patients could not validate its importance [John et al., 2010]. Over time other members of the TNF family came into focus [Randall and Engwerda, 2010] and more recent findings favor a role for LIGHT-lymphotoxin- β and lymphotoxin- α (LT- α), as mice deficient for TNF are fully susceptible to ECM but those deficient for LIGHT-LT β receptor or LT- α do not develop ECM [Randall et al., 2008, Engwerda, 2002]. A possible explanation for these conflicting data is the similarity of TNF and LT- α . Structural similarity and common receptors (TNFR1 and 2), make selective antibody depletion of TNF difficult [Engwerda, 2002]. Therefore, we can only conclude, that members of the TNF super-family were regulated in *Batf3*^{-/-} mice upon PbA-infection.

Taken together, we can conclude a diminished production of inflammatory cytokines in parallel to reduced amounts of possible cellular sources such as T cells and monocytes in brains of ECM-protected *Batf3*^{-/-} mice were contributing to the observed phenotype,

4.1.2.2 Reduced ICAM-1 expression could prevent adhesion of cells in brains of PbA-infected *Batf3*^{-/-} mice

The local action and motility of cytotoxic T cells in the brain is a major factor in ECM development [Shaw et al., 2015]. Adhesion molecules like ICAM-1 help the circulating immune cells to adhere on endothelial cell in order to engage in a local immune response. T cells from spleens and those immigrated to the brain showed significantly increased ICAM-1 expression in PbA-infected WT but not in infected *Batf3*^{-/-} mice (Fig. 3.6D, 3.11D). ICAM-1 is an adhesion molecule whose expression has been shown to be necessary on leukocytes for ECM development [Ramos et al., 2013]. A reduced ICAM-1 expression could be a direct effect of the lacking interaction of CD8⁺ T cells with cross-presenting

DCs, as TC-DC-interactions give rise to a positive-feedback-loop with subsequent induction of ICAM-1 expression [McBride and Fathman, 2002]. In the course of disease development, the lack of an adhesion molecule could be beneficial, as T cells might be less likely to attach to other cells like endothelial cells, platelets or infected erythrocytes which could prevent cluster formation, microvessels occlusion and inflammation in brains during ECM [Ramos et al., 2013, de Kossodo and Grau, 1993, Shaw et al., 2015].

4.1.2.3 Phagocytosis is reduced in microglia of PbA-infected and naive *Batf3*^{-/-} mice

Brain resident microglia are often described as the macrophages of the brain. Next to their role as a possible source of TNF and other cytokines, they can also take up antigen for clearance functions and present antigen to other immune cells. In both, human CM patients as well as in murine ECM studies, activated microglia were found [Deininger et al., 2002, Medana et al., 1997].

In a preliminary experiment, we observed that the capability to take up antigen was increased in microglia isolated from brains of both PbA-infected groups (WT and ko) on 6 dpi compared to their respective naive controls but not early in infection on 3 dpi (compared to naive controls; Fig. 3.7). Interestingly, the frequencies of microglia that had taken up the beads was lower in *Batf3*^{-/-} mice compared to WT mice at all analyzed time points.

Currently, there are no studies regarding putative roles of *Batf3* in development or activity of microglia. However, a recent paper showed that *Batf3* is not necessary for the initial development of pre-CD8a⁺ DCs but is needed for auto-activation of transcription factor interferon regulatory factor 8 (*IRF8*), which is required for the maturation of this DC subtype [Grajales-Reyes et al., 2015]. *IRF8* but not *Batf3* was shown to be also involved in the development of microglia; however functional features such as phagocytosis were not tested and could still be affected through a similar *Batf3-IRF8*-interaction as in the DC development [Kierdorf et al., 2013]. Further investigations are required in order to see how the lack of *Batf3* might influence microglia actions.

4.1.3 Protection from brain pathology in PbA-infected *Batf3*^{-/-} mice apparently resulted from altered immune responses in the spleen

The general lack of inflammatory processes in brains of PbA-infected *Batf3*^{-/-} mice was in strong contrast to the results from susceptible WT mice on 6 dpi (Fig. 3.6). Immune responses to *Plasmodium* parasites are initiated in the spleen, where T cells are primed upon antigen encounter [Engwerda et al., 2005]. These activated T cells then migrate towards a chemokine gradient into the brain where clustering of infected red blood cells leads to an activation of the local tissue and subsequent release of chemokines attracts further immune cells.

Since all of these inflammatory processes were strongly impaired in PbA-infected *Batf3*^{-/-} mice, we hypothesized that reduced inflammation in the brain might be the result of a hampered T cell priming in the spleen of PbA-infected *Batf3*^{-/-} mice that remain ECM free.

It was shown before, that only depletion of DCs at an early time point of infection leads to protection from ECM in otherwise susceptible mice, which favors a role of DCs in the priming phase of PbA-infection [DeWalick et al., 2007]. Lundie et al. specifically showed that CD8a⁺ DCs, that cross-present antigen to CD8⁺ T cells, are essential for priming of CD8⁺ T cells in ECM [Lundie et al., 2008].

4.1.3.1 PbA-infected *Batf3*^{-/-} mice displayed an impaired, but not fully absent CTL response

First of all, we determined strong production of cytotoxic molecules in the periphery in PbA-infected WT mice. Most importantly, the functional ability of endogenously generated T lymphocytes to lyse cells that present parasite-derived antigens was tested and successfully demonstrated for PbA-infected WT mice.

Parasite-specific cytotoxicity can be determined by lysis of peptide-loaded target cells by endogenously generated T cells in an *in vivo* CTL assay. This assay was performed previously in our lab with the help of transgenic PbA parasites that expressed ovalbumin; in addition to the well-described MHC class I peptide from OVA (SIINFEKL), we analyzed also responses towards MHC class I peptides from the endogenous parasite-derived protein MSP-1 (merozoite surface protein) that our group had identified before.

Indeed, in addition to the lack of brain inflammation in PbA-infected *Batf3*^{-/-} mice, they generated only weak CTL responses in their spleens compared to infected WT mice (Fig. 1.2F). Next to generally reduced CD8⁺ T cell frequencies throughout infection (3 dpi and 6 dpi; Fig. 3.10C), an analysis of their splenocyte cultures revealed less cytotoxic molecules, such as granzyme B and IFN γ , as well as reduced expression of markers associated with T cell activation such as ICAM-1, on 3 and 6 dpi when compared to PbA-infected WT mice (Fig. 3.11, 3.12).

The majority of CD8⁺ T cells found in spleens of PbA-infected WT mice expressed CD11c, which is, according to Beyer et al., a marker for cytotoxic T cells [Beyer et al., 2005] and fits to the finding by Tamura et al. that CD11c⁺CD8⁺ T cells are highly activated in PbA-infection and contribute to the ECM pathology by production of inflammatory cytokines and by promoting T cell accumulation in the brain [Tamura et al., 2011]. However, we found in PbA-infected *Batf3*^{-/-} mice, significantly less T cells expressing CD11c, indicating less efficient activation (Fig. 3.12D). In addition, the presence of CD11c⁺CD8⁺ T cells was also described for other ECM-resistant strains such as Balb/c mice [Tamura et al., 2011]. Therefore, the pure presence of this cell subset is apparently not sufficient to induce ECM, but CD11c expression itself might be an interesting marker for T cell activity in ECM.

The reduced ability of splenic CD8⁺ T cells from *Batf3*^{-/-} mice to produce and release granzyme B and IFN γ upon PbA-infection (Fig. 3.11, 3.12) is not only a sign of their hampered activation, but most likely one part in the processes that lead to the observed ECM protection, as both cytotoxic mediators, granzyme B and IFN γ , were shown to be required for development of ECM with the help of knock-out mice [Haque et al., 2011, Rudin et al., 1997]. Our results are in line with observations from Piva et al. (2012), who reported reduced signs of T cell activation in Clec9A-DTR mice, which were depleted of cross-presenting DCs by diphtheria toxin (DT) before PbA-infection [Piva et al., 2012]. Interestingly, they observed an increase in serum IFN γ levels at an early time point of infection, before the onset of ECM symptoms in WT but not Clec9A-DTR mice. In contrast to our results, where serum IFN γ was only reduced in *Batf3*^{-/-} mice on 3 dpi but not on 6 dpi when compared to WT controls (Fig. 3.11C), Piva et al. observed lower IFN γ also on 4 and 6 dpi [Piva et al., 2012]. Those differences could be caused by the different

approaches to eliminate the cross-presenting DCs.

The study from Haque et al. showed that *gzmB*^{-/-} mice (genetically lacking granzyme B) contained more IFN γ positive CD4⁺ and CD8⁺ T cells in their spleens, but were fully protected from ECM. They could also demonstrated by adoptive transfer experiments, that IFN γ deficient OT-I cells were still able to induce ECM-like symptoms in PbA-OVA-infected *gzmB*^{-/-} mice [Haque et al., 2011]. These observations led them to the conclusion that - in contrast to granzyme B - IFN γ is dispensable for ECM development. However, the whole process leading to ECM is multi-factorial and can not be fully explained by the presence or absence of these mediators.

Additionally to reduced T cell activity in PbA-infected *Batf3*^{-/-} mice, we observed an increase of inflammatory Ly6C⁺ monocytes in spleens of WT but not in *Batf3*^{-/-} mice on 3 dpi, but this was not seen at later time points of infection (Fig. 3.18C). The production of TNF was increased in WT mice on 3 dpi but was not changed in *Batf3*^{-/-} mice (Fig. 3.19A). These observations are in line with results from our lab that showed an important role for inflammatory monocytes in the early phase of PbA-infection: early (0 dpi) but not late (3 + 5 dpi) depletion of CCR2⁺ monocytes prevented ECM in usually susceptible Bl/6 mice [Schumak et al., 2015].

Taken together, we concluded that PbA-infected *Batf3*^{-/-} mice were protected from ECM due to an impaired CTL response.

NK cells could contribute to the cytotoxic immune response in *Batf3*^{-/-} mice after PbA-infection

Granzyme B and IFN γ are pro-inflammatory mediators that are usually produced by cytotoxic T cells, but can also be produced by natural killer (NK) and natural killer T (NKT) cells. Importantly, we detected elevated NK and NKT cell frequencies in spleens of PbA-infected *Batf3*^{-/-} mice at an early (3 dpi) and late (6 dpi) time point after infection when compared to samples of infected WT mice (Fig. 3.13). Therefore, we analyzed these cell subset for their ability to produce granzyme B and IFN γ at both time points. MACS-purification by DX5 made it impossible to distinguish between NK and NKT cells, and therefore both cell subsets together will be referred to as NK(T) cells.

In agreement with cytokine analysis from whole spleen cell culture (Fig. 3.11A, B),

granzyme B and IFN γ were detected at very low levels in NK(T) culture supernatant derived from d+3 PbA-infected mice of both strains (Fig. 3.14). NK cells belong to the innate immune system, which would favor an early cytokine production by these cells. However, NK cells as producers of early IFN γ were found to be more important in the brain than in the spleens of PbA-infected mice [Villegas-Mendez et al., 2012]. Interestingly, IFN γ levels in serum from d+3 PbA-infected WT mice were almost 10-fold higher compared to *Batf3*^{-/-} mice (Fig. 3.11C).

In contrast to early infection, we detected high levels of both cytokines in NK(T) cell cultures on 6 dpi (Fig. 3.14). Importantly, supernatants of NK(T) cell culture contained more granzyme B expression in samples from PbA-infected *Batf3*^{-/-} mice compared to samples from infected WT mice, which was in contrast to observations from the whole spleen cell culture where granzyme B level were higher in samples from PbA-infected WT mice (Fig. 3.14A, 3.11A). While IFN γ production is assigned to NKT cells and also CD4⁺ T cells in later *Plasmodium* infection [Deroost et al., 2016], the production of granzyme B has not yet been described in detail. Flow cytometry analysis on 6 dpi could further enforce a cytotoxic role of NK cells in *Batf3*^{-/-} mice, since degranulation marker CD107a was significantly increased in PbA-infected *Batf3*^{-/-} mice, but not in infected WT mice (Fig. 3.15D).

Interestingly, despite observations that *P. falciparum* infected RBCs induce granzyme B in NK cells [Böttger et al., 2012] and these cells are involved in parasite elimination [Chen et al., 2014], the parasitemia was not affected by the higher levels of granzyme B (Fig. 1.2C).

The finding that NK(T) cells from PbA-infected *Batf3*^{-/-} mice produced more granzyme B and were more activated than those from WT animals could indicate a mechanism by which the immune system tries to compensate for the impaired cytotoxicity of CD8⁺ T cells and could at least in part explain the high cytokine levels in spleen cell culture supernatants of ECM-negative *Batf3*^{-/-} mice.

Alternative generation of cross-presenting dendritic cells could contribute to the remaining CTL response in PbA-infected *Batf3*^{-/-} mice

CTL responses and T cell activation in PbA-infected *Batf3*^{-/-} mice were significantly reduced compared to infected WT mice, but not completely absent. Additionally, even if impaired, antigen-specific immune responses were still detectable in these mice (Fig. 3.11, 3.12, 1.2F). Therefore, priming of CD8⁺ T cells was not completely abolished.

Spleens of *Batf3*^{-/-} mice contained almost no XCR1⁺ DCs, but very few cells were still detectable (Fig. 3.16). Next to the possibility of false positive signals or a leaky knock-out phenotype, an explanation for the presence of XCR1⁺ DCs in *Batf3*^{-/-} mice could be a *Batf3*-independent mechanism, as generation of cross-presenting DCs was shown in the absence of *Batf3* [Mott et al., 2015]. Other transcription factors that might compensate the lack of *Batf3* include *Batf2* or interferon regulatory factor 8 (*Irf8*) [Seillet et al., 2013]. Later studies confirmed that pre-CD8a⁺ DCs develop in the absence of *Batf3*, but this transcription factor was needed to maintain auto-activation of *Irf8* which is necessary to preserve the CD8⁺ phenotype of developing DCs [Grajales-Reyes et al., 2015].

One minor difficulty in interpretation of these results is the fact that all mentioned studies defined cross-presenting DCs as CD8a⁺ DCs, which make only up for 80% of this DC subset, with XCR1 being a better marker for the *Batf3*-dependent cross-presenting DCs [Bachem et al., 2012]. This small discrepancy has to be kept in mind when analyzing the results, as CD8a⁺ DCs that emerge in the absence of *Batf3* could be part of the non-cross-presenting subset.

Antigen-cross-presentation by alternative cell subsets could activate CTL responses with the help of IL-6 *trans*-signaling

As the remaining XCR1⁺ DC population was very small in *Batf3*^{-/-} mice, we addressed the question whether other cells were able to induce CD8⁺ T cell responses.

Analysis of XCR1⁻ DCs revealed significantly higher CD40 expression in PbA-infected *Batf3*^{-/-} mice 6 days post infection compared to infected WT mice (Fig. 3.17A). While CD40 expression is associated with the cross-presentation in general, there is no evidence that XCR1⁻ dendritic cells acquire the ability to cross-present when expressing high levels of CD40 [Yin et al., 2015]. Analysis of other APCs like macrophages, monocytes and neutrophils did not show any striking differences between PbA-infected WT and *Batf3*^{-/-} mice in cell numbers (Fig. 3.18) but cells from *Batf3*^{-/-} mice showed reduced phagocytic capacity on 6 dpi (Fig. 3.20). Therefore, alternative cross-presentation within our current analyses needs further explanation.

Liver sinusoidal endothelial cells (LSEC) are liver resident cells that can cross-present exogenous antigen to T cells to induce tolerance [Limmer et al., 2000]. However, also rapid generation of granzyme B-expressing CD8⁺ effector T cells after antigen cross-presentation

by LSECs is possible and was shown to be dependent on IL-6 *trans*-signaling, where the soluble form of IL-6 receptor (sIL-6R) binds IL-6 in order to activate the signaling transducing unit glycoprotein 130 (gp130) [Böttcher et al., 2014]. We did not yet characterize LSECs in the livers of our PbA-infected *Batf3*^{-/-} mice, but we found increased levels of IL-6 production in these mice (Fig. 3.21D, E). Therefore, the framework requirements for cross-presentation of *Plasmodium* antigen and subsequent activation of CD8⁺ effector T cells by LSECs would be present in our model.

Red pulp macrophages and CD169⁺ macrophages are further cell populations that are discussed to be able to cross-present antigen to CD8⁺ T cells [presentation by C. Kurts at the European Congress of Immunology, 2015 in Vienna, Bernhard et al., 2015]. However, while CD169⁺ macrophages were able to induce a CTL response in the absence DCs, the mechanism of cross-presentation was not confirmed in this study.

In summary, the remaining CTL responses in PbA-infected *Batf3*^{-/-} mice are probably induced by other APC populations than CD8a⁺ DCs and should be further investigated in future studies.

4.1.3.2 The lack of *Batf3* resulted in a shift from inflammation to a more regulatory milieu after PbA-infection

Remarkably, besides a strongly reduced cytotoxic immune response in brain and spleen of PbA-infected *Batf3*^{-/-} mice, we could also observe an increase in regulatory characteristics in those mice. *Batf3*^{-/-} mice contained higher total amounts of T_{regs} in their spleens on 3 and 6 dpi and the regulatory programmed death-1 (PD-1) receptor was strongly upregulated on CD4⁺ and CD8⁺ T cells in these mice when compared to PbA-infected WT mice (Fig. 3.22). Cultured spleen cells produced more IL-10 in d+6 PbA-infected *Batf3*^{-/-} mice, especially the production of IL-10 by CD11b⁺ cells was markedly increased (Fig. 3.21A,C). IL-10 producing CD11b⁺ cells might include regulatory B cells [O'Garra et al., 1992], which might play a role in ECM regulation [Liu et al., 2013] or alternatively activated macrophages, which will be discussed in more detail.

In spleens of *Batf3*^{-/-} mice, T_{regs} were slightly elevated but did not produce more IL-10 than cells from WT mice

The increased CD4⁺ vs. CD8⁺ T cell ratio that we observed in PbA-infected *Batf3*^{-/-} mice on 3 and 6 dpi was a first hint that regulatory mechanisms might play a role in the ECM-protection in these mice (Fig. 3.10D). These results were further supported by the finding that absolute amounts of T_{regs} and IL-10 production were increased in spleens of *Batf3*^{-/-} mice after PbA-infection (Fig. 3.22, 3.21).

Our observation that the population of regulatory T cells was increased in ECM-resistant mice is supported by results from others who found that spleens of ECM-resistant Balb/c and DBA/2 mice contain higher amounts of T_{regs} at all time points after PbA-infection, which suggests a role for these cells in controlling the cerebral inflammation in ECM [Wu et al., 2010]. Similar to our results, findings of Wu et al. were accompanied by higher amounts of anti-inflammatory cytokines and a decrease in pro-inflammatory mediators. However, the role of T_{regs} is conversely discussed in *Plasmodium* infection. Depletion of T_{regs} by injection of an anti-CD25 antibody was found to protect mice from ECM development, which reinforces the idea of a complex and multi-factorial role of this cell type in *Plasmodium* infections [Amante et al., 2007]. A possible conflict in this study is the use of anti-CD25 antibody for depletion of T_{regs} as CD25, the receptor for IL-2, is also upregulated on activated cytotoxic T cells and might therefore not be specifically depleting T_{regs} only. Additionally, these results could not be confirmed using DERE mice in which a bacterial artificial chromosome expresses a diphtheria toxin (DT) receptor-enhanced GFP (eGFP) fusion protein under the control of the *foxp3* gene locus which allows specific depletion of T_{regs} by diphtheria toxin injection [Steeg et al., 2009]. Analysis in human patients that had been infected with *Plasmodium falciparum* could not reveal any correlation between the presence of T_{regs} and the severity of malaria symptoms [Torres et al., 2014]. In summary, the role of T_{regs} in ECM is not yet defined completely and needs further investigation.

Could splenic CD8a⁻ DCs induce the generation of a regulatory milieu in PbA-infected *Batf3*^{-/-} mice?

CD8a⁻ dendritic cells are also known to regulate T_{reg} development by interaction

between CD80 / CD86 and CD28 on T_{regs} [Leventhal et al., 2016]. We found more DCs in naive and d+3 PbA-infected $Batf3^{-/-}$ mice compared to WT mice (Fig. 3.16A). As $Batf3^{-/-}$ mice are lacking CD8a⁺ DCs, all remaining DCs are CD8a⁻, which could play a role in T_{reg} regulation. Interestingly, cells from $Batf3^{-/-}$ mice did not show an increase in CD80 or CD86 expression, and even a small reduction compared to WT mice on 3 dpi (Fig. 3.17B). Leventhal et. al showed that T_{reg} regulation by DCs is dependent on CCR7, however, while the expression of this receptor was increased after PbA-infection and could play a role in regulation of the pro-inflammatory immune response, we could not find any differences between WT and $Batf3^{-/-}$ mice 6 days post infection (Fig. 3.17C).

While dendritic cells can also be a source of IL-10, this function is mainly associated with CD8a⁺ CD11b⁻ DCs, which makes a contribution of DCs from $Batf3^{-/-}$ mice to IL-10 production from CD11b⁺ cells unlikely.

Together, these results suggest that the anti-inflammatory milieu observed in $Batf3^{-/-}$ mice is not a direct consequence of altered activation of CD8a⁻ DCs.

Alternatively activated macrophages could play a role in immune regulation in $Batf3^{-/-}$ mice after PbA-infection

T_{regs} are an important regulatory immune cell subset and a major source of IL-10. However, we could not detect differences in IL-10 production from CD4⁺ purified T cells between all experimental groups, but we observed a strong increase in IL-10 production from MACS-purified CD11b⁺ cells that were isolated from PbA-infected $Batf3^{-/-}$ mice compared to almost baseline levels in infected WT mice (Fig. 3.21C).

While analyses in mice and humans did not find any proof for a relevant role of T_{regs} in regulatory immune responses after *Plasmodium* infection, IL-10 is an important regulator. *In vivo* experiments in PbA-infected mice showed that ECM could be induced by neutralization of IL-10 in usually resistant strains and inversely, ECM-susceptible mice could be protected from ECM by injection of recombinant IL-10 [Kossodo et al., 1997].

Alternatively activated M2 macrophages (AAMs) are of particular interest, as they have been shown to promote T_h2 immune responses which are associated with ECM production in resistant Balb/c mice. In our experiments the frequency and total cell number of AAMs was significantly higher in d+6 PbA-infected $Batf3^{-/-}$ mice when compared to WT infection controls (Fig. 3.23). A role of AAMs in our model was further underlined

by increased levels of IL-6 that were found in whole spleen cell cultures and cultures from CD11b⁺ splenocytes from uninfected and PbA-infected *Batf3*^{-/-} mice (Fig. 3.21). While IL-6 is often described as a pro-inflammatory cytokine, it has also immune regulatory properties. In a mouse model for obesity and insulin resistance, it was shown that IL-6 mediated the alternative activation of macrophages, which could in turn promote regulation of the overwhelming pro-inflammatory response [Mauer et al., 2014]. As AAMs can be induced by IL-6 and also produce IL-6 themselves, a connection of both is likely.

Alternatively activated macrophages have not yet been discussed in detail in *Plasmodium* infection, however, innate lymphoid cells (ILCs) were found to participate in immune regulation by inducing M2 macrophage polarization and are thereby be involved in ECM-protection in an IL-33 dependent manner [Besnard et al., 2015]. The analysis of ILCs in PbA-infected *Batf3*^{-/-} mice are a topic of ongoing research in our group.

AAMs were also mentioned in the context of non-lethal *P. chabaudi chabaudi* infection where a shift towards a T_h2 immune response is observed [Fairweather and Cihakova, 2009]. After infection, a shift from T_h1 to T_h2 responses is usually comprehensible in order to limit inflammation and the associated tissue damage, but can also give way to chronic infections. AAMs have been found to play a role in typical T_h2 associated parasite infections like helminth infection [Kreider et al., 2007], but also chronic bacterial infections [Benoit et al., 2008]. In *Plasmodium* infection, a shift towards a T_h2 could would be favorable to avoid an overwhelming immune response that can result in CM development.

Taken together, the immune responses to PbA in *Batf3*^{-/-} mice were shifted to a more immune regulatory milieu which could help to prevent ECM development.

4.1.4 Relevance of impaired CTL responses for PbA-infection in *Batf3*^{-/-} mice

Taken together, we hypothesize that the protection from ECM that was observed in *Batf3*^{-/-} mice upon PbA infection, resulted from an insufficient generation of a CTL response due to the genetic ablation of cross-presenting DCs and an additional immune regulating milieu (characterized by IL-10, AAMs and probably T_{regs}) that was established in these mice (Fig. 4.1).

4.1. CROSS-PRESENTING DENDRITIC CELLS WERE REQUIRED FOR DEVELOPMENT OF ECM IN A PBA MOUSE MODEL

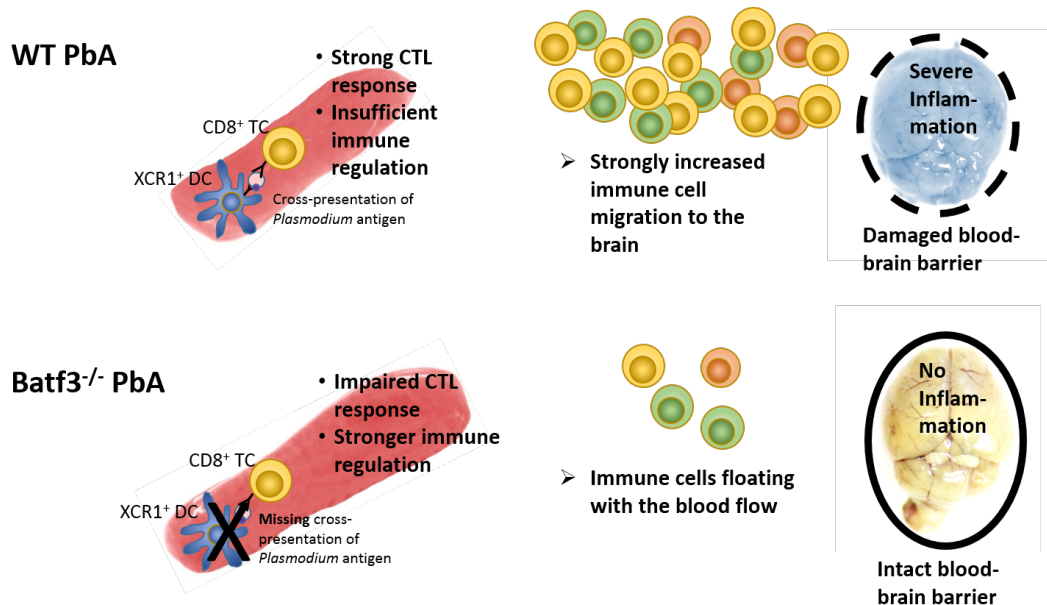


Figure 4.1: *Batf3*^{-/-} mice did not develop ECM as a consequence of impaired T cell priming and subsequent reduction of inflammation in the brain. Differences in the immune response to PbA infection between WT (upper) and *Batf3*^{-/-} (lower) mice are depicted in spleen and brain. In short: PbA-infection in WT mice leads to cross-priming of PbA antigen by XCR1⁺ DCs to CD8⁺ T cells which leads to a strong CTL response in the spleen of those mice. Activated pro-inflammatory immune cells migrate to a cytokine gradient in brain where they promote local inflammation which results in a breakdown of the blood-brain barrier. The lack of cross-presenting DCs in *Batf3*^{-/-} mice prevents efficient T cell priming and therefore the aftereffects, resulting in reduced CTL responses in spleen and brain, but enhancing regulatory mechanisms.

Several disease outcomes have been shown to be dependent on cross-presenting dendritic cells and their ability to prime cytotoxic CD8⁺ T cells. Studies in *Batf3*^{-/-} mice, were the first to specifically analyze animals lacking cross-presenting dendritic cells without affecting other cell populations [Hildner et al., 2008]. Using these mice, Hildner et al. showed that cross-presenting DCs are required for an adjuvant virus-specific immune CTL response after West Nile virus infection [Hildner et al., 2008]. Furthermore, the lack of *Batf3* was associated with impaired antigen-specific CTL responses in syngenic fibrosarcoma transplants and *Leishmania major* infections, which led to a diminished clearance function in both models [Hildner et al., 2008, Ashok et al., 2014].

Our data and also the above mentioned studies strongly indicate that the lack of *Batf3* leads to a diminished CTL response with concomitant induction of immune regulation. In some models, a strong CTL response is beneficial to clear an infection or to control tumor growth [Hildner et al., 2008, Ashok et al., 2014]. The role of CTL responses in

Plasmodium clearance after infection is less clear, however the involvement of cytotoxic T cell responses in the development of CM remains unchallenged [Deroost et al., 2016], which makes the lack of the pro-inflammatory immune response an advantage regarding survival in our model.

Importantly, the success of vaccination with live irradiation-attenuated *P. berghei* sporozoites was also dependent on T cells primed by cross-presenting dendritic cells. *Batf3*^{-/-} mice failed to generate protective IFN γ -producing CD8⁺ effector memory T cells and were not able to establish a sterile and long lasting immunity against *P. berghei* that is described in WT mice [Montagna et al., 2015]. This finding demonstrates, that the generation of CTLs is bivalent in malaria, as these cells are associated with immune damage on the one hand, but are required for immune memory generation on the other hand.

The differences between CM in human patients and ECM in mice have led to passionate discussions between researchers in the malaria field ([Craig et al., 2012]. Most researchers agreed that mouse models can be useful if certain conditions are met, like uniformity of experimental procedures and clear discrimination between investigation of disease development, prevention of disease and therapeutic approaches. In the end, limitations of those models are still outweighed by the advantages of experimental conditions, like defined exposure to pathogens, only specified genetic variability, inclusion of appropriate control groups or the ability to analyze organs of interest before the actual symptoms of CM are present [Craig et al., 2012]. Therefore, we have to keep in mind, that not all findings from a mouse model translate directly to the human disease. However, results from experimental approaches might initiate human studies to confirm the findings.

Taken together, these data confirm a key role for cross-presenting DCs in the immune response against *Plasmodium* parasites and help to understand the disease mechanism.

4.2 Doxycycline prevented ECM by exerting anti-inflammatory properties in susceptible Bl/6 mice

Doxycycline has previously been used in treatment of malaria because of its anti-parasitic effects [WHO, 2010, Budimulja et al., 1997, Batty et al., 2007]. However, doxycycline has also additional anti-inflammatory properties that could be beneficial for patients suffering from cerebral malaria, since neuro-inflammation is thought to contribute to disease manifestations. For a long time, fast parasite elimination was the major goal of CM treatment. However, recent studies explored options to directly target the inflammation in the brain [Miranda et al., 2013, Dende et al., 2015]. Our study here, aimed to elucidate the immune-modulating properties of doxycycline in a mouse model of CM in order to evaluate possible treatment options that directly affect the inflammatory causes of the disease.

Earlier findings from my diploma thesis demonstrated that intravenous injection of 80 mg/kg doxycycline starting from day four post PbA-infection successfully prevented ECM development in susceptible C57Bl/6 WT mice and reduced CTL responses in brains and spleens (Fig. 3.24, 3.25).

Briefly summarized, our initial studies revealed a significant reduction of brain inflammation, when compared to untreated PbA-infected mice (Fig. 3.25A-D), which included strongly reduced mRNA levels of cell adhesion molecules (L- and P-selectin) and several cytokines (CCL2, CCL5, CXCL2 and IL-6) which are all associated with inflammatory processes and are described to be present in brains of ECM-positive mice [Combes et al., 2010, Miu et al., 2008, Miranda et al., 2013]. Furthermore, we detected also lower protein levels of granzyme B in brain tissue of doxycycline treated mice. Most importantly, cytotoxic T cells that are associated with brain damage during ECM, exhibited significantly less cytolytic capacity in spleens of mice after doxycycline treatment (Fig. 3.27E), despite an enlarged spleen and increased total amounts of cells in comparison to control-infected mice (Fig. 3.27F). This was a relevant finding, since the priming of parasite-directed CTLs that is acquired in the spleen, was already completed before treatment start [Engwerda et al., 2005].

Therefore, we concluded that the administration of systemic doxycycline was able to alter the peripheral immune responses that had been already generated in the spleens

of PbA-infected mice by modification of effector cell activities, which resulted finally in reduced inflammation, especially in the brain and protection from ECM. However, doxycycline-treated mice had decreased peripheral parasitemia on 6 dpi, which raised the question whether the protective effect of doxycycline could be attributed to its immune-modulatory properties or / and to the reduced parasite load.

To answer this question, we established a modified experimental infection, and inoculated the mice with an elevated dose of iRBCs before doxycycline treatment, in order to ensure a comparable parasite load in DOX-treated (ECM-negative) and untreated (ECM-positive) mice. With this approach, we aimed to evaluate the immune regulatory effects of doxycycline while reducing the impact of the anti-parasitic effects in this model. Indeed, DOX-treatment of mice with elevated PbA parasite load was still able to prevent ECM, which was mirrored by a stable BBB, reduced amounts of cellular infiltrates in the brain and strongly impaired brain inflammation. Furthermore, we detected strongly impaired functions of cytotoxic T cells in DOX-treated mice, confirming the hypothesis that doxycycline – in addition to its well-described anti-parasitic properties - exerts strong immune modulatory capacities, affecting the activity of effector T cells and attenuating inflammatory immune responses, which finally protected the infected mice from fatal ECM.

4.2.1 Doxycycline treatment in mice infected with higher parasite loads prevented ECM and protected the blood-brain barrier

An unresolved problem in the analysis of the immune responses in mice that had received doxycycline treatment after PbA-infection, was the anti-parasitic effect of DOX. While clearance of the parasite is desirable in actual treatment, the ability to reduce parasitemia made differentiation between immune-modulatory and anti-plasmodial effects difficult. An idea to overcome this obstacle was to inject mice with a higher initial dose of parasites in order to align peripheral parasitemia in untreated mice and DOX treated mice on 6 dpi, when first neurological symptoms occur in the untreated control group. Mice infected with $1e6$ iRBCs before DOX-treatment start on 4 dpi, reached a similar parasitemia on 6 dpi when compared to untreated mice that had received the "normal" infective dose of $5e4$ iRBCs (as used before) (Fig. 3.28C). It is of notice that doxycycline treatment for 3 days was not enough to completely eliminate the parasites and parasitemia increased in all animals later on, leading to anemia but not to later CM symptoms after 10 dpi.

Importantly, despite a similar parasite load to untreated mice on 6 dpi, doxycycline treated mice were still 100% protected from ECM with only minor neuro-pathological symptoms (Fig. 3.28), similar to the results we had gained before with treatment of mice that had been infected with the lower dose of iRBC (Fig. 3.24).

Thus, the absence of ECM despite a high parasitemia in the "PbA 1e6 + DOX" groups confirmed our hypothesis that the protective effect of doxycycline was not only caused by its anti-parasitic effects. However, the later drop in parasitemia in DOX treated mice leaves room for discussion, as we could not exclude the possibility that the parasites were already damaged and maybe less pathogenic. An analysis with a doxycycline-resistant PbA strain could clarify these remaining issues, but unfortunately no such strain is known for use in the mouse model.

Consistently with the ECM-protection upon DOX-treatment, treated mice revealed a stable the blood-brain barrier till 9 dpi, regardless of the initial infective dose of parasites, in contrast to untreated controls which died on 6 dpi with a severely damaged BBB (Fig. 3.29).

Studies in murine ECM model have shown that the BBB disruption in cerebral malaria is not caused by apoptosis of endothelial cells but rather by alteration of the tight junction proteins of cells building the BBB that are caused by CD8⁺ T cells in a perforin-dependent manner [Suidan et al., 2008, Shaw et al., 2015]. These observations were used to explain the fast recovery of the blood-brain barrier after administration of anti-malarial drugs [Shaw et al., 2015], which we also observed in our experiments from 7 dpi (Fig. 3.29). It is possible that doxycycline protects the blood-brain barrier through various mechanisms. In a rat model of middle cerebral artery occlusion and reperfusion, doxycycline reduced the BBB leakage and the cerebral infarct volume by up-regulation of tight-junction proteins [Wang et al., 2011]. In addition, doxycycline could act in an anti-inflammatory manner similar to minocycline, another antibiotic of the tetracycline group, which was shown to alter T cell activation and reduce their contact with microglia [Giuliani and Hader, 2005].

4.2.1.1 PbA-infected mice showed reduced cerebral inflammation after doxycycline treatment: less cellular infiltrates and impaired activity of effector T cells

BBB breakdown and migration of immune cells to the brain, especially of cytotoxic T cells, but also macrophages, is a hall mark of experimental cerebral malaria [Nacer et al., 2014]. The stability of the BBB upon DOX-treatment was further mirrored by less infiltration of cells with hematopoietic origin in brains of 1e6 iRBC PbA-infected mice (+DOX) compared to ECM-positive control-infected mice. However, DOX-treated mice still contained a higher number of leukocytes in their brains compared to uninfected controls (Fig. 3.30).

We found similarly increased T cell frequencies in both infected groups and subsequent reductions in the frequencies of other cell subsets (Fig. 3.31, 3.33, 3.34). Because of the late intervention with doxycycline at 4 dpi, we hypothesized that an effect on cell population migration was less likely compared to alterations in cell activation.

Indeed, T cells from brains of doxycycline treated 1e6 iRBC PbA-infected mice, showed reduced expression of activation markers such as ICAM-1 on their surface and intracellular granzyme B (Fig. 3.32). Granzyme B is an important cytotoxic mediator in ECM. While the pure presence of granzyme B alone is not sufficient ECM induction [Shaw et al., 2015], its absence is clearly beneficial as $gzmB^{-/-}$ mice do not develop ECM [Haque et al., 2011]. Similarly, the lack of ICAM-1 expression on T cells protected mice from ECM [Ramos et al., 2013].

Minocycline, another tetracycline derivate, is able to reduce T cell activation due to its Ca^{2+} chelating activity [Kloppenborg et al., 1995]. As doxycycline shares the chelating ability with minocycline, a similar mechanism is reasonable.

Reduced activation of T cells in doxycycline treated mice after PbA-infection was accompanied by diminished cytokine levels in primary brain cell cultures such as CCL5 (Fig. 3.36), which is an attractant of T cells and important player in development of CM in mice and humans [Belnoue et al., 2003b, Hanum et al., 2003, Sarfo et al., 2004]. Migration of T cells to the brain is a hallmark of ECM and low levels of CCL5 might hinder T cell migration in doxycycline-treated mice. Additionally, binding of CCL5 to its receptors on brain resident cells might activate these cells and result in subsequent BBB breakdown in susceptible animals [Sarfo et al., 2004, Szklarczyk et al., 2007].

Interestingly, a comparison between mice infected with the ECM-inducing parasites *P. berghei* ANKA and mice infected with *P. berghei* NK65 parasites, that do not induce ECM but fatal anemia, revealed that also these PbNK65-infected mice contained cellular infiltrates in their brains, despite the absence of ECM [Shaw et al., 2015]. Interestingly, brains of these protected mice contained activated CD8⁺ T cells that expressed CD11a as a sign of previous antigen experience and similar frequencies of T cells expressing granzyme B as in ECM-positive brains of PbA-infected mice [Shaw et al., 2015]. An important result was that in the non-ECM mice, the CD8⁺ T cells remained in the perivascular space of the brains and showed an increased motility and less cognate interaction with CD31⁺ brain endothelial cells compared to T cells in brains of ECM positive mice.

However, one drawback of the Shaw study is that only frequencies of cells expressing the different markers were shown but not analysis of the geometric mean fluorescence intensity which could give more information about the expression level of these markers which might vary between cells from ECM-negative and ECM-positive mice. Also functional analysis, for example if granzyme B positive T cells would actually release the stored granzyme B *in vivo* is missing in their analysis. All together, these observations show, that ECM cannot simply be explained by infiltration of immune cells to the brain, but also their activity and motility profile have to be considered.

Alterations in antigen-presenting cells might contribute to reduced T cell activation after doxycycline treatment

Doxycycline might directly affect the activity of T cells, but also other immune cells that interact with T cells in the brain. Immigrated and resident APCs in brains of doxycycline-treated mice after PbA-infection expressed less ICAM-1 and MHC molecules (Fig. 3.33, 3.34, 3.35). These cells are involved in T cell priming by antigen-presentation, but also participate in the pro-inflammatory immune responses by production of cytokines like TNF, which was down-regulated in brain cell cultures from doxycycline treated mice, compared to samples from untreated infection controls (Fig. 3.36A). Importantly, the parasite load in brains of doxycycline treated mice was similar to that in untreated mice after PbA-infection (Fig. 3.37B), which suggests a protective mechanism by doxycycline, independently of antigen reduction in the brain.

An effect of doxycycline or other tetracycline-derivates on dendritic cells has not been described yet. As DCs in general are thought to play a role in the early phase of disease [Engwerda et al., 2005, Cockburn and Zavala, 2016], their reduced activation might be more a consequence of generally reduced inflammation and probably not involved in the doxycycline mediated protection in general.

CD11b⁺ macrophages from the periphery (CD45^{hi}) are found in increased numbers in brains of mice with ECM but not in non-ECM mice with hyperparasitemia. Importantly, these cells were not only found in the blood vessels but also in the perivascular space, which makes a possible role in ECM more likely [Nacer et al., 2014]. Additionally, microglia, that also express CD11b, have been associated with inflammation in the context of cerebral malaria development in humans and mice [Deininger et al., 2002, Medana et al., 1997].

Peripheral CD11b⁺ cells and microglia in brains from 1e6 iRBC PbA-infected mice (+DOX) expressed less MHC class II (I-Ab) compared to cells from untreated control mice (Fig. 3.34B, 3.35B).

These results agree with observations, that doxycycline reduced macrophage and microglia activation in general, as measured by production of TNF, IL-1 β , -6 and -8 [Cazalis et al., 2008]. Additionally, studies with minocycline specifically showed that doxycycline is able to reduce MHC class II expression macrophages and microglia by inhibition of Interferon regulatory factor 1 (*IRF-1*) and protein kinase C (PKC) $_{\alpha\beta/II}$ [Nikodemova et al., 2007]. Reduction of MHC class II expression on APCs suggests an impaired ability to activate CD4⁺ T cells, which can also contribute to inflammatory activities in the brain [Monso-Hinard et al., 1997]. Interestingly, *IRF-1*, together with its partner *IRF-8* was shown to play a role in ECM development, as mice deficient for this transcription factor were resistant to ECM [Berghout et al., 2013]. Additionally, doxycycline was shown to reduce microglia activation by inhibition of p38 MAPK and NF-kB signaling pathways by [Santa-Cecília et al., 2016]. While activation of microglia starts early after PbA-infection [Medana et al., 1997], a later reduction of their pro-inflammatory status might still help to prevent brain damage in ECM, for example by inhibiting microglia-T cell-interaction [Giuliani and Hader, 2005]. Further characterization of infiltrated and brain-resident APCs by a phagocytosis assay might provide valuable information about the function of these cells and their impairment by doxycycline treatment in our model.

The role of antigen-presentation in CM is still under debate. Cross-presentation of *Plasmodium*-derived antigen by endothelial cells is a hallmark for ECM in the mouse model [Howland et al., 2013, Howland et al., 2015]. However, we did not measure any significant differences in the ability of brain endothelial cells regarding cross-presentation (kindly tested by S. Howland, L. Réhias; Singapore) between doxycycline treated and untreated PbA-infected mice (Fig. 3.37A). Also, a role for microparticles in antigen-presentation is discussed, based on the finding that these can interact with T cells and trigger their proliferation [Nacer et al., 2014, Wheway et al., 2014].

In summary, doxycycline was able to reduce brain inflammation of PbA-infected mice that had been treated with doxycycline from 4 dpi, which then led to ECM-protection. Doxycycline could either directly target T cells or resident or brain immigrated antigen-presenting cells by attenuating their activity, thereby preventing fatal disease progression of ECM.

4.2.1.2 (Antigen-specific) immune cell activation in spleens of PbA-infected mice was reduced by doxycycline but the treatment did not affect the composition of cell subsets

The spleen is an important organ in ECM development to prime cytotoxic T cells [Engwerda et al., 2005]. Intravenous application of doxycycline in PbA-infected mice from 4 dpi was likely to exert systemic effects and could modify the immune response in the spleen.

We observed a weight increase of spleens after PbA-infection which was similar in both infected groups (\pm DOX), but total splenocyte numbers from single cell suspensions which did not differ between all experimental groups (Fig. 3.38). These observations were unexpected, as our previous results using the lower dose of parasites before DOX-treatment (5×10^4 iRBC) revealed a higher cell count in the spleens of doxycycline treated mice (Fig. 3.25F).

There are different studies on the influence of doxycycline and other tetracycline-derivates on cell proliferation. Minocycline and doxycycline were shown to inhibit proliferation of human T cells *in vitro* in a dose-dependent manner [Kloppenborg et al., 1995, Chang et al., 2010]. However, these results might have been due to toxic effects of doxycycline that were further supported by the description of pro-apoptotic effects of

doxycycline [Chang et al., 2010]. Importantly, *in vivo* studies showed that splenomegaly from *Ehrlichia risticii* infections were rather amplified by doxycycline treatment instead of any suppression of proliferation [Rikihisu and Jiang, 1989]. These findings underline our results, which suggest that the analysis of doxycycline's effect on cell proliferation were probably be dependent on the surrounding circumstances.

Furthermore, we had addressed the question whether the increased frequency of lymphocytes upon DOX-treatment in the mice infected with the lower iRBC number was due to differences in migration capacity, but did neither observe any differences in our transwell approach nor in an *in vivo* proliferation assay (Fig. 3.26, 3.27). Since there was no significant further increase in organ size and cell count in the modified experimental model using $1e6$ iRBC before DOX-treatment, we did not follow up this hypothesis any further.

Impaired CTL responses in PbA-infected mice after doxycycline treatment

Similar to the brain, the composition of T cells in the spleen did not differ between doxycycline treated and untreated PbA-infected mice (Fig. 3.39). More important was the finding that the activity of these T cells, measured by intracellular and secreted granzyme B and $IFN\gamma$ as well as by antigen-specific cytotoxicity of spleen cells from doxycycline treated mice, was significantly lower compared to that of untreated mice (Fig. 3.40, 3.41), thus demonstrating an attenuated inflammatory response upon DOX-treatment. However, we did not observe any differences in immune-regulatory IL-10 (Fig. 3.41D).

Our results showed that the reduced activation of T cells in the brains of doxycycline treated, PbA-infected mice was not a local phenomenon but probably due to a systemic effect of doxycycline. As some T cell activation has already taken place before start of the treatment on 4 dpi, the CTL response was not completely abolished in the treated group ("PbA $1e6$ + DOX") but clearly impeded.

As discussed before, doxycycline and other tetracycline-derivates are described to impair T cell proliferation and activity, partly through Ca^{2+} chelating activity [Kloppenburger et al., 1995]. Additionally, doxycycline might inhibit T cell activity indirectly by down-regulation of CD40 ligand, which is needed for T cell - APC interaction [Giuliani and Hader, 2005].

CD11b⁺ cells were not affected regarding their activation but less splenic Ly6C⁺ monocytes were present in doxycycline treated mice

Frequencies of dendritic cells and CD11b⁺ cells did not differ significantly between control infected and DOX-treated PbA groups of mice (Fig. 3.42A, 3.43A). Most interestingly, the frequency of inflammatory Ly6C⁺ monocytes among the CD11b⁺ splenocytes was reduced in DOX-treated PbA-infected mice compared to untreated infection-controls (Fig. 3.43B). The importance of this cell subset was shown recently since mice depleted from inflammatory monocytes at the time point of PbA-infection were resistant to ECM [Schumak et al., 2015], thus fitting to the generally reduced inflammation in spleens of doxycycline treated PbA-infected mice.

Surprisingly, the activity of splenic CD11b⁺ cells (as defined by up-regulation of MHC class I and II as well as ICAM-1 expression) in spleens of DOX-treated PbA-infected mice was not reduced on 6 dpi (Fig. 3.43D-F). These results were contrary to our observations in the brain, where CD11b⁺ microglia but also immigrated CD11b⁺ cells expressed less MHC class II (Fig. 3.34B, 3.35B). However, since the initial activation of splenic antigen-presenting cells was probably initiated upon PbA-infection, thus before start of the DOX-treatment, any conceivable effects of doxycycline, like regulation of MHC class II expression [Nikodemova et al., 2007], might either take more time to be detectable or do not visibly affect these cells.

4.2.2 Sub-antimicrobial doses of doxycycline prevented ECM without affecting parasitemia

Administration of 80 mg/kg/d doxycycline from 4 dpi protected PbA-infected Bl/6 mice to 100% (Fig. 3.24A). However, this dose did also significantly affect parasitemia from 6 dpi (Fig. 3.24B), which made it impossible to distinguish between direct anti-inflammatory effect of doxycycline and reduced inflammation as a consequence of parasite reduction, as discussed before.

Studies regarding human periodontitis and atherosclerosis had shown beneficial effects of sub-antimicrobial doses of doxycycline on inflammatory processes [Walker et al., 2000, Brown et al., 2004]. Based on these findings, we decided to titrate the dose of doxycycline down to achieve a sub-antimicrobial dose that would not affect parasite replication but

protect mice by anti-inflammatory effects. Survival studies with doxycycline doses ranging from only 8 mg/kg/d to 80 mg/kg/d (original dose), we showed that the lower doses were still able to protect around 50% of PbA-infected mice which received the drug daily from 4 to 6 dpi (Fig. 3.44). Even more important, we could show that single mice survived a high parasitemia, which leaves the anti-inflammatory effects of doxycycline as the sole cause of protection (Fig. 3.45). However, these results were not stable as we observed this broad range of parasitemia and only around 50% protection. Another problem was that mice with reduced parasitemia also died from cerebral malaria (with normal or reduced parasitemia on the day of death). Due to this inconsistency, *ex vivo* analysis in this approach would be difficult unless we could discover a diagnostic marker to predict which mice would survive despite high parasitemia and which would die regardless of treatment.

Nonetheless, these results are very important, as they showed that ECM-protection by doxycycline could be achieved with only anti-inflammatory effects.

4.2.3 Outlook - Prevention of ECM due to altered shedding of microparticle

In the last years, small particles called microparticles (MPs) came into focus in malaria research [Wassmer et al., 2011, El-Assaad et al., 2014]. MPs are small vesicles with a size between 0.1 and 1 μm that originate from the cell walls in a Ca^{2+} -dependent process called shedding. Therefore, microparticle show similar expression of surface molecules as their parental cell and can also contain mRNA, miRNA and proteins, which they can transfer to neighboring cells. Microparticle shedding is increased in activated cells, which makes them a marker for cell activation, but they can also contribute to inflammation by recruitment and activation of other immune cells [Distler et al., 2006]. The involvement of microparticles in CM development was shown in human patients, where plasma of *P. falciparum* infected CM positive children contained higher levels of endothelial MPs compared to children with uncomplicated disease or severe anemia [Combes et al., 2004]. Murine models did not only confirm this finding but furthermore linked endothelial-derived MPs to the development of neurological symptoms, as the transfer of MPs from activated endothelial cells led to ECM-like symptoms in naive recipient mice [El-Assaad et al., 2014]. Furthermore, evidence was found that endothelial MPs might interact with CD4^+ and CD8^+ T cells, resulting in enhanced T cell activity and proliferation [Wheway et al., 2014]. These examples show that microparticles might be worth further investigation.

Interestingly, TNF plasma levels correlated with the amount of circulating MPs in CM patients [Sahu et al., 2013] and doxycycline inhibited TNF production in macrophages and microglia [Cazalis et al., 2008, Santa-Cecília et al., 2016]. As TNF was significantly reduced in brains of our DOX-treated PbA-infected mice (Fig. 3.36A), a direct effect of doxycycline might be possible.

A key event in MP shedding is the flopping of phosphatidylserine (PS) to the outer leaflet of the plasma membrane, which is dependent on calcium levels in the cell [Morel et al., 2011]. This finding hints to another possible mechanism of doxycycline: tetracycline and its derivatives are able to decrease intracellular calcium levels in plant and human cells [Bowman et al., 2011, Szeto et al., 2011]. Hence, we hypothesize that doxycycline might lower intracellular calcium levels in endothelial cells and thereby inhibiting shedding of microparticles and subsequently improving the disease development. The importance of PS flopping and microparticles in ECM was also shown in ATP-binding cassette transporter A1 knock-out mice ($ABCA1^{-/-}$ mice). The ATP-binding cassette transporter A1 is involved in MP shedding, since it is required for the translocation of PS to the outer leaflet of the plasma membrane. After *P. berghei* infection, $ABCA1^{-/-}$ mice were completely protected from ECM development and contained significantly reduced MPs levels compared to susceptible WT controls [Combes et al., 2005].

Several experiments are conceivable to test the hypothesis that doxycycline might be able to prevent microparticle shedding and therefore disease development. First of all, quantification and identification of circulating microparticles via electron microscopy and / or flow cytometry should clarify whether doxycycline treated mice contain less MPs in their blood compared to untreated mice. The direct impact of doxycycline on microparticle shedding might be tested by *in vitro* generation of MPs with or without the presence of doxycycline in the culture. Finally, a transfer of MPs from untreated, PbA-infected mice into doxycycline treated mice would show whether these MPs are able to promote ECM in doxycycline treated mice.

In summary, microparticles might play a substantial role in (E)CM development and possible doxycycline-driven prevention of MP release might help to control CM progression by directly ameliorating cerebral inflammation. However, further research is needed to confirm this hypothesis.

Interestingly, we detected low TNF levels in ECM-resistant $Batf3^{-/-}$ mice (Fig. 3.6E);

this could be a result of the generally reduced inflammatory milieu, and might be a hint for successful prevention of MP shedding in this model, contributing to the protection.

4.2.4 Anti-inflammatory drugs offer promising treatment options in ECM

Although an estimated 5-20% of patients with neurological CM symptoms are still dying after immediate treatment [de Souza et al., 2010], the current WHO treatment guidelines for CM focus solely on parasite clearance [WHO, 2015]. As CM is associated with severe inflammation in the patients' brains, targeting this aspect of the disease could be beneficial for the patients and reduce the mortality rate.

Our results indicate, that doxycycline is able to regulate the immune responses in ECM (summarized in Fig. 4.2), resulting in improved survival chances of PbA-infected mice, even in mice with elevated parasitemia (Fig. 3.44).

WT 1e6 PbA after doxycycline treatment

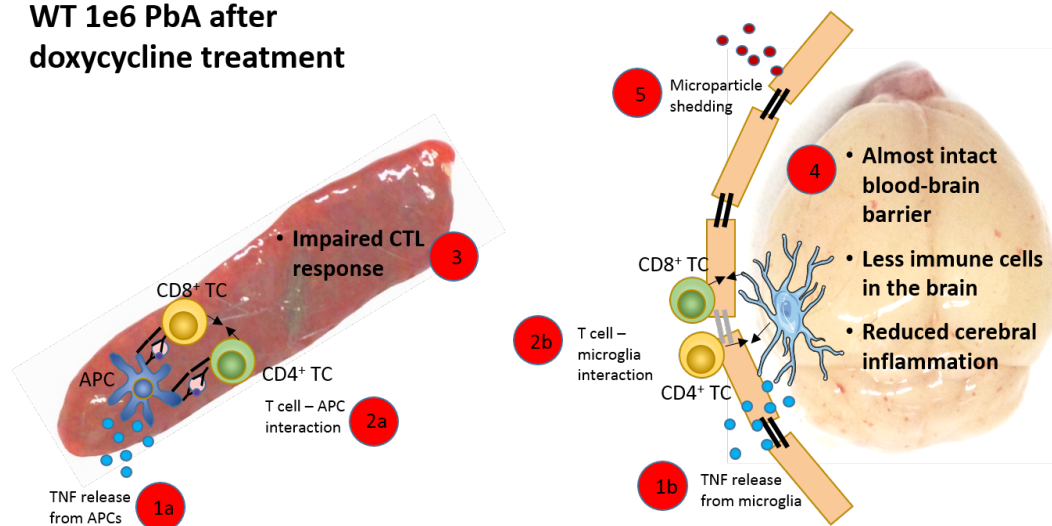


Figure 4.2: **Doxycycline treatment protected PbA-infected WT mice from ECM by dampening their inflammatory immune responses.** Doxycycline treatment in PbA-infected mice prevented ECM in usually susceptible mice. Doxycycline was discussed to reduce TNF production from antigen-presenting cells in spleen (1a) and brain (1b) and to impair their interaction with T cells in both organs (2a, 2b). These effects (together with other, unknown mechanisms) led to reduced CTL response in the spleen (3) and subsequently a protected blood-brain barrier, reduced immune cell migration to the brain and a generally dampened immune response in the brain (4). Another hypothetical target of doxycycline could be microparticle shedding (5). Source microglia: Servier Medical Art - <http://www.servier.com/Powerpoint-image-bank>

These findings suggest treating parasitemia and inflammation at the same time. Doxycycline is usually a well-tolerated drug that could dampen the immune response in CM patients and improve their survival, which should be beneficial in addition to the standard

treatment regimen.

Recently, the topic of specific treatment for cerebral inflammation in CM has also been addressed by others using experimental mouse models. Artesunate is widely used as a fast-acting drug in *Plasmodium* infection. A single dose of artesunate on 4 dpi was shown to prevent ECM in susceptible Bl/6 mice, which contained reduced mRNA expression of different pro-inflammatory cytokines in their brains on 5 dpi, when first neuro-pathological symptoms occurred [Miranda et al., 2013]. However, artesunate is a fast-acting anti-plasmodial drug and parasitemia was significantly reduced in treated mice on the day of analysis, when compared to untreated controls [Miranda et al., 2013]. Therefore, it could not be ruled out that the strongly reduced parasitemia was responsible for the observed regulation of pro-inflammatory factors in artesunate-treated mice.

In contrast, curcumin, which has been described to exert anti-inflammatory properties [Jurenka, 2009], did not affect parasitemia but protected PbA-infected mice from ECM when given before the onset of symptoms from 3 dpi. More importantly, treatment 12h after onset of symptoms (but before coma) was still able to delay the death of infected animals, which died 6-9 days later from anemia [Dende et al., 2015]. Similar to our suggestions, the authors of this study proposed administration of curcumin in combination with artether (a artemisinin derivate) for additional fast elimination of the parasite.

Taken together, our results and the cited studies above recommend an optimization of the current standard treatment regarding CM, expanding it from solely targeting the parasite to also addressing the pro-inflammatory immune responses in CM. In future, also other drugs with anti-inflammatory and / or neuro-protective effects should be tested in CM models. One promising example are Cerebralcare Granule[®], which were shown to ameliorate BBB permeability in a rat model for ischemic stroke [Huang et al., 2012].

In conclusion, we suggest to consider doxycycline for the treatment of CM patients in combination with other fast-working anti-parasitic drugs.

Bibliography

- [Alvarez et al., 2010] Alvarez, I. B., Pasquinelli, V., Jurado, J. O., Abbate, E., Musella, R. M., de la Barrera, S. S., and García, V. E. (2010). Role Played by the Programmed Death-1–Programmed Death Ligand Pathway during Innate Immunity against *Mycobacterium tuberculosis*. *The Journal of Infectious Diseases*, 202(4):524–532.
- [Amante et al., 2007] Amante, F. H., Stanley, A. C., Randall, L. M., Zhou, Y., Haque, A., McSweeney, K., Waters, A. P., Janse, C. J., Good, M. F., Hill, G. R., and Engwerda, C. R. (2007). A role for natural regulatory T cells in the pathogenesis of experimental cerebral malaria. *The American journal of pathology*, 171(2):548–59.
- [Ashok et al., 2014] Ashok, D., Schuster, S., Ronet, C., Rosa, M., Mack, V., Lavanchy, C., Marraco, S. F., Fasel, N., Murphy, K. M., Tacchini-Cottier, F., and Acha-Orbea, H. (2014). Cross-presenting dendritic cells are required for control of *Leishmania major* infection. *European Journal of Immunology*, 44(5):1422–1432.
- [Bachem et al., 2012] Bachem, A., Hartung, E., Güttler, S., Mora, A., Zhou, X., Hege-
mann, A., Plantinga, M., Mazzini, E., Stoitzner, P., Gurka, S., Henn, V., Mages, H. W.,
and Kroccek, R. a. (2012). Expression of XCR1 characterizes the Batf3-dependent lin-
eage of dendritic cells capable of antigen cross-presentation. *Frontiers in Immunology*,
3(July):1–12.
- [Banisadr et al., 2005] Banisadr, G., Gosselin, R.-D., Mechighel, P., Kitabgi, P., Rostène,
W., and Parsadaniantz, S. M. (2005). Highly regionalized neuronal expression of mono-
cyte chemoattractant protein-1 (MCP-1/CCL2) in rat brain: evidence for its colocaliza-
tion with neurotransmitters and neuropeptides. *The Journal of comparative neurology*,
489(3):275–92.
- [Baptista et al., 2010] Baptista, F. G., Pamplona, A., Pena, A. C., Mota, M. M., Pied,
S., and Vigário, A. M. (2010). Accumulation of *Plasmodium berghei*-infected red blood
cells in the brain is crucial for the development of cerebral malaria in mice. *Infection
and immunity*, 78(9):4033–9.

- [Batty et al., 2007] Batty, K. T., Law, A. S. F., Stirling, V., and Moore, B. R. (2007). Pharmacodynamics of doxycycline in a murine malaria model. *Antimicrobial agents and chemotherapy*, 51(12):4477–9.
- [Belnoue et al., 2003a] Belnoue, E., Costa, F., Vigário, A., Voza, T., Gonnet, F., Landau, I., Van Rooijen, N., Mack, M., Kuziel, W. A., and Rénia, L. (2003a). Chemokine receptor CCR2 is not essential for the development of experimental cerebral malaria. *Infection and immunity*, 71(6):3648.
- [Belnoue et al., 2003b] Belnoue, E., Kayibanda, M., Deschemin, J.-C., Viguier, M., Mack, M., Kuziel, W. A., and Rénia, L. (2003b). CCR5 deficiency decreases susceptibility to experimental cerebral malaria. *Blood*, 101(11):4253–9.
- [Belnoue et al., 2002] Belnoue, E., Kayibanda, M., Vigario, A. M., Deschemin, J.-C., Rooijen, N. V., Viguier, M., Snounou, G., and Renia, L. (2002). On the Pathogenic Role of Brain-Sequestered $\alpha\beta$ CD8+ T Cells in Experimental Cerebral Malaria. *J. Immunol.*, 169(11):6369–6375.
- [Belnoue et al., 2008] Belnoue, E., Potter, S. M., Rosa, D. S., Mauduit, M., Grüner, A. C., Kayibanda, M., Mitchell, A. J., Hunt, N. H., and Rénia, L. (2008). Control of pathogenic CD8+ T cell migration to the brain by IFN-gamma during experimental cerebral malaria. *Parasite Immunology*, 30(10):544–553.
- [Benoit et al., 2008] Benoit, M., Desnues, B., and Mege, J.-L. (2008). Macrophage Polarization in Bacterial Infections. *The Journal of Immunology*, 181(6):3733–3739.
- [Berghout et al., 2013] Berghout, J., Langlais, D., Radovanovic, I., Tam, M., Macmicking, J. D., Stevenson, M. M., and Gros, P. (2013). Irf8-Regulated Genomic Responses Drive Pathological Inflammation during Cerebral Malaria. *PLoS pathogens*, 9(7):e1003491.
- [Bernhard et al., 2015] Bernhard, C. A., Ried, C., Kochanek, S., and Brocker, T. (2015). CD169+ macrophages are sufficient for priming of CTLs with specificities left out by cross-priming dendritic cells. *Proceedings of the National Academy of Sciences*, 112(17):5461–5466.
- [Besnard et al., 2015] Besnard, A. G., Guabiraba, R., Niedbala, W., Palomo, J., Reverchon, F., Shaw, T. N., Couper, K. N., Ryffel, B., and Liew, F. Y. (2015). IL-33-Mediated Protection against Experimental Cerebral Malaria Is Linked to Induction of Type 2 Innate Lymphoid Cells, M2 Macrophages and Regulatory T Cells. *PLoS Pathogens*, 11(2):1–21.
- [Beyer et al., 2005] Beyer, M., Wang, H., Peters, N., Doths, S., Koerner-Rettberg, C., Openshaw, P. J. M., and Schwarze, J. (2005). The beta2 integrin CD11c distinguishes a subset of cytotoxic pulmonary T cells with potent antiviral effects in vitro and in vivo. *Respiratory Research*, 6(1):70.

- [Böttcher et al., 2014] Böttcher, J. P., Schanz, O., Garbers, C., Zaremba, A., Hegenbarth, S., Kurts, C., Beyer, M., Schultze, J. L., Kastenmüller, W., Rose-John, S., and Knolle, P. A. (2014). IL-6 trans-Signaling-Dependent Rapid Development of Cytotoxic CD8+ T Cell Function. *Cell Reports*, 8(5):1318–1327.
- [Böttger et al., 2012] Böttger, E., Multhoff, G., Kun, J. F. J., and Esen, M. (2012). Plasmodium falciparum-Infected Erythrocytes Induce Granzyme B by NK Cells through Expression of Host-Hsp70. *PLoS ONE*, 7(3):e33774.
- [Bowman et al., 2011] Bowman, S. M., Drzewiecki, K. E., Mojica, E.-R. E., Zielinski, A. M., Siegel, A., Aga, D. S., and Berry, J. O. (2011). Toxicity and reductions in intracellular calcium levels following uptake of a tetracycline antibiotic in Arabidopsis. *Environmental science & technology*, 45(20):8958–64.
- [Brown et al., 2004] Brown, D. L., Desai, K. K., Vakili, B. a., Nouneh, C., Lee, H.-M., and Golub, L. M. (2004). Clinical and biochemical results of the metalloproteinase inhibition with subantimicrobial doses of doxycycline to prevent acute coronary syndromes (MIDAS) pilot trial. *Arteriosclerosis, thrombosis, and vascular biology*, 24(4):733–8.
- [Budimulja et al., 1997] Budimulja, A. S., Tapchaisri, P., Wilairat, P., and Marzuki, S. (1997). The sensitivity of Plasmodium protein synthesis to prokaryotic ribosomal inhibitors. *Molecular and biochemical parasitology*, 84:137–141.
- [Carroll et al., 2010] Carroll, R. W., Wainwright, M. S., Kim, K. Y., Kidambi, T., Gómez, N. D., Taylor, T., and Haldar, K. (2010). A rapid murine coma and behavior scale for quantitative assessment of murine cerebral malaria. *PLoS ONE*, 5(10):1–12.
- [Castro et al., 2011] Castro, J. E. Z., Vado-Solis, I., Perez-Osorio, C., and Fredeking, T. M. (2011). Modulation of cytokine and cytokine receptor/antagonist by treatment with doxycycline and tetracycline in patients with dengue Fever. *Clinical & developmental immunology*, 2011.
- [Cazalis et al., 2008] Cazalis, J., Bodet, C., Gagnon, G., and Grenier, D. (2008). Doxycycline reduces lipopolysaccharide-induced inflammatory mediator secretion in macrophage and ex vivo human whole blood models. *Journal of periodontology*, 79(9):1762–8.
- [Centers for Disease Control and Prevention, 2015] Centers for Disease Control and Prevention (2015). Malaria - About Malaria - Disease. <http://www.cdc.gov/malaria/about/disease.html>, date accessed 2016-03-09.
- [Centers for Disease Control and Prevention, 2016a] Centers for Disease Control and Prevention (2016a). Malaria - About Malaria - Biology. <http://www.cdc.gov/malaria/about/biology/index.html>, date accessed 2016-03-09.
- [Centers for Disease Control and Prevention, 2016b] Centers for Disease Control and Prevention (2016b). The History of Malaria, an Ancient Disease. <http://www.cdc.gov/malaria/about/history/>, date accessed 2016-02-24.

- [Chang et al., 2010] Chang, W. Y. C., Clements, D., and Johnson, S. R. (2010). Effect of doxycycline on proliferation, MMP production, and adhesion in LAM-related cells. *American journal of physiology. Lung cellular and molecular physiology*, 299(3):L393–400.
- [Chen et al., 2011] Chen, C.-J., Ou, Y.-C., Chang, C.-Y., Pan, H.-C., Liao, S.-L., Raung, S.-L., and Chen, S.-Y. (2011). TNF- α and IL-1 β mediate Japanese encephalitis virus-induced RANTES gene expression in astrocytes. *Neurochemistry international*, 58(2):234–42.
- [Chen et al., 2000] Chen, L., Zhang, Z., and Sendo, F. (2000). Neutrophils play a critical role in the pathogenesis of experimental cerebral malaria. *Clinical and experimental immunology*, 120(1):125–133.
- [Chen et al., 2014] Chen, Q., Amaladoss, A., Ye, W., Liu, M., Dummler, S., Kong, F., Wong, L. H., Loo, H. L., Loh, E., Tan, S. Q., Tan, T. C., Chang, K. T. E., Dao, M., Suresh, S., Preiser, P. R., and Chen, J. (2014). Human natural killer cells control Plasmodium falciparum infection by eliminating infected red blood cells. *Proceedings of the National Academy of Sciences of the United States of America*, 111(4):1479–84.
- [Clark et al., 2003] Clark, I., Awburn, M., Whitten, R., Harper, C., Liomba, N. G., Molyneux, M., and Taylor, T. (2003). Tissue distribution of migration inhibitory factor and inducible nitric oxide synthase in falciparum malaria and sepsis in African children. *Malaria Journal*, 2(1):6.
- [Clark et al., 2004] Clark, I. A., Alleva, L. M., Mills, A. C., and Cowden, W. B. (2004). Pathogenesis of malaria and clinically similar conditions. *Clinical Microbiology ...*, 17(3):509–539.
- [Clark and Cowden, 2003] Clark, I. A. and Cowden, W. B. (2003). The pathophysiology of falciparum malaria. *Pharmacology & Therapeutics*, 99(2):221–260.
- [Clark and Rockett, 1994] Clark, I. A. and Rockett, K. A. (1994). The cytokine theory of human cerebral malaria. *Parasitology today (Personal ed.)*, 10(10):410–2.
- [Cockburn and Zavala, 2016] Cockburn, I. A. and Zavala, F. (2016). Dendritic cell function and antigen presentation in malaria. *Current Opinion in Immunology*, 40:1–6.
- [Coisne et al., 2006] Coisne, C., Faveeuw, C., Delplace, Y., Dehouck, L., Miller, F., Cecchelli, R., and Dehouck, B. (2006). Differential expression of selectins by mouse brain capillary endothelial cells in vitro in response to distinct inflammatory stimuli. *Neuroscience letters*, 392(3):216–20.
- [Coles et al., 2002] Coles, R. M., Mueller, S. N., Heath, W. R., Carbone, F. R., and Brooks, A. G. (2002). Progression of Armed CTL from Draining Lymph Node to Spleen Shortly After Localized Infection with Herpes Simplex Virus 1. *J. Immunol.*, 168(2):834–838.

- [Combes et al., 2005] Combes, V., Coltel, N., Alibert, M., van Eck, M., Raymond, C., Juhan-Vague, I., Grau, G. E., and Chimini, G. (2005). ABCA1 gene deletion protects against cerebral malaria: potential pathogenic role of microparticles in neuropathology. *The American journal of pathology*, 166(1):295–302.
- [Combes et al., 2010] Combes, V., El-Assaad, F., Faille, D., Jambou, R., Hunt, N. H., and Grau, G. E. R. (2010). Microvesiculation and cell interactions at the brain-endothelial interface in cerebral malaria pathogenesis. *Progress in neurobiology*, 91(2):140–51.
- [Combes et al., 2004] Combes, V., Taylor, T. E., Juhan-Vague, I., Mège, J.-L., Mwenechanya, J., Tembo, M., Grau, G. E., and Molyneux, M. E. (2004). Circulating endothelial microparticles in malawian children with severe falciparum malaria complicated with coma. *JAMA : the journal of the American Medical Association*, 291(21):2542–4.
- [Craig et al., 2012] Craig, A. G., Grau, G. E. R., Janse, C., Kazura, J. W., Milner, D., Barnwell, J. W., Turner, G., and Langhorne, J. (2012). The Role of Animal Models for Research on Severe Malaria. *PLoS pathogens*, 8(2):e1002401.
- [Dahl et al., 2006] Dahl, E. L., Shock, J. L., Shenai, B. R., Gut, J., DeRisi, J. L., and Rosenthal, P. J. (2006). Tetracyclines specifically target the apicoplast of the malaria parasite Plasmodium falciparum. *Antimicrobial agents and chemotherapy*, 50(9):3124–31.
- [Day et al., 1999] Day, N. P., Hien, T. T., Schollaardt, T., Loc, P. P., Chuong, L. V., Chau, T. T., Mai, N. T., Phu, N. H., Sinh, D. X., White, N. J., and Ho, M. (1999). The prognostic and pathophysiologic role of pro- and antiinflammatory cytokines in severe malaria. *The Journal of infectious diseases*, 180(4):1288–97.
- [de Kossodo and Grau, 1993] de Kossodo, S. and Grau, G. E. R. (1993). Role of cytokines and adhesion molecules in malaria immunopathology. *Stem cells (Dayton, Ohio)*, 11(1):41–8.
- [de Souza et al., 2010] de Souza, J. B., Hafalla, J. C. R., Riley, E. M., and Couper, K. N. (2010). Cerebral malaria: why experimental murine models are required to understand the pathogenesis of disease. *Parasitology*, 137(5):755–72.
- [Deininger et al., 2002] Deininger, M. H., Kremsner, P. G., Meyermann, R., and Schluesener, H. (2002). Macrophages/microglial cells in patients with cerebral malaria. *European cytokine network*, 13(2):173–85.
- [Dende et al., 2015] Dende, C., Meena, J., Nagarajan, P., Panda, A. K., Rangarajan, P. N., and Padmanaban, G. (2015). Simultaneously targeting inflammatory response and parasite sequestration in brain to treat Experimental Cerebral Malaria. *Scientific Reports*, 5(February):12671.
- [Deroost et al., 2016] Deroost, K., Pham, T. T., Opdenakker, G., and Van den Steen, P. E. (2016). *The immunological balance between host and parasite in malaria*, volume 40.

- [DeWalick et al., 2007] DeWalick, S., Amante, F. H., McSweeney, K. A., Randall, L. M., Stanley, A. C., Haque, A., Kuns, R. D., MacDonald, K. P. A., Hill, G. R., and Engwerda, C. R. (2007). Cutting edge: conventional dendritic cells are the critical APC required for the induction of experimental cerebral malaria. *Journal of immunology (Baltimore, Md. : 1950)*, 178(10):6033–7.
- [Distler et al., 2006] Distler, J. H. W., Huber, L. C., Gay, S., Distler, O., and Pisetsky, D. S. (2006). Microparticles as mediators of cellular cross-talk in inflammatory disease. *Autoimmunity*, 39(8):683–90.
- [El-Assaad et al., 2014] El-Assaad, F., Wheway, J., Hunt, N. H., Grau, G. E. R., and Combes, V. (2014). Production, fate and pathogenicity of plasma microparticles in murine cerebral malaria. *PLoS pathogens*, 10(3):e1003839.
- [Engwerda, 2002] Engwerda, C. (2002). Locally Up-regulated Lymphotoxin alpha, Not Systemic Tumor Necrosis Factor alpha, Is the Principle Mediator of Murine Cerebral Malaria. *Journal of Experimental Medicine*, 195(10):1371–1377.
- [Engwerda et al., 2005] Engwerda, C. R., Beattie, L., and Amante, F. H. (2005). The importance of the spleen in malaria. *Trends in parasitology*, 21(2):75–80.
- [Enose-Akahata et al., 2012] Enose-Akahata, Y., Matsuura, E., Tanaka, Y., Oh, U., and Jacobson, S. (2012). Minocycline modulates antigen-specific CTL activity through inactivation of mononuclear phagocytes in patients with HTLV-I associated neurologic disease. *Retrovirology*, 9(1):16.
- [Fairweather and Cihakova, 2009] Fairweather, D. and Cihakova, D. (2009). Alternatively activated macrophages in infection and autoimmunity. *Journal of Autoimmunity*, 33(3-4):222–230.
- [Finney et al., 2010] Finney, O. C., Riley, E. M., and Walther, M. (2010). Regulatory T cells in malaria—friend or foe? *Trends in immunology*, 31(2):63–70.
- [Giuliani and Hader, 2005] Giuliani, F. and Hader, W. (2005). Minocycline attenuates T cell and microglia activity to impair cytokine production in T cell-microglia interaction. *Journal of leukocyte biology*, 78(July):135–143.
- [Grajales-Reyes et al., 2015] Grajales-Reyes, G. E., Iwata, A., Albring, J., Wu, X., Tussiwand, R., Kc, W., Kretzer, N. M., Briseño, C. G., Durai, V., Bagadia, P., Haldar, M., Schönheit, J., Rosenbauer, F., Murphy, T. L., and Murphy, K. M. (2015). Batf3 maintains autoactivation of Irf8 for commitment of a CD8 α + conventional DC clonogenic progenitor. *Nature Immunology*, 16(7):708–717.
- [Grau et al., 1987] Grau, G. E. R., Fajardo, L. F., Piguet, P.-F., Allet, B., Lambert, P.-H., and Vassalli, P. (1987). Tumor Necrosis Factor (Cachectin) as an Essential Mediator in Murine Cerebral Malaria. *Science (New York, N.Y.)*, 237:1210–1212.

- [Griffin et al., 2011] Griffin, M. O., Ceballos, G., and Villarreal, F. J. (2011). Tetracycline compounds with non-antimicrobial organ protective properties: possible mechanisms of action. *Pharmacological research : the official journal of the Italian Pharmacological Society*, 63(2):102–7.
- [Hansen et al., 2007] Hansen, D. S., Bernard, N. J., Nie, C. Q., and Schofield, L. (2007). NK Cells Stimulate Recruitment of CXCR3 + T Cells to the Brain during Plasmodium berghei-Mediated Cerebral Malaria. *The Journal of Immunology*, 178(9):5779–5788.
- [Hanum et al., 2003] Hanum, S. P., Hayano, M., and Kojima, S. (2003). Cytokine and chemokine responses in a cerebral malaria-susceptible or -resistant strain of mice to Plasmodium berghei ANKA infection: early chemokine expression in the brain. *International Immunology*, 15(5):633–640.
- [Haque et al., 2011] Haque, A., Best, S. E., Unosson, K., Amante, F. H., de Labastida, F., Anstey, N. M., Karupiah, G., Smyth, M. J., Heath, W. R., and Engwerda, C. R. (2011). Granzyme B expression by CD8+ T cells is required for the development of experimental cerebral malaria. *Journal of immunology (Baltimore, Md. : 1950)*, 186(11):6148–56.
- [Hildner et al., 2008] Hildner, K., Edelson, B. T., Purtha, W. E., Diamond, M., Matsushita, H., Kohyama, M., Calderon, B., Schraml, B. U., Unanue, E. R., Diamond, M. S., Schreiber, R. D., Murphy, T. L., and Murphy, K. M. (2008). Batf3 deficiency reveals a critical role for CD8alpha+ dendritic cells in cytotoxic T cell immunity. *Science (New York, N.Y.)*, 322(November):1097–1100.
- [Horne-Debets et al., 2013] Horne-Debets, J., Faleiro, R., Karunarathne, D., Liu, X., Lineburg, K., Poh, C., Grotenbreg, G., Hill, G., MacDonald, K. A., Good, M., Renia, L., Ahmed, R., Sharpe, A., and Wykes, M. (2013). PD-1 dependent exhaustion of CD8+ T cells drives chronic malaria. *Cell Reports*, 5(5):1204–1213.
- [Howland et al., 2013] Howland, S. W., Poh, C. M., Gun, S. Y., Claser, C., Malleret, B., Shastri, N., Ginhoux, F., Grotenbreg, G. M., and Rénia, L. (2013). Brain microvessel cross-presentation is a hallmark of experimental cerebral malaria. *EMBO molecular medicine*, 5(7):916–31.
- [Howland et al., 2015] Howland, S. W., Poh, C. M., and Rénia, L. (2015). Activated Brain Endothelial Cells Cross- Present Malaria Antigen. *PLoS pathogens*, 11(6).
- [Huang et al., 2012] Huang, P., Zhou, C.-M., Qin-Hu, Liu, Y.-Y., Hu, B.-H., Chang, X., Zhao, X.-R., Xu, X.-S., Li, Q., Wei, X.-H., Mao, X.-W., Wang, C.-S., Fan, J.-Y., and Han, J.-Y. (2012). Cerebralcare Granule® attenuates blood-brain barrier disruption after middle cerebral artery occlusion in rats. *Experimental neurology*, 237(2):453–63.
- [Hunt, 2003] Hunt, N. (2003). Cytokines: accelerators and brakes in the pathogenesis of cerebral malaria. *Trends in Immunology*, 24(9):491–499.

- [Hunt et al., 2006] Hunt, N. H., Golenser, J., Chan-Ling, T., Parekh, S., Rae, C., Potter, S., Medana, I. M., Miu, J., and Ball, H. J. (2006). Immunopathogenesis of cerebral malaria. *International journal for parasitology*, 36(5):569–82.
- [John et al., 2010] John, C. C., Kutamba, E., Mugarura, K., and Opoka, R. O. (2010). Adjunctive therapy for cerebral malaria and other severe forms of *Plasmodium falciparum* malaria. *Expert Reviews in Anti-Infection Therapy*, 8(9):997–1008.
- [Johns Hopkins Bloomberg School of Public Health (Organization), 2016] Johns Hopkins Bloomberg School of Public Health (Organization) (2016). "Life cycle of the malaria parasite" from Epidemiology of Infectious Diseases.
- [Jurenka, 2009] Jurenka, J. S. (2009). Anti-inflammatory properties of curcumin, a major constituent of *Curcuma longa*: A review of preclinical and clinical research. *Alternative Medicine Review*, 14(2):141–153.
- [Kast, 2008] Kast, R. E. (2008). Minocycline in cerebral malaria. *Journal of neuroscience research*, 86(15):3257.
- [Kierdorf et al., 2013] Kierdorf, K., Erny, D., Goldmann, T., Sander, V., Schulz, C., Perdiguero, E. G., Wieghofer, P., Heinrich, A., Riemke, P., Hölscher, C., Müller, D. N., Luckow, B., Brocker, T., Debowski, K., Fritz, G., Opdenakker, G., Diefenbach, A., Biber, K., Heikenwalder, M., Geissmann, F., Rosenbauer, F., and Prinz, M. (2013). Microglia emerge from erythromyeloid precursors via Pu.1- and Irf8-dependent pathways. *Nature neuroscience*, 16(3):273–80.
- [Kinra and Dutta, 2013] Kinra, P. and Dutta, V. (2013). Serum TNF alpha levels: a prognostic marker for assessment of severity of malaria. *Tropical Biomedicine*, 30(4):645–653.
- [Kloppenburg et al., 1995] Kloppenburg, M., Verweij, C., Miltenburg, A., Verhoeven, A., Daha, M., Dijkmans, B., and Breedveld, F. (1995). The influence of tetracyclines on T cell activation. *Clinical and experimental immunology*, 102:635–641.
- [Koch et al., 2002] Koch, O., Awomoyi, A., Usen, S., Jallow, M., Richardson, A., Hull, J., Pinder, M., Newport, M., and Kwiatkowski, D. (2002). IFNGR1 gene promoter polymorphisms and susceptibility to cerebral malaria. *The Journal of infectious diseases*, 185(11):1684–7.
- [Kossodo et al., 1997] Kossodo, S., Monso, C., Juillard, P., Velu, T., Goldman, M., and Grau, G. E. (1997). Interleukin-10 modulates susceptibility in experimental cerebral malaria. *Immunology*, 91(4):536–540.
- [Krakauer and Buckley, 2003] Krakauer, T. and Buckley, M. (2003). Doxycycline Is Anti-Inflammatory and Inhibits Staphylococcal Exotoxin-Induced Cytokines and Chemokines. *JAMA*, 47(11):3630–3633.

- [Kreider et al., 2007] Kreider, T., Anthony, R. M., Urban, J. F., and Gause, W. C. (2007). Alternatively activated macrophages in helminth infections. *Current Opinion in Immunology*, 19(4):448–453.
- [Kurtzhals et al., 1998] Kurtzhals, J. A. L., Adabayeri, V., Goka, B. Q., Akanmori, B. D., Oliver-Commey, J. O., Nkrumah, F. K., Behr, C., and Hviid, L. (1998). Low plasma concentrations of interleukin-10 in severe malarial anaemia compared with cerebral and uncomplicated malaria. *Lancet*, 351(9118):1768–1772.
- [Lalloo et al., 2007] Lalloo, D. G., Shingadia, D., Pasvol, G., Chiodini, P. L., Whitty, C. J., Beeching, N. J., Hill, D. R., Warrell, D. A., and Bannister, B. A. (2007). UK malaria treatment guidelines. *The Journal of infection*, 54(2):111–21.
- [Langhorne et al., 2002] Langhorne, J., Quin, S. J., and Sanni, L. A. (2002). Immunity and Regulation Mouse Models of Blood-Stage Malaria Infections : Immune Responses and Cytokines Involved in Protection and Pathology. *Chemical immunology*, 80:204–228.
- [Leventhal et al., 2016] Leventhal, D. S., Gilmore, D. C., Berger, J. M., Nishi, S., Lee, V., Malchow, S., Kline, D. E., Kline, J., Vander Griend, D. J., Huang, H., Socci, N. D., and Savage, P. A. (2016). Dendritic Cells Coordinate the Development and Homeostasis of Organ-Specific Regulatory T Cells. *Immunity*, 44(4):847–859.
- [Li et al., 2001] Li, C., Seixas, E., and Langhorne, J. (2001). Rodent malarial: the mouse as a model for understanding immune responses and pathology induced by the erythrocytic stages of the parasite. *Medical microbiology and immunology*, 189(3):115–26.
- [Lieberman et al., 1989] Lieberman, A. P., Pitha, P. M., Shin, H. S., and Shin, M. L. (1989). Production of tumor necrosis factor and other cytokines by astrocytes stimulated with lipopolysaccharide or a neurotropic virus. *Proceedings of the National Academy of Sciences of the United States of America*, 86(16):6348–52.
- [Limmer et al., 2000] Limmer, a., Ohl, J., Kurts, C., Ljunggren, H. G., Reiss, Y., Groettrup, M., Momburg, F., Arnold, B., and Knolle, P. a. (2000). Efficient presentation of exogenous antigen by liver endothelial cells to CD8+ T cells results in antigen-specific T-cell tolerance. *Nature medicine*, 6(12):1348–1354.
- [Liu et al., 2013] Liu, Y., Chen, Y., Li, Z., Han, Y., Sun, Y., Wang, Q., Liu, B., and Su, Z. (2013). Role of IL-10-producing regulatory B cells in control of cerebral malaria in *Plasmodium berghei* infected mice. *European Journal of Immunology*, 43(11):2907–2918.
- [Lou et al., 1998] Lou, J., Gasche, Y., Zheng, L., Critico, B., Monso-Hinard, C., Juillard, P., Morel, P., Buurman, W. A., and Grau, G. E. R. (1998). Differential reactivity of brain microvascular endothelial cells to TNF reflects the genetic susceptibility to cerebral malaria. *European Journal of Immunology*, 28(12):3989–4000.

- [Lundie et al., 2008] Lundie, R. J., de Koning-Ward, T. F., Davey, G. M., Nie, C. Q., Hansen, D. S., Lau, L. S., Mintern, J. D., Belz, G. T., Schofield, L., Carbone, F. R., Villadangos, J. a., Crabb, B. S., and Heath, W. R. (2008). Blood-stage Plasmodium infection induces CD8+ T lymphocytes to parasite-expressed antigens, largely regulated by CD8alpha+ dendritic cells. *Proceedings of the National Academy of Sciences of the United States of America*, 105(38):14509–14.
- [MacPherson et al., 1985] MacPherson, G. G., Warrell, M. J., White, N. J., Looareesuwan, S., and Warrell, D. A. (1985). Human cerebral malaria. A quantitative ultrastructural analysis of parasitized erythrocyte sequestration. *The American journal of pathology*, 119(3):385–401.
- [Mauer et al., 2014] Mauer, J., Chaurasia, B., Goldau, J., Vogt, M. C., Ruud, J., Nguyen, K. D., Theurich, S., Hausen, A. C., Schmitz, J., Brönneke, H. S., Estevez, E., Allen, T. L., Mesaros, A., Partridge, L., Febbraio, M. A., Chawla, A., Wunderlich, F. T., and Brüning, J. C. (2014). Signaling by IL-6 promotes alternative activation of macrophages to limit endotoxemia and obesity-associated resistance to insulin. *Nature immunology*, 15(5):423–30.
- [McBride and Fathman, 2002] McBride, J. M. and Fathman, C. G. (2002). A complicated relationship: fulfilling the interactive needs of the T lymphocyte and the dendritic cell. *The pharmacogenomics journal*, 2(6):367–76.
- [Medana et al., 1997] Medana, I. M., Hunt, N. H., and Chan-Ling, T. (1997). Early activation of microglia in the pathogenesis of fatal murine cerebral malaria. *Glia*, 19(2):91–103.
- [Miranda et al., 2013] Miranda, A. S., Brant, F., Rocha, N. P., Cisalpino, D., Rodrigues, D. H., Souza, D. G., Machado, F. S., Rachid, M. a., Teixeira, A. L., and Campos, A. C. (2013). Further evidence for an anti-inflammatory role of artesunate in experimental cerebral malaria. *Malaria journal*, 12:388.
- [Mitchell et al., 2005] Mitchell, A. J., Hansen, A. M., Hee, L., Ball, H. J., Potter, S. M., Walker, J. C., and Hunt, N. H. (2005). Early cytokine production is associated with protection from murine cerebral malaria. *Infection and immunity*, 73(9):5645–53.
- [Miu et al., 2008] Miu, J., Mitchell, A. J., Muller, M., Carter, S. L., Manders, P. M., McQuillan, J. A., Saunders, B. M., Ball, H. J., Lu, B., Campbell, I. L., and Hunt, N. H. (2008). Chemokine Gene Expression during Fatal Murine Cerebral Malaria and Protection Due to CXCR3 Deficiency. *J. Immunol.*, 180(2):1217–1230.
- [Monso-Hinard et al., 1997] Monso-Hinard, C., Lou, J. N., Behr, C., Juillard, P., and Grau, G. E. R. (1997). Expression of major histocompatibility complex antigens on mouse brain microvascular endothelial cells in relation to susceptibility to cerebral malaria. *Immunology*, 92(1):53–9.

- [Montagna et al., 2015] Montagna, G. N., Biswas, A., Hildner, K., Matuschewski, K., and Dunay, I. R. (2015). Batf3 deficiency proves the pivotal role of CD8+ dendritic cells in protection induced by vaccination with attenuated Plasmodium sporozoites. *Parasite Immunology*, 37(10):533–543.
- [Morel et al., 2011] Morel, O., Jesel, L., Freyssinet, J. M., and Toti, F. (2011). Cellular mechanisms underlying the formation of circulating microparticles. *Arteriosclerosis, Thrombosis, and Vascular Biology*, 31(1):15–26.
- [Mott et al., 2015] Mott, K. R., Maazi, H., Allen, S. J., Zandian, M., Matundan, H., Ghiasi, Y. N., Sharifi, B. G., Underhill, D., Akbari, O., and Ghiasi, H. (2015). Batf3 deficiency is not critical for the generation of CD8 α + dendritic cells. *Immunobiology*, 220:518–524.
- [Murphy et al., 2008] Murphy, K. M., Travers, P., and Walport, M. (2008). *Janeway's Immunobiology*. Garland Science, 7 edition.
- [Nacer et al., 2014] Nacer, A., Movila, A., Sohet, F., Girgis, N. M., ahesh Gundra, U. M., Loke, P., Daneman, R., and Frevert, U. (2014). Experimental cerebral malaria pathogenesis–hemodynamics at the blood brain barrier. *PLoS pathogens*, 10(12):e1004528.
- [Nikodemova et al., 2007] Nikodemova, M., Watters, J. J., Jackson, S. J., Yang, S. K., and Duncan, I. D. (2007). Minocycline down-regulates MHC II expression in microglia and macrophages through inhibition of IRF-1 and protein kinase C (PKC) α /betaII. *The Journal of biological chemistry*, 282(20):15208–16.
- [Nitcheu et al., 2003] Nitcheu, J., Bonduelle, O., Combadiere, C., Tefit, M., Seilhean, D., Mazier, D., and Combadiere, B. (2003). Perforin-Dependent Brain-Infiltrating Cytotoxic CD8+ T Lymphocytes Mediate Experimental Cerebral Malaria Pathogenesis. *J. Immunol.*, 170(4):2221–2228.
- [O'Garra et al., 1992] O'Garra, a., Chang, R., Go, N., Hastings, R., Haughton, G., and Howard, M. (1992). Ly-1 B (B-1) cells are the main source of B cell-derived interleukin 10. *European journal of immunology*, 22(3):711–717.
- [Pais and Chatterjee, 2005] Pais, T. F. and Chatterjee, S. (2005). Brain macrophage activation in murine cerebral malaria precedes accumulation of leukocytes and CD8+ T cell proliferation. *Journal of neuroimmunology*, 163(1-2):73–83.
- [Piva et al., 2012] Piva, L., Tetlak, P., Claser, C., Karjalainen, K., Renia, L., and Ruedl, C. (2012). Cutting edge: Clec9A+ dendritic cells mediate the development of experimental cerebral malaria. *Journal of immunology (Baltimore, Md. : 1950)*, 189:1128–32.
- [Prall et al., 2002] Prall, A. K., Longo, G. M., Mayhan, W. G., Waltke, E. A., Fleckten, B., Thompson, R. W., and Baxter, B. T. (2002). Doxycycline in patients with abdominal aortic aneurysms and in mice: Comparison of serum levels and effect on aneurysm growth in mice. *Journal of Vascular Surgery*, 35(5):923–929.

- [Ramos et al., 2013] Ramos, T. N., Bullard, D. C., Darley, M. M., McDonald, K., Crawford, D. F., and Barnum, S. R. (2013). Experimental Cerebral Malaria Develops Independently of Endothelial Expression of Intercellular Adhesion Molecule-1 (ICAM-1). *The Journal of biological chemistry*, 288(16):10962–6.
- [Randall et al., 2008] Randall, L. M., Amante, F. H., Zhou, Y., Stanley, A. C., Haque, A., Rivera, F., Pfeffer, K., Scheu, S., Hill, G. R., Tamada, K., and Engwerda, C. R. (2008). Cutting Edge: Selective Blockade of LIGHT-Lymphotoxin {beta} Receptor Signaling Protects Mice from Experimental Cerebral Malaria Caused by Plasmodium berghei ANKA. *J. Immunol.*, 181(11):7458–7462.
- [Randall and Engwerda, 2010] Randall, L. M. and Engwerda, C. R. (2010). TNF family members and malaria: old observations, new insights and future directions. *Experimental parasitology*, 126(3):326–31.
- [Renia et al., 2012] Renia, L., Howland, S. W., and Claser, C. (2012). Cerebral malaria: Mysteries at the blood-brain barrier. *Virulence*, 3(2):1–9.
- [Rénia et al., 2006] Rénia, L., Potter, S. M., Mauduit, M., Rosa, D. S., Kayibanda, M., Deschemin, J.-C., Snounou, G., and Grüner, A. C. (2006). Pathogenic T cells in cerebral malaria. *International journal for parasitology*, 36(5):547–54.
- [Renno et al., 1995] Renno, T., Krakowski, M., Piccirillo, C., Lin, J. Y., and Owens, T. (1995). TNF-alpha expression by resident microglia and infiltrating leukocytes in the central nervous system of mice with experimental allergic encephalomyelitis. Regulation by Th1 cytokines. *Journal of immunology (Baltimore, Md. : 1950)*, 154(2):944–53.
- [Rikihiya and Jiang, 1989] Rikihiya, Y. and Jiang, B. M. (1989). Effect of antibiotics on clinical, pathologic and immunologic responses in murine Potomac horse fever: Protective effects of doxycycline. *Veterinary Microbiology*, 19(3):253–262.
- [Roetynck et al., 2006] Roetynck, S., Baratin, M., Johansson, S., Lemmers, C., Vivier, E., and Ugolini, S. (2006). Natural killer cells and malaria. *Immunol Rev*, 214:251–263.
- [Rudin et al., 1997] Rudin, W., Favre, N., Bordmann, G., and Ryffel, B. (1997). Interferon-gamma is essential for the development of cerebral malaria. *European journal of immunology*, 27(4):810–5.
- [Safeukui et al., 2015] Safeukui, I., Gomez, N. D., Adelani, A. a., Burte, F., Afolabi, N. K., Akondy, R., Sodeinde, O., Kazura, J., Ahmed, R., Mohandas, N., Fernandez-reyes, D., and Haldar, K. (2015). Malaria induces anemia through CD8+ T cell-dependent parasite clearance and erythrocyte removal in the spleen. *mBio*, 6(1):e02493–14.
- [Sahu et al., 2013] Sahu, U., Sahoo, P. K., Kar, S. K., Mohapatra, B. N., and Ranjit, M. (2013). Association of TNF level with production of circulating cellular microparticles during clinical manifestation of human cerebral malaria. *Human immunology*, 74(6):713–21.

- [Santa-Cecília et al., 2016] Santa-Cecília, F. V., Socias, B., Ouidja, M. O., Sepulveda-Diaz, J. E., Acuña, L., Silva, R. L., Michel, P. P., Del-Bel, E., Cunha, T. M., and Raisman-Vozari, R. (2016). Doxycycline Suppresses Microglial Activation by Inhibiting the p38 MAPK and NF- κ B Signaling Pathways. *Neurotoxicity Research*, 29(4):447–59.
- [Sarfo et al., 2005] Sarfo, B. Y., Armah, H. B., Irune, I., Adjei, A. A., Olver, C. S., Singh, S., Lillard, J. W., and Stiles, J. K. (2005). Plasmodium yoelii 17XL infection up-regulates RANTES, CCR1, CCR3 and CCR5 expression, and induces ultrastructural changes in the cerebellum. *Malaria journal*, 4(63):1–13.
- [Sarfo et al., 2004] Sarfo, B. Y., Singh, S., Lillard, J. W., Quarshie, A., Gyasi, R. K., Armah, H., Adjei, A. A., Jolly, P., and Stiles, J. K. (2004). The cerebral-malaria-associated expression of RANTES, CCR3 and CCR5 in post-mortem tissue samples. *Annals of tropical medicine and parasitology*, 98(3):297–303.
- [Schofield and Grau, 2005] Schofield, L. and Grau, G. E. R. (2005). Immunological processes in malaria pathogenesis. *Nature reviews. Immunology*, 5(9):722–35.
- [Schumak et al., 2015] Schumak, B., Klocke, K., Kuepper, J. M., Biswas, A., Djie-Maletz, A., Limmer, A., van Rooijen, N., Mack, M., Hoerauf, A., and Dunay, I. R. (2015). Specific Depletion of Ly6Chi Inflammatory Monocytes Prevents Immunopathology in Experimental Cerebral Malaria. *Plos One*, 10(4):e0124080.
- [Seillet et al., 2013] Seillet, C., Jackson, J. T., Markey, K. a., Brady, H. J. M., Hill, G. R., MacDonald, K. P. a., Nutt, S. L., and Belz, G. T. (2013). CD8+ DCs can be induced in the absence of transcription factors Id2, Nfil3, and Batf3. *Blood*, 121(9):1574–1583.
- [Shaw et al., 2015] Shaw, T. N., Stewart-Hutchinson, P. J., Strangward, P., Dandamudi, D. B., Coles, J. A., Villegas-Mendez, A., Gallego-Delgado, J., van Rooijen, N., Zindy, E., Rodriguez, A., Brewer, J. M., Couper, K. N., and Dustin, M. L. (2015). Perivascular Arrest of CD8+ T Cells Is a Signature of Experimental Cerebral Malaria. *PLOS Pathogens*, 11(11):e1005210.
- [Sherman et al., 2003] Sherman, I. W., Eda, S., and Winograd, E. (2003). Cytoadherence and sequestration in Plasmodium falciparum: defining the ties that bind. *Microbes and Infection*, 5(10):897–909.
- [Starzengruber et al., 2009] Starzengruber, P., Thriemer, K., Haque, R., Khan, W. A., Fuehrer, H. P., Siedl, A., Hofecker, V., Ley, B., Wernsdorfer, W. H., and Noedl, H. (2009). Antimalarial activity of tigecycline, a novel glycylycylcine antibiotic. *Antimicrobial agents and chemotherapy*, 53(9):4040–2.
- [Steege et al., 2009] Steege, C., Adler, G., Sparwasser, T., Fleischer, B., and Jacobs, T. (2009). Limited role of CD4+Foxp3+ regulatory T cells in the control of experimental cerebral malaria. *J Immunol*, 183(11):7014–22.

- [Stojanovic et al., 2014] Stojanovic, A., Fiegler, N., Brunner-Weinzierl, M., and Cerwenka, A. (2014). CTLA-4 is expressed by activated mouse NK cells and inhibits NK Cell IFN- γ production in response to mature dendritic cells. *Journal of immunology (Baltimore, Md. : 1950)*, 192(9):4184–91.
- [Su and Stevenson, 2000] Su, Z. and Stevenson, M. M. (2000). Central role of endogenous gamma interferon in protective immunity against blood-stage *Plasmodium chabaudi* AS infection. *Infection and immunity*, 68(8):4399–406.
- [Suidan et al., 2008] Suidan, G. L., Mcdole, J. R., Chen, Y., Pirko, I., and Johnson, A. J. (2008). Induction of blood brain barrier tight junction protein alterations by CD8 T cells. *PloS one*, 3(8):e3037.
- [Szeto et al., 2011] Szeto, G. L., Pomerantz, J. L., Graham, D. R. M., and Clements, J. E. (2011). Minocycline suppresses activation of nuclear factor of activated T cells 1 (NFAT1) in human CD4+ T cells. *The Journal of biological chemistry*, 286(13):11275–82.
- [Szklarczyk et al., 2007] Szklarczyk, A., Stins, M., Milward, E. A., Ryu, H., Fitzsimmons, C., Sullivan, D., and Conant, K. (2007). Glial activation and matrix metalloproteinase release in cerebral malaria. *Journal of neurovirology*, 13(1):2–10.
- [Tamura et al., 2011] Tamura, T., Kimura, K., Yuda, M., and Yui, K. (2011). Prevention of experimental cerebral malaria by Flt3 ligand during infection with *Plasmodium berghei* ANKA. *Infection and Immunity*, 79(10):3947–3956.
- [Togbe et al., 2008] Togbe, D., de Sousa, P. L., Fauconnier, M., Boissay, V., Fick, L., Scheu, S., Pfeffer, K., Menard, R., Grau, G. E. R., Doan, B.-T., Beloeil, J.-C., Renia, L., Hansen, A. M., Ball, H. J., Hunt, N. H., Ryffel, B., and Quesniaux, V. F. J. (2008). Both functional LTbeta receptor and TNF receptor 2 are required for the development of experimental cerebral malaria. *PloS one*, 3(7):e2608.
- [Torres et al., 2014] Torres, K. J., Villasis, E., Bendezú, J., Chauca, J., Vinetz, J. M., and Gamboa, D. (2014). Relationship of regulatory T cells to *Plasmodium falciparum* malaria symptomatology in a hypoendemic region. *Malaria journal*, 13(1):108.
- [Vaughan et al., 2013] Vaughan, A. M., Kappe, S. H. I., Ploss, A., and Mikolajczak, S. A. (2013). Development of humanized mouse models to study human malaria parasite infection Ashley. *Future Microbiology*, 7(5):657–665.
- [Villegas-Mendez et al., 2012] Villegas-Mendez, A., Greig, R., Shaw, T. N., de Souza, J. B., Gwyer Findlay, E., Stumhofer, J. S., Hafalla, J. C. R., Blount, D. G., Hunter, C. A., Riley, E. M., and Couper, K. N. (2012). IFN- γ -Producing CD4+ T Cells Promote Experimental Cerebral Malaria by Modulating CD8+ T Cell Accumulation within the Brain. *Journal of immunology (Baltimore, Md. : 1950)*, 189(2):968–79.
- [Vinay and Kim, 2009] Vinay, D. and Kim, C. (2009). Origins and functional basis of regulatory CD11c+ CD8+ T cells. *European journal of . . .*, 39(6):1552–1563.

- [Walker et al., 2000] Walker, C., Thomas, J., Nangó, S., Lennon, J., Wetzel, J., and Powala, C. (2000). Long-term treatment with subantimicrobial dose doxycycline exerts no antibacterial effect on the subgingival microflora associated with adult periodontitis. *Journal of periodontology*, 71(9):1465–71.
- [Wang et al., 2011] Wang, Z., Xue, Y., Jiao, H., Liu, Y., and Wang, P. (2011). Doxycycline-Mediated Protective Effect Against Focal Cerebral Ischemia – Reperfusion Injury Through the Modulation of Tight Junctions and PKC δ Signaling in Rats. *Journal of Molecular Neuroscience*.
- [Wassmer et al., 2011] Wassmer, S. C., Combes, V., and Grau, G. E. R. (2011). Platelets and microparticles in cerebral malaria: the unusual suspects. *Drug Discovery Today: Disease Mechanisms*, 8(1-2):e15–e23.
- [Wassmer et al., 2010] Wassmer, S. C., Moxon, C. A., Taylor, T., Grau, G. E. R., Molyneux, M. E., and Craig, A. G. (2010). Vascular endothelial cells cultured from patients with cerebral or uncomplicated malaria exhibit differential reactivity to TNF. *Cellular microbiology*.
- [Wheway et al., 2014] Wheway, J., Latham, S. L., Combes, V., and Grau, G. E. R. (2014). Endothelial Microparticles Interact with and Support the Proliferation of T Cells. *Journal of immunology (Baltimore, Md. : 1950)*, 193(7):3378–87.
- [White et al., 2010] White, N. J., Turner, G. D. H., Medana, I. M., Dondorp, A. M., and Day, N. P. J. (2010). The murine cerebral malaria phenomenon. *Trends in parasitology*, 26(1):11–5.
- [WHO, 2010] WHO (2010). Guidelines for the treatment of malaria, second edition. Technical report, World Health Organization.
- [WHO, 2014] WHO (2014). World Malaria Report 2014. Technical report, World Health Organization.
- [WHO, 2015] WHO (2015). Guidelines for the treatment of malaria, third edition. Technical report, World Health Organization.
- [WHO, 2016] WHO (2016). Malaria - Fact Sheet. <http://www.who.int/mediacentre/factsheets/fs094/en/>, last update April 2016, accessed 2016-04-23.
- [Wu et al., 2010] Wu, J.-J., Chen, G., Liu, J., Wang, T., Zheng, W., and Cao, Y.-M. (2010). Natural regulatory T cells mediate the development of cerebral malaria by modifying the pro-inflammatory response. *Parasitology international*, 59(2):232–41.
- [Yañez et al., 1996] Yañez, D. M., Manning, D. D., Cooley, A. J., Weidanz, W. P., and van der Heyde, H. C. (1996). Participation of lymphocyte subpopulations in the pathogenesis of experimental murine cerebral malaria. *Journal of immunology (Baltimore, Md. : 1950)*, 157(4):1620–4.

- [Yin et al., 2015] Yin, W., Gorvel, L., Zurawski, S., Li, D., Ni, L., Duluc, D., Upchurch, K., Kim, J. R., Gu, C., Ouedraogo, R., Wang, Z., Xue, Y., Joo, H. M., Gorvel, J. P., Zurawski, G., and Oh, S. K. (2015). Functional Specialty of CD40 and Dendritic Cell Surface Lectins for Exogenous Antigen Presentation to CD8+ and CD4+ T Cells. *EBioMedicine*, 5:46–58.
- [Zhao et al., 2014] Zhao, H., Aoshi, T., Kawai, S., Mori, Y., Konishi, A., Ozkan, M., Fujita, Y., Haseda, Y., Shimizu, M., Kohyama, M., Kobiyama, K., Eto, K., Nabekura, J., Horii, T., Ishino, T., Yuda, M., Hemmi, H., Kaisho, T., Akira, S., Kinoshita, M., Tohyama, K., Yoshioka, Y., Ishii, K. J., and Coban, C. (2014). Olfactory plays a key role in spatiotemporal pathogenesis of cerebral malaria. *Cell host & microbe*, 15(5):551–63.

Supplements

Proof of *Batf3* knock-out

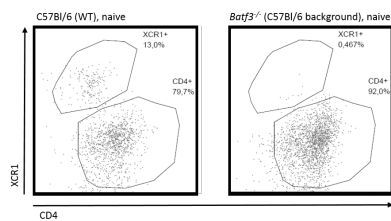


Figure S1: **XCR1⁺ cross-presenting dendritic cells are missing in *Batf3*^{-/-} mice.** Dendritic cells from spleens of naive WT and *Batf3*^{-/-} mice were analyzed for XCR1 and CD4. As expected, the population of XCR1⁺ was missing in *Batf3*^{-/-} mice, which confirmed the genetic knock-out of this DC subset.

Referring to Figure 1.2 and 3.1

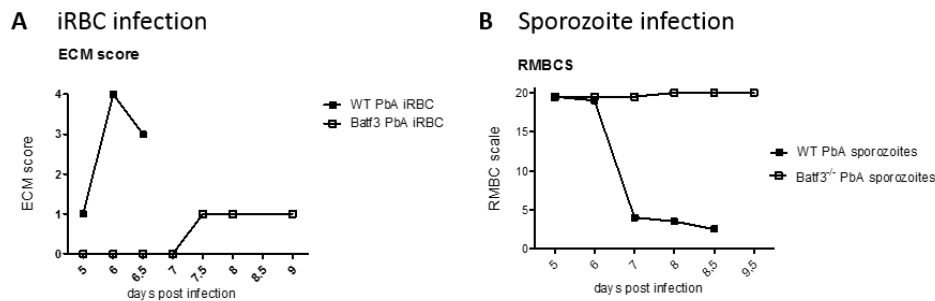


Figure S2: ***Batf3*^{-/-} mice did not develop cerebral malaria.** A: ECM scores (disease score, from 0 = healthy to 6 = severely sick) of WT Bl/6 mice (filled squares, n = 10) and *Batf3*^{-/-} mice (empty squares, n = 10) after infection with 5e4 iRBC i.v. till 9 dpi. B: RMCBS scores (fitness score, from 20 = healthy to 0 = severely sick) of WT (filled squares, n=6) and *Batf3*^{-/-} mice (empty squares, n =6) after inoculated with 1,000 sporozoites from dpi 17 infected mosquitoes is shown.

Referring to Figure 3.4 and 3.5

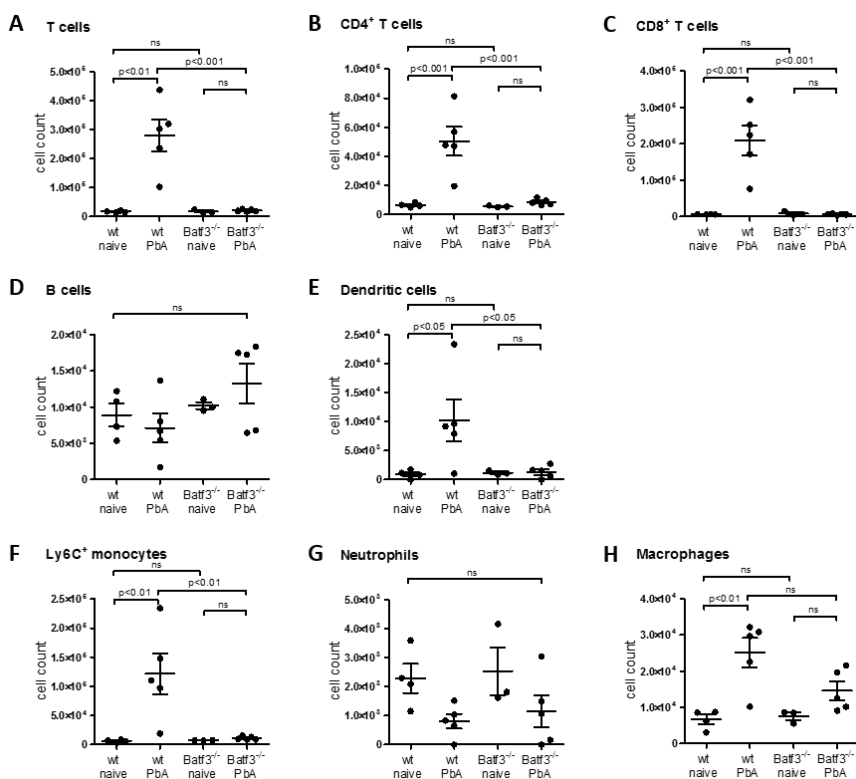


Figure S3: Very low levels of total cells found in brains of PbA-infected *Batf3*^{-/-} mice on 6 dpi. Brain-infiltrated CD45^{high} lymphocytes from PbA-infected (6 dpi) and naive WT and *Batf3*^{-/-} mice were differentiated by flow cytometry (n=3-5) into were T cells (CD3³, A), which were further differentiated in CD4⁺ (B) and CD8a⁺ cells (C), B cells (CD3⁻B220⁺, D), dendritic cells (CD11c⁺I-Ab⁺ from CD3⁻B220⁺, E), Ly6C⁺ monocytes (Ly6C⁺Ly6G⁻; F), neutrophils (Ly6C⁺Ly6G⁺; G) and macrophages (Ly6C⁻Ly6G⁻; H).

Referring to Figure 3.8

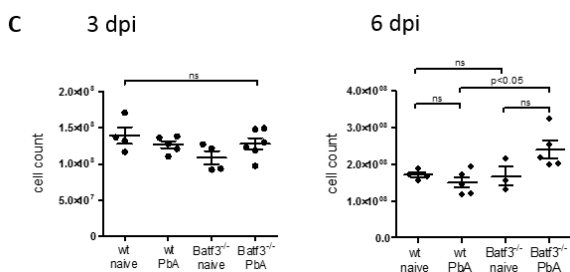


Figure S4: Total amount of splenocytes did increase in PbA-infected *Batf3*^{-/-} mice at 6 dpi. C: Spleens from dpi 3 and 6 infected WT and *Batf3*^{-/-} mice (n=5-6) as well as naive control mice (n=3-4) were digested with collagenase and homogenized. The cell concentration of in this suspension was counted and the total amount of splenocytes was calculated. Values are presented as mean \pm SEM. Significance was tested with ANOVA followed by Tukey post-test, p < 0.05 was considered significant (* = p < 0.05, ** = p < 0.01, *** = p < 0.001).

Referring to Figure 3.10

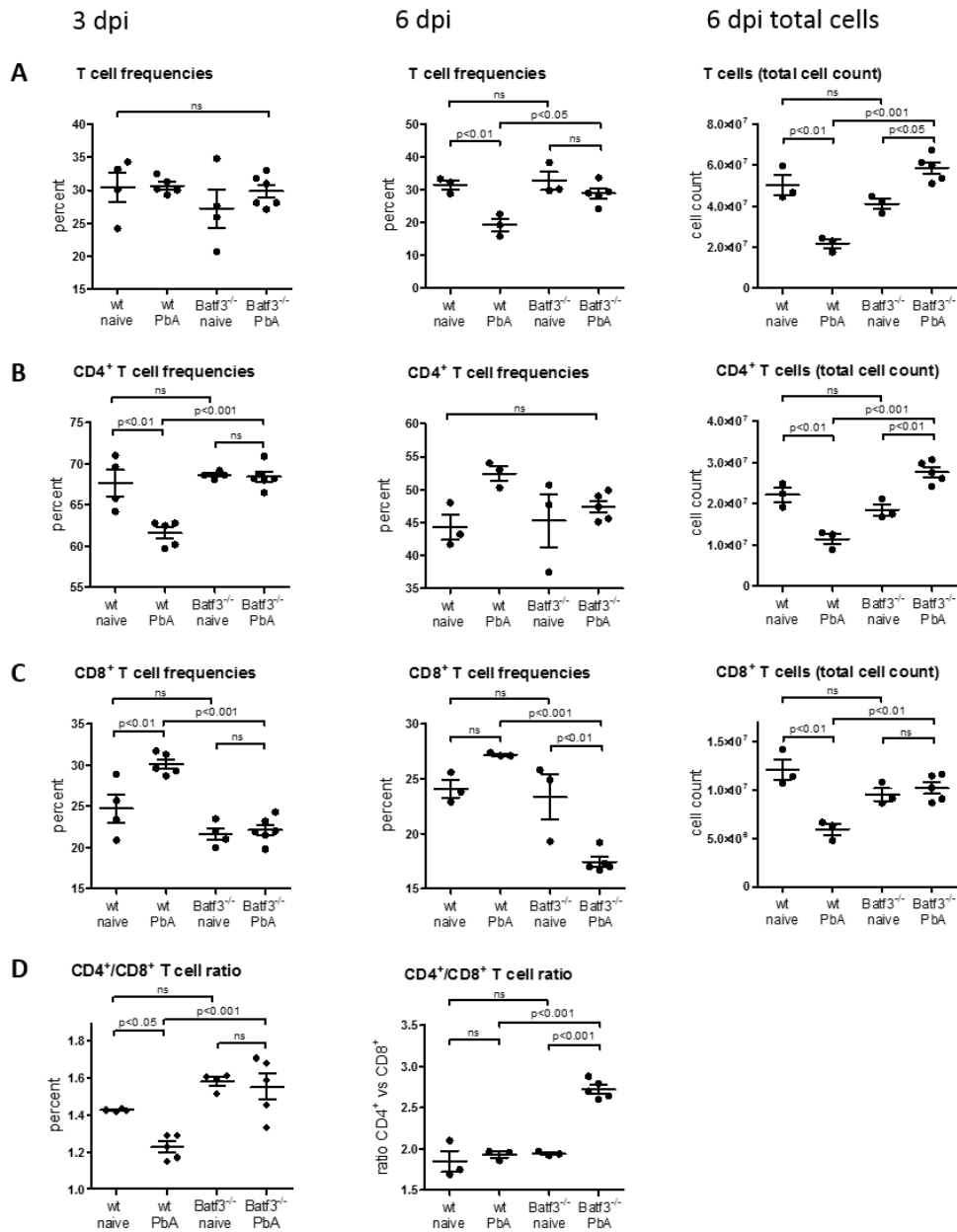


Figure S5: Increased CD4⁺ vs. CD8⁺ T cell ratios in *Batf3*^{-/-} mice at all tested time points after PbA-infection. (A) T cell frequencies of d+3 or d+6 PbA-infected mice (n=5-6) and naive controls (n=3-4) were identified by surface marker CD3. Total cell counts are shown for 6 dpi. CD3⁺ T cells were further differentiated into CD4⁺ (B) and CD8a⁺ (C) T cells (both calculated from frequency from CD3⁺ cells). (D) The ratio between CD4⁺ and CD8⁺ T cells was calculated. Values are presented as mean ± SEM. Differences were tested with ANOVA followed by the Tukey post-test; p values below 0.05 were considered significant (* = p < 0.05, ** = p < 0.01, *** = p < 0.001).

Referring to Figure 3.11

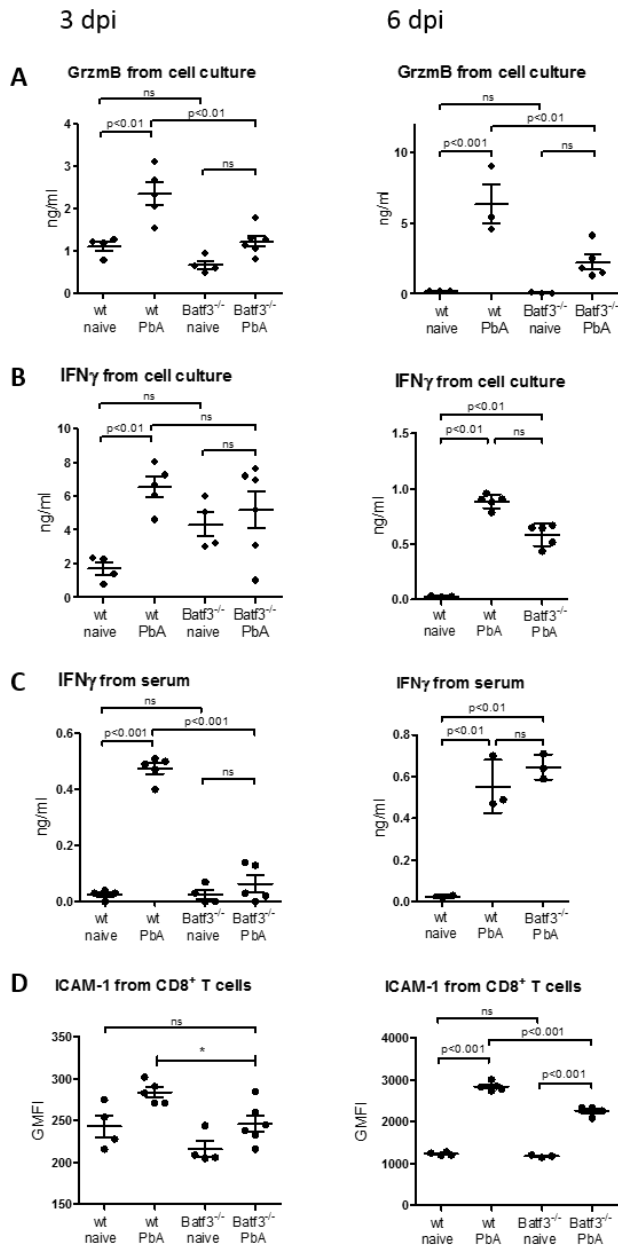


Figure S6: **Cytotoxicity was reduced in *Batf3*^{-/-} mice.** PbA-infected WT and *Batf3*^{-/-} mice were analyzed on 3 and 6 dpi together with naive control mice (n=3-5). A and B: Granzyme B (GrzmB) and IFN γ were measured by ELISA in supernatant of 24h splenocyte culture. C: IFN γ was determined by ELISA in serum of all experimental animals. D: Presence of surface marker ICAM-1 on CD8a⁺ was analyzed by flow cytometry. Values are presented as mean \pm SEM. Differences were tested with ANOVA followed by the Tukey post-test; p values below 0.05 were considered significant (* = p < 0.05, ** = p < 0.01, *** = p < 0.001).

Referring to Figure 3.11 and 3.12

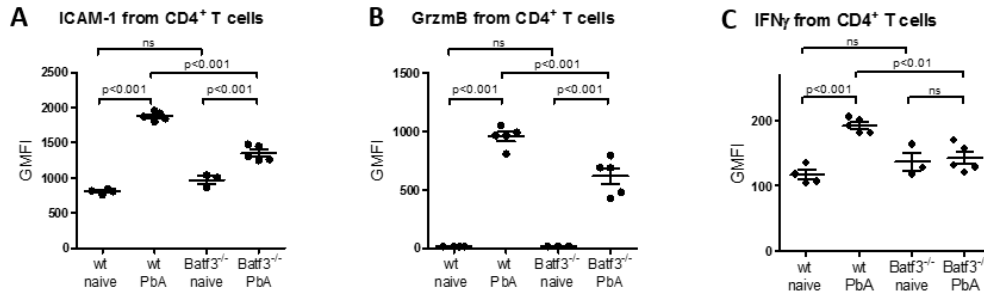


Figure S7: **Activation of CD4⁺ T cells was reduced in *Batf3*^{-/-} mice.** PbA-infected WT and *Batf3*^{-/-} mice were analyzed on 3 and 6 dpi together with naive control mice (n=3-5). Presence of surface markers on CD4⁺ were analyzed by flow cytometry: ICAM-1 (A), granzyme B (B) and IFN γ (C). Values are presented as mean \pm SEM. Differences were tested with ANOVA followed by the Tukey post-test; p values below 0.05 were considered significant (* = p < 0.05, ** = p < 0.01, *** = p < 0.001).

Referring to Figure 3.13

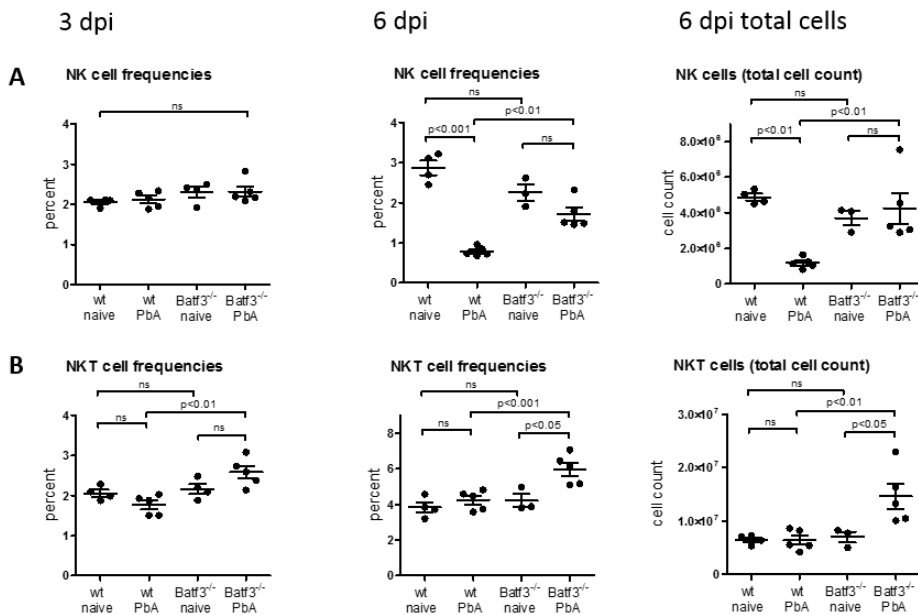


Figure S8: **NK and NKT cells were elevated in *Batf3*^{-/-} mice after PbA-infection, compared to infected WT mice.** Splens of d+3 and d+6 PbA-infected WT and *Batf3*^{-/-} mice (n=5-6) as well as naive controls (n=3-4) were processed for FACS analysis and stained with surface markers CD3 and NK1.1 to identify NK cells (CD3⁻NK1.1⁺; A) and NKT cells (CD3⁺NK1.1⁺; B). Values are presented as mean \pm SEM. Differences were tested with ANOVA followed by the Tukey post-test; p values below 0.05 were considered significant (* = p < 0.05, ** = p < 0.01, *** = p < 0.001).

Referring to Figure 3.14

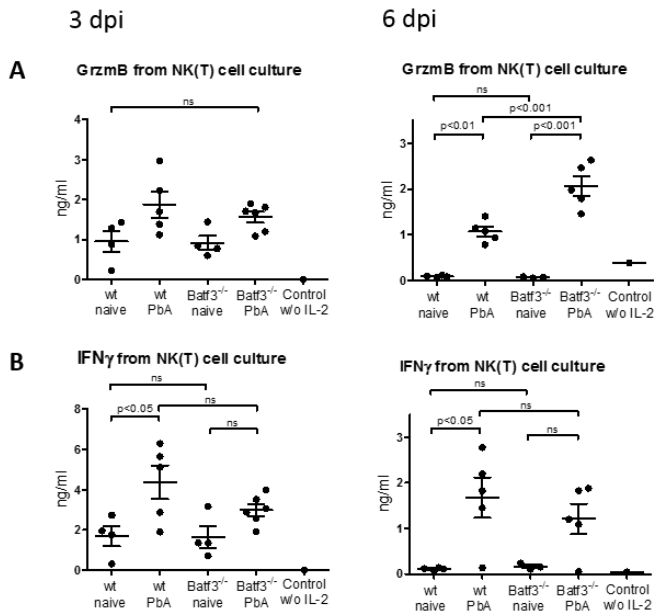


Figure S9: NK and NKT cells from *Batf3*^{-/-} mice produced significantly more granzyme B after PbA-infection than infected WT mice. NK and NKT cells from all experimental groups (n=3-5; 3 and 6 dpi for PbA-infected mice) were sorted via MACS sorting after labeling with magnetically labeled beads coupled to DX-5 antibody. Sorted cells were incubated with IL-2 and BMDCs from naive WT donor mice that were cultured with GM-CSF for a week prior to the experiment. A pooled sample of DX-5 sorted cells on BMDCs without IL-2 was used as simulation control. Supernatant was collected the next day and subjected to sandwich-ELISAs for granzyme B (A) and IFN γ (B). Values are presented as mean \pm SEM. Differences were tested with ANOVA followed by the Tukey post-test; p values below 0.05 were considered significant (* = p < 0.05, ** = p < 0.01, *** = p < 0.001).

Referring to Figure 3.15

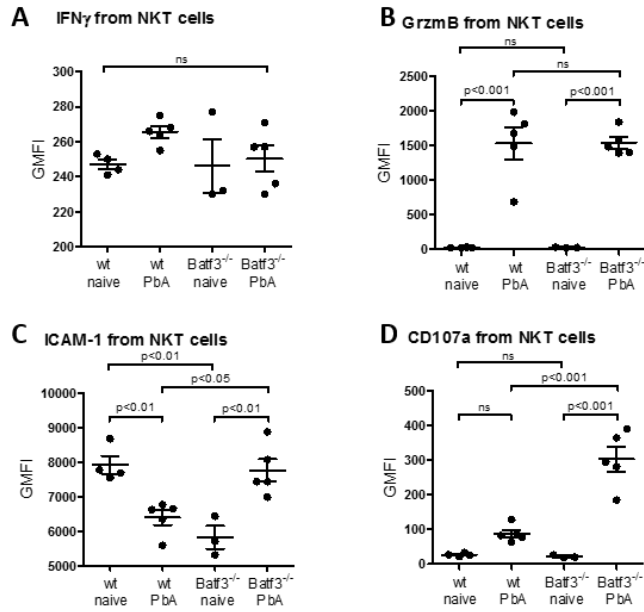


Figure S10: NKT cells from *Batf3*^{-/-} mice did not produce more IFN γ or granzyme B after PbA-infection than infected WT mice. NKT cells from spleens of PbA-infected and naive mice of WT and *Batf3*^{-/-} strains (n=3-5) were defined as described before. Cells were then analyzed via flow cytometry for intracellular cytokines IFN γ (A) and granzyme B (B) and surface markers ICAM-1 (C) and CD107a (D). Values are presented as mean \pm SEM. Differences were tested with ANOVA followed by the Tukey post-test; p values below 0.05 were considered significant (* = p < 0.05, ** = p < 0.01, *** = p < 0.001).

Referring to Figure 3.16

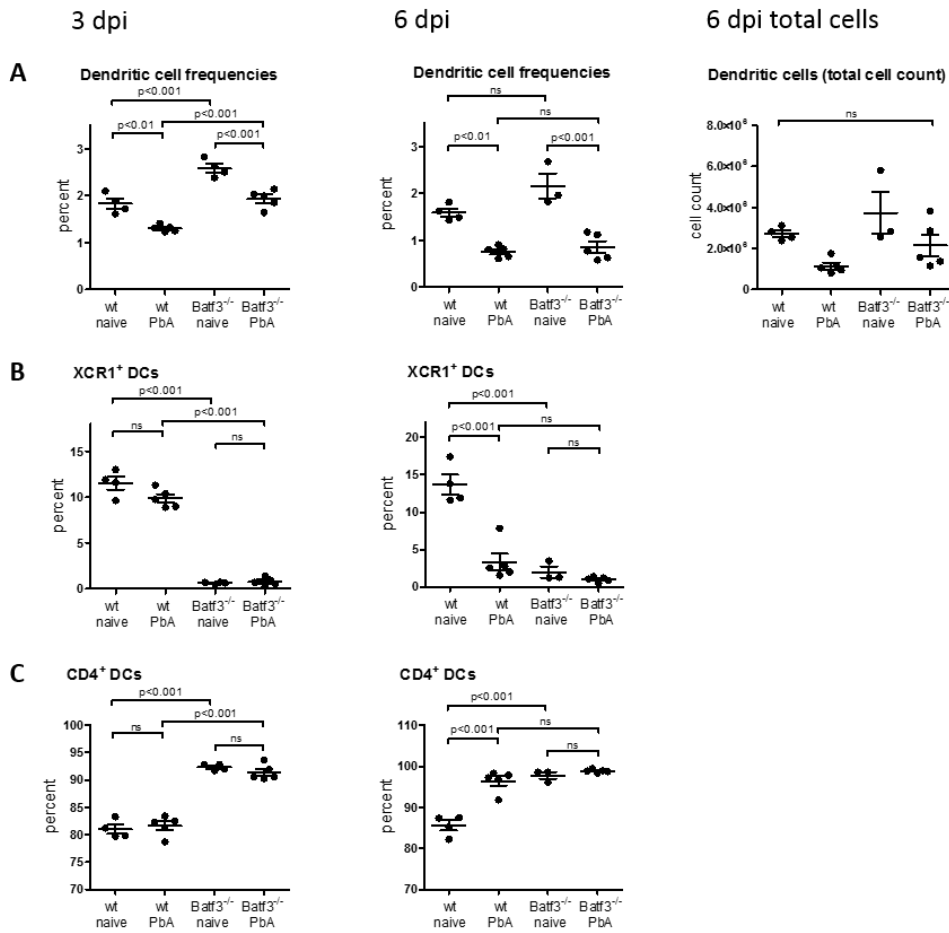


Figure S11: Dendritic cell numbers decreased in spleens of PbA-infected WT and *Batf3*^{-/-} mice. Spleens of d+3 and d+6 PbA-infected WT and *Batf3*^{-/-} mice and their respective naive controls were processed for FACS staining (n=3-6). A: Dendritic cells were defined as CD11c⁺I-Ab⁺ from CD3⁻NK1.1⁻B220⁻ cells. Dendritic cells were further subdivided into XCR1⁺ DCs (B) and CD4⁺ DCs (C). Values are presented as mean ± SEM. Differences were tested with ANOVA followed by the Tukey post-test; p values below 0.05 were considered significant (* = p < 0.05, ** = p < 0.01, *** = p < 0.001).

Referring to Figure 3.17

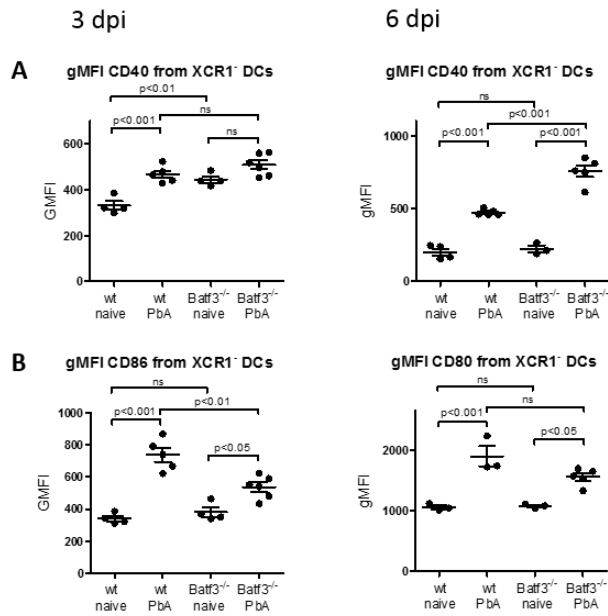


Figure S12: CD40 was increased on splenic DCs in d+6 PbA-infected *Batf3*^{-/-} mice. CD4⁺ dendritic cells that were identified from spleens of d+3 and d+6 PbA-infected *Batf3*^{-/-} and WT mice and their respective uninfected controls (Fig. 3.16), were analyzed for expression of surface marker CD40 (A), CD80/CD86 (B) and CCR7 (C, 6 dpi only) by flow cytometry (n=3-6). Values are presented as mean ± SEM. Differences were tested with ANOVA followed by the Tukey post-test; p values below 0.05 were considered significant (* = p < 0.05, ** = p < 0.01, *** = p < 0.001).

Referring to Figure 3.18

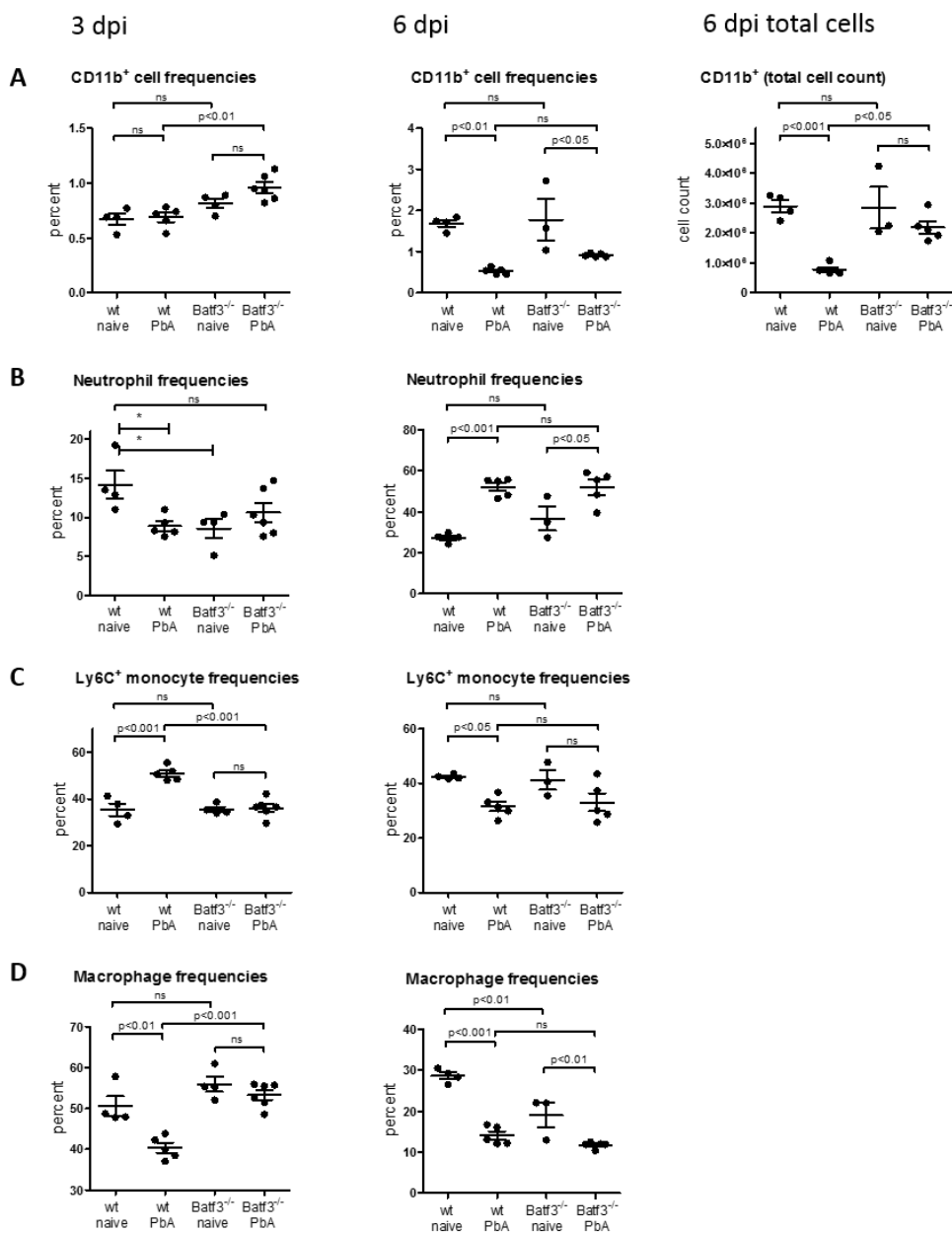


Figure S13: Inflammatory monocytes were not increased in *Batf3*^{-/-} but in WT mice on dpi 3. Splens of PbA-infected (3 and 6 dpi) and naive WT and *Batf3*^{-/-} mice (n=3-6) were analyzed for CD11b⁺ cells by FACS (A), after exclusion of other cell subsets and further differentiated into neutrophils (Ly6C⁺Ly6G⁺, B), Ly6C⁺ monocytes (Ly6C⁺Ly6G⁻, C) or macrophages (Ly6C⁻Ly6G⁻, D). Values are presented as mean ± SEM. Differences were tested with ANOVA followed by the Tukey post-test; p values below 0.05 were considered significant (* = p < 0.05, ** = p < 0.01, *** = p < 0.001).

Referring to Figure 3.21

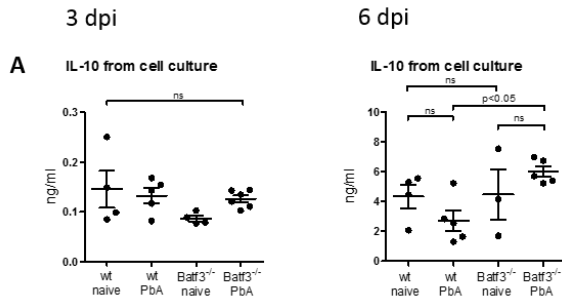


Figure S14: **IL-10 and IL-6 production from splenic CD11b⁺ cells was increased in PbA-infected *Batf3*^{-/-} mice.** WT and *Batf3*^{-/-} mice were infected with PbA (n=3-5) and spleens were analyzed 3 and 6 days later. Naive mice (n=3) served as controls. IL-10 was measured in supernatant of 24h incubated splenocyte culture with whole spleen cell suspension (A). Results from are presented as mean (\pm SEM). All differences were tested with ANOVA followed by the Tukey post-test; p values below 0.05 were considered significant (* = p < 0.05, ** = p < 0.01, *** = p < 0.001).

Referring to Figure 3.22

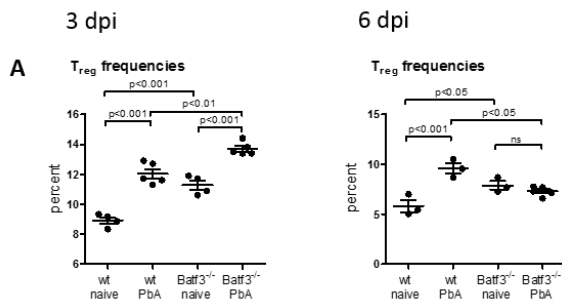


Figure S15: **The total amount of T_{regs} was increased in PbA-infected *Batf3*^{-/-} mice on 6 dpi.** WT and *Batf3*^{-/-} mice were infected with PbA (n=3-6) and spleens were analyzed at 3 and 6 dpi. Naive mice (n=3-4) were used as controls. A: T cells were identified via FACS as described before and CD4⁺ cells were analyzed via flow cytometry for CD25 and FoxP3 double positive cells (T_{regs}). Fractions were calculated to present the percentage of T_{regs} from all T cells. Results are presented as mean (\pm SEM). All differences were tested with ANOVA followed by the Tukey post-test; p values below 0.05 were considered significant (* = p < 0.05, ** = p < 0.01, *** = p < 0.001).

Referring to Chapter 3.1.5.7

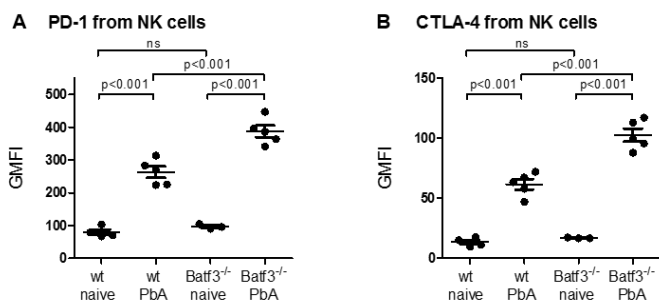


Figure S16: **PD-1 and CTLA-4 were increased in PbA-infected *Batf3*^{-/-} mice on 6 dpi.** WT and *Batf3*^{-/-} mice were infected with PbA (n=3-6) and spleens were analyzed at 3 and 6 dpi. Naive mice (n=3-4) were used as controls. NK cells were identified as described before and analyzed for expression of PD-1 (A) and CTLA-4 (B) by flow cytometry. Results are presented as mean (\pm SEM). All differences were tested with ANOVA followed by the Tukey post-test; p values below 0.05 were considered significant (* = p < 0.05, ** = p < 0.01, *** = p < 0.001).

Referring to Figure 3.32

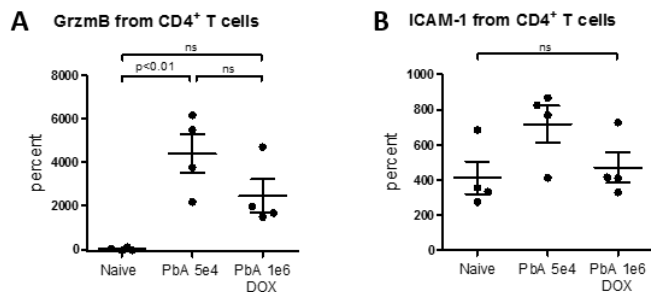


Figure S17: **CD4⁺ T cells in the brain were less activated after doxycycline treatment.** CD4⁺ T cells from brains of doxycycline treated (PbA 1e6 + DOX), untreated (PbA 5e4) and naive animals (n=4) were analyzed for different activation markers by flow cytometry. A: intracellular granzyme B staining, B: surface staining for ICAM-1. Statistics were performed with ANOVA and Tukey post-test with p < 0.05 considered significant.

Scientific Contributions

Publications

- Alferink J, Specht S, Arends H, Schumak B, Schmidt K, Ruland C, Lundt R, Kempter A, Dlugos A, **Kuepper JM**, Poppensieker K, Findeiss M, Albayram Ö, Otte DM, Marazzi J, Gertsch J, Foerster I, Maier W, Scheu S, Hoerauf A, and Zimmer A, *Cannabinoid receptor 2 modulates susceptibility to experimental cerebral malaria through a CCL17-dependent mechanism.*, The Journal of Biological Chemistry, 2016 July 29
- Schumak B, Klocke K, **Kuepper JM**, Biswas A, Djie-Maletz A, Limmer A, van Rooijen N, Mack M, Hoerauf A, Dunay IR, *Specific Depletion of Ly6Chi Inflammatory Monocytes Prevents Immunopathology in Experimental Cerebral Malaria.*, PLoS One, 2015 April 17
- Kreer C, **Kuepper JM**, Zehner M, Schumak B, Burgdorf S, *N-glycosylation converts non-glycoproteins into Mannose Receptor ligands and reveals antigen-specific T cell responses in vivo.*, under review with Oncotarget, first submission 2016 May 03

Oral & Poster Presentations

- **Kuepper JM**, Borsche M, Korir PJ, Hoerauf A, Dunay IR, Schumak B, *Cross-presenting dendritic cells in the pathogenesis of experimental cerebral malaria*, 27th Annual Meeting of the German Society for Parasitology, Göttingen (Germany), March 2016 (oral presentation)

- **Kuepper JM**, Borsche M, Korir PJ, Hoerauf A, Dunay IR, Schumak B, *Cross-presenting dendritic cells in the pathogenesis of experimental cerebral malaria*, 13th Malaria Meeting, Hamburg (Germany), November 2015 (oral presentation)
- **Kuepper JM**, Borsche M, Korir PJ, Hoerauf A, Dunay IR, Schumak B, *CD8a⁺ dendritic cells in the pathogenesis of experimental cerebral malaria*, 3rd Cluster Science Days of the ImmunoSensation Cluster of Excellence, Bonn (Germany), November 2015 (short oral & poster presentation)
- **Kuepper JM**, Borsche M, Korir PJ, Hoerauf A, Dunay IR, Schumak B, *CD8a⁺ dendritic cells in the pathogenesis of experimental cerebral malaria*, 4th European Congress of Immunology (ECI), Vienna (Austria), September 2015 (poster presentation)
- **Kuepper JM**, Schmidt KE, Alferink J, Schumak B, Limmer A, Specht S, Hoerauf A, *Doxycycline inhibits experimental cerebral malaria by altering T cell responses and reducing inflammatory and tissue-degrading mediators*, 12th Malaria Meeting, Bonn (Germany), November 2014 (oral presentation)
- **Kuepper JM**, Borsche M, Korir PJ, Hoerauf A, Dunay IR, Schumak B, *CD8a⁺ dendritic cells in the pathogenesis of experimental cerebral malaria*, 2nd Cluster Science Days of the ImmunoSensation Cluster of Excellence, Bonn (Germany), November 2014 (poster presentation)
- **Kuepper JM**, Borsche M, Hoerauf A, Dunay IR, Schumak B, *CD8a⁺ dendritic cells in the pathogenesis of experimental cerebral malaria*, 44th Annual Meeting German Society for Immunology (DGfI), Bonn (Germany), September 2014 (poster presentation)
- **Kuepper JM**, Schmidt KE, Alferink J, Schumak B, Limmer A, Specht S, Hoerauf A, *Doxycycline inhibits experimental cerebral malaria by altering T cell responses and reducing inflammatory and tissue-degrading mediators*, Summer School on Infection Research, Dresden (Germany), June 2014 (poster presentation)
- **Kuepper JM**, Borsche M, Hoerauf A, Dunay IR, Schumak B, *CD8a⁺ dendritic cells in the pathogenesis of experimental cerebral malaria*, 18th Symposium “Infektion und Immunabwehr“, Rothenfels (Germany), March 2014 (oral presentation)
- Schmidt KE, **Kuepper JM**, Alferink J, Schumak B, Limmer A, Specht S, Hoerauf A, *Doxycycline inhibits experimental cerebral malaria by altering T cell responses and reducing inflammatory and tissue-degrading mediators*, Annual meeting of the Bonner Forum Biomedizin, Bonn (Germany), February 2014 (poster presentation)
- Schmidt KE, **Kuepper JM**, Specht S, Alferink J, Hoerauf A, *Doxycycline targets several pathological processes during Plasmodium berghei ANKA induced experimental cerebral malaria*, 16th Symposium “Infektion und Immunabwehr“, Rothenfels (Germany), March 2012 (oral presentation)

Curriculum Vitae

Janina Melanie Küpper

Acknowledgments

First of all I would like to thank Prof. Dr. Achim Hörauf who gave me the opportunity to do my thesis in his institute. I always appreciated his support and scientific input on the projects.

I would like to thank Prof. Dr. Waldemar Kolanus for agreeing to be my co-supervisor, despite his busy schedule.

I would further like to thank PD Dr. Gerhild van Echten-Deckert and Prof. Dr. Ulrich Kubitscheck for joining the committee board for my defense.

My deepest thanks goes to Dr. Beatrix Schumak for excellent supervision and support throughout my thesis. You always had an open ear for my problems and ideas, supported me throughout my PhD and gave me very helpful input. Without you, this thesis wouldn't exist.

A special thank you to PD Dr. Sabine Specht and Dr. Kim Schmidt who welcomed me to the institute and introduced me to research. Thank you both for your support and help, even after you left Bonn.

A very big thank you to all members of the AG Schumak, especially to Max Borsche for help in the lab and to Patricia Korir who has gone all this way with me and even up to Mt. Kilimanjaro (also Hi to Missa here!). I'm still in for the Kenya beach plan ;). Also thanks to all IMMIP members, who always provided the essentials of lab-life: help, happiness and coffee. Thanks to Dr. Ute Klarmann-Schulz and Dr. Andrea Hofmann

ACKNOWLEDGMENTS

who helped with statistical analysis. Also, we should not forget our small four-legged colleagues, who dedicated their lives to science. Thank you all!

I further want to express my gratitude to Dr. Ildiko Dunay from Magdeburg who provided us with the *Batf3*^{-/-} mice, Dr. Ann-Kristin Müller and her lab in Heidelberg for the generation of the transgenic *Plasmodium* strain PbA AMA1, Laurent Rénia and Shanshan Howland who performed the cross-presentation assay for brain microvessels in their lab in Singapore and the Flow Cytometry Core Facility Bonn for excellent technical support.

I'm very grateful for my friends - near and far - who give me a wonderful life outside of work and always gave me a reason to forget about the lab.

Special thanks to my family, especially my parents, who provided unlimited support throughout my life and always believed in me. I can't thank you enough!

My biggest thanks goes to Daniel, not only for helping me with L^AT_EX and programming, but even more importantly for always being by my side. Thank you for catching my falls literally as well as figuratively. I love you!